Synthesis and Mechanistic Studies of Sulfur Heterocyclic (Benzodithiolanone-oxide) and Dioxirane Compounds

by

NAHED SAWWAN

A dissertation submitted to the Graduate Faculty in Chemistry in partial fulfillment of the requirements for the degree of Doctor of Philosophy

The City University of New York

2007

UMI Number: 3295016

ProQuest Information and Learning Company
300 North Zeeb Road
P.O. Box 1346
Ann Arbor, MI 48106-1346

This manuscript has been read and accepted for the Graduate Faculty in Chemistry in satisfaction of the dissertation requirement for the degree of Doctor of Philosophy.

PROFESSOR ALEXANDER GREER

Date

Chair of Examining Committee

PROFESSOR GERALD KOEPPL

Date

Executive Officer

PROFESSOR ROBERT BITTMAN

PROFESSOR KLAUS GROHMANN

PROFESSOR DAVID R. MOOTOO

Supervision Committee

THE CITY UNIVERSITY OF NEW YORK

Abstract

Synthesis and Mechanistic Studies of Sulfur Heterocyclic (Benzodithiolanone-oxide) and Dioxirane Compounds

by

Nahed Sawwan

Advisor: Professor Alexander Greer

This research studies the idea of neighboring group interactions as important variables in the chemistry of sulfur heterocycles (benzodithiolanone-oxide) and 3-membered ring peroxides (dioxiranes). The thesis consists of four parts. The first part of the thesis describes the synthesis of *ortho*- and *para*-substituted benzo-1,2-dithiolan-3-one 1-oxides, and investigates their reactivity toward *n*-propyl thiol reactions in acetonitrile-water mixtures. The reaction with thiol is facilitated by reducing the electron density at the *para* position, or by placing substituents bearing lone pair electrons *ortho* to the dithiolanone-oxide reaction center. Through-space and through-bond effects both contribute to the conversion of polysulfane products. The second part of the thesis describes studies of dioxirane stability. Our study of "bis-dioxiranes" aimed to provide an understanding of their stabilities compared to "mono-dioxiranes". Biacetyl reacts with oxone to give bis-dioxirane [3,3'-dimethyl-(3,3')bidioxirane, **3**] and mono-dioxirane [1-(3-methyl-dioxiran-3-yl)-ethanone, **2**)]. Bis-dioxirane **3** is formed when two oxygens are

incorporated into biacetyl, while mono-dioxirane **2** incorporated only one. A greater stability is observed in **3** compared to **2**, which is attributed to an α-dioxiranyl (anomeric) effect in the former. In contrast, **2** suffers from a destabilizing π-electron withdrawing effect from the adjacent carbonyl group. The third part of the thesis involves the attempted synthesis of a 1,5-bis-dioxirane from 3,7-dimethyl-1,5-cyclooctanedione (**4**). The idea here is that the two dioxirane groups might be situated in a *syn* orientation. It was found that, **4** reacts with oxone to form the monoester compound presumably via a mono-dioxirane, although work on the project is incomplete. There is no evidence was obtained for the 1,5-bis-dioxirane intermediate in this system. Finally, a review of the literature on heteroatom-containing dioxiranes was accomplished, which represents the last chapter of the thesis.

ACKNOWLEDGMENTS

First and foremost, I wish to extend my appreciation and gratitude to my mentor, Professor Alexander Greer, for his guidance, support and encouragement throughout the course of my Ph.D. studies. Without his encouragement, it would have been impossible to complete my graduate work and develop adequate understanding of the research subjects, which is necessary for my professional growth and development.

I also extend special thanks to my advisory committee, Prof. K. Grohmann, Prof. R. Bittman, and Prof. D. R. Mootoo for putting forth their time and thoughts during my research period. I also thank all my teachers and colleagues who helped, supported and encouraged me along the way. In particular, I like to thank my friend Dr. Edyta M. Greer, Dr. David Aebisher, Matibur Zamadar, Alvaro Castillo, Mahendran Adaickapillai, and Nikolay Azar. Finally, I like to extend special thanks to my family, especially, my husband, Osman, and my kids, Gennine, Ronny, Jasmine, and Sherine, who were patient with me and who gave their unconditional support and love.

To My Parents My Great Husband My children Gennine Ronny Jasmine Sherine my brothers and sister. And All the Other Wonderful People in My Life

TABLE OF CONTENTS

LIST OF SYMBOLS AND ABBREVIATIONS

Å	angstrom
Ac	acetyl
Ac_2O	acetic anhydride
B3LYP/6-31G(d)	Becke-type-parameter density functional theory
brine	saturated aqueous sodium chloride solution
br	broad
^oC	degree Celsius
calcd	calculated
kcal	kilocalorie
^{13}C NMR	carbon-13 nuclear magnetic resonance
δ	chemical shift in ppm
d	doublet
DCM	dichloromethane
DMAP	4-(dimethylamino)pyridine
DFT	density Functional Theory
DMF	N,N-dimethylformamide
Et_2O	diethyl ether
EtOAc	ethyl acetate
eq	equivalent
g	gram
GC	gas chromatography
GCMS	gas chromatography mass spectroscopy

hr	hour
^{1}H NMR	proton nuclear magnetic resonance
Hz	hertz
IR	infrared spectroscopy
J	coupling constant
L	liter
LAH	lithium aluminum hydride
m	multiplet
MeOH	methanol
mg	milligram
min	minute
mL	milliliter
mmol	millimole
NBO	natural bond order
PCM	polarized continuum model
*p*H	potential of hydrogen
*p*Ka	ionization constant
ppm	parts per million
q	quartet
rt	room temperature
s	singlet
t	triplet
TBAF	tetrabutylammonium fluoride

THF	tetrahydrofuran
TLC	thin-layer chromatography
TMEDA	tetramethylethylenediamine
TS	transition state
TsOH	*p*-toluenesulfonic acid
UV	ultraviolet spectroscopy

LIST OF FIGURES

Chapter 1

Chapter 2

Figure Page

Chapter 3

Figure Page

Chapter 4

Figure Page

LIST OF CHARTS

Chapter 5

Chart Page

LIST OF SCHEMES

Chapter 1

1

Chapter 2

Chapter 3

Scheme Page

Chapter 4

Scheme Page

LIST OF TABLES

Chapter 1

Chapter 4

Chapter 1. Substituent Effects on the Reactivity of Benzo-1,2-Dithiolan-3-one 1-Oxides and Its Possible Application to the Synthesis of DNA-Targeting Drugs

1.1 Introduction

Benzo-1,2-dithiolan-3-one 1-oxide (**1**) contains a thiosulfinate ester heterocycle[1] and possesses DNA-cleaving activity, albeit reduced, compared to the natural product leinamycin (**2**) (Scheme 1).[2-5] The DNA-cleaving[2-5] and antitumor[6-13] activities of leinamycin **2** and other dithiolanone-oxide compounds are thought to arise by an initial attack of thiol or another nucleophile onto the dithiolanone-oxide ring system.[14-16] According to the mechanism proposed by Gates and co-workers, computations predict that a thiolate ion attacks the central sulfur (S2) of leinamycin and is probably reasonable for thiol-trigered activation of leinamycin (Scheme 2).[14-16] The attack of thiolate ion at (S1) is a reversible pathway and unlikely to open the heterocyclic ring. The reaction of leinamycin with thiolate ion suggested that the attack on (C3) is also unlikely from an energetic standpoint. A structure-activity study in which the structure of the benzene core of **1** is varied by introduction of substituents may provide insight into the factors influencing the thiol reaction with dithiolanone-oxide drugs. We have examined *ortho* [X = Cl (**3**), CH_3 (**4**), OCH_3 (**5**)] and *para* [Y = Cl (**6**), CH_3 (**7**), OCH_3 (**8**)] substituted 1,2-dithiolan-3-one 1-oxides that contain different substituent groups, which also differ in being nearer to farther from the sulfinate sulfur (S1) (Scheme 3). The *ortho* and *para* positions are relative to the sulfinyl sulfur (S1) and refer to the 3- and 5-positions of the fused benzene ring.

1.2 Results and Discussion

1.2.1 Synthesis of Benzo-1,2-dithiolan-3-one 1-oxides

The preparation of dithiolanone-oxides **1** and **3-8** is shown in Scheme 2 where a modification of the method of Beaucage[17] was used. Treatment of a 3- or 5-substituted anthranilic acid with $NaNO_2$ yielded the diazonium salt compound. Sodium sulfide and elemental sulfur were added to the diazonium compound to give the dithiosalicylic acid derivative and, after reduction, thiosalicylic acid. Thiolacetic acid was then added to the thiosalicylic acid, which after oxidation with dimethyldioxirane, gave the substituted benzodithiolanone-oxides **3-8** in 20-30% overall yield; the final product from the polysulfane produced (Scheme 3). The yield for each step in the reaction sequence (the yield of the diazo compound, thiosalicylic acid and dithiolanone) may differ according to substituent effects, and their yields were not measured. The synthetic method gave higher yields with structures possessing the methyl (30%) or methoxy groups (25%) compared to the chloro substituent (20%). A likely reason is that the generation of the diazo group should depend on an electron-donating ability to add stability. The substituent may affect the intrinsic stability of the final product (**1**, **3-8** Scheme 3). The issue of unimolecular stability was not studied; however, these materials seemed to be long lived and remained of good purity when stored in the refrigerator. Compounds **3-8** were synthesized and characterized as described in the Experimental Section[18] (Section 2.3). The known dithiolanone-oxide **1**[1] was prepared by oxidation of commercially available 3*H*-1,2-benzodithiolan-3-one with dimethyldioxirane.

The reactivity of **1, 3-8** with thiol was investigated, and the overall yield of the polysulfane generated from this reaction and the rate of consumption of these substrates indicate a difference in reactivity of **1, 3-8** towards the thiol and substituent effects in certain pathway.

Experiments to analyze the substituent effect were carried out for the reaction of **1** and **3**-**8** with *n*-propyl thiol in a mixture of CD_3CN and D_2O (Table 1; Scheme 4). We selected the CD_3CN:D_2O (7:3) mixture for the study because it gave rates such that after 15 minutes products arose in different overall yields. The thiol was added to **1** and **3**-**8** in a 7:3 mixtures of acetonitrile:water. Compound **3** reacted in the presence of the thiol (100% conversion) to form the corresponding polysulfide products **C-G** (83% yield) (Scheme 4), while **4** decomposed (60% conversion) to generate polysulfane products **C-G** (11% yield). The lower yield of products may be caused by a lower rate, depending on the low percent of conversion in the same period. The study of the kinetics of polysulfur products in a reaction can be complicated due to the fact that subsequent equilibrations can take place. We evaluated the products in the reaction since we are unsure about whether they are previous products or intermediates in the reaction. A thermodynamic equilibrium appears to be established by the time we analyzed the material. Thus, kinetic analyses were not conducted. The detection of the intermediate **A** and **B** was not possible; therefore the percent of conversion the substrate and the overall yields (Table 1) were assessed as an indication of the reactivity and substituent effect. No reaction took place between **1**, **3**-**8** and *n*-PrSH over a 3-day period in CD_3CN alone (entry 1, Table 2). The reaction rate increases upon increasing the D_2O content in CD_3CN (entries 2-4) since the acidity of *n*-PrSH is enhanced where *n*-PrS^- ion can act as a nucleophile. We speculate that **A** is protonated; however, the pH was not measured during the reaction. We note however, that substrate solubility becomes a problem at CD_3CN:D_2O 1:10 (entry 4).

The nature of the solvent dependence constraining reductive thiol activation

reported here may be of importance for dithiolanone-oxide compounds capable of noncovalently associating with DNA.[19-21] The dithiolanone-oxide compounds might intercalate or weakly associate to the minor groove of DNA. The structure of thiol may also play an important role in the activity of dithiolanone-oxide drugs.[22,23] Control experiments show that the above dithiolanone-oxide decomposition is a thiol-dependent process. There is no reaction of the benzodithiolanone-oxides in the CD_3CN:D_2O (7:3) mixture over 2 h in the absence of thiol. Each dithiolanone-oxide (**1** and **3**-**8**)—*n*-PrSH reaction forms at least 5 products (Table 1), which are similar to the product distribution observed previously by Gates and co-workers for the reaction of **1** with *n*-PrSH.[1]

The polysulfane products observed are proposed to arise from the interconversion of sulfenic acid (**A**) and oxathiolane species (**B**) on the reaction surface (Scheme 3). A similar mechanism has been proposed previously by Gates and co-workers for compound **1**.[1] Compounds **A** and **B** are unstable intermediates and are not detected in the reaction. Electrophilic oxathiolane **B** can potentially undergo a reaction with PrS^- or $PrSS^-$ to give rise to 3- or 5-substituted-2-propyldisulfuranyl benzoic acid (**C**) and 3- or 5-substituted-2-propyltrisulfuranyl benzoic acid (**D**), respectively. Equilibrium and exchange processes may also contribute to the production of **C** and **D**. The reactive byproduct hydrodisulfide (PrSSH) will likely undergo reactions in the presence of PrSH and O_2 to account for formation of polysulfanes [di-*n*-propyl-disulfane (**E**), di-*n*-propyl-trisulfane (**F**), and di-*n*-propyl-tetrasulfane (**G**)]. Similar thiol-disulfide equilibria (redox) processes have been observed in biological systems.[24]

Ortho-chloro (**3**) and *ortho* -methoxy substituted dithiolanone-oxides (**5**) yield higher concentrations of polysulfane products (**C**-**G**) compared to **1**, **4**, **7**, and **8**, which

may depend on the generation and reactivity of intermediate **B**. Intermediate **B** generated in higher concentration in reaction of **3** and **5** with thiol that can be explained in terms of two reaction steps according to the proposed mechanism (Scheme 4). Reaction of **3** and **5** with thiol can be facilitated in the first step by increasing the electrophilicity for compound **3** and **5** by decreasing the electron density on the hererocyclic ring (through bond effects). Moreover, substrate bearing a lone pair of electrons can be donated to S1 through space, elongate the S-S bond and increase the positive charge on S2 which is susiptable to thiol attack. Second step was cyclization of compound **A** to compound **B**. In this step through space effects may play the key role in increasing the neucleophilicity of the oxygen in sulfenic acid **A**. However, the consumption of the intermediate **B** to the final product polysulfane **C** and **D** may be affected by the substituent since the chloro and methoxy in ortho positions reduce the electron density of the heterocyclic ring and increase the reactivity of the intermediate **B**.

Para-chlorodithiolanone-oxide (**6**) yielded higher concentrations of polysulfanes **C-D** compared to **8**, this can be explained by ehectron-withdrawing character for the chlorine over the methoxy group. The chloro substituent can reduce the electron density by through bond effects and increase the positive charge on S2 which can facilitate step one, on the other hand, it may slow the cyclization in step 2. However, the reactivity of the intermediate **B** would be increased by reducing the electron density which leads to increasing in the polysulfane products formation (**C-D**) (79% overall yields). The methoxy sustituent may stabilize the substrate **8** as well as the intermediate **B** leading to a reduction of the generation of the polysulfane products **C-D** (27% overall yields).

Generation of polysulfane **E-G** occur via the oxidation and equilibration processes of the

reactive hydrodisulfide. These processes may lead to formation of undefined products reducing the polysulfane **E-G** yield in favor of the **C-D** polysulfane. However, the sustituent effect can facilitate one step in the proposed mechanism and on the other hand, slow down other steps. Because of this complexity, the final product of the polysulfane or the percent of convertion of the dithiolanone compounds **1, 3-8** can be used to determine the efficiency of dithiolanone oxide reaction with thiol.

A possible through-space effect emerges[25] with substituents bearing lone pair electrons positioned near the dithiolanone-oxide sulfinate sulfur (S1). *Ortho*-chloro (**3**) and -methoxy substituted dithiolanone-oxides (**5**) yield higher concentrations of polysulfane products (**C-G**) compared to **1**, **4**, **7**, and **8**, which may be explained by intramolecular S1—Cl or S1—$O_{(methoxy)}$ dipole-dipole interactions that enhance the ease of ring opening of the heterocycle. According to B3LYP/6-31G(d) calculations, the 1,4-S—X perturbation (X = Cl, OMe) influences the structure of dithiolanone-oxide **3** and **5** (Table 3). The calculated S2-S1-O1 bond angles in **3** (110.9°) and **5** (111.1°) are less than other dithiolanone-oxides **1** (113.1°), **4** (111.9°), **6** (113.1°), **7** (113.1°), and **8** (113.1°).[26] The 1,4-S—X perturbation [X=Cl (**3**), OMe (**5**)] influences the S1-O1 and C1-S2 bond distances, but has little or no effect on the S1-S2 bond distance. We observed decreases in the S1-O1 and C1-S2 bond distance when comparing **3** and **5** with **1**, **4**, and **6-8**. The S—X perturbation also influences the calculated dihedral angle (θ = O1-S1-S2-C1). The torsion angle θ in **3** (104.7°) and **5** (105.9°) are reduced compared with **1** (113.1°), **4** (110.1°), **6** (113.2°), **7** (112.9°), and **8** (112.9°).

The *para*-chloro substituent in **6** had an unexpected influence on product generation. A reason for the enhanced reactivity of **6** is a suggested thiol attack at S2,

which should depend on electron-withdrawing through-bond effects in *ortho* or *para* positions to enhance reactivity. There is a small reduction of electron-density at S2, when comparing the natural bond order (NBO) positive charge in **3** (0.020) and **6** (0.017) with compounds **1** (0.007), **4** (0.016), **5** (0.005), **7** (0.004), and **8** (0.007) (Table 3). We believe the destabilizing substitution of chlorine in the *ortho* or *para* position accounts for the increase in the rate of thiol activation. Finally, a chemical consequence from the perturbation of the sulfinyl center in **3** could be accounted for by combined through-space S—Cl interaction and electron withdrawing substituent effect responsible for increased product formation (Table 1). This is shown in **3**, where unlike others in the series, the through-bond and through-space effects both contribute in the same direction to product conversion.

1.3 Conclusion

In conclusion, mechanistic evidence suggests that an electron-withdrawing chlorine substituent in the *para* position (such as Cl) or a neighboring group interaction involving lone pair electrons on methoxy or chlorine substituents as factors that enhance benzodithiolanone-oxide reactivity toward thiol. The substituent effect on intermediates **A** and **B** is uncertain; we were unable to detect these intermediates, and in our mechanism speculated to their existence. The substituent effects have been analyzed by using an acetonitrile water 7:3 solvent mixture, but up to now the only substrates considered have limited water solubility. The relationship between the substituent effects in thiol activation of the dithiolanone-oxide heterocycle may be dramatic *in vivo* because of substrate-DNA noncovalent associations where dipolar aprotic and aqueous solvent environments are both contributors. Use of remote and near-by functional groups as a

mechanistic tool enables one to bias the yield of the polysulfane products **C**-**G**. Polysulfane autoxidation and subsequent Fenton chemistry can take place. Oxygen radicals, such as OH radical, are produced in a trace metal-dependent Fenton reaction previously reported for the oxidative DNA cleavage by the antitumor antibiotic leinamycin and synthetic dithiolanone-oxide analogs.[2,4,5,27,28] However, unlike compounds **1** and **3**-**8**, leinamycin **2** can also act as a DNA alkylating agent because of an intramolecular reaction of an alkene moiety on the oxathiolane heterocycle.[6,8,9,11-13,16,29]

1.4 Experimental Section

1.4.1 Materials and Instrumentation 2-amino-3-methylbenzoic acid, 2-amino-3-methoxybenzoic acid, 2-amino-3-chlorobenzoic acid, 2-amino-5-methylbenzoic acid, 2-amino-5-chlorobenzoic acid, 2-amino-5-methoxybenzoic acid, 1,3,5-trimethoxybenzene, sodium nitrate, sodium sulfide, elemental sulfur (S_8), sodium hydroxide, sodium bicarbonate, zinc dust, hydrochloric acid solution (12 M), sulfuric acid solution (1 M), glacial acetic acid, thiolacetic acid, magnesium sulfate, potassium bromide, acetone, ethanol, $CHCl_3$, $CDCl_3$, CH_3CN, CD_3CN, hexane, and *n*-propyl thiol were obtained commercially and used as received. Proton and carbon NMR data were acquired on a Bruker 400-MHz NMR spectrometer. Mass spectrometry data were collected on one of two GC/MS instruments, a Hewlett-Packard GC/MS instrument consisting of a 6890 series GC and a 5973N series mass selective detector, or a Hewlett-Packard GC/MS instrument consisting of a 5890 series GC and a 5988A series mass selective detector. IR data were collected on a Nicolet Magna FI-IR 760 spectrometer. UV data were collected on a Hitachi V-2001 spectrometer.

1.4.2 Dithiolanone-oxide Synthesis Dithiolanone-oxide compounds were synthesized with modifications of the Beaucage method.[17] The synthesis involved adding a 3- or 5-substituted anthranilic acid (6.6 mmol) to a 4 mL aqueous solution of 2 mL of concentrated HCl and $NaNO_2$ (6.6 mmol) at 5 °C to generate the diazo compound. A separate solution was prepared by mixing Na_2S (7.3 mmol) with elemental sulfur (7.3 mmol) at 24 °C, which was heated and made alkaline by the addition of 10 M NaOH. The mixture of the two solutions resulted in a precipitate upon addition of HCl. The sulfurization gave the dithiosalicylic acid derivative, which after purification was mixed with Zn dust in glacial acetic acid and refluxed yielding thiosalicylic acid. Thiolacetic acid (0.110 mol) was added to thiosalicyclic acid (0.005 mol) in concentrated H_2SO_4 at 24 °C. Oxidations of the benzo-substituted dithiolanone-oxides were carried out with dimethyldioxirane.

1. 4. 2 Characterization of Dithiolanone-oxides 1 and 3-8 (Figure 1-13)

1-Oxo-1H-1λ^4-benzo[1,2]dithiol-3-one (1) (Figure 1 and 2). The overall yield 25%, ^{1}H NMR (CD_3CN): δ 7.95 (t, J = 7.35 Hz, 1H), 7.82 (t, J = 7.47 Hz, 1H), 8.07 (d, J = 7.77 Hz, 1H), 8.02 (d, J = 7.60 Hz, 1H). ^{13}C NMR 152.1, 135.7, 133.2, 131.3, 128.1, 127.0. MS *m/z* (% rel. intensity) 68 (26), 76 (37), 108 (28), 136 (100), 184 (M^+, 3). FT-IR (KBr) 1703 (C=O), 1071 (S=O). UV (CH_2Cl_2) λ_{max} 281 nm.

7-Chloro-1-oxo-1H-1λ^4-benzo[1,2]dithiol-3-one (3) (Figure 3 and 4). The overall yield 20%, ^{1}H NMR (CD_3CN): δ 7.98 (dd, J_1 = 1.18, J_2 = 7.98, 1H), 7.93 (dd, J_1 = 1.19, J_2 = 7.67, 1H), 7.86 (t, J = 7.75, 1H). ^{13}C NMR (CD_3CN): 190.6, 148.1, 136.6, 135.2, 134.0, 133.1, 125.5. MS *m/z* (% rel. intensity) 53 (4), 69 (25), 75 (35), 95 (17), 110 (21),

130 (5), 142 (22), 154 (4), 170 (100), 186 (5), 202 (3), 218 (M^+, 17). FT-IR (KBr) 1690 (C=O), 1100 (S=O).

7-Methyl-1-oxo-1H-1λ^4-benzo[1,2]dithiol-3-one (4) (Figure 5). The overall yield 30%, ^{1}H NMR (CD_3CN): δ 7.68 (d, J = 5.10 Hz, 2H), 7.84 (t, J = 4.2 Hz, 1H), 2.78 (s, 3H, CH_3). ^{13}C NMR (CD_3CN): 191.4, 149.6, 139.1, 137.9, 133.4, 130.8, 124.5, 16.9. MS *m/z* (% rel. intensity): 51 (23), 63 (43), 78 (20), 90 (44), 109 (8), 121 (64), 123 (2), 150 (100), 166 (8), 182 (2), 198 (M^+, 25). FT-IR (KBr) 1690 (C=O), 1100 (S=O). UV (CH_2Cl_2) λ_{max} 290 nm.

7-Methoxy-1-oxo-1H-1λ^4-benzo[1,2]dithiol-3-one (5) (Figure 6 and 7). The overall yield 25%, ^{1}H NMR (CD_3CN): δ 7.55 (dd, J_1 = 0.87, J_2 = 7.61 Hz, 1H), 7.34 (dd, J_1 = 0.58 J_2 = 8.17 Hz, 1H), 7.74 (t, J = 7.76, 1H), 4.07 (s, 3H, OCH_3). ^{13}C NMR (CD_3CN): 191.5, 158.1, 137.8, 136.0, 132.8, 118.9, 118.0, 56.6. MS *m/z* (% rel. intensity) 51 (18), 69 (42), 76 (45), 95 (17), 108 (21), 123 (10), 138 (23), 150 (12), 166 (100), 182 (8), 198 (2), 214 (M^+, 28). FT-IR (KBr) at 1710 (C=O), 1690, 1080 (S=O). UV(CH_2Cl_2) λ_{max} 323 nm.

5-Chloro-1-oxo-1H-1λ^4-benzo[1,2]dithiol-3-one (6) (Figure 8 and 9). The overall yield 22%, ^{1}H NMR (CD_3CN): δ 7.82 (dd, J_1 = 1.98, J_2 = 8.26 Hz, 1H), 7.90 (t, J = 8.27 Hz, 2H). ^{13}C NMR (CD_3CN): 190.0, 150.5, 139.5, 135.6, 132.9, 129.1, 126.1. MS *m/z* (% rel. intensity): 37 (6), 50 (12), 63 (20), 75 (39), 84 (5), 95 (31), 110 (25), 130 (9), 142 (38), 170 (100), 172 (40), 186 (4), 202 (18), 218 (M^+, 31). FT-IR (KBr) 1720, 1690 (C=O), 1080 (S=O), 780, 820 (C-Cl). UV (CH_2Cl_2) λ_{max} 280 nm.

5-Methyl-1-oxo-1H-1λ^4-benzo[1,2]dithiol-3-one (7) (Figure 10 and 11). The overall yield 27%, ^{1}H NMR (CD_3CN): δ 7.92 (d, J = 7.97 Hz, 1H), 7.79 (s, 1H), 7.73 (d, J = 8.0

Hz, 1H), 2.56 (s, 3H, CH_3). ^{13}C NMR (CD_3CN): 191.2, 149.6, 144.8, 136.6, 131.0, 127.7 126.5, 20.0. MS *m/z* (% rel. intensity): 39 (54), 45 (25), 51 (49), 63 (78), 69 (51), 77 (54), 78 (54), 89 (71), 110 (23), 121 (92), 150 (100), 153 (41), 166 (12), 182 (55), 198 (M^+, 17). FT-IR (KBr) 1700 (C=O), 1087 (S=O). UV (CH_2Cl_2) λ_{max} 280 nm.

5-Methoxy-1-oxo-1H-1λ^4-benzo[1,2]dithiol-3-one (8) (Figure 12 and 13). The overall yield 23%, ^1H NMR (CD_3CN): δ 8.01 (d, J = 8.63 Hz, 1H), 7.51 (dd, J_1 = 2.57, J_2 = 8.65 Hz, 1H), 7.42 (d, J = 2.5 Hz, 1H), 3.95 (s, 3H, OCH_3). ^{13}C NMR (CD_3CN): 190.8, 163.6, 143.7, 133.5, 129.0, 122.1, 109.9, 56.0. MS *m/z* (% rel. intensity): 44 (16), 64 (57), 69 (20), 95 (20), 106 (9), 123 (45), 138 (21), 155 (14), 166 (100), 183 (27), 207 (6), 214 (M^+, 14).

1.4.3 Reaction of Thiol with Substituted Dithiolanone-oxides. Reactions of **1** and **3**-**8** (10 mM) were carried out in the presence of *n*-PrSH (20-40 mM) in 70% CD_3CN:30% D_2O. The volume of the reaction mixture was 5 or 10 mL and the internal standard was 1,3,5-trimethoxybenzene (4 mM). The overall percent yield of the products was determined after 15 minutes at 25 °C. The reaction of **3** or **5** with *n*-propyl thiol in CD_3CN:D_2O (1:10) was too rapid to discern a possible substituent effect by NMR spectroscopy. ^1H NMR data on the dithiolanone-oxide (**1**, **3**-**8**)—*n*-PrSH reaction provided evidence for the formation of unsymmetrical and symmetrical sulfane products similar to that observed previously by Gates et al. for the **1**—*n*-PrSH reaction.[1] The assignment of unsymmetrical products [3- or 5-substituted-2-propyl disulfanyl benzoic acid (**C**) and 3- or 5-substituted-2-propyl trisulfanyl benzoic acid (**D**)] are based on 2 sets of triplets; a downfield set at about δ=2.8 ppm (2H, SCH_2) and a downfield set at about δ=2.9 ppm (2H, SCH_2), respectively (Figure 14-17). The chemical shifts for the δ-

methylene and methyl protons are often obscured by reagent peaks. Downfield chemical shifts of polysulfane neighboring protons with higher numbers of sulfur atoms have been reported previously.[30-32] For reaction of **1** with *n*-PrSH, we utilized GC/MS data of the polysulfane mixture to corroborate the NMR method of analysis. The percent yields of **C** and **D** were determined by analysis of products in the respective reaction mixtures.

Unsymmetrical polysulfane products 3-Chloro-2-propyl disulfanyl-benzoic acid (**3A**): ^{1}H NMR (CD_3CN): δ 2.73 (t, J = 7.0 Hz, 2H, SCH_2). 3-Methyl-2-propyl disulfanyl-benzoic acid (**4A**): ^{1}H NMR (CD_3CN): δ 2.77 (t, J = 7.0 Hz, 2H, SCH_2). 3-Methoxy-2-propyl disulfanyl-benzoic acid (**5A**): ^{1}H NMR (CD_3CN): δ 2.74 (t, J = 7.0 Hz, 2H, SCH_2). 5-Methyl-2-propyl disulfanyl-benzoic acid (**6A**): ^{1}H NMR (CD_3CN): δ 2.84 (t, J = 7.2 Hz, 2H, SCH_2). 2-Propyl disulfanyl-benzoic acid (**1A**): ^{1}H NMR (CD_3CN): δ 2.85 (t, J = 7.2 Hz, 2H, SCH_2). MS *m/z* (% rel. intensity): 55 (44), 69 (46), 97 (27), 108 (20), 136 (26), 153 (23), 168 (100), 228 (M^+, 34). 3-Chloro-2-propyl trisulfanyl-benzoic acid (**3B**)**:** ^{1}H NMR (CD_3CN): δ 2.964 (t, J = 7.2 Hz, 2H, SCH_2). 3-Methyl-2-propyl trisulfanyl-benzoic acid (**4B**): ^{1}H NMR (CD_3CN): δ 2.960 (t, J = 7.2 Hz, 2H, SCH_2). 3-Methoxy-2-propyl trisulfanyl-benzoic acid (**5B**): ^{1}H NMR (CD_3CN): δ 2.96 (t, J = 7.0 Hz, 2H, SCH_2). 5-Chloro-2-propyl trisulfanyl-benzoic acid (**6B**): ^{1}H NMR (CD_3CN): δ 2.96 (t, J = 7.2 Hz, 2H, SCH_2). 5-Methyl-2-propyl trisulfanyl-benzoic acid (**7B**): ^{1}H NMR (CD_3CN): δ 2.96 (t, J = 7.2 Hz, 2H, SCH_2). 5-Methoxy-2-propyl trisulfanyl-benzoic acid (**8B**): ^{1}H NMR (CD_3CN): δ 2.96 (t, J = 7.0 Hz, 2H, SCH_2). 2-Propyl trisulfanyl-benzoic acid (**1B**): ^{1}H NMR (CD_3CN): δ 2.96 (t, J = 7.2 Hz, 2H, SCH_2). MS *m/z* (% rel. intensity): 64 (47), 76 (28), 93 (26), 105 (20), 121 (35), 160 (22), 185 (100), 213 (21), 224 (10), 258 (M^+, 6).

Symmetrical polysulfane products were detected using the SCH_2 protons as signals.[7] Di-*n*-propyl disulfide (**C**): ^{1}H NMR (CD_3CN): δ 2.72 (t, *J* = 7.2 Hz, 4H, SCH_2). MS *m/z* (% rel intensity): 55 (65), 66 (51), 71 (47), 81 (27), 85 (36), 99 (42), 108 (100), 125 (11), 135 (5), 150 (M^+, 97). Di-*n*-propyl trisulfide (**D**): ^{1}H NMR (CD_3CN): δ 2.89 (t, *J* = 7.2 Hz, 4H, SCH_2). MS *m/z* (% rel. intensity): 64 (5), 75 (100), 98 (10), 111 (3), 139 (6), 156 (2), 182 (M^+, 36). Di-*n*-propyl tetrasulfide (**E**): ^{1}H NMR (CD_3CN): δ 3.00 (t, *J* = 7.0 Hz, 4H, SCH_2). MS *m/z* (% rel. intensity): 55 (8), 64 (23), 73 (100), 97 (11), 108 (86), 130 (4), 139 (3), 150 (3), 172 (4), 214 (M^+, 66).

Scheme 1

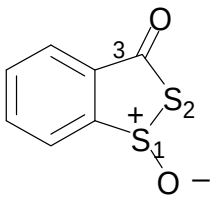

1

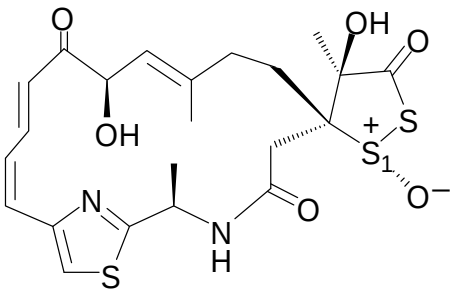

2

Scheme 2

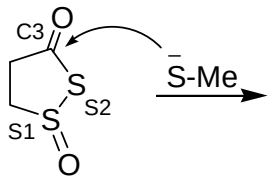

reaction pathway high in energy 26.9 kcal/mol

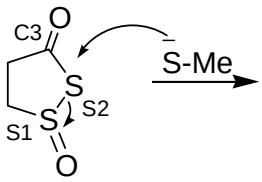

energetically prefered pathway 6 kcal/mol

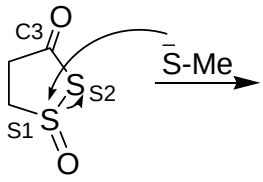

reaction pathway high in energy >40 kcal/mol

Scheme 3

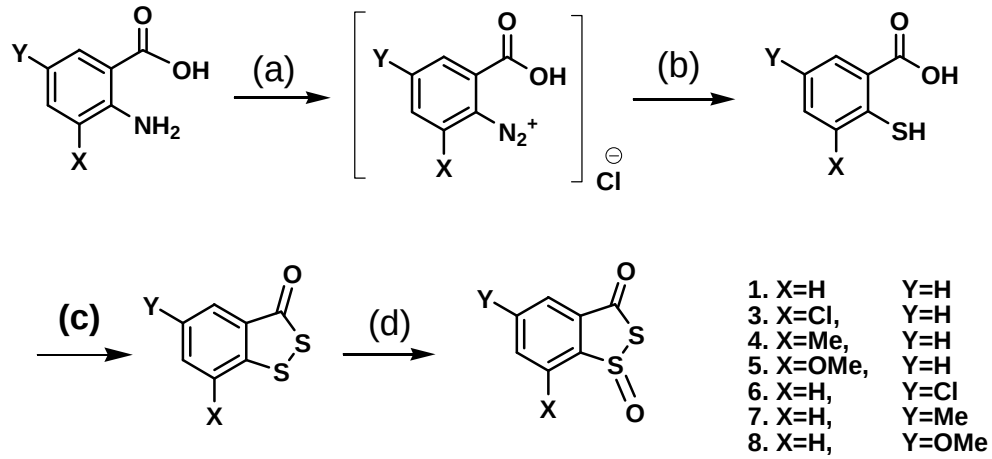

Reagents and conditions: (a) HCl, $NaNO_2$, 5 °C; (b) (i) Na_2S, elemental S_x, NaOH, 5 °C; (ii) Zn, glacial CH_3CO_2H, reflux, 48 h; (c) H_2SO_4, CH_3COSH, 24 °C, 15 min; (d) dimethyldioxirane, 0 °C, 2 h, 20-30%.

Scheme 4

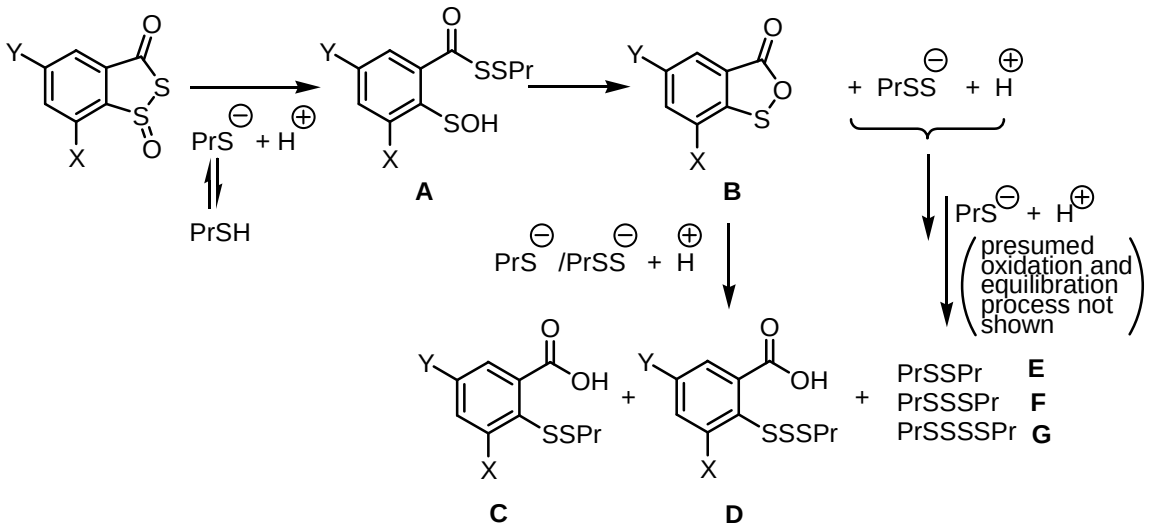
Y
X
O
S
S
O
PrS⊖ + H⊕
PrSH
SSPr
SOH
A
B
+ PrSS⊖ + H⊕
PrS⊖ + H⊕
presumed oxidation and equilibration process not shown
PrS⊖ /PrSS⊖ + H⊕
OH
C
D
PrSSPr E
PrSSSPr F
PrSSSSPr G

Table 1. Efficiency of Polysulfane Product Generation (%) Measured for Propyl Thiol Reactions with Substituted Dithiolanone-oxides **1** and **3**-**8** by NMR Spectroscopy

		Relative Yields[a,b]			
		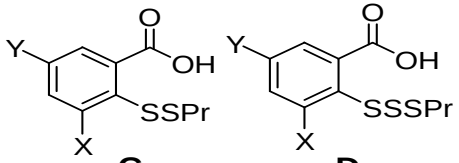 **C** **D**	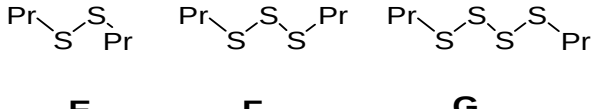 **E** **F** **G**		
compound	substituent[c]	Ar polysulfane products	Pr polysulfane products	overall product yield	% conversion
1	H	18	16	34	63
3	*o*-Cl	63	20	83	100
4	*o*-Me	9	2	11	60
5	*o*-MeO	51	26	77	79
6	*p*-Cl	53	26	79	86
7	*p*-Me	5	2	7	
8	*p*-MeO	15	12	27	

[a] Reaction of *ortho* [X = Cl (**3**), CH_3 (**4**), OCH_3 (**5**)] and *para* [Y = Cl (**6**), CH_3 (**7**), OCH_3 (**8**)] substituted 1,2-dithiolan-3-one 1-oxides (10 mM) were carried out in the presence of *n*-PrSH (20-40 mM) in 70% CD_3CN:30% D_2O. [b] Relative yields were determined by ^1H NMR after 15 min at 25 °C and are the average of 2 runs [see Experimental Section (Section 1.4.3)]. [c] *Ortho* or *para* substituent positions are relative to the sulfinate sulfur (S1) of compounds **3**-**8**.

Table 2. Relationship between the $CD_3CN:D_2O$ Ratio for the Reaction of Substituted Benzodithiolanone-oxides **1** and **3**-**8** with *n*-Propyl Thiol[a]

entry	$CD_3CN:D_2O$	comment
1	1:0	no reaction (after 3 days)
2	8:2	12 h to reach approx. 50% conversion
3	7:3	2 h to reach approx. 50% conversion
4	1:10	minutes to reach 100% conversion

[a] 10 mM **1** and **3**-**8**; 30 mM *n*-PrSH.

Table 3. Calculated Substituted Benzo-1,2-dithiolan-3-one 1-oxides (**1** and **3**-**8**) Stuctural Parameters[a,b]

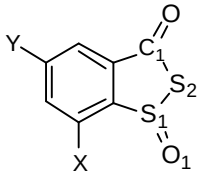

	Substituent							NBO Charges		
	X	Y	S1-S2	S1-O1	C1-S2	S2-S1-O1	θ[c]	S1	S2	O
1	H	H	2.215	1.497	1.822	113.1	113.1	1.150	0.007	-0.862
3	Cl	H	2.213	1.493	1.815	110.9	104.7	1.155	0.020	-0.853
4	Me	H	2.202	1.499	1.821	111.9	110.1	1.138	0.016	-0.874
5	OMe	H	2.218	1.495	1.817	111.1	105.9	1.159	0.005	-0.862
6	H	Cl	2.217	1.496	1.819	113.1	113.2	1.154	0.017	-0.859
7	H	Me	2.217	1.497	1.822	113.1	112.9	1.150	0.004	-0.863
8	H	OMe	2.222	1.497	1.818	113.1	112.9	1.153	0.007	-0.863

[a] Structures optimized at the B3LYP/6-31G(d) level. [b] Distances in Å, angles in deg. [c] The dihedral angle θ=O1-S1-S2-C1 is positive for a clockwise movement from O1 to C1 as one looks down the bond from S1 to S2.

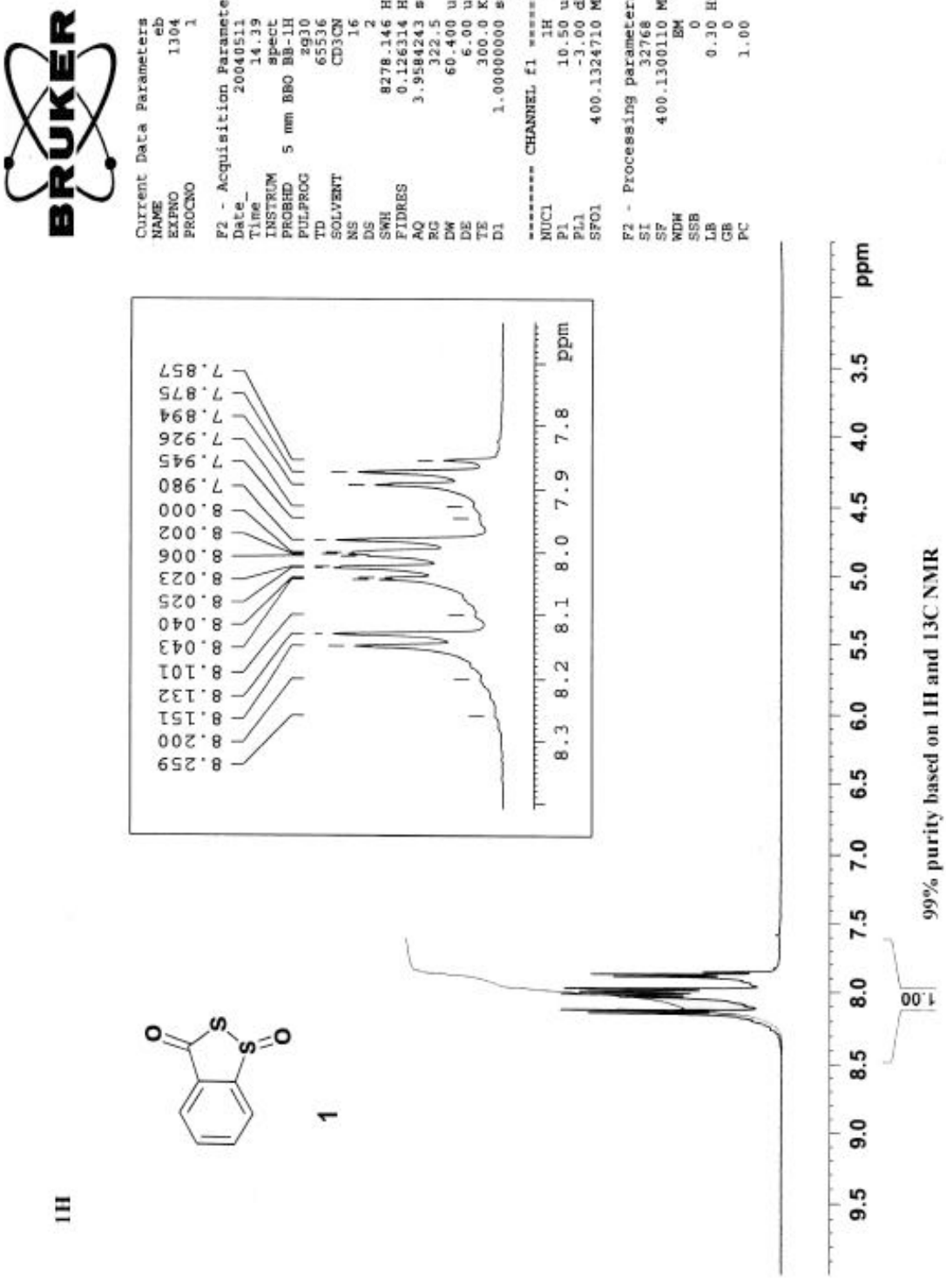

Figure 1. ^{1}H NMR sprctrum of oxo-1H-1λ^{4}-benzo[1,2]dithiol-3-one (**1**)

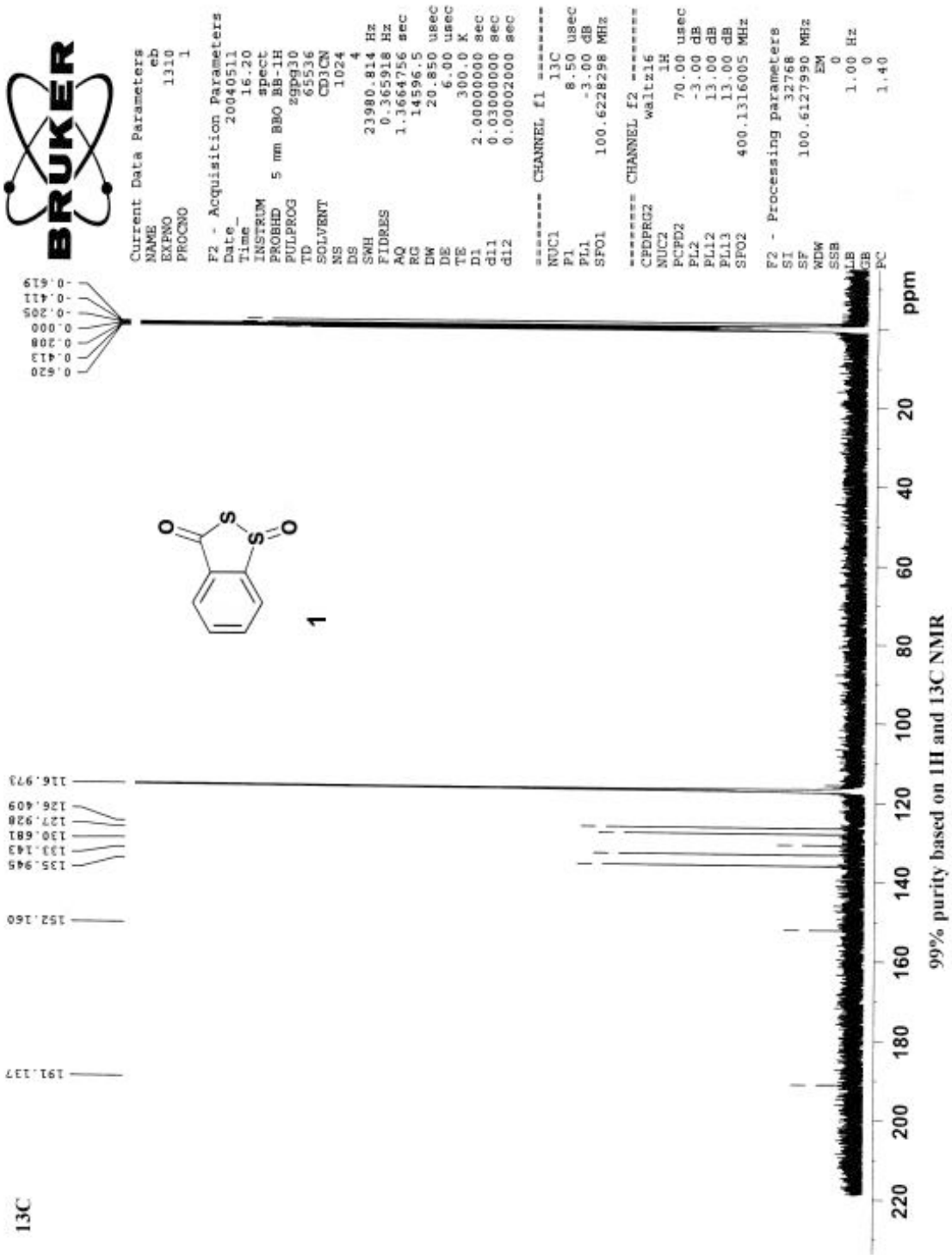

Figure 2. ^{13}C NMR sprctrum of oxo-1H-1λ^4-benzo[1,2]dithiol-3-one (**1**)

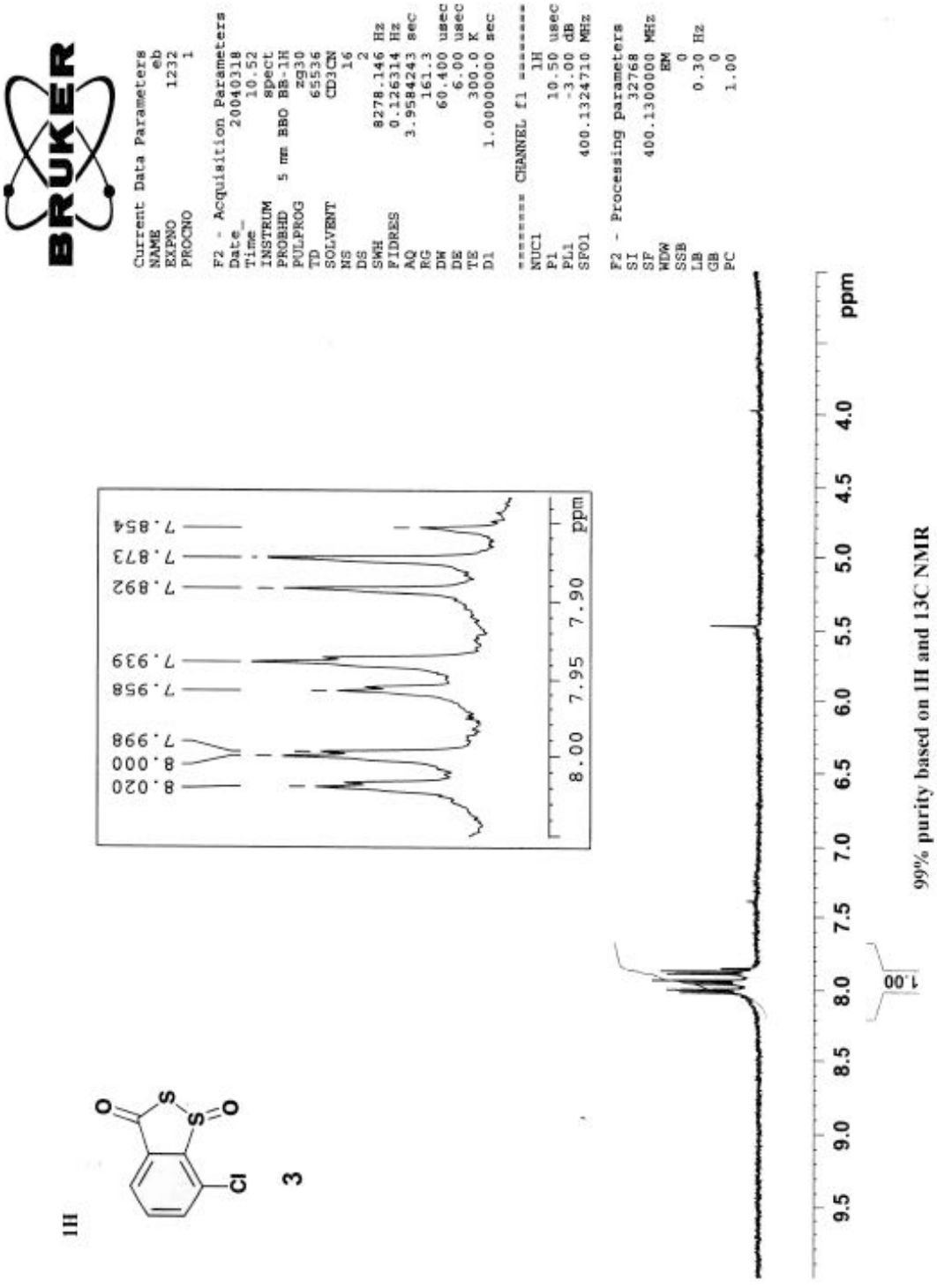

Figure 3. ^{1}H NMR spectrum of 7-Chloro-1-oxo-1H-1λ^{4}-benzo[1,2]dithiol-3-one (**3**)

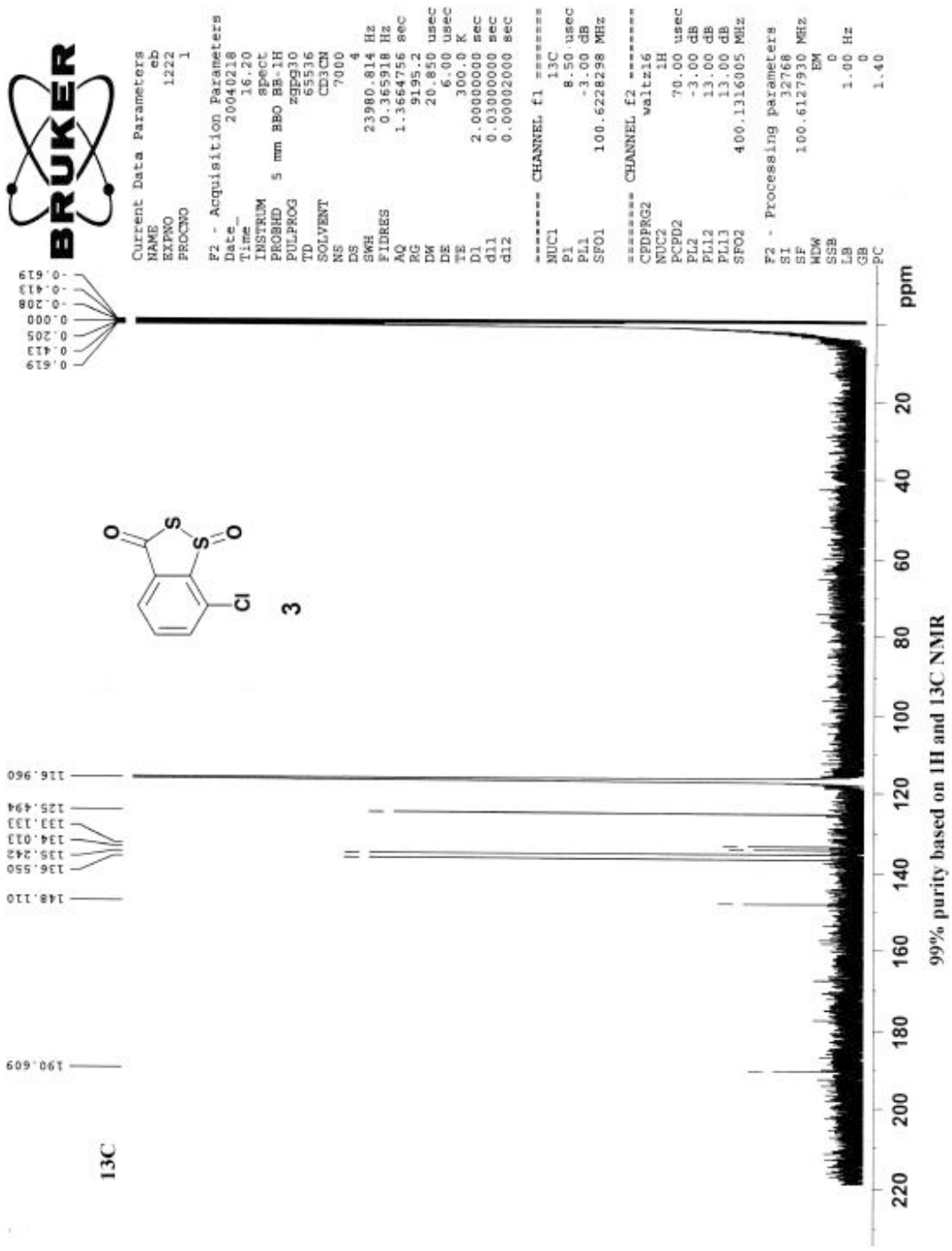

Figure 4. ^{13}C NMR spectrum of 7-Chloro-1-oxo-1H-1λ^4-benzo[1,2]dithiol-3-one (**3**)

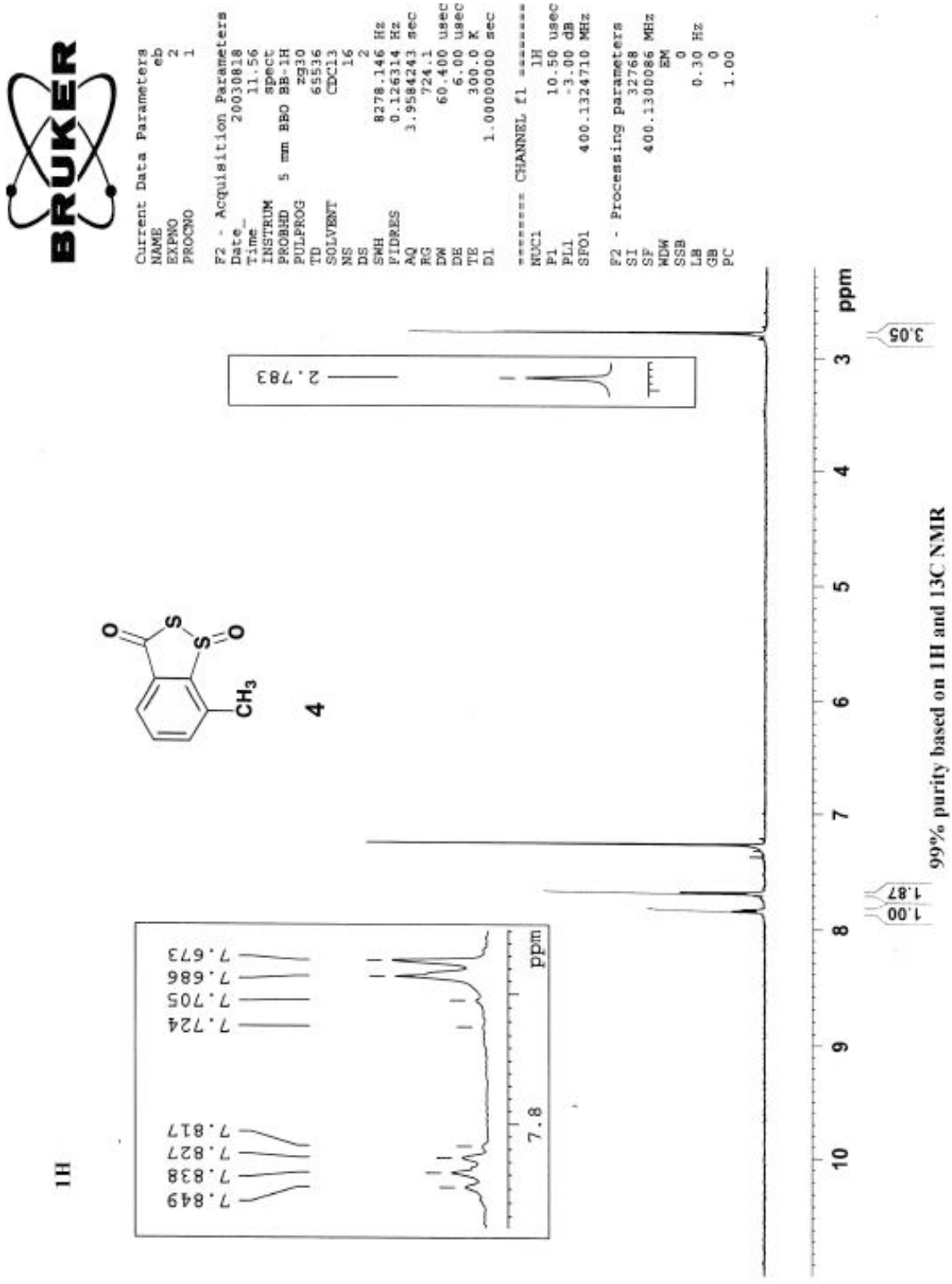

Figure 5. ^{1}H NMR spectrum of 7-Methyl-1-oxo-1H-1λ^{4}-benzo[1,2] dithiol-3-one (**4**)

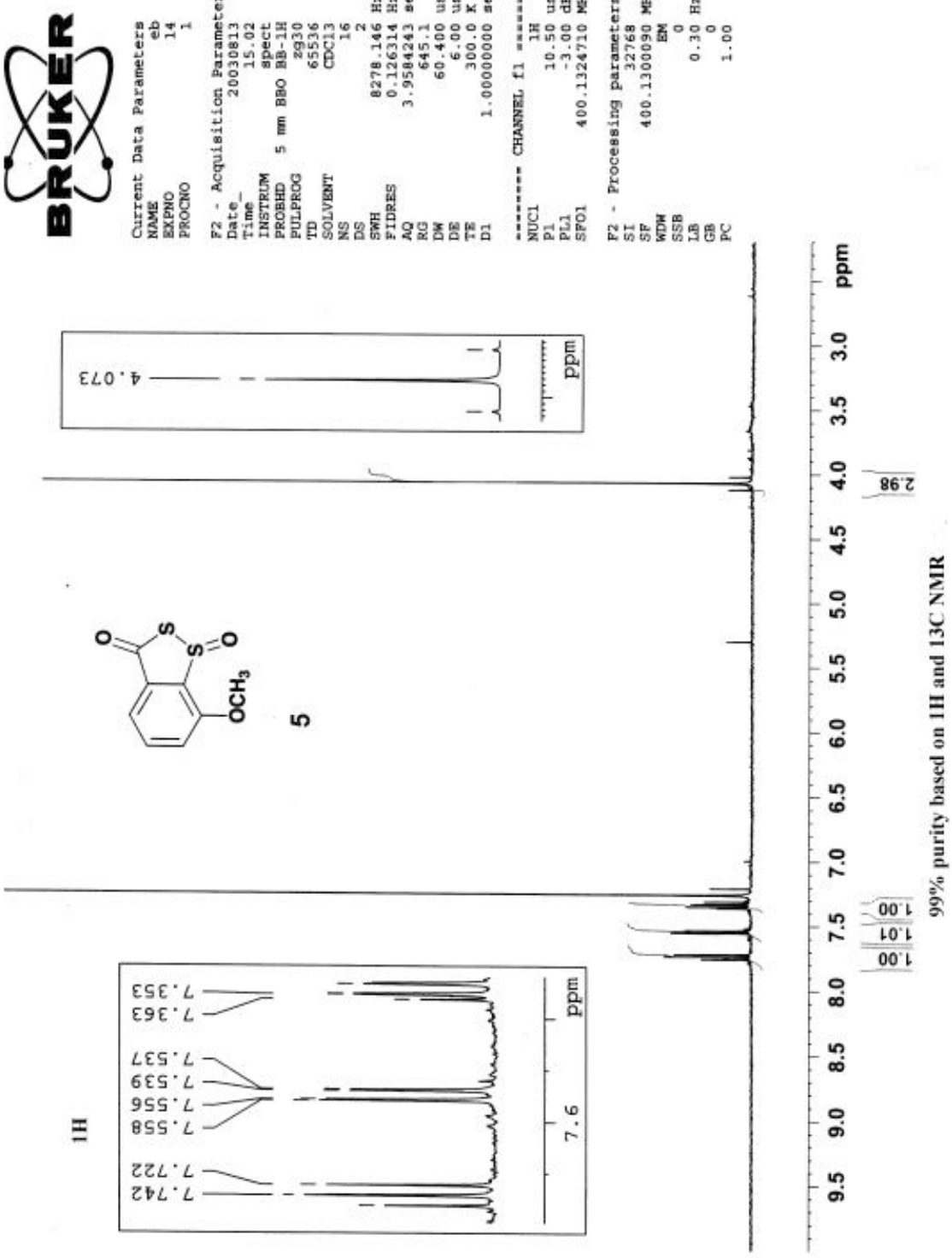

Figure 6. ^{1}H NMR spectrum of 7-Methoxy-1-oxo-1H-1λ^{4}-benzo[1,2]dithiol-3-one (**5**)

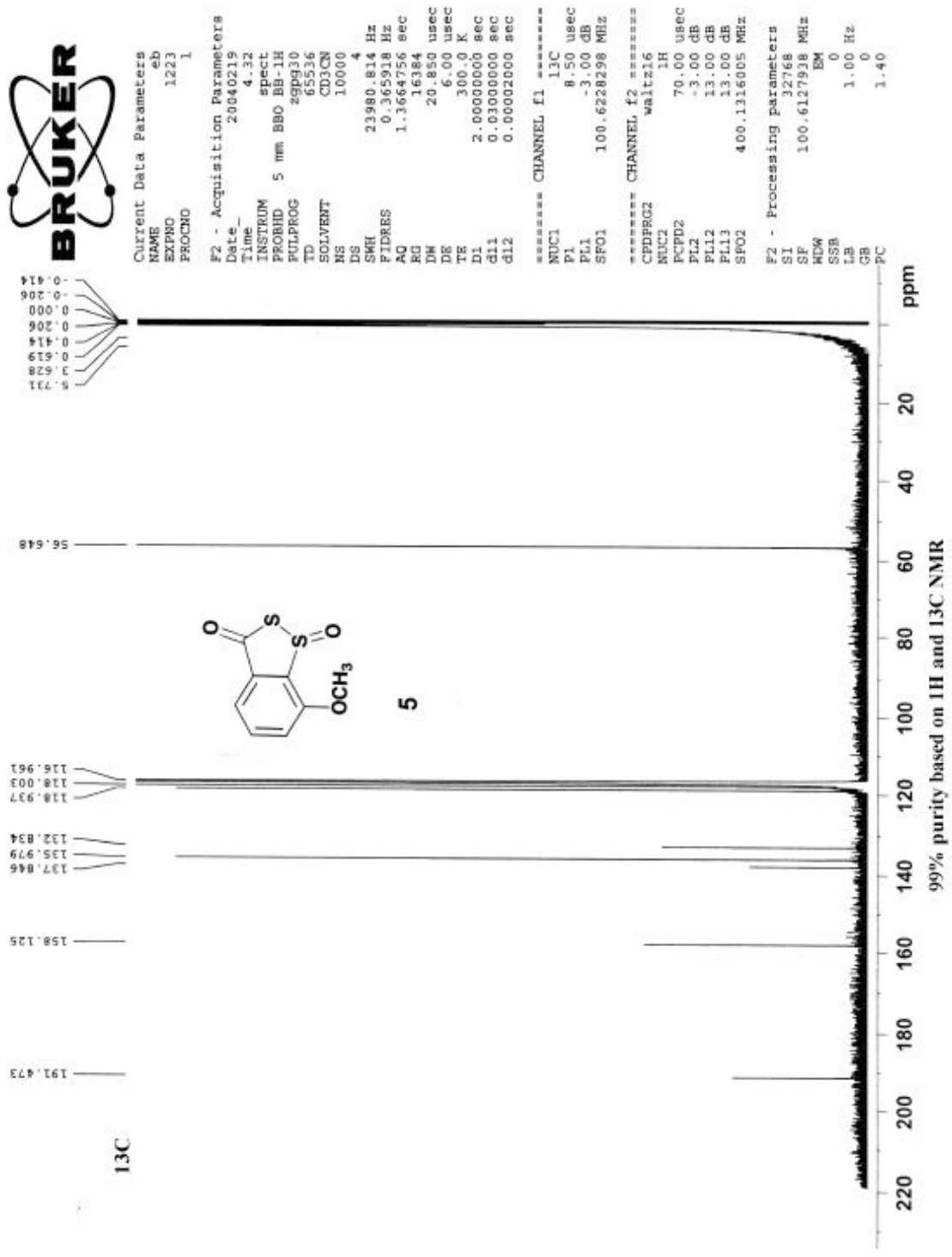

Figure 7. ^{13}C NMR spectrum of 7-Methoxy-1-oxo-1H-1λ^4-benzo[1,2]dithiol-3-one (**5**)

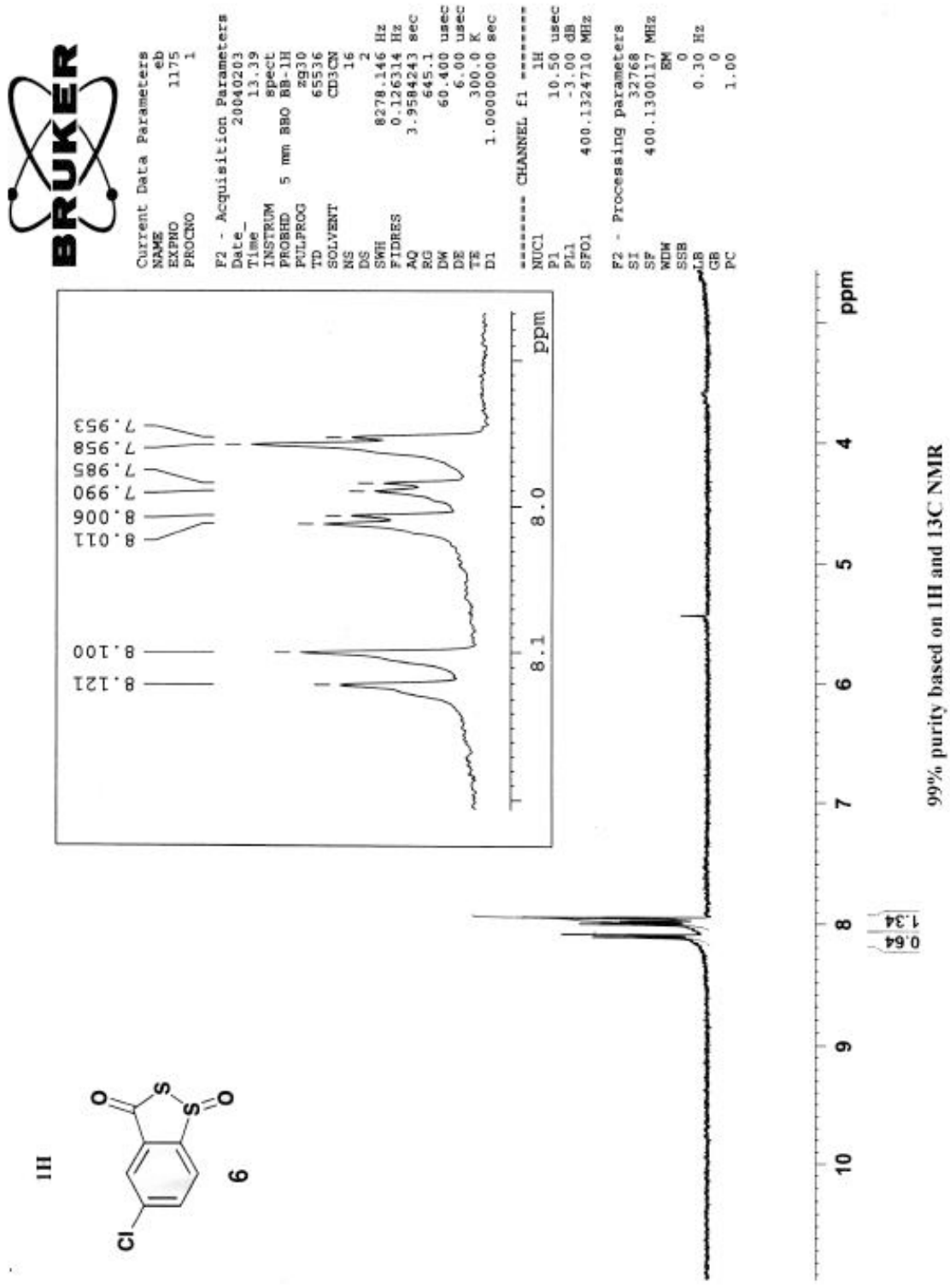

Figure 8. ^{1}H NMR spectrum of 5-Chloro-1-oxo-1H-1λ^{4}-benzo[1,2]dithiol-3-one (**6**)

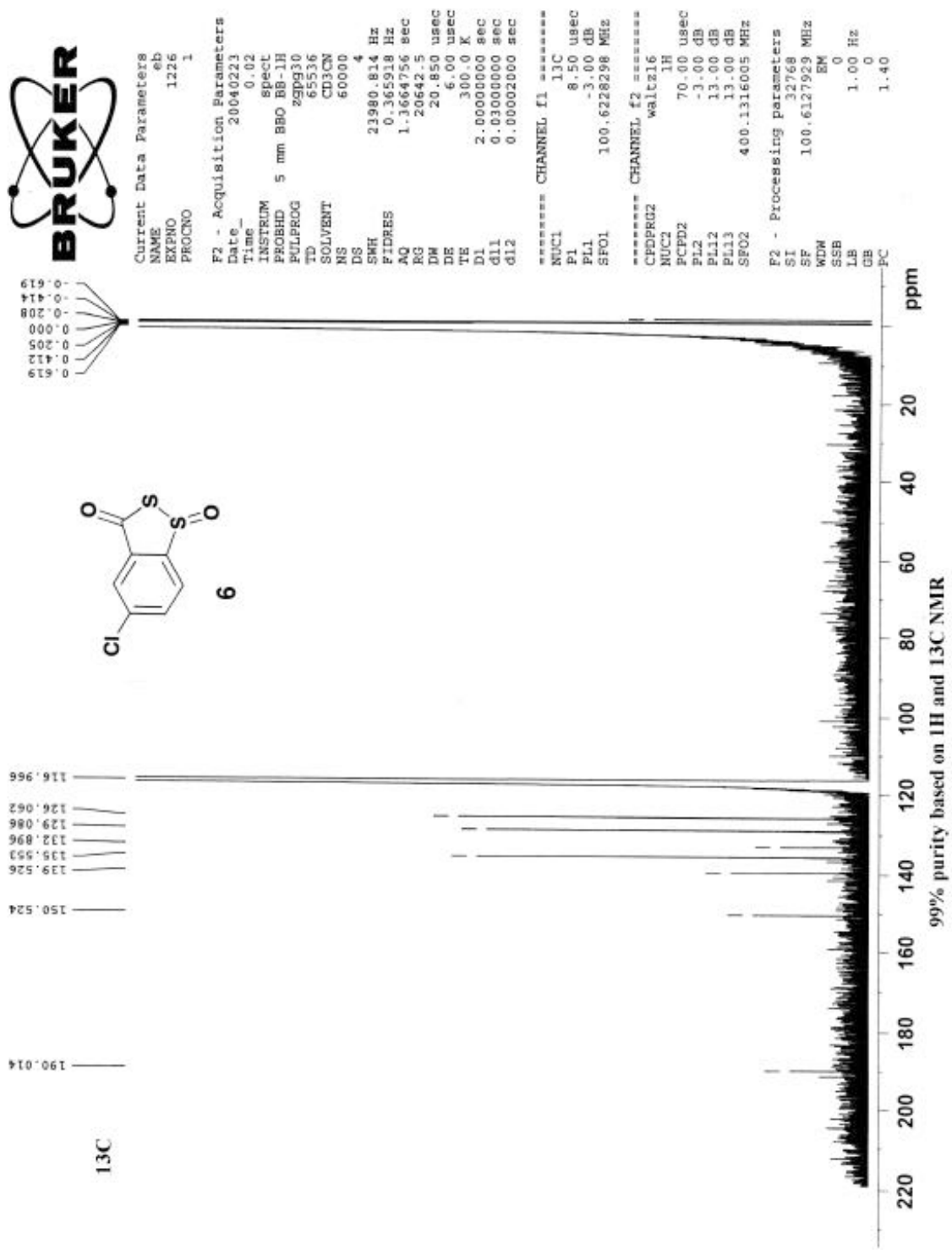

Figure 9. ^{13}C NMR spectrum of 5-Chloro-1-oxo-1H-1λ^4-benzo[1,2]dithiol-3-one (**6**)

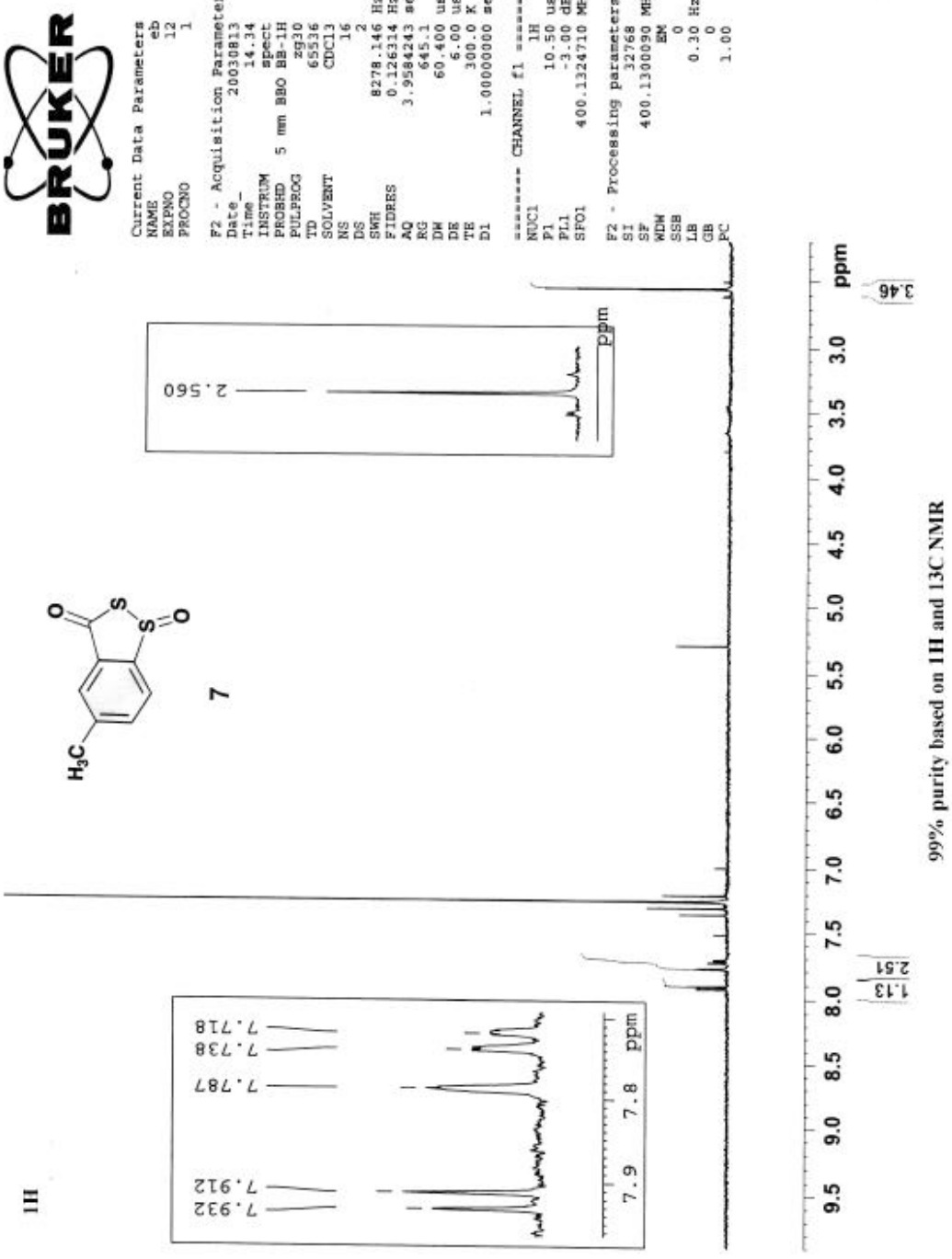

Figure 10. ^{1}H NMR spectrum of 5-Methyl-1-oxo-1H-1λ^{4}-benzo[1,2]dithiol-3-one (**7**)

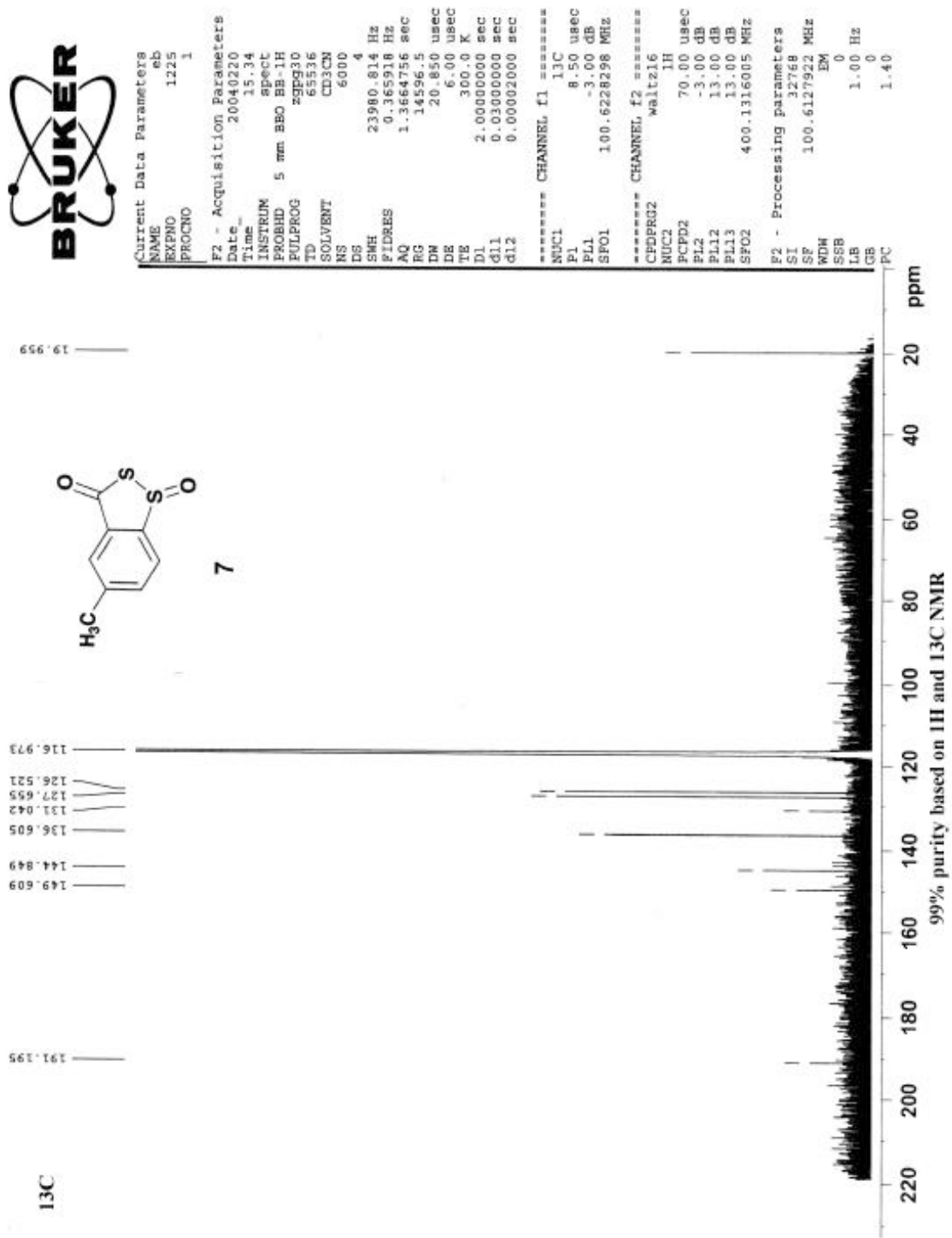

Figure 11. ^{13}C NMR spectrum of 5-Methyl-1-oxo-1H-1λ^4-benzo[1,2]dithiol-3-one (**7**)

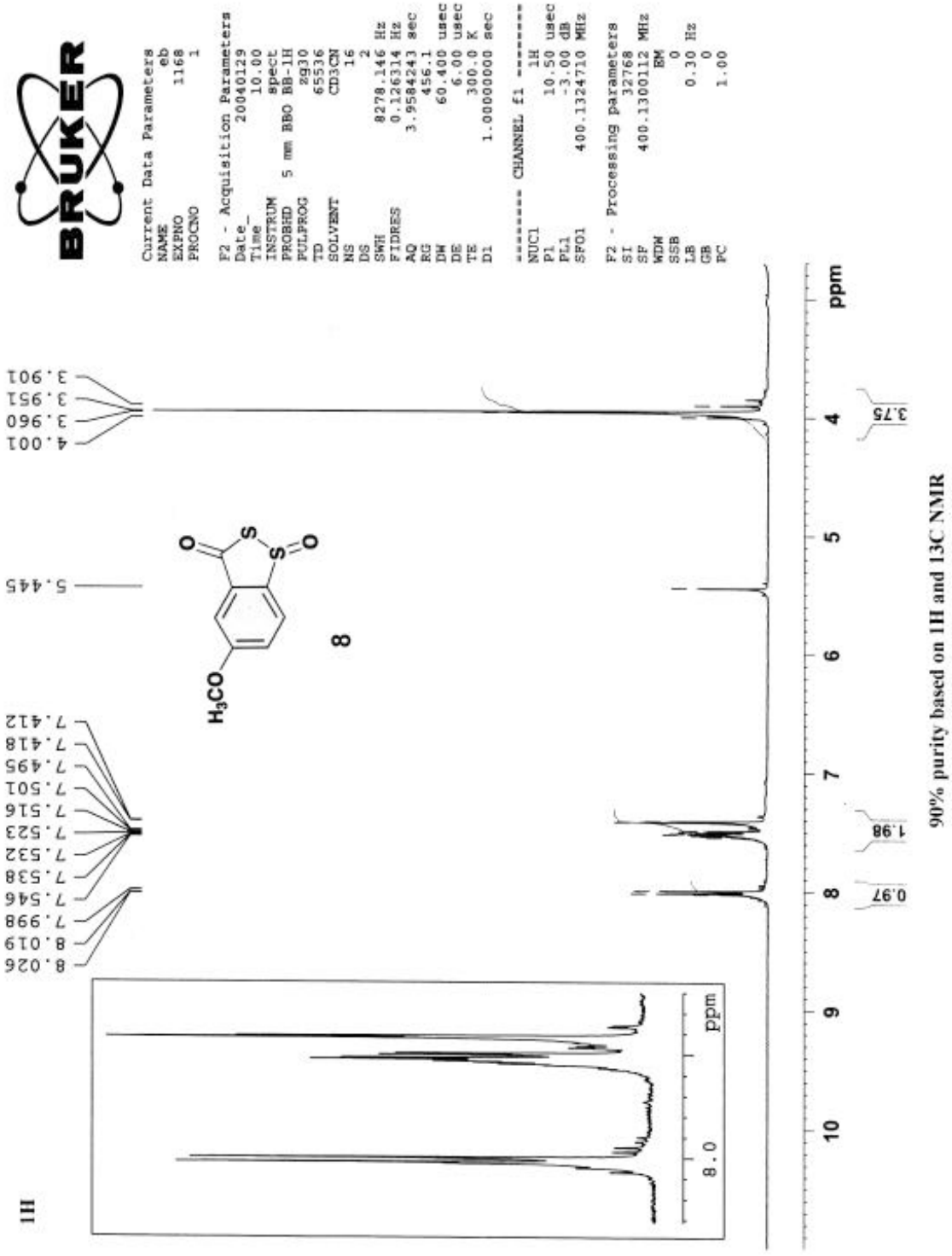

Figure 12. ^{1}H NMR spectrum of 5-Methoxy-1-oxo-1H-1λ^{4}-benzo[1,2]dithiol-3-one (**8**)

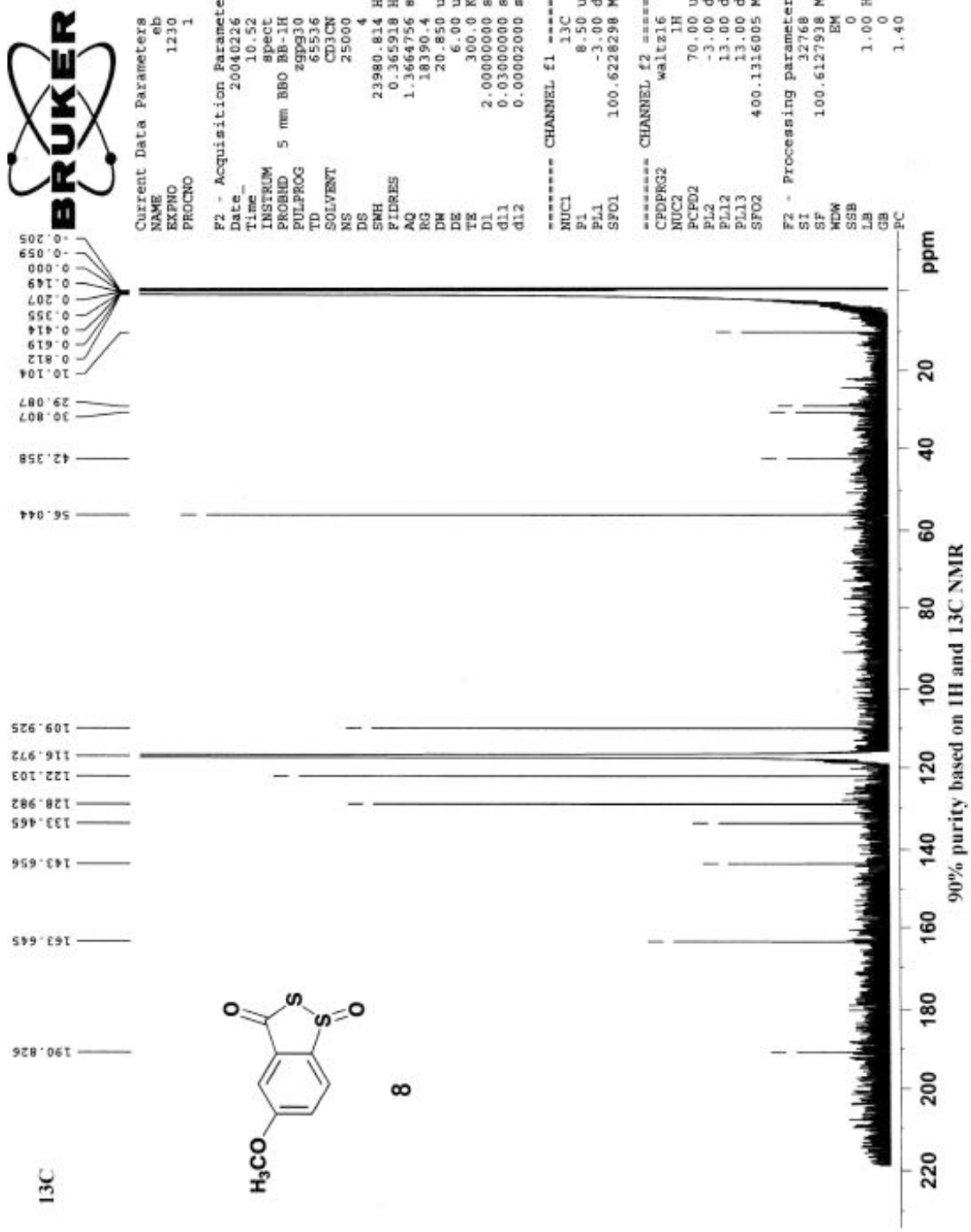

Figure 13. ^{13}C NMR spectrum of 5-Methoxy-1-oxo-1H-1λ^4-benzo[1,2]dithiol-3-one (**8**)

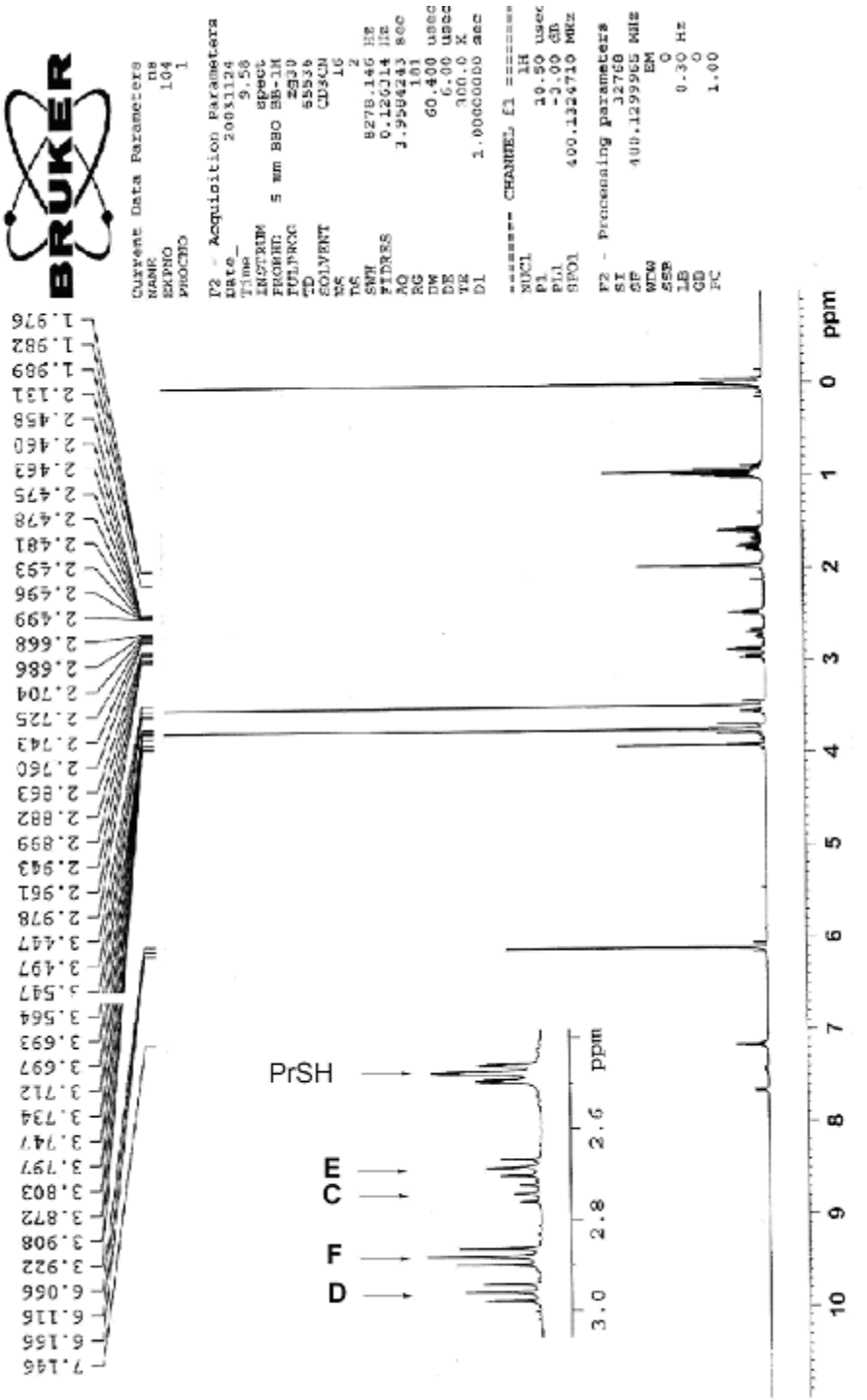

Figure 14. ^{1}H NMR spectrum for reaction of 7-Methoxy-1-oxo-1H-1λ^{4}-benzo[1,2]dithiol-3-one (**5**) with *n*-propylthiol in 70% CD_3N:30% D_2O for 15 min. **C** and **D** are the di- and tri-sulfide unsymmetrical products, while **E** and **F** are the di-, tri-sulfide symmetrical product.

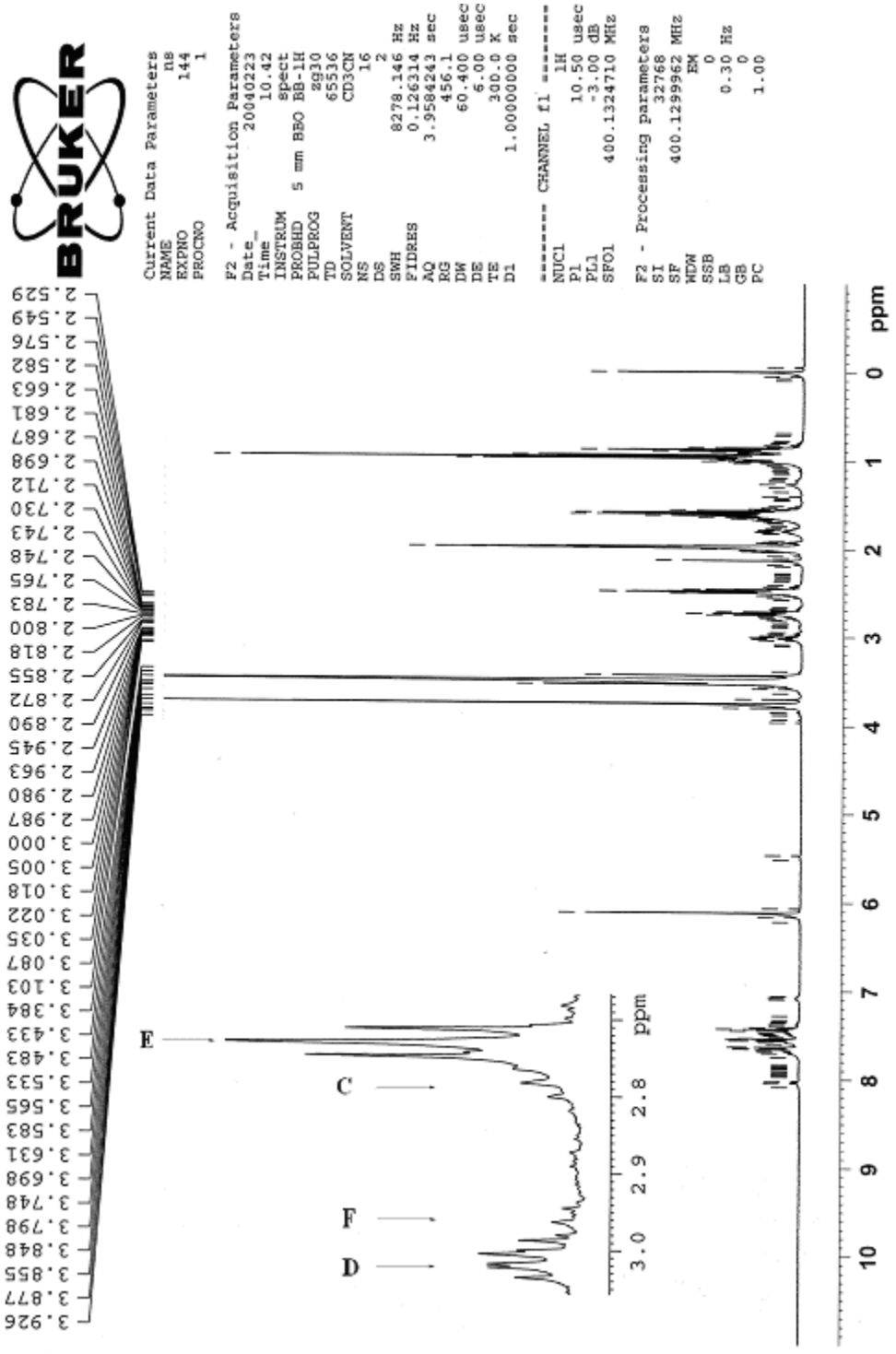

Figure 15. ^{1}H NMR spectrum for reaction of 7-Chloro-1-oxo-1H-1λ^{4}-benzo[1,2]dithiol-3-one (**3**) with *n*-propylthiol in 70% CD_3N:30% D_2O for 15 min. **C** and **D** are the di- and tri-sulfide unsymmetrical products, while **E** and **F** are the di-, tri-sulfide symmetrical product.

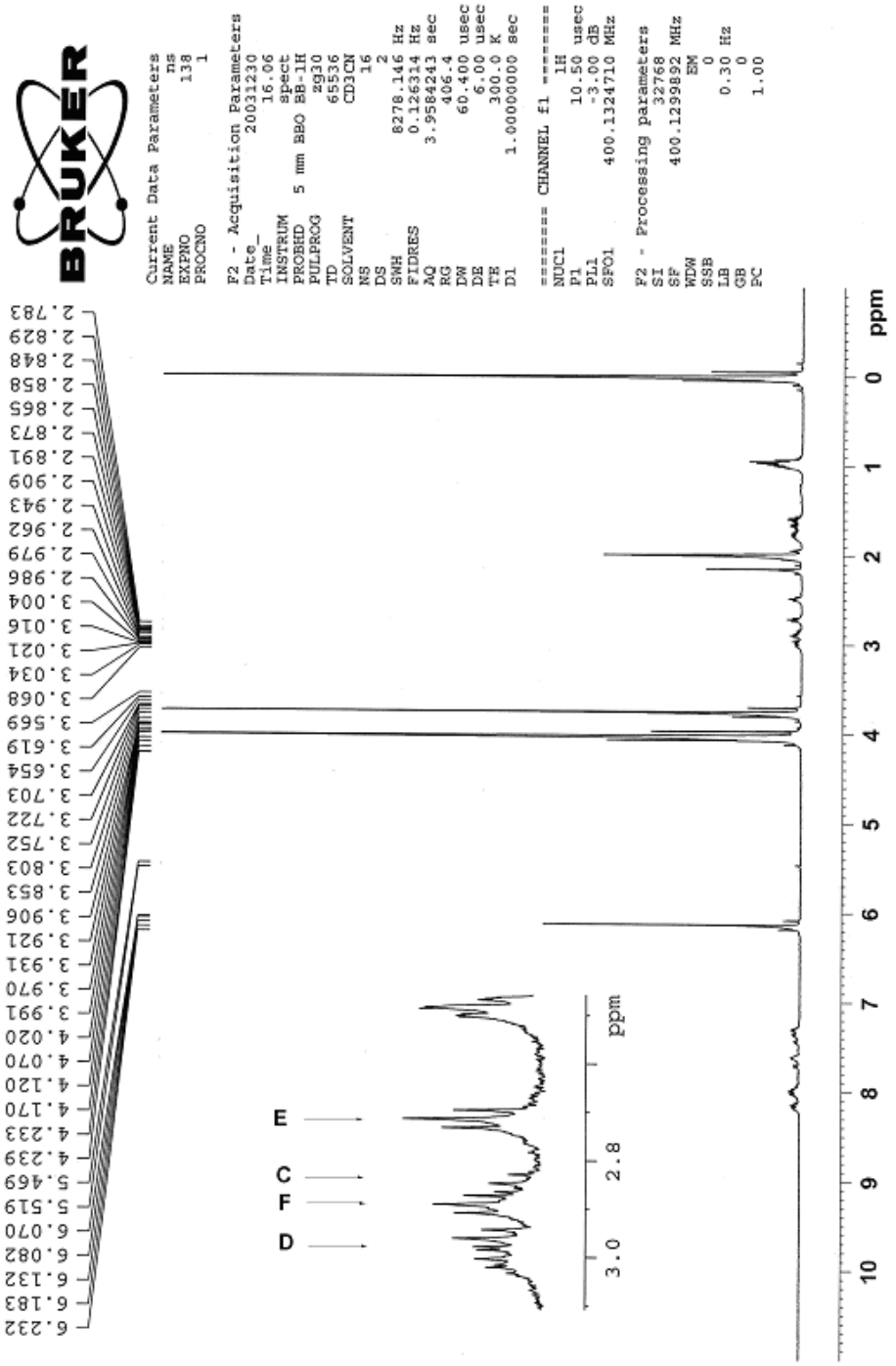

Figure 16. ^{1}H NMR spectrum for reaction of oxo-1H-1λ^{4}-benzo[1,2]dithiol-3-one (**1**) with n-propylthiol in 70% CD_3N:30% D_2O for 15 min. **C** and **D** are the di- and tri-sulfide unsymmetrical products, while **E** and **F** are the di-, tri-sulfide symmetrical product.

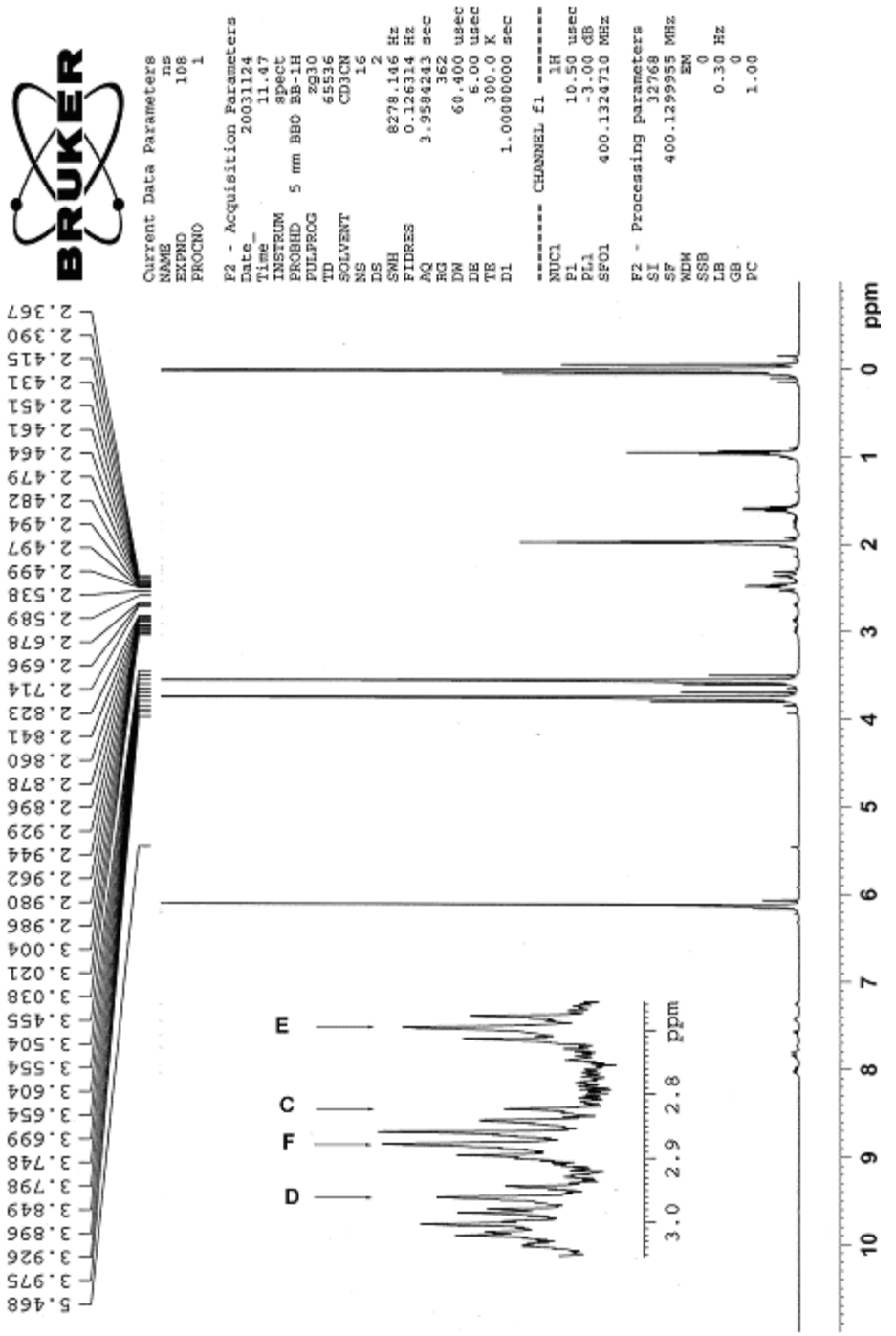

Figure 17. ^{1}H NMR spectrum for reaction of 5-Methoxy-1-oxo-1H-1λ^{4}-benzo[1,2]dithiol-3-one (**8**) with n-propylthiol in 70% CD_3N:30% D_2O for 15 min. **C** and **D** are the di- and tri-sulfide unsymmetrical products, while **E** and **F** are the di-, tri-sulfide symmetrical product.

1.5 References

(1) Behroozi, S. J.; Kim, W., Gates, K. S. *J. Org. Chem.* **1995**, *60*, 3964.

(2) Behroozi, S. J.; Kim, W.; Dannaldson, J.; Gates, K. S. *Biochemistry* **1996**, *5*, 1768.

(3) Hara, M.; Saitoh, Y.; Nakano, H. *Biochemistry* **1990**, *29*, 5676.

(4) Mitra, K.; Kim, W.; Daniels, J. S.; Gates, K. S. *J. Am. Chem. Soc.* **1997**, *119*, 11691.

(5) Gates, K. S. *Chem. Res. Toxicol.* **2000**, *13*, 953.

(6) Kanda, Y.; Ashizawa, T.; Saitoh, Y.; Saito, H.; Gomi, K.; Okabe, M. *Bioorg. Med. Chem. Lett.* **1998**, *8*, 909.

(7) Lee, A. H. F.; Chan, A. S. C.; Li, T. *Tetrahedron* **2003**, *59*, 833.

(8) Kanda, Y.; Ashizawa, T.; Kakita, S.; Takahashi, Y.; Kono, M.; Yoshida, M.; Saitoh, Y., Okabe, M. *J. Med. Chem.* **1999**, *42*, 1330.

(9) Ashizawa, T.; Kawashima, K.; Kanda, Y.; Gomi, K.; Okabe, M.; Ueda, K.; Tamaoki, T. *Anti-Cancer Drugs* **1999**, *10*, 829.

(10) Kanda, Y.; Ashizawa, T.; Kawashima, K.; Ikeda, S. I.; Tamaoki, T. *Bioorg. Med. Chem. Lett.* **2003**, *13*, 455.

(11) Asai, A.; Hara, M.; Kakita, S.; Kanda, Y.; Yoshida, M.; Saito, H.; Saitoh, Y. *J. Am. Chem. Soc.* **1996**, *118*, 6802.

(12) Zang, H.; Gates, K. S. *Chem. Res. Toxicol.* **2003**, *16*, 1539.

(13) Chatterji, T.; Kizil, M.; Keerthi, K.; Chowdhury, G.; Pospisil, T.; Gates, K. S. *J. Am. Chem. Soc*. **2003**, *125*, 4996.

(14) Zang, H.; Breydo, L.; Mitra, K.; Dannaldson, J.; Gates, K. S. *Bioorg. Med. Chem. Lett.* **2001**, *11*, 1511.

(15) Breydo, L.; Gates, K. S. *J. Org. Chem.* **2002**, *67*, 9054.

(16) Breydo, L.; Zang, H.; Mitra, K.; Gates, K. S. *J. Am. Chem. Soc.* **2001**, *123*, 2060.

(17) Iyer, R. P.; Phillips, L. R.; Egan, W.; Regan, J. B.; Beaucage, S. L. *J. Org. Chem.* **1990**, *55*, 4693.

(18) Synthetic and biosynthetic processes leading to dithiolanone-oxide and related compounds have been reported. (a) Pattenden, G.; Shuker, A. J. *Tetrahedron Lett.* **1991**, *32*, 6625. (b) Pattenden, G.; Shuker, A. J. *J. Chem. Soc., Perkin Trans. 1* **1992**, 1215. (c) Kanda, Y.; Fukuyama, T. *J. Am. Chem. Soc.* **1993**, *115*, 8451. (d) Glass, R. S.; Liu, Y. *Tetrahedron Lett.* **1994**, *35*, 3887. (e) Marchan, V.; Gilbert, M.; Messeguer, A.; Pedroso, E.; Grandas, A. *Synthesis* **1999**, 43. (f) Cheng, Y. Q.; Tang, G.-L.; Shen, B. *J. Bacteriol.* **2002**, *184*, 7013. (g) Pattenden, G.; Sinclair, D. J. *J. Organomet. Chem.* **2002**, *653*, 261. (h) Cheng, Y. O.; Tang, G.-L.; Shen, B. *Proc. Nat. Acad. Sci.* **2003**, *100*, 3149. (i) Du, L.; Chen, M.; Zhang, Y.; Shen, B. *Biochemistry* **2003**, *42*, 9731. (j) Lee, A. H. F.; Chan, A. S. C.; Li, T. *Tetrahedron* **2003**, *59*, 833. (k) Salvetti, R.; Martinetti, G.; Ubiali, D.; Pregnolato, M.; Pagani, G. *Farmaco* **2003**, *58*, 995. (l) Lee, A. H. F.; Chen, J.; Chan, A. S. C.; Li, T. *Phosphorus Sulfur Silicon Rel. Elem.* **2003**, *178*, 1163. (m) Gargadennec, S.; Legouin, B.; Burgot, J.-L. *Phosphorus Sulfur Silicon Rel. Elem.* **2003**, *178*, 1721. (n) Garcia-Valverde, M.; Pascual, R.; Torroba, T. *Org. Lett.* **2003**, *5*, 929. (o) Hutchinson, C. R. *Proc. Nat. Acad. Sci.* **2003**, *100*, 3010. (p) Tang, G.-L.; Cheng, Y.-Q.; Shen, B. *Chem. Biol.* **2004**, *11*, 35. (q) Barriga, S.; Fuertes, P.; Marcos, C. F.; Torroba, T. *J. Org. Chem.* **2004**, *69*, 3672. (r) Szilágyi, A.; Pelyvás, I. F.; Majercsik, O.; Herczegh, P. *Tetrahedron Lett.* **2004**, *45*, 4307.

(19) Galm, U.; Hager, M. H.; Van Lanen, S. G.; Ju, J.; Thorson, J. S.; Shen, B. *Chem. Rev.* **2005**, *105*, 739.

(20) Paz, M. M.; Das, A.; Palom, Y.; He, Q.-Y.; Tomasz, M. *J. Med. Chem.* **2001**, *44*, 2834.

(21) Lopez-Larraza, D. M.; Moore, K., Jr.; Dedon, P. C. *Chem. Res. Toxicol.* **2001**, *14*, 528.

(22) Kuo, H.-M.; Lee Chao, P.-D.; Chin, D.-H. *Biochemistry* **2002**, *41*, 897.

(23) Wolkenberg, S. E.; Boger, D. L. *Chem. Rev.* **2002**, *102*, 2477.

(24) Buckberry, L. D.; Teesdale-Spittle, P. H. Sulfur-Hydrogen Compounds in *Biological Interactions of Sulfur Compounds*; Mitchel, S., Ed.; Taylor & Francis; London, 1996, pp 113.

(25) Through-space effects to perturb the reactivity of chalcogen centers have been reported: (a) Burling, F. T.; Goldstein, B. M. *J. Am. Chem. Soc.* **1992**, *114*, 2313. (b) Nagao, Y.; Hirata, T.; Goto, S.; Sano, S.; Kakehi, A.; Iizuka, K.; Shiro, M. *J. Am. Chem. Soc.* **1998**, *120*, 3104. (c) Iwaoka, M.; Takemoto, S.; Okada, M.; Tomoda, S. *Chem. Lett*. **2001**, *2*, 132. (d) Iwaoka, M.; Takemoto, S.; Okada, M.; Tomoda, S. *Bull. Chem. Soc. Jpn*. **2002**, *75*, 1611. (e) Iwaoka, M.; Katsuda, T.; Tomoda, S.; Harada, J., Ogawa, K. *Chem. Lett.* **2002**, *5*, 518. (f) Iwaoka, M.; Takemoto, S.; Tomoda, S. *J. Am. Chem. Soc*. **2002**, *124*, 10613. (g) Iwaoka, M.; Komatsu, H.; Katsuda, T.; Tomoda, S. *J. Am. Chem. Soc.* **2004**, *126*, 5309. (h) Leriche, P.; Turbiez, M.; Monroche, V.; Frère, P.; Blanchard, P.; Skabara, P. J.; Roncali, J. *Tetrahedron Lett.* **2003**, *44*, 649. (i) Wu, S., Greer, A. *J. Org. Chem.* **2000**, *65*, 4883. (j) Reznik, R.; Greer, A. *Chem. Res. Toxicol.* **2000**, *13*, 1193. (j) Schöneich, C.;

Pogocki, D.; Wisniowski, P.; Hug, G. L.; Bobrowski, K. *J. Am. Chem. Soc.* **2000**, *122*, 10224. (k) Pogocki, D.; Schöneich, C. *J. Org. Chem.* **2002**, 67, 1526. (l) Schöneich, C.; Pogocki, D.; Hug, G. L.; Bobrowski, K. *J. Am. Chem. Soc.* **2003**, *125*, 13700. (m) Bobrowski, K.; Hug, G. L.; Marciniak, B.; Miller, B.; Schöneich, C. *J. Am. Chem. Soc.* **1997**, *119*, 8000. (n) Pogocki, D.; Serdiuk, K.; Schöneich, C. *J. Phys. Chem. A.* **2003**, *107*, 7032.

(26) The calculated features of benzodithiolanone-oxide **1** compare well with those obtained from its X-ray structure. Behroozi, S. J.; Barnes, C. L.; Gates, K. S. *J. Chem. Crystallogr.* **1998**, *28*, 689.

(27) Burrows, C. J.; Muller, J. G. *Chem. Rev.* **1998**, *98*, 1109.

(28) Bassett, S.; Urrabaz, R.; Sun, D. *Anti-Cancer Drugs* **2004**, *15*, 689.

(29) (a) Zang, H.; Gates, K. S. *Chem. Res. Toxicol.* **2003**, *16*, 1539. (b) Shipova, E.; Gates, K. S. *Bioorg. Med. Chem. Lett.* **2005**, *15*, 2111.

(30) Zysman-Colman, E. 2003, Ph. D Thesis, McGill University, Montreal, Quebec.

(31) Clennan, E. L.; Stensaas, K. L. *J. Org. Chem.* **1996**, *61*, 7911.

(32) Kustos, M.; Steudel, R. *J. Org. Chem.* **1995**, *60*, 8056.

Chapter 2. The Generation of Mono- and Bis-dioxiranes from 2,3-Butanedione

2.1 Introduction

Dimethyldioxirane **1** possesses low strain energy (11 kcal/mol) compared to oxirane (26 kcal/mol) and cyclopropane (27 kcal/mol) based on *ab initio* calculations.[1] The low strain energy of **1** was rationalized assuming gem-dioxa anomeric stabilization (Scheme 1).[1] Vicinal gem-dioxa-containing molecules are known. Thus, structures bearing 1,2-bis acetals would be topologically similar to a hypothetical bis-dioxirane (**3B**, Scheme 2). The comparison of **1** with butane-2,3-bisacetal (**2**), such as the 1,1,2,2-oxygenation generated as a protecting group for 1,2-diols, led us to raise the following question: *Can more than one dioxirane center occupy a molecule?* Despite the intense interest in the synthesis of dioxiranes,[2] in studies gauging dioxirane stability[3] and in oxone-mediated cleavage of 1,2-dicarbonyl compounds,[4] no studies have yet focused on molecules containing adjacent α-dioxirane groups (1,2-bis-dioxiranes). The juxtaposition of two dioxirane groups would represent a new type of structure in dioxirane chemistry.

In the present work, we focus on the synthesis of a molecule containing α-dioxirane groups, **3B**, along with mono-dioxirane **3A**. A rationale is presented to account for the greater stability of **3B** compared to **3A**.

2.2 Results and Discussion

2.2.1 NMR Spectroscopy and Chemical Trapping The oxidation of biacetyl (1.23 M) in buffered aqueous solution at pH 7 was conducted in the presence of oxone (0.48 M) at

–17 °C. Separation of the organic-soluble fraction at –17 °C led to the detection of the mono-dioxirane **3A** and the bis-dioxirane **3B** along with carbon dioxide, acetic acid, and other by-products (discussed later). The low temperature separation method permitted an NMR analysis at –17 °C of unstable **3A** and **3B**. Two sets of peaks disappeared as a result of addition of sulfide or on warming the sample to 25 °C, according to NMR. An HMBC experiment on **3A** shows a long-range correlation of H2 (1.59 ppm) with the dioxirane carbon (94.5 ppm) and carbonyl carbon (208.0 ppm) (Figure 1). The directly attached methyl carbon of H2 was identified at 24.4 ppm by a HSQC experiment. However, the methyl α to the carbonyl group (2.41 ppm) is obscured by the biacetyl peak. With a HMBC experiment on **3B**, the correlation between H1 (1.41 ppm) and dioxirane carbon (110.5 ppm) was identified while a HSQC experiment confirmed the directly attached methyl carbon at 21.6 ppm (Figure 2). The measured integral values indicate that the relative ratio of **3A**:**3B** is 5:1. Dioxiranes **3A** and **3B** are stable at –17 °C, but cannot be obtained in pure form to enable their complete characterization. Chemical trapping studies[5] provided strong evidence for the presence of the dioxirane intermediates **3A/3B**. Oxygenation of added Ph_2S or $(p\text{-}CH_3OC_6H_4)_2S$ proceeded at –17 °C in the presence of the organic-soluble fraction of the biacetyl—oxone mixture, and was monitored by GC/MS and ^1H NMR, respectively. (Control reactions demonstrate that oxone was not present in the organic-soluble fraction after the extraction and is not responsible for the sulfide oxidation reaction, see page 38.) The products formed are the corresponding Ph_2SO and $(p\text{-}CH_3OC_6H_4)_2SO$. The concentrations of sulfoxides were determined to be 0.06 M based upon calibration curve for authentic samples (see the experimental section page 39). The sulfoxide concentration indicates that a peroxide is

present in the organic layer. The NMR data shows that concentration of the monodioxirane is 5 times the concentration of the bisdioxirane (Figure 7). Combining the data from the sulfide trapping studies and from NMR detection allowed us to calculate that the –17 °C organic-fraction contains 0.05 M **3A** and 0.01 M **3B**. The observation that diacetyl peroxide **7** reacted slowly with Ph_2S and $(p\text{-}CH_3OC_6H_4)_2S$ leads us to suggest that the oxygen-transfer chemistry is derived from **3A** and **3B**. A quantitative study of biacetyl with oxone with added olefins also showed oxygen-transfer chemistry expected of **3A** and **3B**. 2,3-Dimethyl-2-butene and *trans*-stilbene reacted in the presence of the –17 °C $CHCl_3$ fraction (see page 39). GC/MS analyses of these reactions revealed the formation of the corresponding epoxides, 2,2,3,3-tetramethyl-oxirane (41.7% yield) and *trans*-2,3-diphenyl-oxirane (47.0% yield). These percent yields were determined after 8 hours of stirring at –17 °C.

2.2.2 Reaction Products. The biacetyl—oxone reaction is an effective reaction to generate **3A** and **3B**, but the reaction also gives by-products. Separation of the organic-soluble fraction at –17 °C led to the detection of seven stable by-products: acetic anhydride (**4**), acetic acid (**5**), succinaldehyde (**6**), diacetyl peroxide (**7**), acetone (**8**), methyl acetate (**9**), and CO_2 (**10**) (Scheme 3). Some compounds exist as hydrates and reside to a greater extent in the aqueous layer making quantification difficult.[6] The percent conversion of the biacetyl ranged from 30 to 40%. Carbon dioxide, acetic anhydride, and acetic acid are the major components of this reaction in the organic layer, where acetic acid presumably arises from the hydrolysis of acetic anhydride which formed from a Baeyer-Villiger rearrangement of **3A**. Evidence for the formation of **4**, **5**, and **7-9** was provided by ^{1}H NMR. Carbon dioxide was detected by ^{13}C NMR. The

evidence for the existence of monomeric **6** was provided using ^{1}H and ^{13}C NMR, although **6** may also exist as the hydrate or in dimeric or trimeric forms.

The experimental evidence suggests that intermediates **3A/3B** decompose to the final stable products **4-10** (Scheme 4). We believe that acyloxy and alkyl radicals play a role in the decomposition of **3A** and **3B**, which arises from homolysis of the O-O bond.[7] Dioxirane **3A** can react to give dialdehyde **6**, and **3B** can convert to the stable diacetyl peroxide **7**, by losing CO_2. A process involving methyl radical cleavage can give intermediates $CH_3C(O)CO_2^{\bullet}$ and $CH_3C(O_2)CO_2^{\bullet}$, subsequently yielding $CH_3C^{\bullet}(O)$ and $CH_3C^{\bullet}(O_2)$, respectively, upon loss of CO_2. There is reason to believe that rearrangements via [$^{\bullet}CH_2CHO \leftrightarrow CH_2{=}CHO^{\bullet}$] precede tail-to-tail dimerization to **6**, and $CH_3CO_2^{\bullet}$ precedes dimerization to **7**. Subsequent methyl radical recombination reactions give **8** and **9**. Previous work has been conducted on thermolytic dioxirane fragmentation; electron transfer and radical formations have been suggested.[7,8] The mono-dioxirane **3A** can also produce the stable anhydride by a Baeyer-Villager type rearrangement in an intramolecular process.

The data suggest that formation of **3B** does not take place efficiently due to a reduced reactivity of the hydrated form of mono-dioxirane with oxone (**11**), which may predominant in the aqueous buffered solution (Scheme 5). Similarly, in a previous study it was reported that the equilibrium constant for the mono hydration of biacetyl to $CH_3C(OH)_2C(O)CH_3$ is 2.1.[6c]

The amount of **3A** and **3B** formed is a function of temperature. After heating the –17 °C organic-soluble fraction of the biacetyl—oxone mixture to 25 °C, concentrations of **4-10** increased and **3A** and **3B** decreased. Biacetyl serves as the co-solvent and

reagent and the yield of **3A** and **3B** depends on the ratio of biacetyl to oxone used in the reaction. Using an equivalent or excess of oxone to biacetyl (that is, 1:1 and 2:1) resulted in lower concentrations of **3A** and **3B**, but increased concentrations of **4-10**. Past a certain point, decomposition of both **3A** and **3B** is facilitated by higher oxone concentrations. Under high oxone to biacetyl ratios (5:1 and 10:1), **3A** and **3B** were not observed. The decomposition of **3A** and **3B** and formation of stable products **4-10** also take place rapidly when chloroform, acetonitrile, or buffer is added as a co-solvent with higher added oxone concentrations. This observation suggests that stabilization of **3A** and **3B** depends in part on the presence of biacetyl solvent. Using a higher oxone-biacetyl ratio led to difficulties in detection **3A** and **3B** from extraction of the organic layer. A higher amount of oxone facilitated the decomposition of the dioxirane intermediates. Acetic anhydride, acetone, and acetic acid were the major product in the reaction when excesses of oxone were used.

2.2.3 Origin of the Stability of Dioxiranes 3A/3B. The mono-dioxirane **3A** and the bis-dioxirane **3B** differ in their relative stability as revealed by NMR. For example, **3A** decomposes rapidly at 0 °C, while at the same temperature **3B** is stable for 30 minutes (referring to NMR data the decomposition increased the formation of the corresponding anhydride). An explanation on dioxirane stability could follow Bach's lead.[1] The decreased stability of **3A** vs **3B** can be viewed from the greater role of the π-resonance contributor compared to the α-dioxiranyl (anomeric) resonance contributor in terms of α-electron withdrawing capacity (Scheme 6). In contrast to bis-dioxirane **3B**, the mono-dioxirane **3A** will have a weaker O-O bond, as anticipated from a π-electron withdrawing effect from the adjacent carbonyl group. The reactivity of the monodioxirane may be due

to an electronic effect, since the NMR data has shown an increase in the stable product (anhydride) after the decomposition. It has been previously shown that substituting one of the methyl groups on dimethyldioxirane **1** with the electron-withdrawing CF_3 group substantially decreases stability.[9]

2.2.4 Conclusion

In conclusion, the data showed that the biacetyl—oxone reaction provides the generation of the mono- and bis-dioxirane, **3A** and **3B**. This result demonstrates that dioxirane units in molecules can be doubled (or even possibly multiplied) to produce new dioxirane structures. A new synthetic utility for **3A** and **3B** has not yet been demonstrated.

2.3 Experimental Section

2.3.1 Materials and Instrumentation

Low-temperature and room-temperature NMR data were acquired on a Bruker 400-MHz NMR spectrometer and an Oxford 600-MHz NMR spectrometer. GC/MS data were collected on an Agilent Technologies GC/MS instrument consisting of a 6890 Series GC with 5973N series mass selective detector. Reagents and solvents [chloroform, chloroform-*d*, 2,3-butanedione, oxone (monopersulfate triple salt, $2KHSO_5$, $KHSO_4$, and K_2SO_4), sodium phosphate monobasic, sodium phosphate dibasic heptahydrate, sodium sulfite (anhydrous), *m*-chloroperoxybenzoic acid (MCPBA), diphenyl sulfide, diphenyl sulfoxide, 2,3-dimethyl-2-butene, *trans*-stilbene, and triphenylmethane] were obtained commercially and were used as received. The purity of the reagents was checked by ^1H NMR and GC/MS prior to use. 2,2,3,3-Tetramethyl-

oxirane and *trans*-2,3-diphenyl-oxirane were synthesized via MCPBA oxidation of their corresponding alkenes and are known compounds previously described in the literature.[10]

2.3.2 Oxone—Biacetyl Reaction (Figure 3-7)

A salted ice bath was used at (–10 °C), where oxone (25 g, 0.0401 mol) in 25 mL deionized water was added to a solution containing sodium phosphate (pH 7.4, 10 mL), sodium bicarbonate (12 g, 0.14285 mol), chloroform (10 mL), deionized water (10 mL), and 1 g of ice. A –5 °C solution of biacetyl (8 mL, 0.0916 mol) and chloroform (5 mL) was added to the mixture simultaneously with the oxone. Sodium bicarbonate (12.6 g) was used to maintain the pH between 7.4-7.8. The reaction mixture was then poured into a beaker cooled to –17 °C containing anhydrous Na_2SO_4:$NaH_2PO_4(H_2O)$:$NaH_2PO_4(7H_2O)$ (4:2:1). The organic layer was separated at low temperature (–17 °C) and dried with magnesium sulfate. Chloroform-*d* was added to a 1 mL sample of the chloroform layer of the reaction mixture, which was then analyzed by low-temperature and room-temperature NMR spectroscopy (Figure 3-7) and GC/MS. The data used to generate Figures 1 and 2 were collected at –17 °C. Mono-dioxirane [1-(3-methyl-dioxiran-3-yl)-ethanone (**3A**)]: ^{1}H NMR ($CDCl_3$): δ 1.59 (s, 3H), 2.40 (s, 3H); ^{13}C NMR 208, 94. Bis-dioxirane [(3,3'-dimethyl-[3,3']bidioxirane (**3B**)]: ^{1}H NMR ($CDCl_3$): δ 1.41 (s, 3H); ^{13}C NMR 114. The data collected for **4-10** are consistent with literature values of NMR and/or GC mass spectroscopy.

Control Experiment

Oxone was found not to be present in the organic-soluble solution after extraction. This conclusion is based on a control experiment. To a solution of 50 mL acetonitrile, sodium phosphate (pH 7.4, 30 mL), and chloroform 10 mL was slowly added to a

mixture of 25 g (0.04 mol) and sodium bicarbonate 12 g (0.143 mol). The mixture was stirred for 2 h. After the organic layer was isolated, 0.18 g (1.0 mmol) of *trans*-stilbene was added, the solution was stirred at room temperature overnight. After the solvent was removed under vacuum and the residue was analyzed by GC/MS, NMR could not detect the epoxide. Identical experiment was done for the sulfide reaction with biacetyl-oxone.

Reaction of Oxone-Biacetyl System with Sulfide (Figure 8)

A solution of (1 mL) of 1.57 M oxone-biacetyl reaction in choroform was prepared and stored in a freezer at -10 ^{o}C. To the cooled solution, 131 mL (0.78 mmol) of diphenyl sulfide was added. The mixture was stirred for 2 h at -10 ^{o}C and allowed to warm to room temperature. The concentration of the sulfoxide was determined by GC/MS using a calibration curve for diphenyl sulfoxide and diphenyl sulfone. NMR data were collected for a similar experiment using (p-$MeOC_6H_4)_2S$ instead of diphenyl sulfide: ^{1}H NMR ($CDCl_3$): δ 3.82 (s, 3H) for the methoxy group in the (p-MeO $C_6H_4)_2SO$; and 3.79 (s, 3H) for the methoxy group in (p-$MeOC_6H_4)_2S$.

The concentrations of dioxiranes **3A/3B** were measured by GC/MS with the generation of Ph_2SO from Ph_2S with reference to a calibration curve for Ph_2SO and internal standard, triphenylmethane, and are an average of 4 runs. The concentrations of dioxirane were also measured by NMR by measuring the generation of (p-CH_3O-$C_6H_4)_2SO$ from (p-$CH_3OC_6H_4)_2S$ with reference to the internal standard triphenyl-methane.

The concentrations of 2,2,3,3-tetramethyl-oxirane and *trans*-2,3-diphenyl-oxirane were determined by GC/MS where triphenylmethane was used as an internal standard along with prior-determined calibration curves from authentic samples.

2.3.3 Epoxidation and sulfoxidation reactions

Biacetyl (0.008 mol) neat at –5 °C was added to the mixture simultaneously with oxone (24.5 g, 0.04 mol). The organic layer was extracted with $CHCl_3$, washed 3 times with deionized water, dried over anhydrous magnesium sulfate, and added to –10 °C solutions containing 2,3-dimethyl-2-butene (0.001 mol), and *trans*-stilbene (0.001 mol) in 50 mL of acetonitrile. The solutions were stirred for 8 h at –10 °C. Product distributions of the epoxides are the average of 4 runs. ^{1}H NMR ($CDCl_3$): δ 1.31 (s, 12H) for 2,3-dimethyl-2-butene (figure 9).

Scheme 1

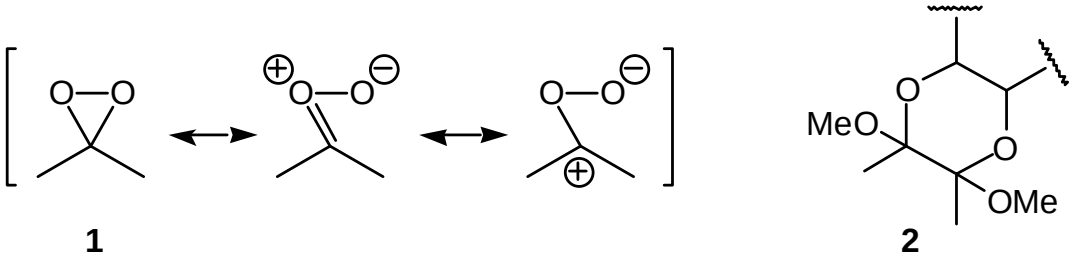

1 **2**

Scheme 2

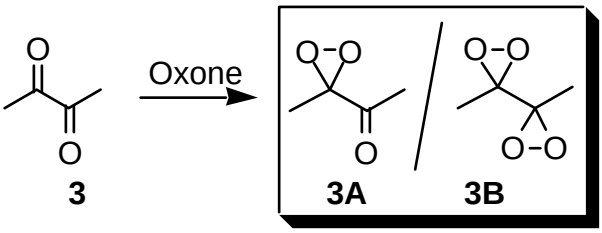

3 **3A** **3B**

Scheme 3

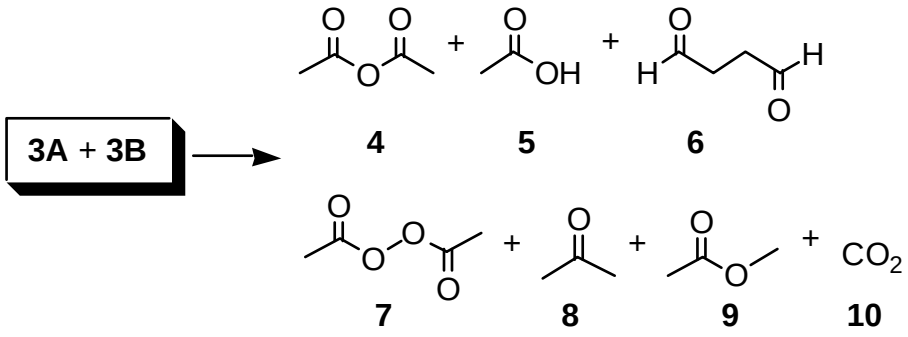

4 **5** **6** **7** **8** **9** **10**

Scheme 4

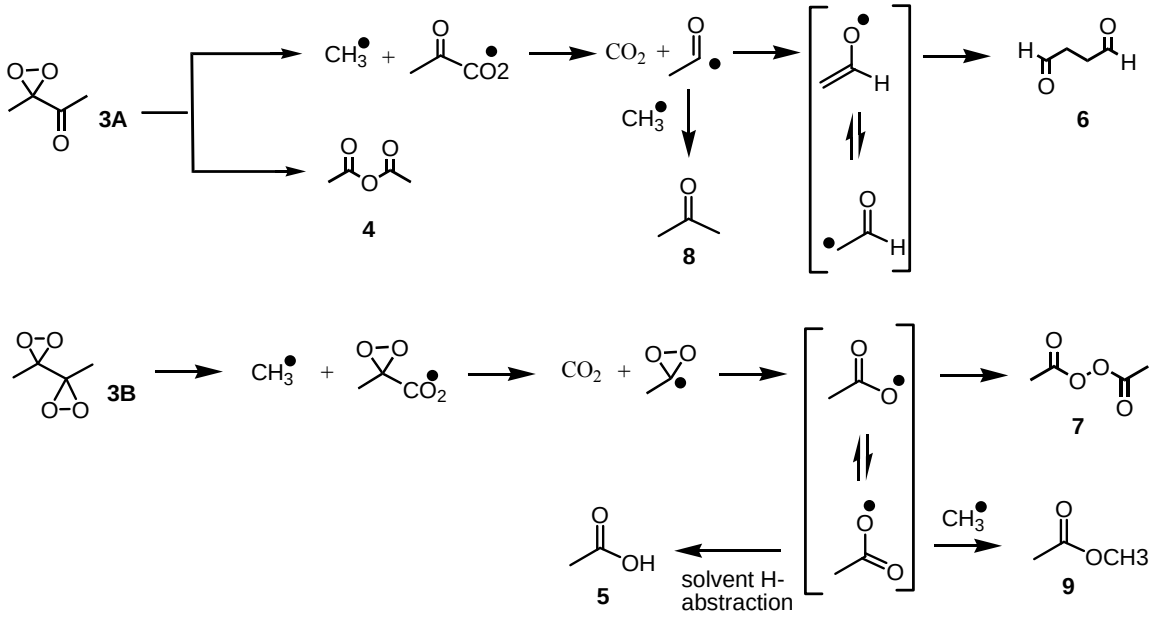

Scheme 5

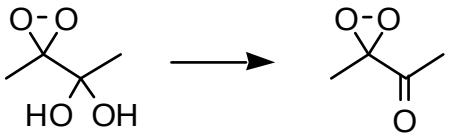

Scheme 6

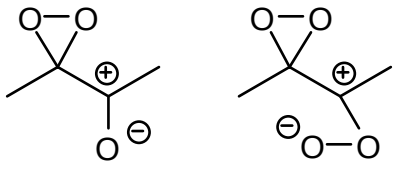

3A
π-resonance contributor

3B
anomeric resonance contributor

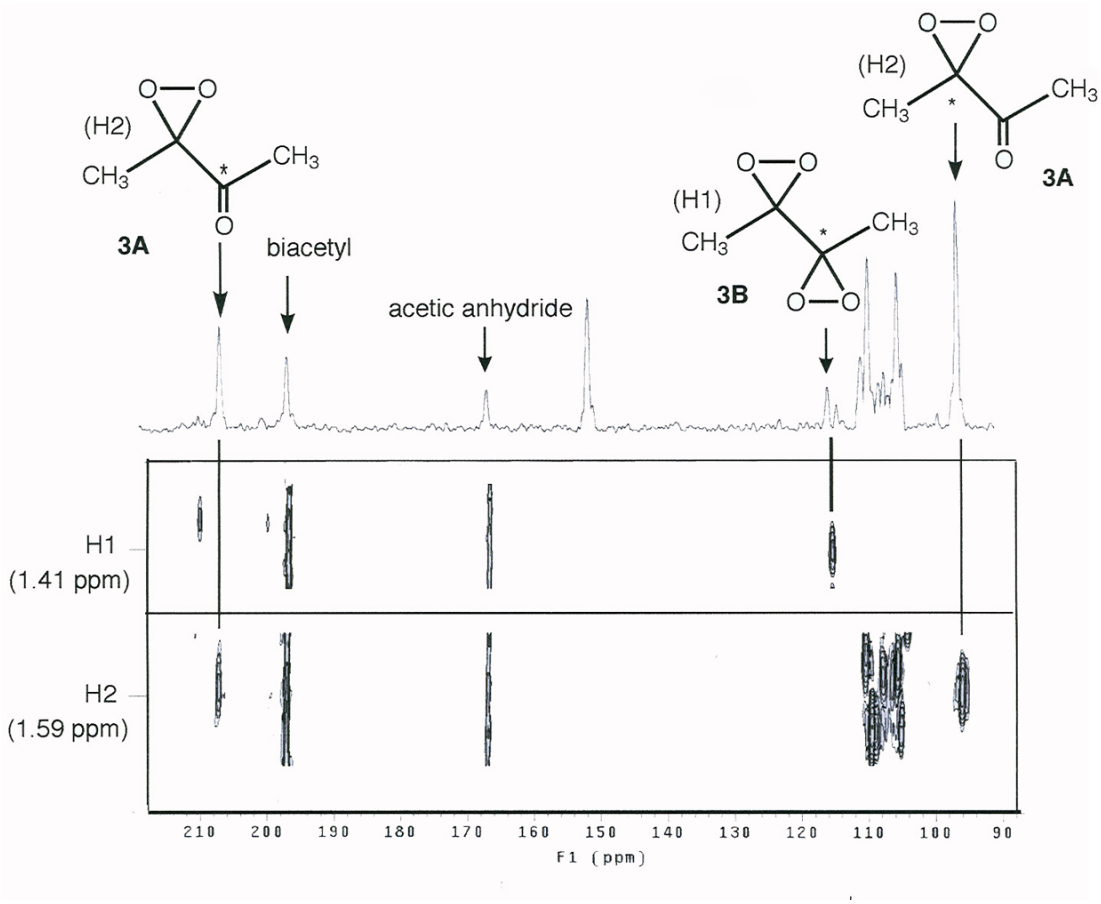

Figure 1. HMBC –17 °C spectra [600 MHz, $CDCl_3$:$CHCl_3$ (4:1 ratio)] of **3A** and **3B** taken from the $CHCl_3$ extract of the biacetyl (1.23 M) oxone (0.48 M) buffer mixture. The extra cross peaks are attributed to solvents and hydrated compounds.

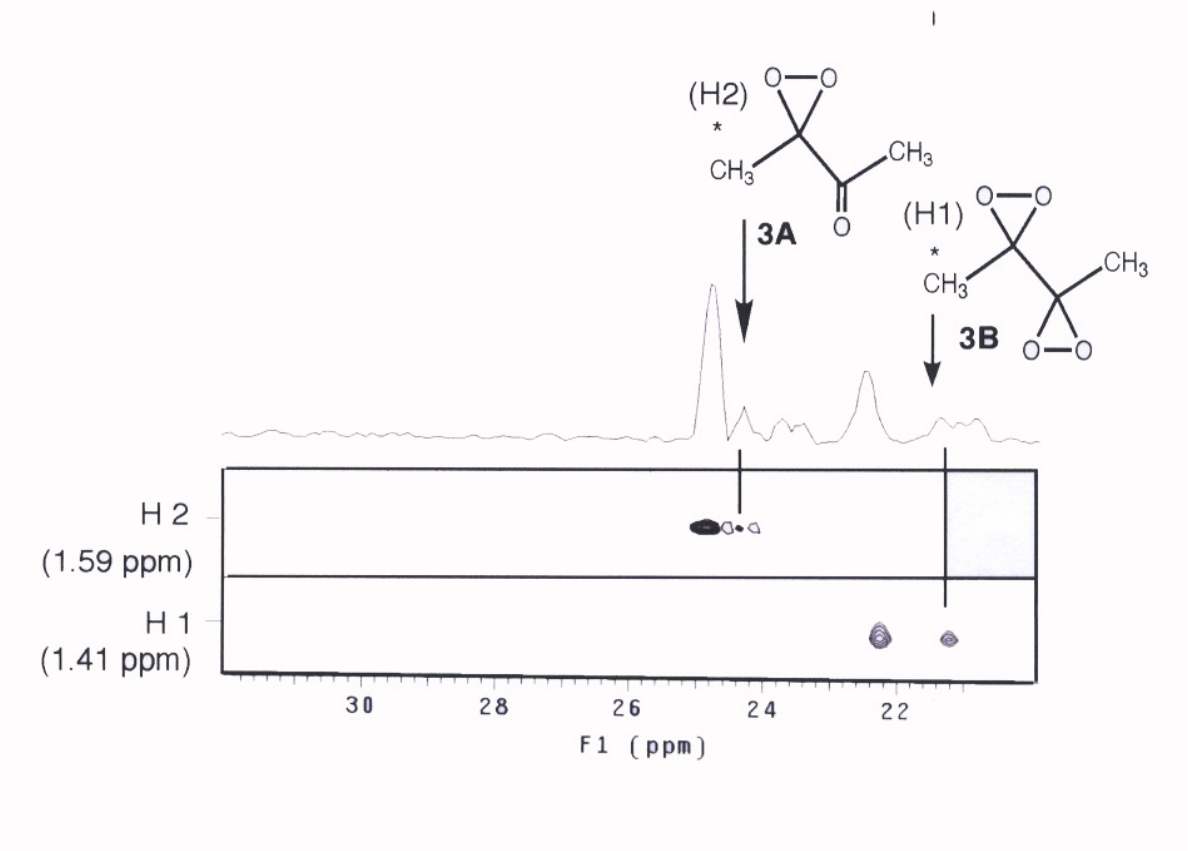

Figure 2. HSQC –17 °C spectra [600 MHz, $CDCl_3$:$CHCl_3$ (4:1 ratio)] of **3A** and **3B** taken from the $CHCl_3$ extract of the biacetyl (1.23 M) oxone (0.48 M) buffer mixture. The extra cross peaks are attributed to solvents and hydrated compounds.

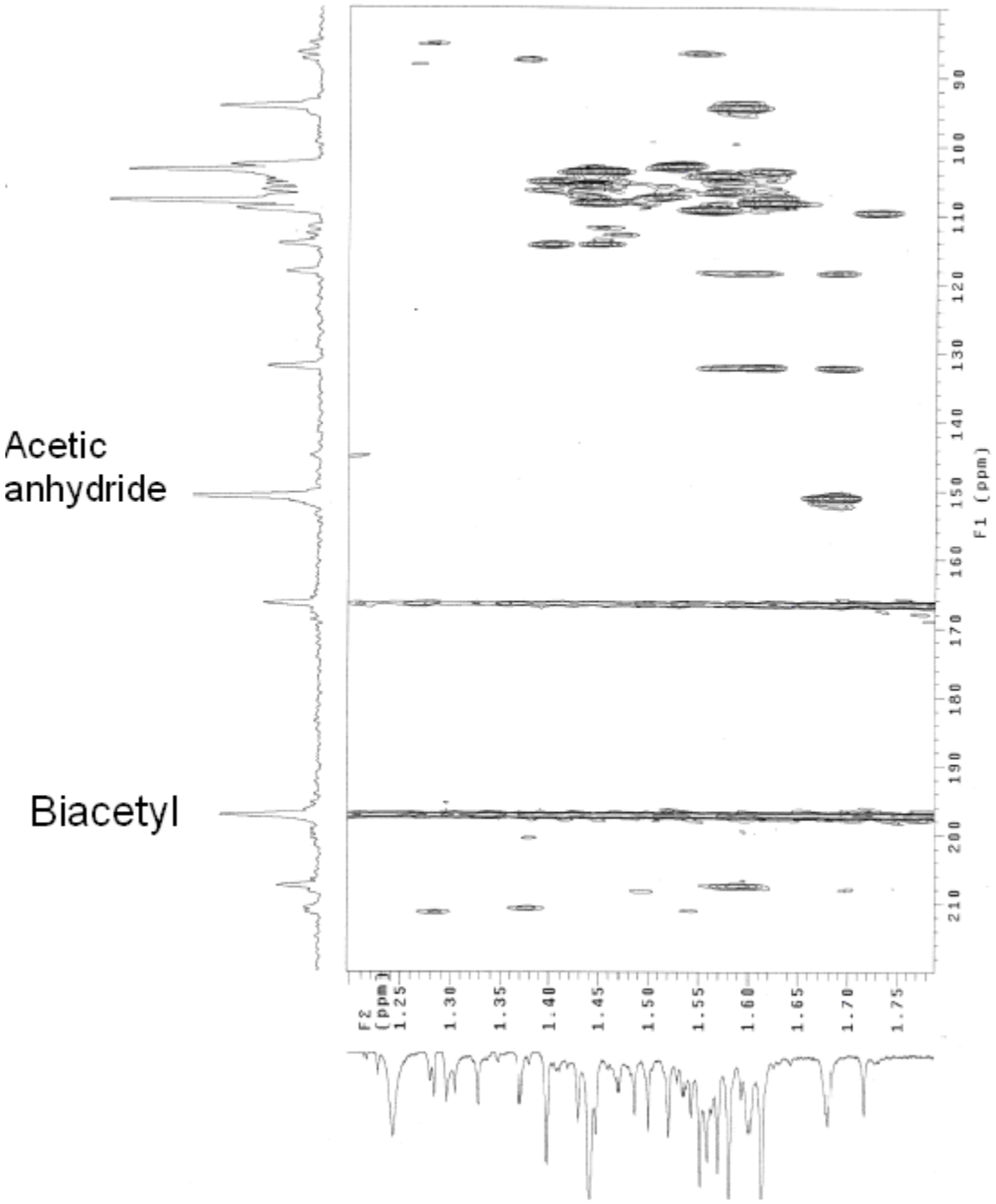

Figure 3. HMBC –17 °C spectrum [600 MHz, $CDCl_3$:$CHCl_3$ (4:1 ratio)] taken from the $CHCl_3$ extract of the biacetyl (1.23 M) oxone (0.48 M) buffer mixture: Proton range 1.2-1.8 ppm.

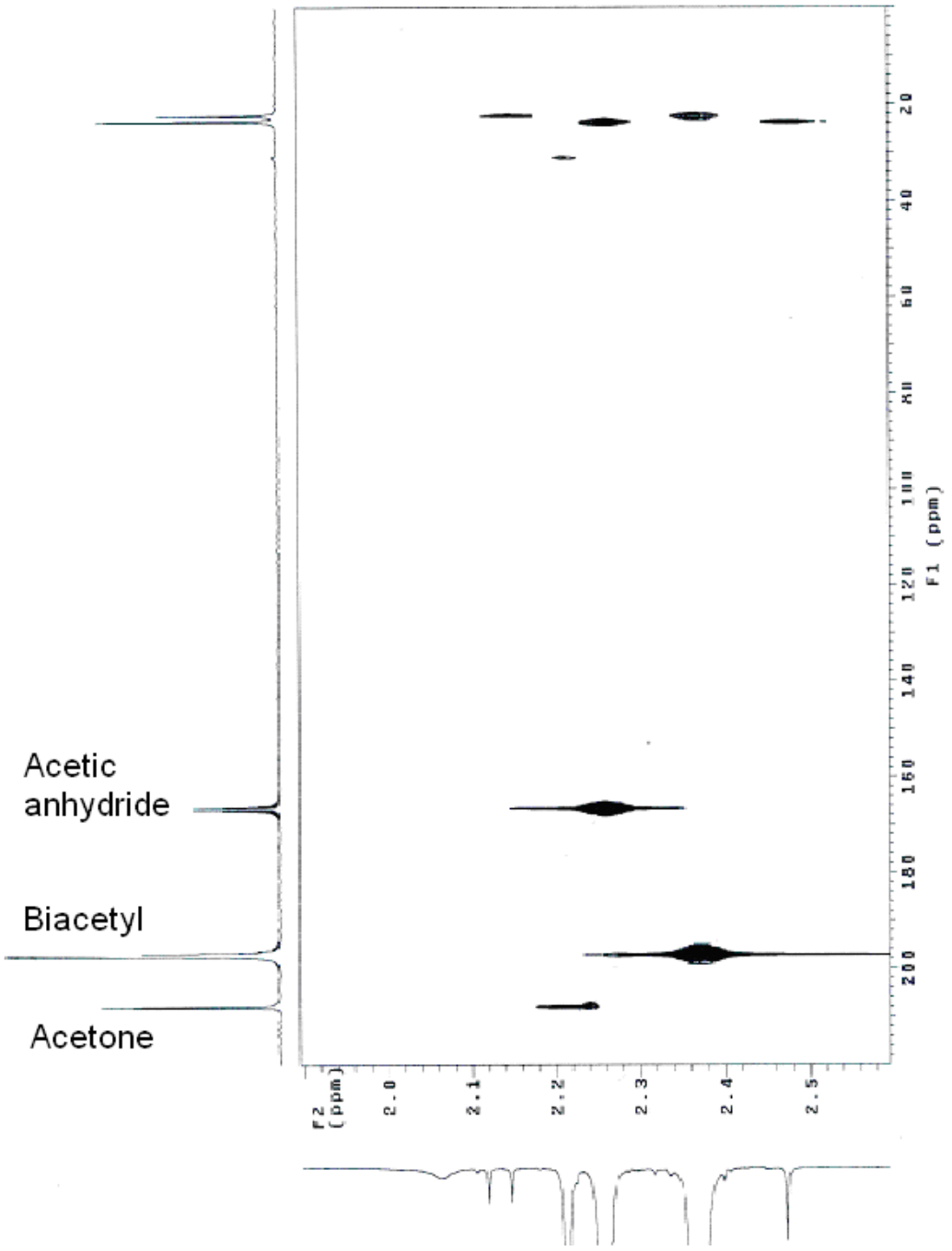

Figure 4. HMBC –17 °C spectrum [600 MHz, $CDCl_3$:$CHCl_3$ (4:1 ratio)] taken from the $CHCl_3$ extract of the biacetyl (1.23 M) oxone (0.48 M) buffer mixture: Proton range 1.8-2.6 ppm.

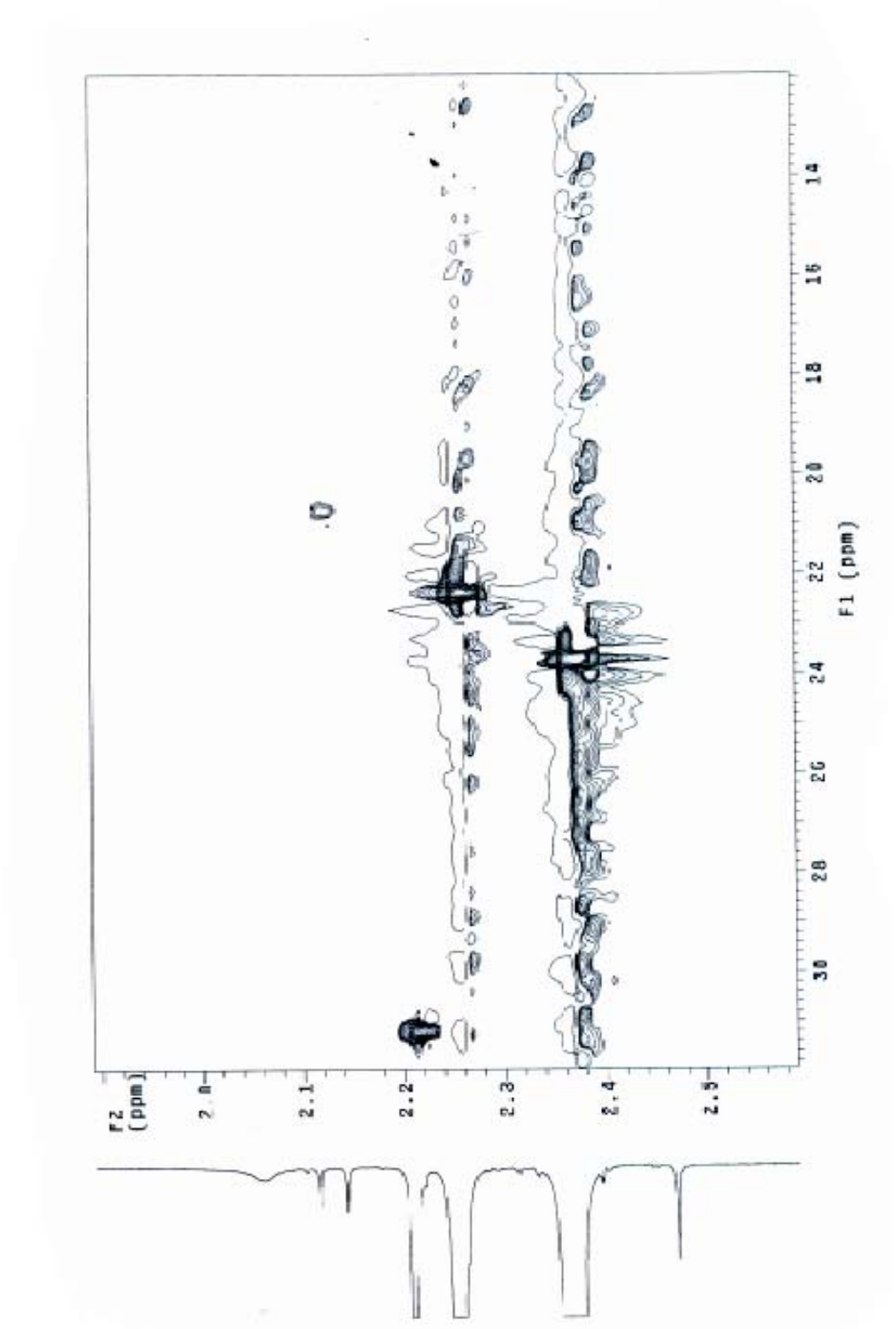

Figure 5. HSQC –17 °C spectrum [600 MHz, $CDCl_3$:$CHCl_3$ (4:1 ratio)] taken from the $CHCl_3$ extract of the biacetyl (1.23 M) oxone (0.48 M) buffer mixture: Proton range 1.7-1.9 ppm.

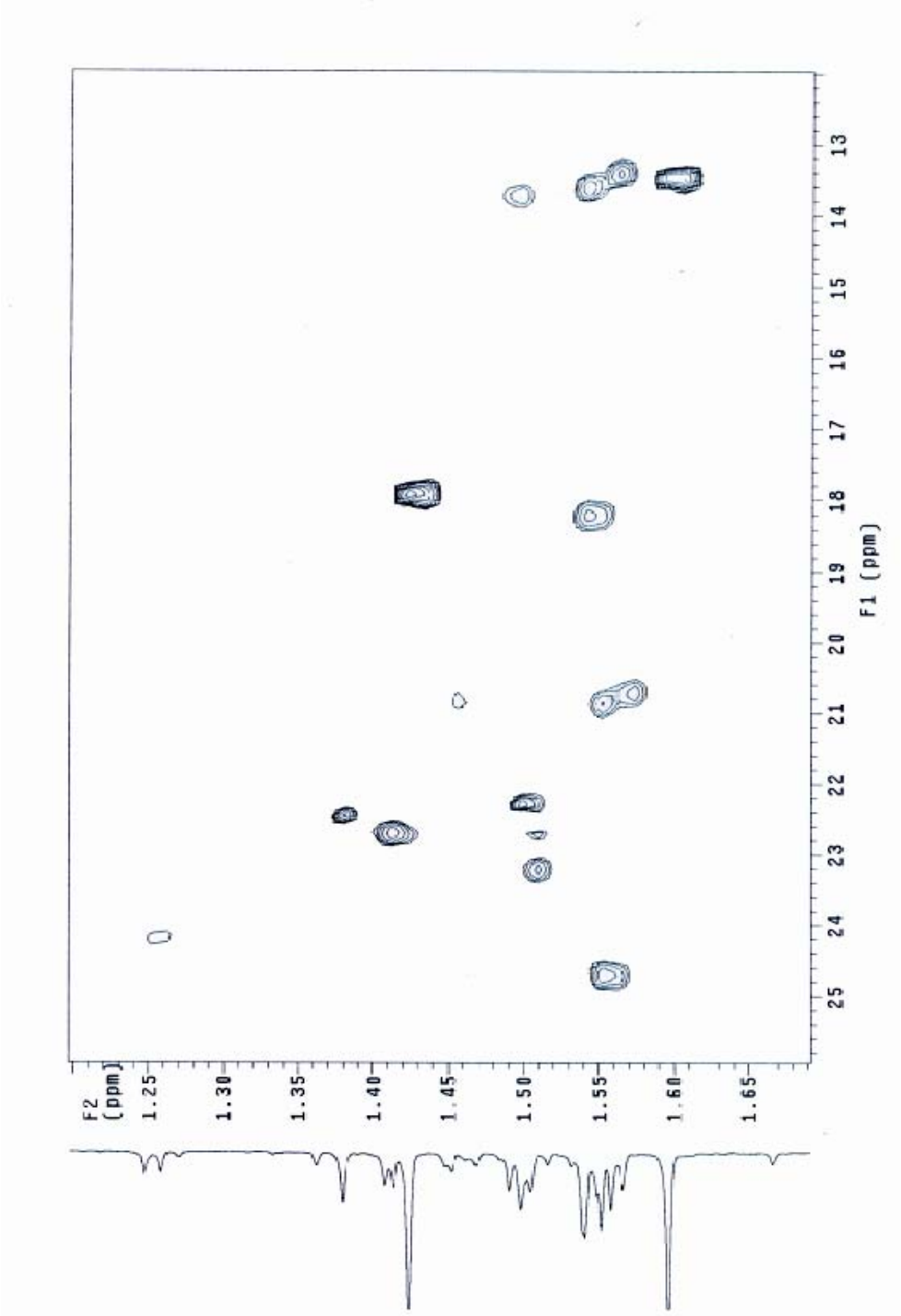

Figure 6. HSQC –17 °C spectrum [600 MHz, $CDCl_3$:$CHCl_3$ (4:1 ratio)] taken from the $CHCl_3$ extract of the biacetyl (1.23 M) oxone (0.48 M) buffer mixture: Proton range 1.2-1.7 ppm.

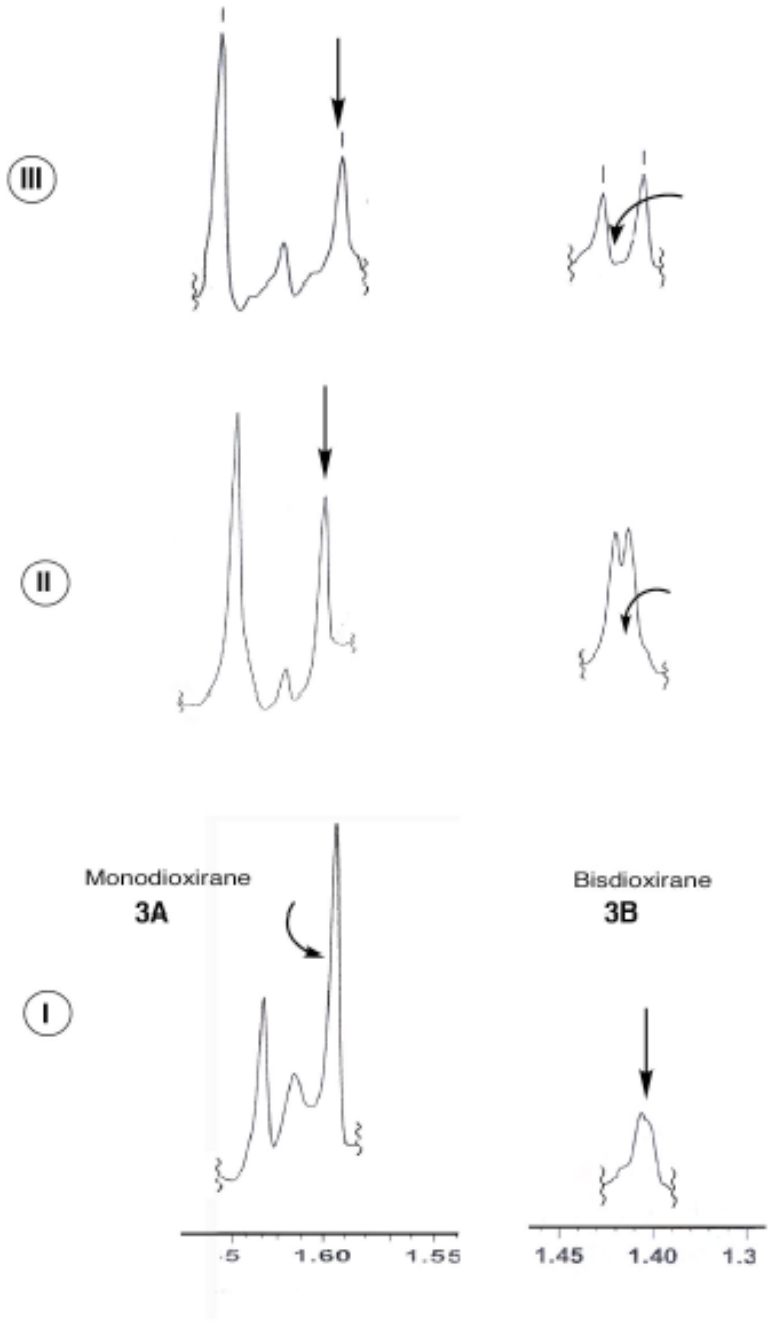

Figure 7. ^{1}H NMR spectra [600 MHz, $CDCl_3$:$CHCl_3$ (4:1 ratio)] taken from the $CHCl_3$ extract of the biacetyl (1.23 M) oxone (0.48 M) buffer mixture. Disappearance of peaks attributed to **3A** and **3B**: -17 °C (I); 0 °C (II); 25 °C (III). A peak from an unidentified stable hydrated compound overlaps with bis-dioxirane **3B**, and becomes more prominent at 0 °C and 25 °C.

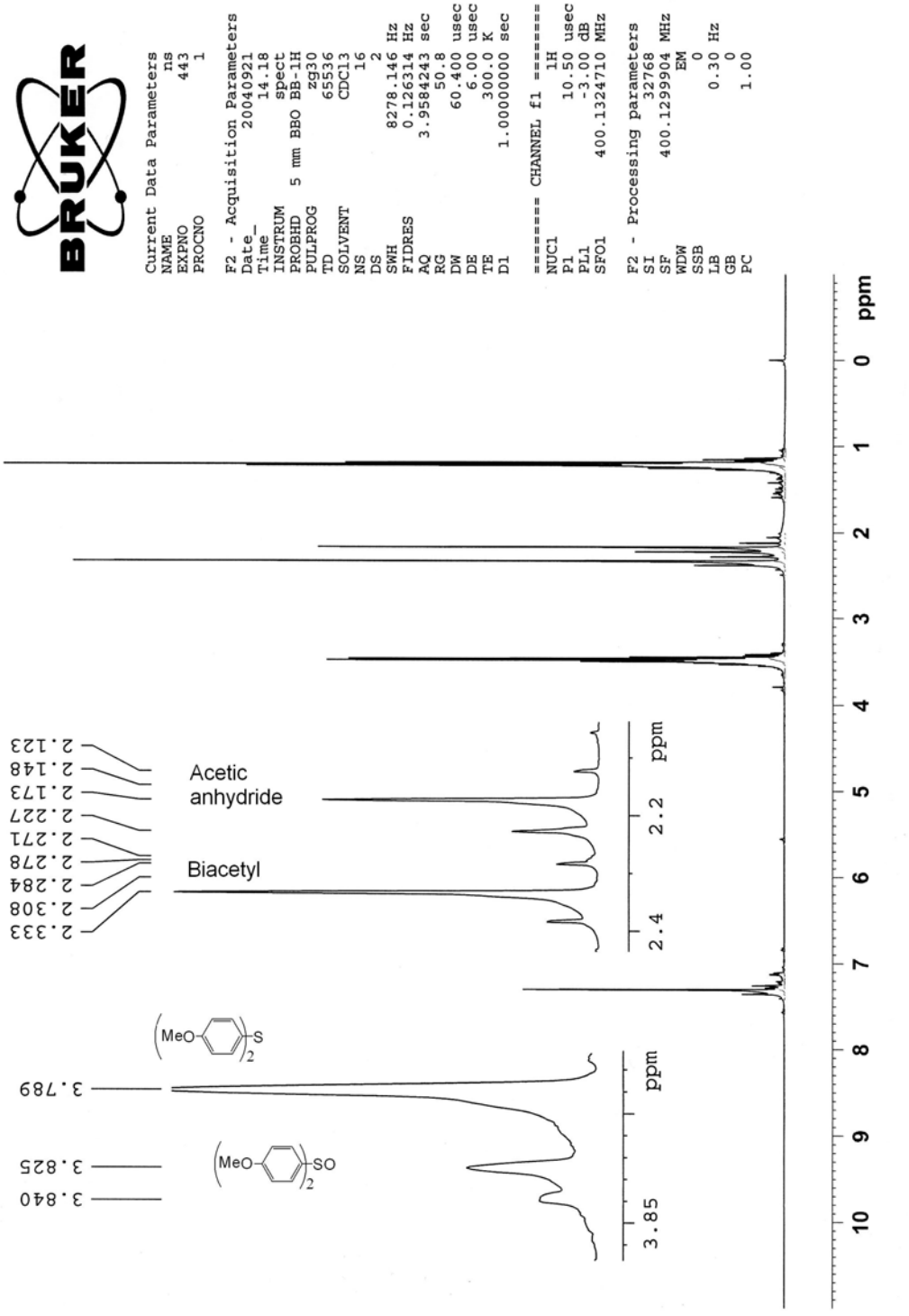

Figure 8. ^{1}H NMR spectrum for reaction oxone-biacetyl with bis-(*p*-methoxyphenyl) sulfide.

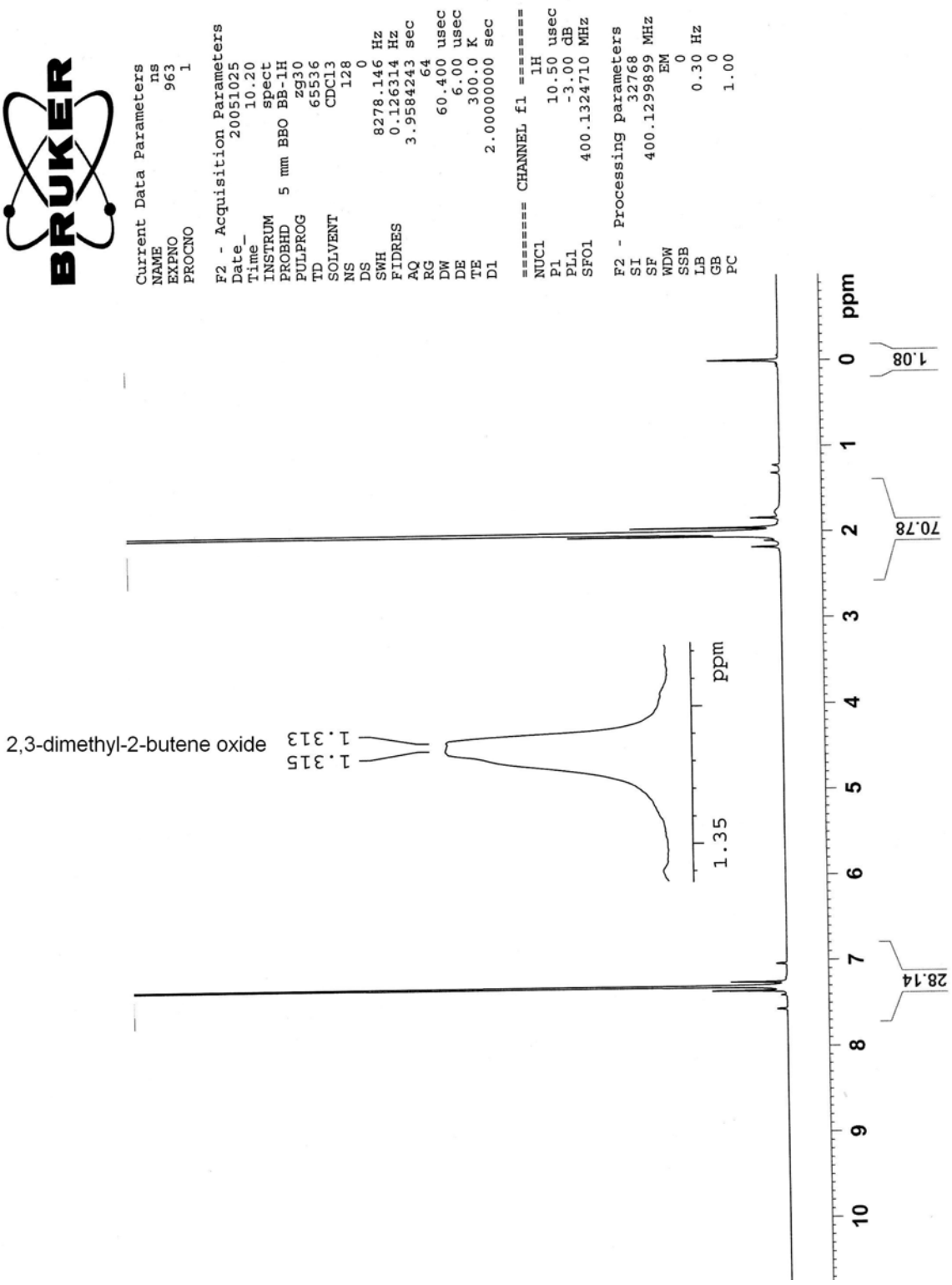

Figure 9. ^{1}H NMR spectrum for reaction oxone-biacetyl with 2,3-tetramethyl-2-butene.

2.4 References

1. (a) Bach, R. D.; Dmitrenko, O. *J. Org. Chem.* **2002**, *67*, 3884. (b) Bach, R. D.; Dmitrenko, O. *J. Org. Chem*. **2002**, *67*, 2588.
2. A very abbreviated list of the literature includes: (a) Murray, R. W. *Chem. Rev.* **1989**, *89*, 1187. (b) Adam, W.; Curci, R.; Edwards, J. O. *Acc. Chem. Res.* **1989**, *22*, 205. (c) Wu, X.-Y.; She, X.; Shi, Y. *J. Am. Chem. Soc.* **2002**, *124*, 8792. (d) Sartori, G.; Armstrong, A.; Maggi, R.; Mazzacani, A.; Sartorio, R.; Bigi, F.; Dominguez-Fernandez, B. *J. Org. Chem.* **2003**, *68*, 3232. (d) Yang, D. *Acc. Chem. Res.* **2004**, *37*, 497. (e) Curci, R.; D'Accolti, L.; Fusco, C. *Acc. Chem. Res.* **2006**, *39*, 1. (f) Chan, T.-C.; Chan, W.-Y.; Chan, W.-K.; Vrijmoed, L. L. P.; O'Toole, D. K.; Wong, M.-K.; Che, C.-M. *Environ. Sci. Technol.* **2006**, *40*, 625.
3. (a) Cassidei, L.; Fiorentino, M.; Mello, R.; Sciacovelli, O.; Curci, R. *J. Org. Chem.* **1987**, *52*, 699. (b) Murray, R. W.; Singh, M.; Jeyaraman, R. *J. Am. Chem. Soc.* **1992**, *114*, 1346. (c) Tomioka, H.; Mizutani, K.; Matsumoto, K.; Hirai, K. *J. Org. Chem.* **1993**, *58*, 7128. (d) Kirschfeld, A.; Muthusamy, S.; Sander, W. *Angew. Chem., Int. Ed. Engl.* **1994**, *33*, 2212. (e) Sander, W.; Schroeder, K.; Muthusamy, S.; Kirschfeld, A.; Kappert, W.; Boese, R.; Kraka, E.; Sosa, C.; Cremer, D. *J. Am. Chem. Soc*. **1997**, *119*, 7265. (f) Block, K.; Kappert, W.; Kirschfeld, A.; Muthusamy, S.; Schroeder, K.; Sander, W.; Kraka, E.; Sosa, C.; Cremer, D. *Peroxide Chem.* **2000**, 139. (g) Schroeder, K.; Sander, W. *Eur. J. Org. Chem.* **2005**, *3*, 496.

4. (a) Ashford, S. W.; Greta, K. C. *J. Org. Chem.* **2001**, *66*, 1523. (b) Yang, D.; Chen, F.; Dong, Z.-M.; Zhang, D.-W. *J. Org. Chem.* **2004**, *69*, 2221. (c) Yan, J.; Travis, B. R.; Borhan, B. *J. Org. Chem.* **2004**, *69*, 9299.

5. Sulfides have been used previously to assay dioxirane content: (a) Murray, R. W.; Jeyaraman, R.; Pillay, M. K. *J. Org. Chem.* **1987**, *52*, 746. (b) Gonzalez-Nunez, M. E.; Mello, R.; Royo, J.; Rios, J. V.; Asensio, G. *J. Am. Chem. Soc.* **2002**, *124,* 9154.

6. Hydrated ketones and aldehydes related to this study have been reported: (a) Lin, T. F.; Christian, S. D.; Affsprung, H. E. *J. Phys. Chem.* **1967**, *71*, 968. (b) Lee, Y. J.; Burr, J. G. *Chem. Phys. Lett.* **1976**, *43*, 146-8. (c) Buschmann, H. J.; Fueldner, H. H.; Knoche, W. *Chem. Berichte.* **1980**, *84*, 41. (d) Burkey, T. J.; Fahey, R. C. *J. Am. Chem. Soc.* **1983**, *105*, 868. (e) Segretario, J. P.; Sleszynski, N.; Partch, R. E.; Zuman, P.; Horak, V. *J. Org. Chem.* **1986**, *51*, 5393.

7. (a) Singh, M.; Murray, R. W. *J. Org. Chem.* **1992**, *57*, 4263-70. (b) Cremer, D.; Kraka, E.; Szalay, P. G. *Chem. Phys. Lett.* **1998**, *292*, 97-109.

8. (a) Adam, W.; Asensio, G.; Curci, R.; Gonzalez-Nunez, M. E.; Mello, R. *J. Am. Chem. Soc.* **1992**, *114*, 8345. (b) Houk, K. N.; Liu, J.; DeMello, N. C.; Condroski, K. R. *J. Am. Chem. Soc.* **1997**, *119*, 10147. (c) Bravo, A.; Fontana, F.; Fronza, G.; Minisci, F.; Zhao, L. *J. Org. Chem.* **1998**, *63*, 254. (d) Freccero, M.; Gandolfi, R.; Sarzi-Amade, M.; Rastelli, A. *J. Org. Chem.* **2003**, *68*, 811.

9. (a) Mello, R.; Fiorentino, M.; Sciacovelli, O.; Curci, R. *J. Org. Chem.* **1988**, *53*, 3890. (b) Yang, D.; Wong, M.-K.; Yip, Y.-C. *J. Org. Chem.* **1995**, *60*, 3887. (c) Denmark, S. E.; Wu, Z. *Synlett* **1999**, 847. (d) Frohn, M.; Zhou, X.; Zhang, J.-R.; Tang, Y.; Shi, Y. *J. Am. Chem. Soc.* **1999**, *121*, 7718. (e) Armstrong, A.; Washington, I.; Houk, K.

N. *J. Am. Chem. Soc.* **2000**, *122,* 6297. (f) Li, W.; Fuchs, P. L. *Org. Lett.* **2003**, *5*, 2853. (g) Bach, R. D.; Dmitrenko, O.; Adam, W.; Schambony, S. *J. Am. Chem. Soc.* **2003**, *125*, 924.

10. (a) Pocker, Y.; Ronald, B. P. *J. Am. Chem. Soc*. **1980**, *102*, 5311. (b) Neimann, K.; Neumann, R. *Org. Lett*. **2000**, *2*, 2861. (c) Jitsukawa, K.; Shiozaki, H.; Masuda, H. *Tetrahedron Lett.* **2002**, *43*, 1491. (d) Denmark, S. E.; Matsuhashi, H. *J. Org. Chem*. **2002**, *67*, 3479.

Chapter 3. Attempted Generation of Mono- and Bis-dioxiranes from *cis*-3,7-Dimethyl-1,5-cyclooctanedione

3.1 Introduction

Chapter 2 was focused on a molecule containing adjacent α-dioxirane groups, namely 3,3'-dimethyl-(3,3')-bidioxirane (**1**) (Figure 1). Bis-dioxirane **1** was generated from low temperature reactions of biacetyl with oxone.[1] An enhanced stability was observed in **1** compared to its mono-dioxirane counterpart, 1-(3-methyl-dioxiran-3-yl)-ethanone. This enhanced stability was attributed to a α-dioxiranyl (anomeric) effect in **1**. With a continued interest in the generation of unusual bis-dioxirane structures, we decided to study the production and stability of homochiral 1,5-bis-dioxirane **2B**. Compound **2B** contains remotely located dioxirane substituents in which through-space (transannular) interactions might become important. The transannular juxtaposition of the two dioxirane groups in **2B** represents a new type of structure in dioxirane chemistry. 1,5-Bis-dioxirane **2B** may situate its pair of dioxiranes in a *syn* orientation depending on the conformational preference, which is presently unknown. In contrast, 1,2-bis-dioxirane **1** likely situates the adjacent pair of dioxiranyl groups in an *anti* orientation. The goal was to gain new insight about the molecule's stability with respect to the position of two dioxirane groups within it.

It is worth noting that the main goal was not concerned with the oxygen-transfer chemistry of these unique dioxiranes. Many research groups are studying the synthetic applications of dioxiranes for oxygen-atom transfer reactions. However, these studies tend to neglect the underlying factors governing dioxirane stability which are largely

unexplored.[2] Thus, we sought to study bis-dioxirane **2B**, with the intent that data may emerge to provide additional understanding for bis-dioxirane stabilities relative to their mono-dioxiranes counterparts. A deeper understanding of stability may permit dioxirane units in molecules to be doubled or multiplied to produce new (and perhaps somewhat exotic) dioxirane structures.

Herein, the reaction of known *cis*-3,7-dimethyl-1,5-cyclooctanedione (**3**) with oxone will be described (Scheme 1). The homochirality of 1,5-bis-dioxirane **2B** might be useful as a mechanistic tool to follow its decomposition or rearrangement. Compound **2B**, if successfully generated, may convert to a C_2-symmetric diester, or a C_s-symmetric diester via a double Baeyer-Villiger reaction. The hydrolysis of the mono- and di-ester products to ring-opened compounds will also be studied. The potentially complicated issue of conformational dynamics available to **2A** and **2B** is of interest and will be examined.

Conformational Analysis. For generation of the eight-member rings **2A** and **2B**, a consideration of their possible conformational dynamics is required. In this regard, prior studies will be reviewed, which examine conformational dynamics of other 8-membered ring systems. 1,5-Cyclooctane-dione **4** has been studied previously experimentally and theoretically, and appears to exist mainly as two conformers: chair-chair and boat-chair (Figure 2).[3,4] The boat-chair form is predicted to be the most stable conformation according to molecular mechanics (MM2) calculations. The strain energy for the 1,5-cyclooctanedione chair-chair conformation is about 14.6 kcal/mol, whereas the boat-chair conformation is about 13.2 kcal/mol.[3] Other conformers have higher strain energies. The theoretical predictions agree with experimental data, in which IR

spectroscopy in solution and the solid state and X-ray data point to a preferred boat-chair conformation.[4-7] Based on these data, it appears that the two carbonyl groups prefer a *syn* orientation in 1,5-cyclooctanedione. Furthermore, these studies suggest that transannular interactions[8-13] are important for the structure of 1,5-cyclooctanedione. Through-space interactions may also affect the reactivity.[13]

A number of studies have been reported on the conformations of cyclooctane (**5**), both experimentally[14-19] and theoretically.[20-23] Cyclooctane **5** can adopt ten possible conformations[6] but tends to populate the boat-chair and to a lesser extent the chair-chair conformation (Figure 3). Based on the molecular mechanics (MM2) calculations, the boat-chair is lower in energy than the chair-chair conformation by 2 kcal/mol. These data agree with the experimental results, which show that the boat-chair conformation is the predominant form for cyclooctane by ^{1}H NMR, with a small (ca. 6%) fraction of another conformer of the chair-chair conformation at room temperature.[15] At the same time X-ray, IR, and Raman data in the gas phase similarly implicate the boat-chair form for **5**.[24,16]

Experimental data for the conformations of the corresponding 8-memberd ring diketone *cis*-3,7-dimethyl-1,5-cyclooctanedione **3** are somewhat sparse. However, an X-ray crystal structure of **3** has been reported in which the molecule was found to adopt a chair-boat conformation (Figure 4).[25] Apparently, the two sp^{2}-hybridized carbon atoms are located in "flagpole" positions next to each other, by which strain can be minimized that would otherwise result from transannular interactions across the ring (a reduction in strain energy has been reasoned for why the location of the two carbonyl groups are *syn* to each other). With this previous work conducted, it was surmised that the generation of

bis-dioxirane **2B** may also adopt a conformation situating the two dioxirane groups in a *syn* orientation.

3.2 Results and Discussion

3.2.1 Synthesis of Starting Material 3. *cis*-3,7-Dimethyl-1,5-cyclooctanedione (**3**) was synthesized from methyl-2,6-dimethyl-4-oxo-5,6-dihydro-4*H*-pyran-3-carboxylate (**6**) according to a literature procedure that was slightly modified (Scheme 2).[27] Compound **6** was prepared by condensation of methyl acetate with crotonyl chloride in the presence of magnesium methylate. Evidence for the formation of **6** came from a GC/MS analysis. After removal of the solvent and purification by recrystallization from hexane, an 80% yield of **6** was obtained in 95% purity.

Sodium hydroxide was added to **6** at room temperature, which led to ring opening to give the β-ketoester product **7**. β-Ketoester **8** is formed as a side product by elimination of acetic acid (the % yield of **8** was not determined). Compound **8** was neither isolated nor characterized in our reaction, although Gelin and Gelin[27] reported the isolation of **8** by distillation. Dimethyl-2,6-dimethyl-4,8-dioxocyclooctane-1,5-dicarboxylate (**9)** was obtained after 2 hours and is thought to be formed by the dimerization of β-ketoester **7** by a nucleophilic substitution mechanism.[4] Compound **7** can dimerize which is a minor route to **9** (2-6% yield); the major route gives polymers (~95%) that were not characterized. The mass spectrometry data for **9** matched well with the data of Gelin and Gelin.[27]

Dimethyl-2,6-dimethyl-4,8-dioxocyclooctane-1,5-dicarboxylate (**9**) was then acidified with an excess of hydrochloric acid to provide **3** in 80% yield. Diketone **3** was

characterized by ^{1}H NMR, ^{13}C NMR, and GC/MS spectroscopy, which matched well with the available literature data.[27].

Additional support for the assignment of **3** came from 2D NMR experiments (COSY, HSQC, and HMBC) (see Experimental Section). Compound **3** appears to possess a *cis* and not *trans* stereochemistry based on Gelin's reported data and on comparison to dimethyl cyclooctaneone NMR data. X-ray crystal structure for this compound showed that it is indeed in the *cis* configuration (Figure 5).

3.2.2 Attempted Synthesis of Mono-dioxirane 2A and Bis-dioxirane 2 via the Reaction of Oxone with 3. Oxidation of 3,7-dimethylcyclooctane-1,5-dione (**3**) by oxone in buffer solution at pH 7-8 leads to formation of the mono-dioxirane **2A**. The peaks at δ 1.05 and 1.19 ppm were detected at -17 °C (after extraction with $CDCl_3$) and disappear after decomposition with ring expansion to the monoester. The decomposition of intermediate **2A** produces the monoester, 4,8-dimethyloxonane-2,6-dione (**10**), and likely occurs via a Baeyer-Villiger rearrangement. The monoester 4,8-dimethyloxonane-2,6-dione (**10**), can be produced from intramolecular reaction of the intermediate **2A.**

It was found that ester **10** can be formed even more rapidly in the presence of an ionic liquid (1-butyl-3-methylimidazolium tetrafluoroborate) in the **3**-oxone reaction. A 50% conversion to the mono-ester form was found in a 4 h. period in the presence of an ionic liquid. The ionic liquid may facilitate the reaction because of an enhanced solubility of **3**. 4,8-Dimethyloxonane-2,6-dione ester (**10**) was formed from the reaction of **3** with oxone bicarbonate system over time. Hydrolysis of compound **10** involves

opening the ester ring to a chain form containing a hydroxyl group and a carboxylic acid functionality in compound **11** (Scheme 3).

Further oxidation of **10** with oxone bicarbonate in buffer solution was attempted, but no evidence for the formation of the C_1-symmetric diester **12** or C_s–symmetric diester **13** was obtained. Oxidation of **10** to **12** and **13** is in progress. Ester hydrolysis of **12** would be expected to produce 1-hydroxy-2-methylbutanoic acid (**14)**, while the hydrolysis of diester **13** produces two fragments, 2-methyl-1,3-dihydroxypropanediol (**15)** and 2-methyl-1,5-pentanedioic acid (**16)** (Scheme 4). Formation of **12** and **13** from bis-dioxirane **2B** can occur via a double Baeyer-Villiger rearrangement. If the rearrangements take place in the same sense **13** will be formed, while if the two dioxirane rings rearranged in the opposite sense **12** will be formed. The hydrolysis of **12** and **13** will generate different fragments; compound **14** is expected, from hydrolysis of diester **12,** and **15** is expected from hydrolysis of **13**. Compound **16** is derived from hydrolysis of diester **13**. Formation of **11, 14, 15**, and **16** will be studied to provide evidence for the diester formation. We can speculate that the absence of diester compound **12** under our reaction conditions is due to deactivation of the second ketone (after formation of **10**) through a transannual interaction. This agrees with the results obtained by Sironi and co-workers who oxidized the monoester **10** using triflouromethyl peracetic acid which gave 10 % compound **12** after 2 days.

Chemical trapping studies provided evidence for the presence of dioxirane intermediates. A quantitative study of **3** with oxone with added *trans*-stilbene showed oxygen-transfer chemistry expected of **2A** and/or **2B**. *trans*-Stilbene reacted in situ. The reaction revealed the formation of the corresponding epoxide, *trans*-2,3-diphenyl-oxirane

(67% yield), based on ^{1}H NMR data. These percent yields were determined after 4 h of stirring at –10 °C, then 8 h at room temperature.

3.2.3 Conclusion

This chapter has described the synthesis of the monoester **10** from the reaction of *cis*-3,7-dimethyl-1,5-cyclooctanedione with oxone via a Baeyer-Villiger rearrangement of the mono-dioxirane **2A**. Attempts to generate the bis-dioxirane **2B** and detect its corresponding rearranged diesters **12** and **13** are in progress.

3.3 Experimental Section

3.3.1 Materials and instrumentation

Reagents and solvents [chloroform, chloroform-*d*, oxone (monopersulfate triple salt: $2KHSO_5$, $KHSO_4$, and K_2SO_4), sodium phosphate monobasic, sodium phosphate dibasic heptahydrate, sodium sulfite (anhydrous), *trans*-stilbene, *trans*-stilbeneoxide, *trans*-crotonyl chloride, methyl acetoacetate, magnesium powder, methanol (anhydrous), magnesium methoxide 6-10 wt.% solution in methanol, benzene, diethyl ether, cyclohexane, hexane, toluene, ethanol, iodine solid, sulfuric acid concentrated, hydrochloric acid concentrated, sodium chloride, 1-butyl-3-methylimidazolium tetrafluoroborate, and sodium bicarbonate] were obtained commercially and were used as received. The purity of the reagents was checked by ^{1}H NMR and GC/MS prior to use. TLC-sheets silica gel 60 F 254 plates were used.

3.3.2 Synthesis of 5-Acetyl-2,6-dimethyl-2,3-dihydropyran-4-one 6 (Figure 6-8). This compound was prepared by two literature methods: A and B.[27] **Method A:** To a solution

of 300 mL of dry benzene in a 1 L round-bottom flask were added slowly 26 g (1.06 mol) magnesium 120 mL of anhydrous methanol and a crystal of iodine. The solution was allowed to react with gentle heating for 2 h. Methyl acetoacetate (116 g, 1.0 mol) was added dropwise under reflux for 2 h. The temperature was cooled to 0^{o}C using an ice bath, after which the solution was warmed to room temp. Crotonyl chloride (115 g, 1.1 mol) was added slowly and dropwise, and the solution was allowed to react at 0^{o}C for 4 h The solution was stirred at room temperature overnight. Concentrated sulfuric acid 20% (250 mL) was added, and the organic larger was extracted with ether. The organic layer was washed with a saturated solution of $NaHCO_3$ and NaCl, then dried over $MgSO_4$. The solvent was removed by distillation. Purification the crude product by recrystallization from hexane afforded 150 g (81.5 %) of compound **6** as yellow oil, 95% purity according to GC/MS. ^{1}H NMR spectrum (400 MHz, $CDCl_3$) was identical to the published spectrum.[26] Another product is seen by GC/MS with the same molecular weight (possibly an isomer) which is present in a minor amount. ^{1}H NMR ($CDCl_3$) δ 1.48 (d, *J* = 6.4 Hz, 3H), 2.22 (s, 3H), 2.48 (d, *J* = 8.3 Hz, 2H), 3.81 (s, 3H), 4.57 (m, 1H) (Figure 5). ^{13}C NMR ($CDCl_3$) δ 20.14, 20.40, 42.36, 51.92, 75.68, 111.93, 166.07, 177.48, 188.05. MS *m/z* 184 (M+).[28]

Method B: To a solution of toluene (400 mL) and methyl acetoacetate (50 mL, 0.47 mol) in a 1 L flask equipped with an addition funnel was added magnesium methoxide (750 mL of 8-10 wt % solution in MeOH) (0.57 mol). After the addition was complete, the excess methanol was removed by distillation. The reaction mixture was heated at reflux for 2 h, then cooled to 0^{o}C in an ice bath. *trans*-Crotonyl chloride (48 mL, 0.49 mol) was added slowly, and the solution was allowed to react 4 h at -5^{o}C and stirred

overnight at room temperature. This method gave 55 g (60%) yield of product **6**. The crude product was purified by flash chromatography using hexane:ethyl acetate (5:4).

3.3.3 Preparation of Dimethyl (2*S*,6*S*)-2,6-Dimethyl-4,8-dioxocyclooctane-1,5-dicarboxylate (9) (Figure 9-14). 5-Acetyl-2,6-dimethyl-2,3-dihydropyran-4-one (**6**) 52.9 g (0.23 mol) was added to a 250 mL of an aqueous solution of sodium hydroxide (1 N) at room temperature. After 2 h a precipitate formed. After extraction 4 times with 50 mL of diethyl ether, and evaporation of the ether a residue was obtained. Hot ethanol (50 mL) was added, and the solution was stored overnight, and white crystals were isolated. The crystals were washed with cold ethanol. Then the crystals were recrystallized in alcohol (ethanol) to afford 2 g of compound **9** (4 % yield). Mass spectral fragments are shown in (Scheme 5). After product **9** was recrystallized from ethanol, GC/MS showed that it was still impure; 60% purity, but we used it as it is for the next step. ^{1}H NMR ($CDCl_3$) δ 1.12 (d, *J* = 6.6 Hz, 6H), 3.35 (d, *J* = 10.5 Hz, 2H), 3.71 (s, 6H), 2.93 (m, 2H), 2.65 (d, *J* = 6.9 Hz, 4H). ^{1}H NMR ($CDCl_3$) spectrum was identical to the published spectrum[27] MS: *m/z* 284 (M+), 253 [(M+) – OCH_3], 221 [(M+)- 2(OCH_3)], 127, 156, 169.

(3*S*,7*S*)-3,7-Dimethyl-1,5-cyclooctanedione (3) (Figure 15-20). After a solution of (2*S*,6*S*)-dimethyl 2,6-dimethyl-4,8-dioxocyclooctane-1,5-dicarboxylate **9** (3.0 g, 10.0 mmol), in 50 mL of 3 M HCl was refluxed for 4 h, the solution was cooled to room temperature. The organic layer was extracted with ether 3 times, and the solvent was evaporated by rotary evaporation leaving 2.7 g of a white solid. The crude product was recyrstallized from cyclohexane. The product was characterized by GC/MS *m/z* 168 (M+). ^{1}H NMR ($CDCl_3$) δ 1.1 (d, *J* = 6 Hz, 6 H), 2.38-2.7 (m, 10 H). ^{13}C NMR ($CDCl_3$)

δ 22.82, 32.33, 50.97, 212.38. DEPT 135, 50.9 (CH_2), 32.3 (CH_3), 22.8 (CH). MS *m/z* 168 (M^+), 126, 98, 69 (Scheme 6). HMBC data show a long rang correlation of the methyl peaks (1.1 ppm) with the methylene carbon (50 ppm) and also with the carbonyl carbon (212).

3.3.5 Oxone experiment:

3.3.5.1 Synthesis of the monoester (4R,8S)-4,8-dimethyloxonane-2,6-dione (10) (Figure 21-24). To a cold stirred solution at -5 ^oC in 15 mL of sodium phosphate buffer (pH 7.8), 10 mL of acetonitrile and 0.2 g (1.0 mmol) **2** of in a three neck round bottom flask equipped with an addition funnel, were added a mixture of oxone (5.8 g, 9.0 mmol) and sodium bicarbonate (2.6 g, 31.0 mmol) in a period of 30 min. The reaction mixture was stirred for 2 h in a salt ice bath, and then for 2 days at room temperature. The solution was filtered and the organic layer was extracted with dichloromethane. The organic layer was dried over anhydrous magnesium sulfate and concentrated under vacuum. Analysis of the residue by GC/MS showed the conversion of the starting material to monoester **10**. Yield was 0.18 g (90%) of **10** as a yellow oil, (purity >95

^1H NMR ($CDCl_3$) δ 0.92 (d, *J* = 6.8 Hz, 3 H), 1.03 (d, *J* = 6.6 Hz, 3H), 1.96 (t, *J* = 13.5 Hz, 1H), 2.11 (t, *J* = 12.5 Hz, 2H), 2.38 (t, *J* = 12.2 Hz, 1H), 2.40 (d, *J* = 13.5 Hz, 1H), 2.44 (d, *J* = 13.3 Hz, 1H), 2.47-2.65 (m, 2H), 3.73 (t, *J* = 11.26 Hz, 1H), 4.18 (dd, *J* = 6.2 Hz, 10.7 Hz, 1H). ^{13}C NMR 17.30, 23.10, 31.07, 34.89, 42.04, 50.39, 67.86, 171.63, 212.21 (Figure 20-23).

3.3.5.2 Low temperature NMR to attempt to detect intermediate 2A. To a cooled solution of *cis*-3,7-dimethyl-1,5-cyclooctanedione (**3**) (0.1 g, 0.6 mmol) in 5 ml $CDCl_3$ and 5 mL buffer solution were added a mixture of oxone (0.5 g 0.8 mmol) and sodium

bicarbonate (0.25 g, 2.9 mmol) over a period of 1 h. After the reaction the mixture was stirred at -5 ^{o}C for 1 h and the organic layer was separated in a cold separatory funnel and the organic layer was dried over magnesium sulfate and stored in the freezer. The ^{1}H NMR spectrum was recorded at – 10 ^{o}C. ^{1}H NMR (**2A)** ($CDCl_3$) δ 1.05 (d, J = 6 Hz, 3H), 1.19 (d, J = 6.2 Hz, 3H).

3.3.5.3 Epoxidation of *trans*-stilbene. An epoxidation reaction was conducted as follows: To a 5 mL solution of buffer pH 9.8 (from 5 mL concentrated acetic acid and 100 mL 0.1 M solution of potassium carbonate) and 3 mL of ionic liquid (1-butyl-3-methylimidazolium tetrafluoroborate) were added a solution of *trans*-stilbene (10.0 mg, 60.0 μmol) in 5 mL of acetonitrile. The solution was stirred for 5 min, then a solution of cis-4,8-dimethyloxacyclooctane-2,6-dione **3** in 2 mL acetonitrile was added to the solution mixture. The solution mixture was cooled to 0^{o}C. A mixture of oxone (0.73 g, 1.0 mmol) and potassium carbonate (0.28 g) were added to the solution slowly. The reaction mixture was stirred in an ice bath for 2 h and then at room temperature for 2 days. The formation of the product was followed by TLC. The organic layer was extracted and washed five times with deionized water and dried over magnesium sulfate. The product was analyzed by ^{1}H NMR to show *trans*-stilbene oxide formation. The ^{1}H NMR spectrum of the *trans*-stilbene oxide sample was compared with that of the commercial sample.

Figure 1

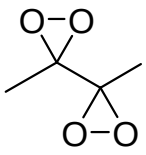

1

achiral
bis-dioxirane

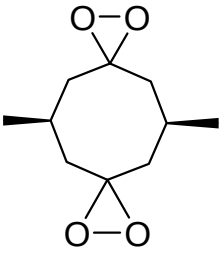

2B

homochiral
bis-dioxirane

Figure 2

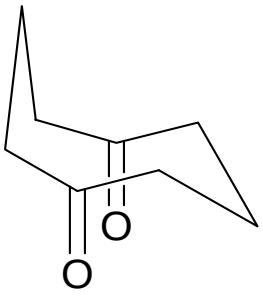

4
boat-chair

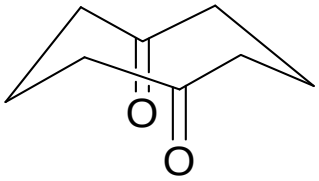

4
chair-chair

Figure 3

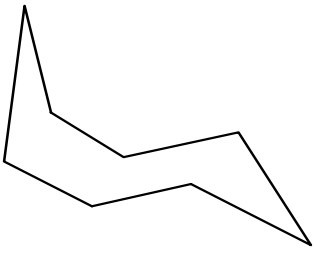

5
boat-chair

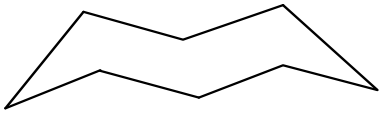

5
chair-chair

Figure 4

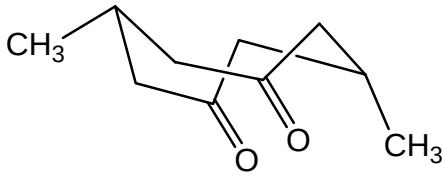

3

Figure 5

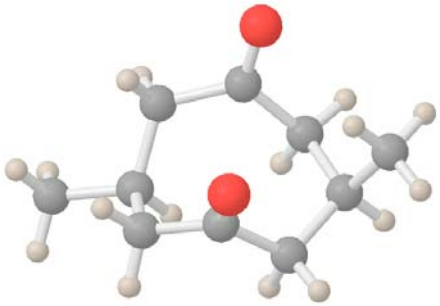

X-ray structure of **3** (dark gray = oxygen, medium gray = carbon, light gray = hydrogen)

Scheme 1

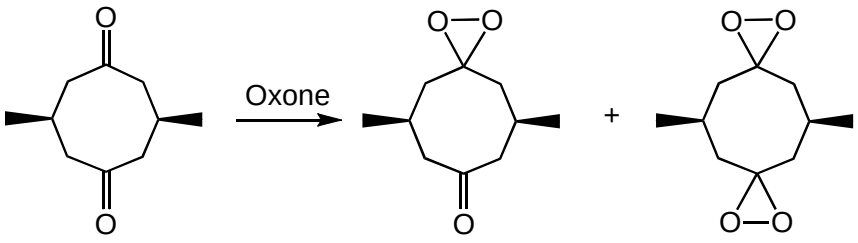

3 mono-dioxirane **2A** bis-dioxirane **2B**

Scheme 2

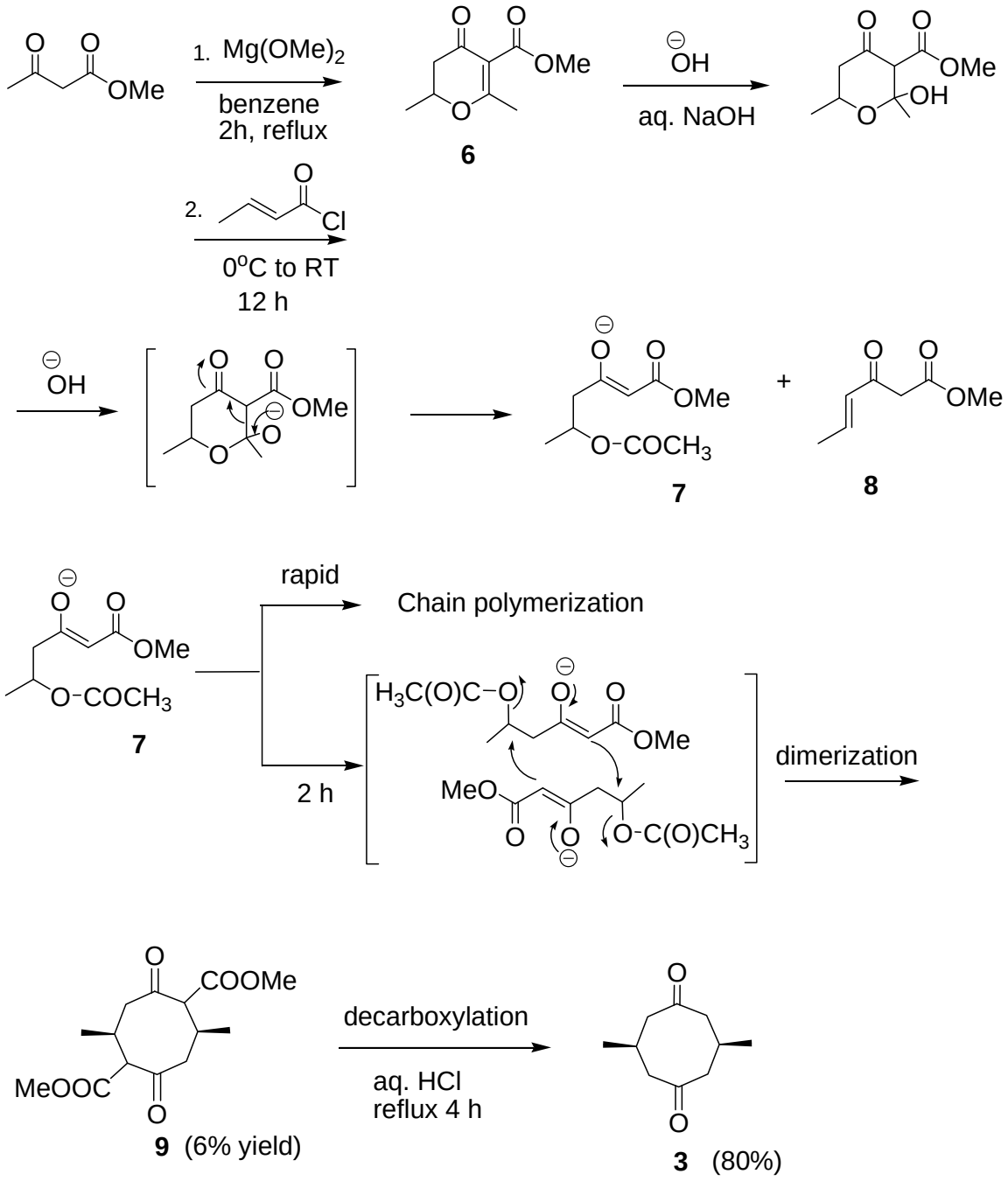
1. Mg(OMe)2
benzene
2h, reflux
2.
0°C to RT
12 h
OH
aq. NaOH
6
7
8
rapid
Chain polymerization
2 h
dimerization
decarboxylation
aq. HCl
reflux 4 h
9 (6% yield)
3 (80%)

Scheme 3

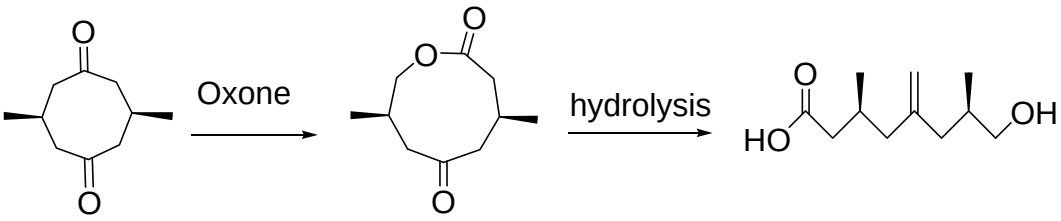

3 **10** **11**

Scheme 4

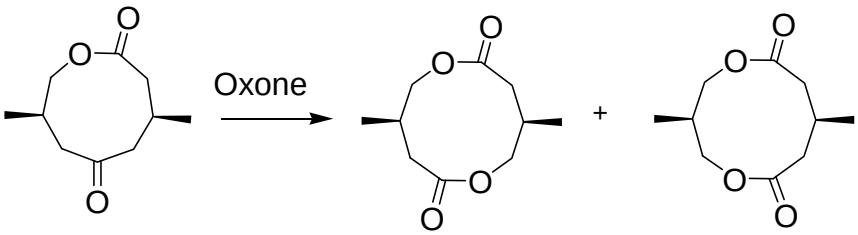

10 **12** **13**

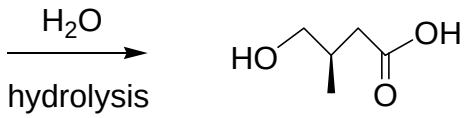

14

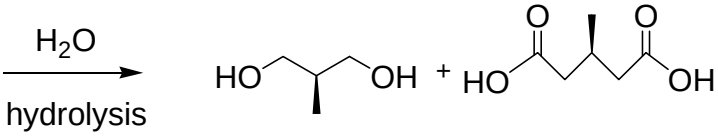

15 **16**

Scheme 5. MS fragmentation of **9**

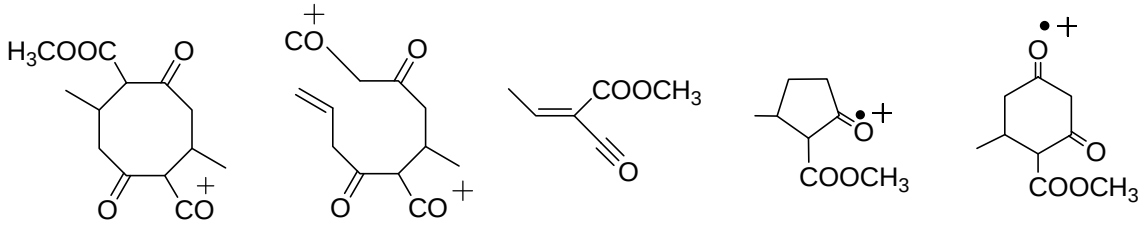

253 m/z 221 m/z 127 m/z 156 m/z 169 m/z

Scheme 6

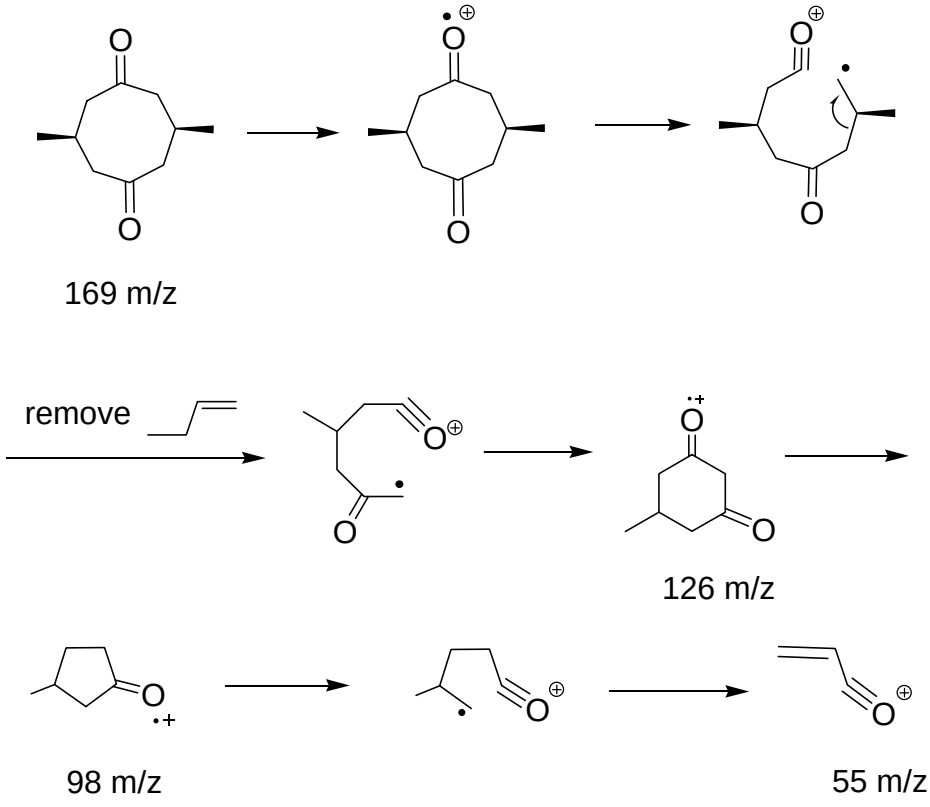

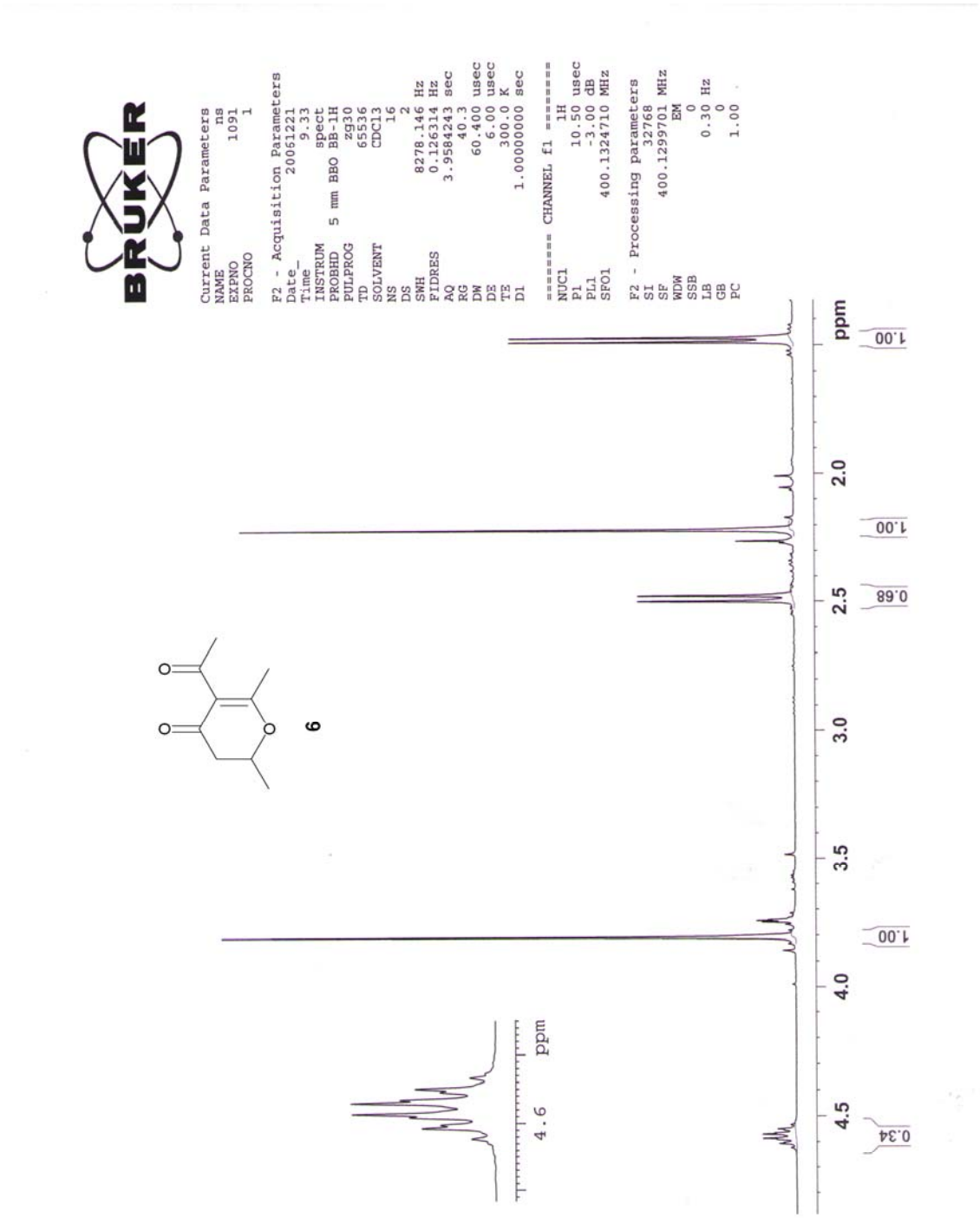

Figure 6. ^{1}H NMR spectrum of methyl 2,6-dimethyl-4-oxo-5,6-dihydro-4H-pyran-3-carboxylate (**6**).

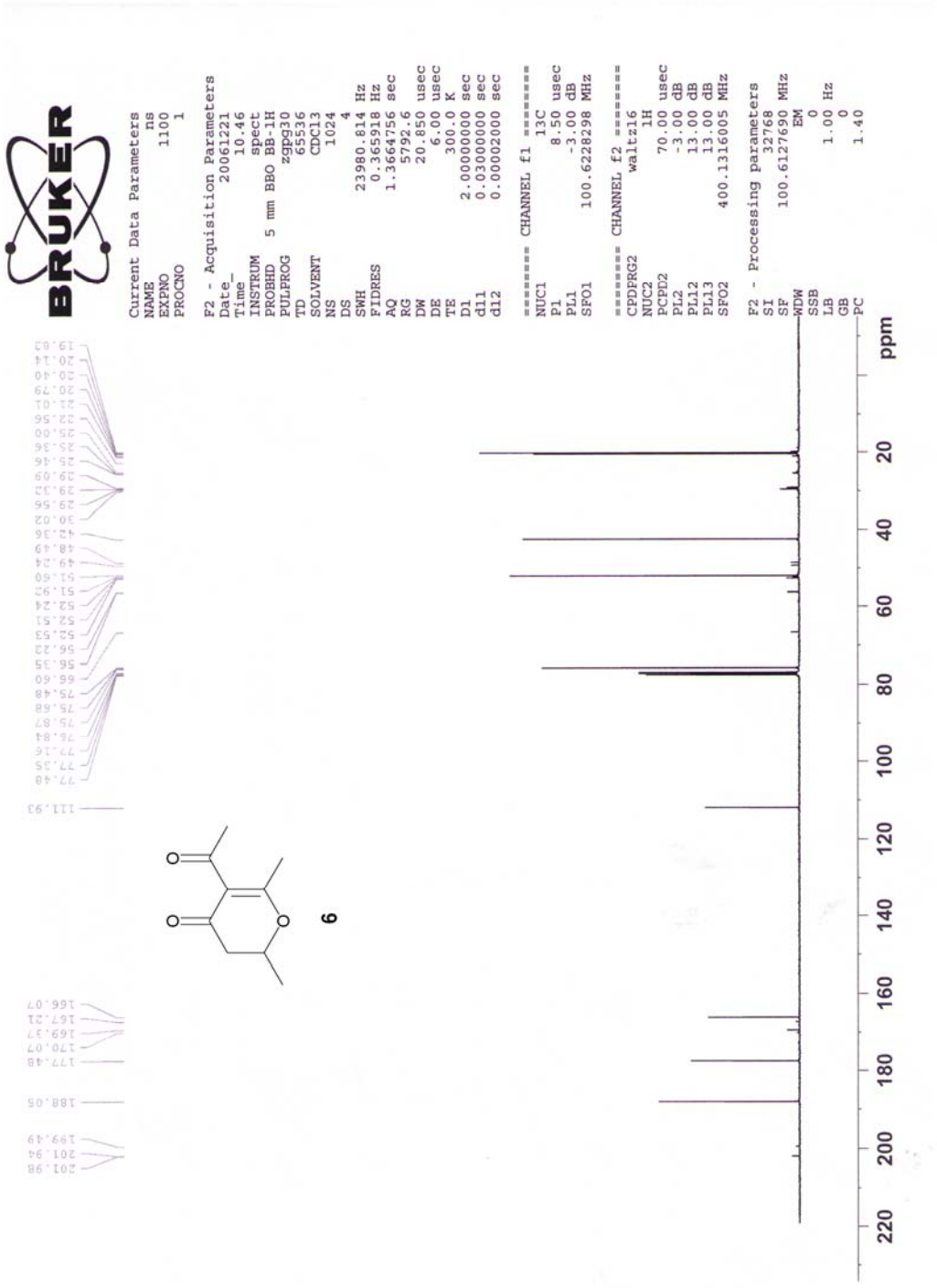

Figure 7. ^{13}C NMR spectrum of methyl 2,6-dimethyl-4-oxo-5,6-dihydro-4H-pyran-3-carboxylate (**6**).

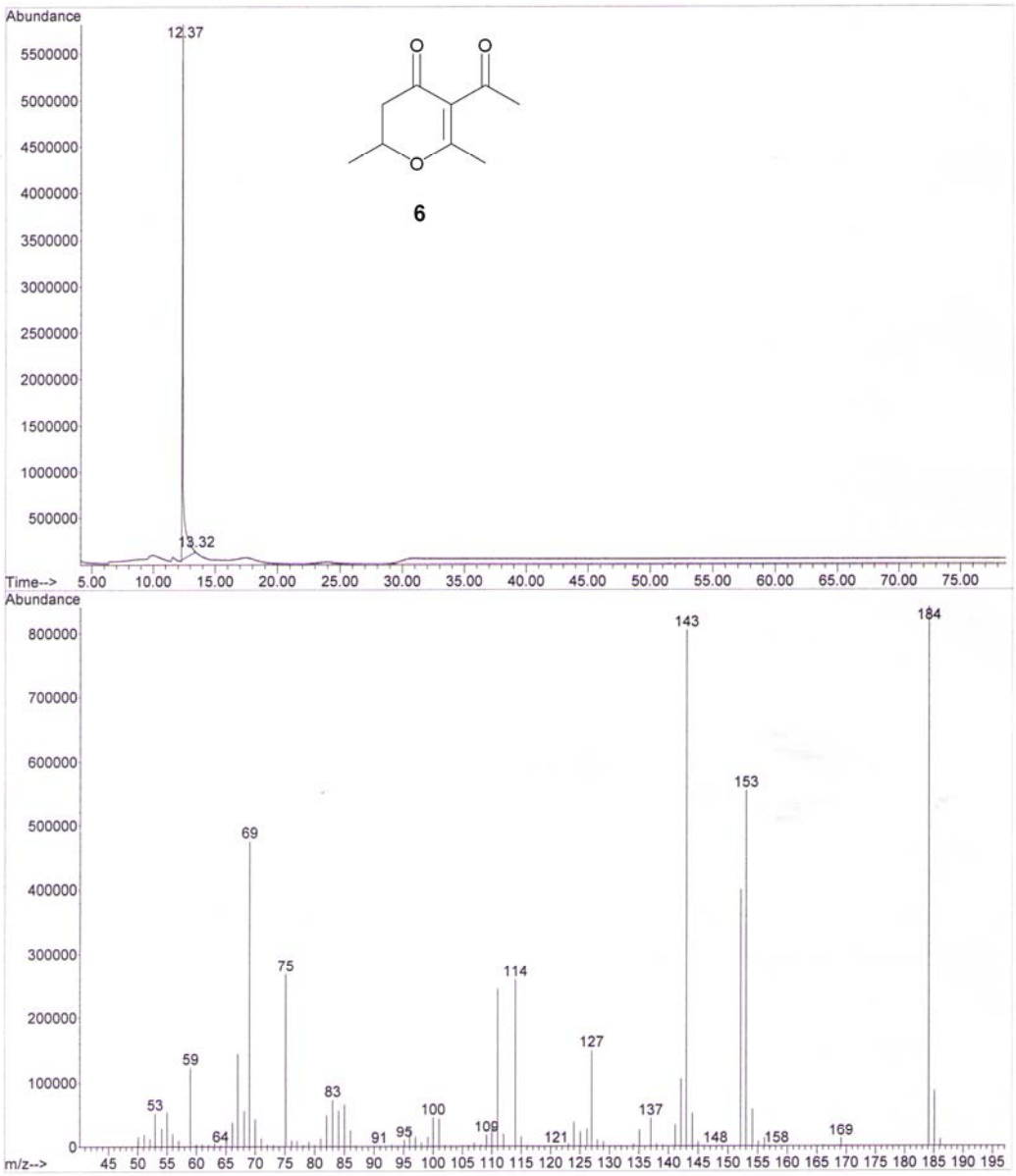

Figure 8. GC/MS of methyl 2,6-dimethyl-4-oxo-5,6-dihydro-4H-pyran-3-carboxylate (**6**).

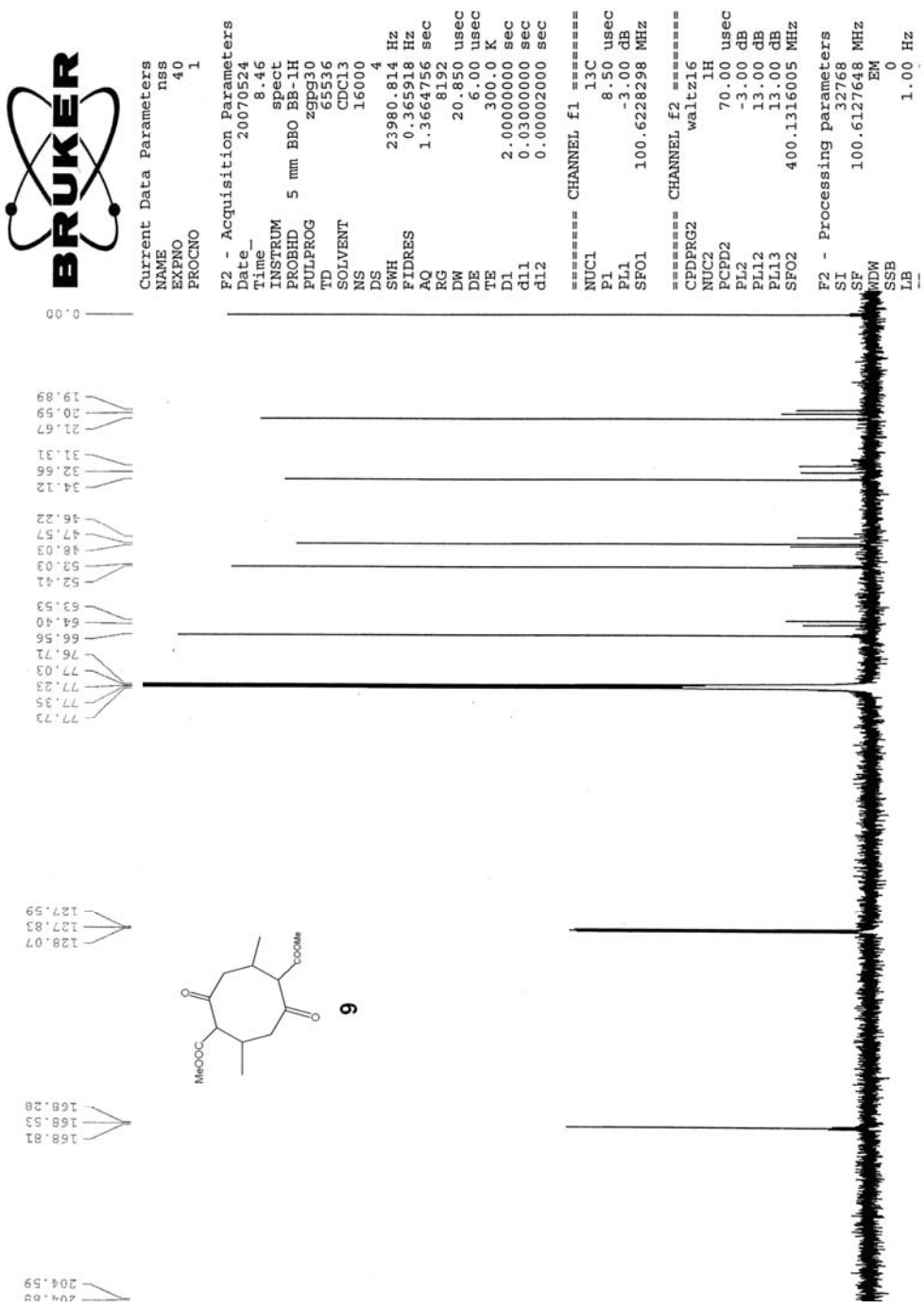

Figure 9. ^{13}C NMR spectrum of dimethyl 2,6-dimethyl-4,8-dioxocyclooctane-1,5-dicarboxylate (**9**)**.**

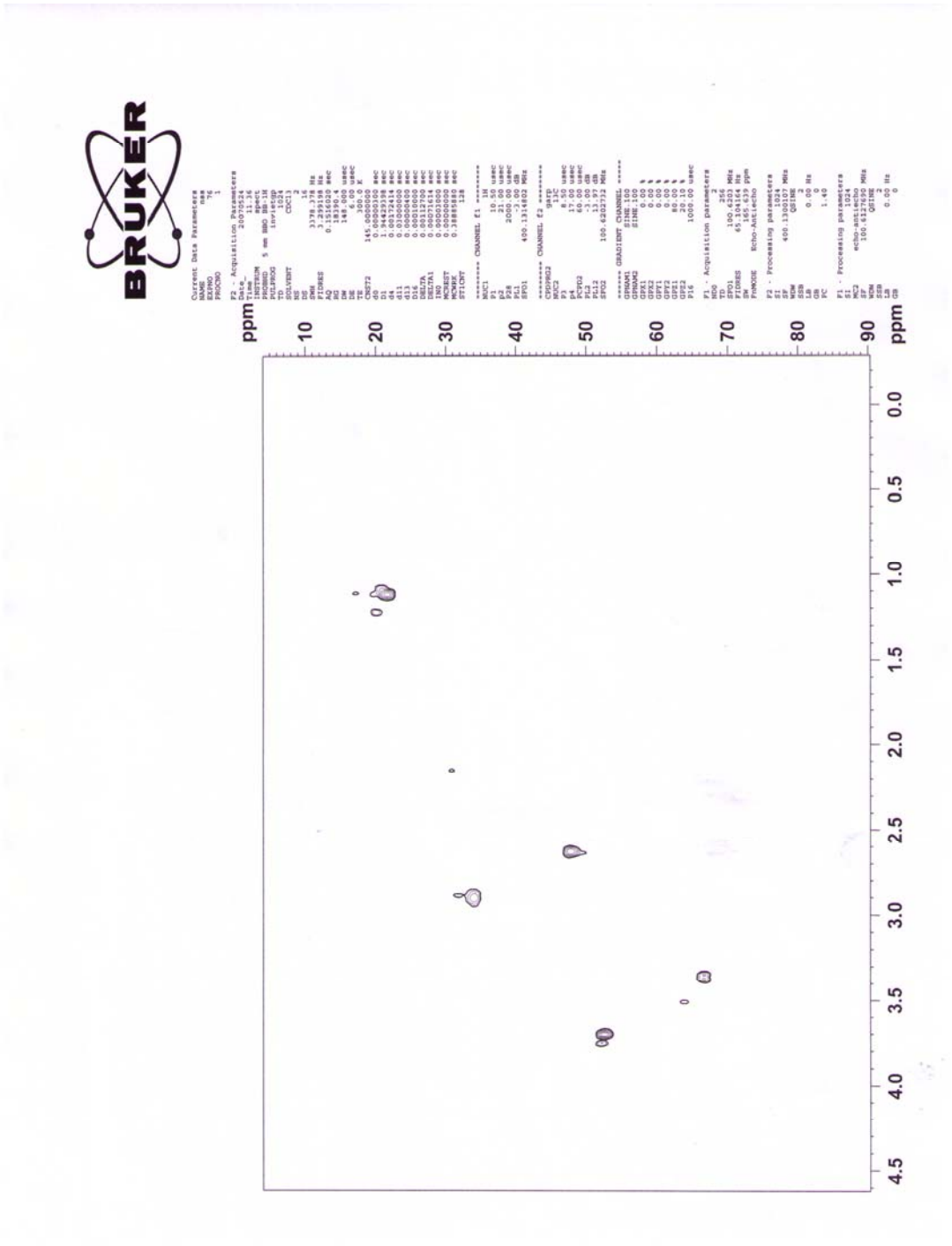

Figure 10. HSQC of dimethyl 2,6-dimethyl-4,8-dioxocyclooctane-1,5-dicarboxylate (**9**).

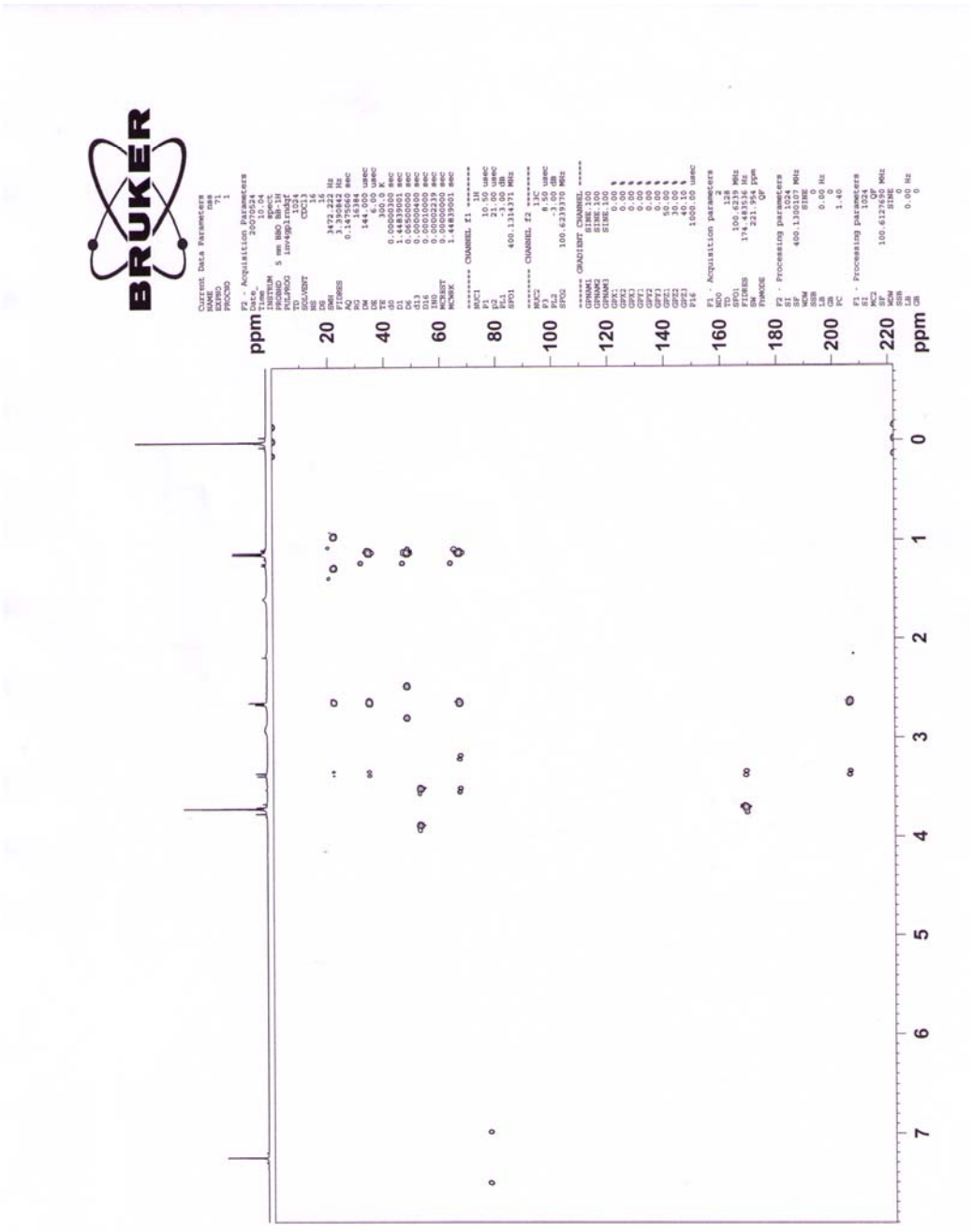

Figure 11. HMBC of dimethyl 2,6-dimethyl-4,8-dioxocyclooctane-1,5-dicarboxylate (**9**).

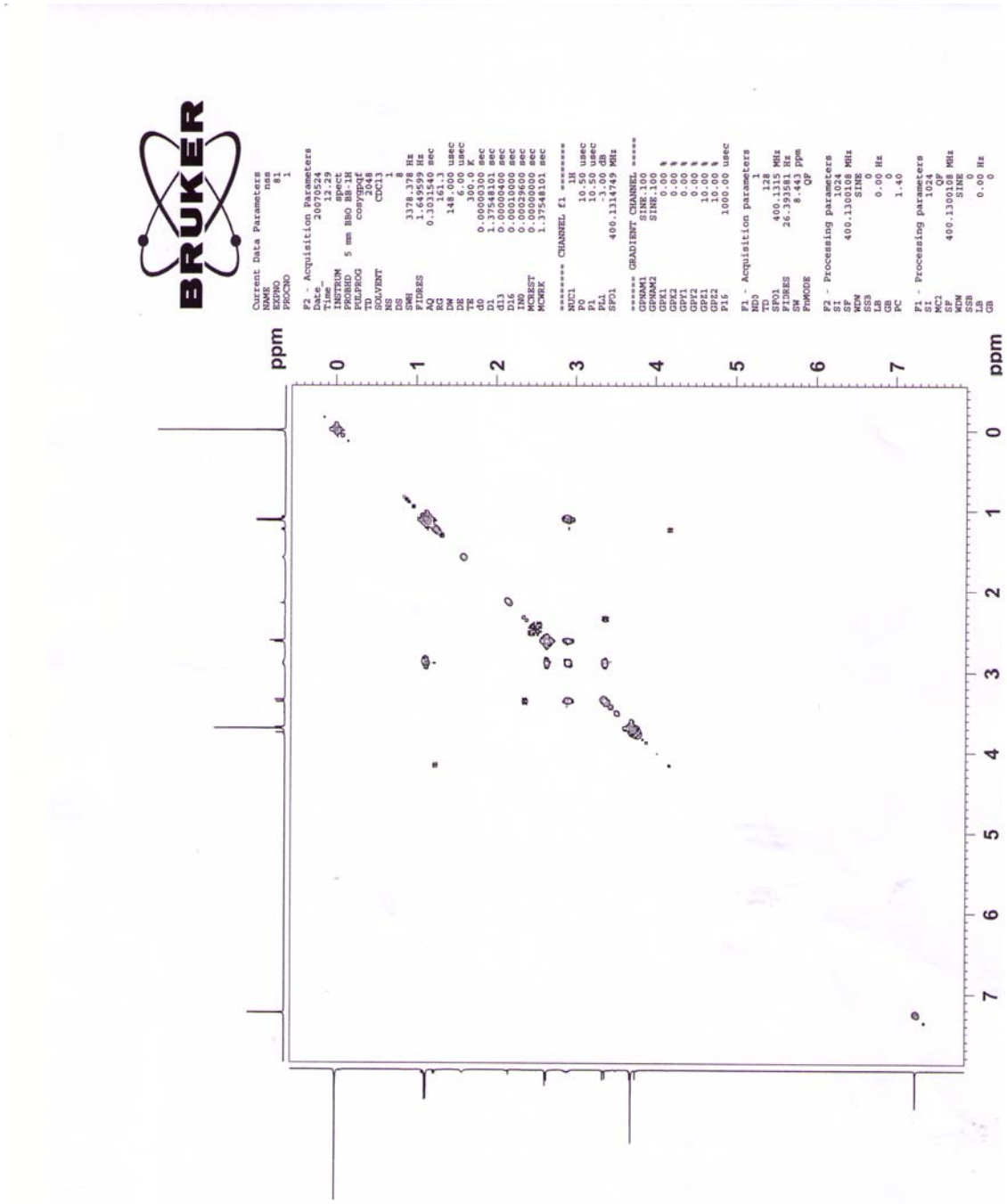

Figure 12. cosy NMR spectrum of dimethyl 2,6-dimethyl-4,8-dioxocyclooctane-1,5-dicarboxylate (**9**).

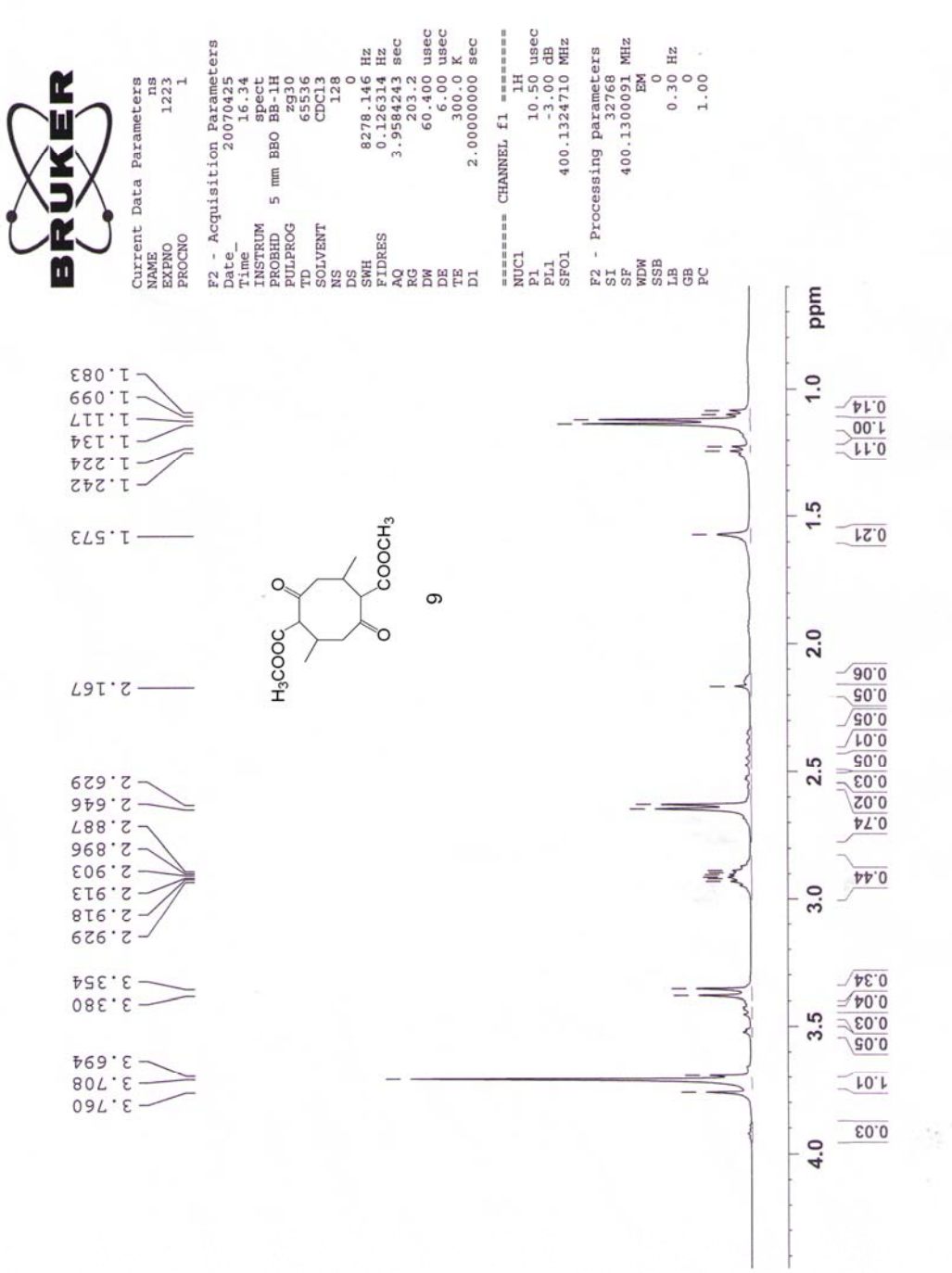

Figure 13. ^{1}H NMR spectrum of dimethyl 2,6-dimethyl-4,8-dioxocyclooctane-1,5-dicarboxylate (**9**)**.**

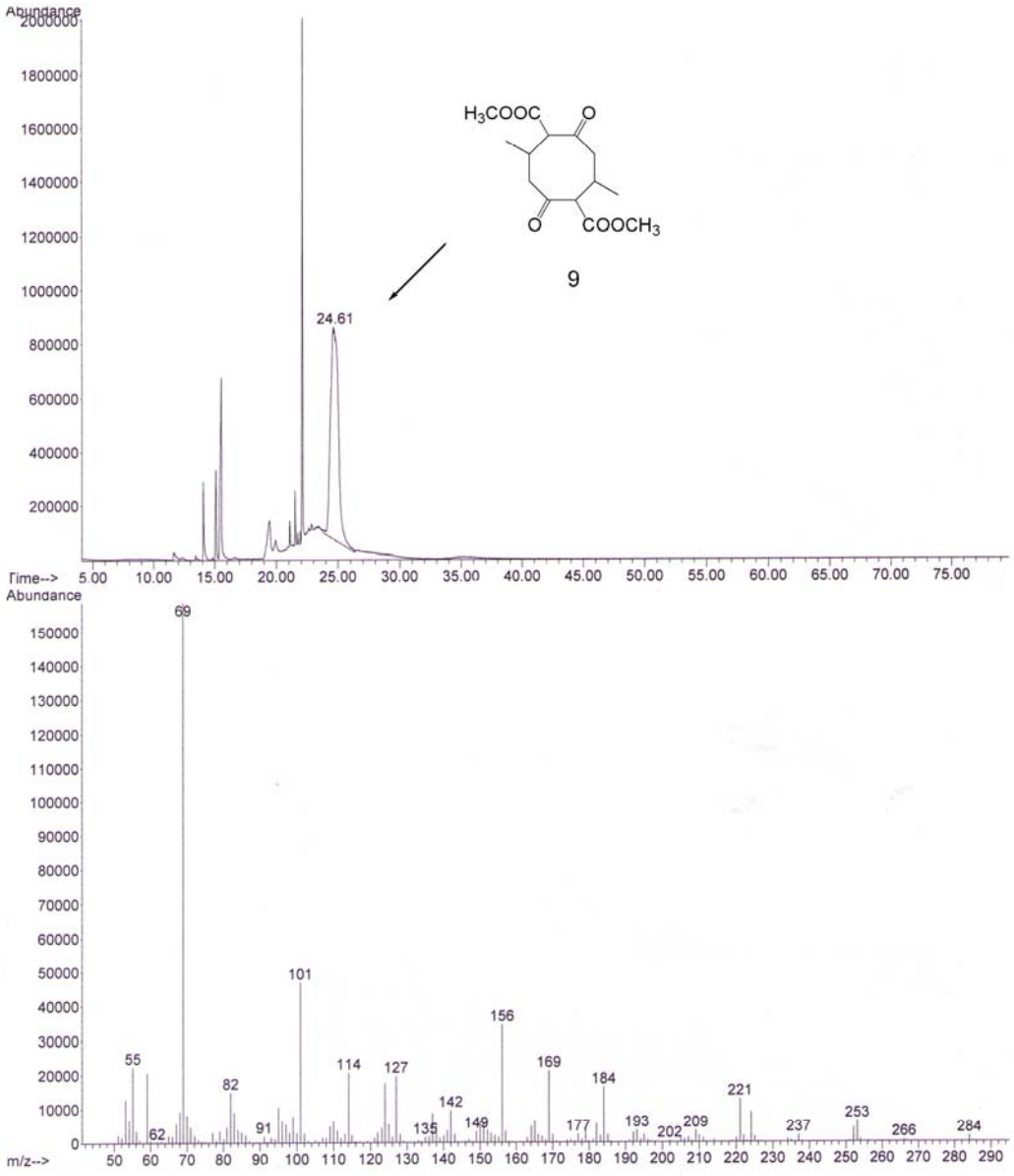

Figure 14. GC/MS of dimethyl 2,6-dimethyl-4,8-dioxocyclooctane-1,5-dicarboxylate (**9**).

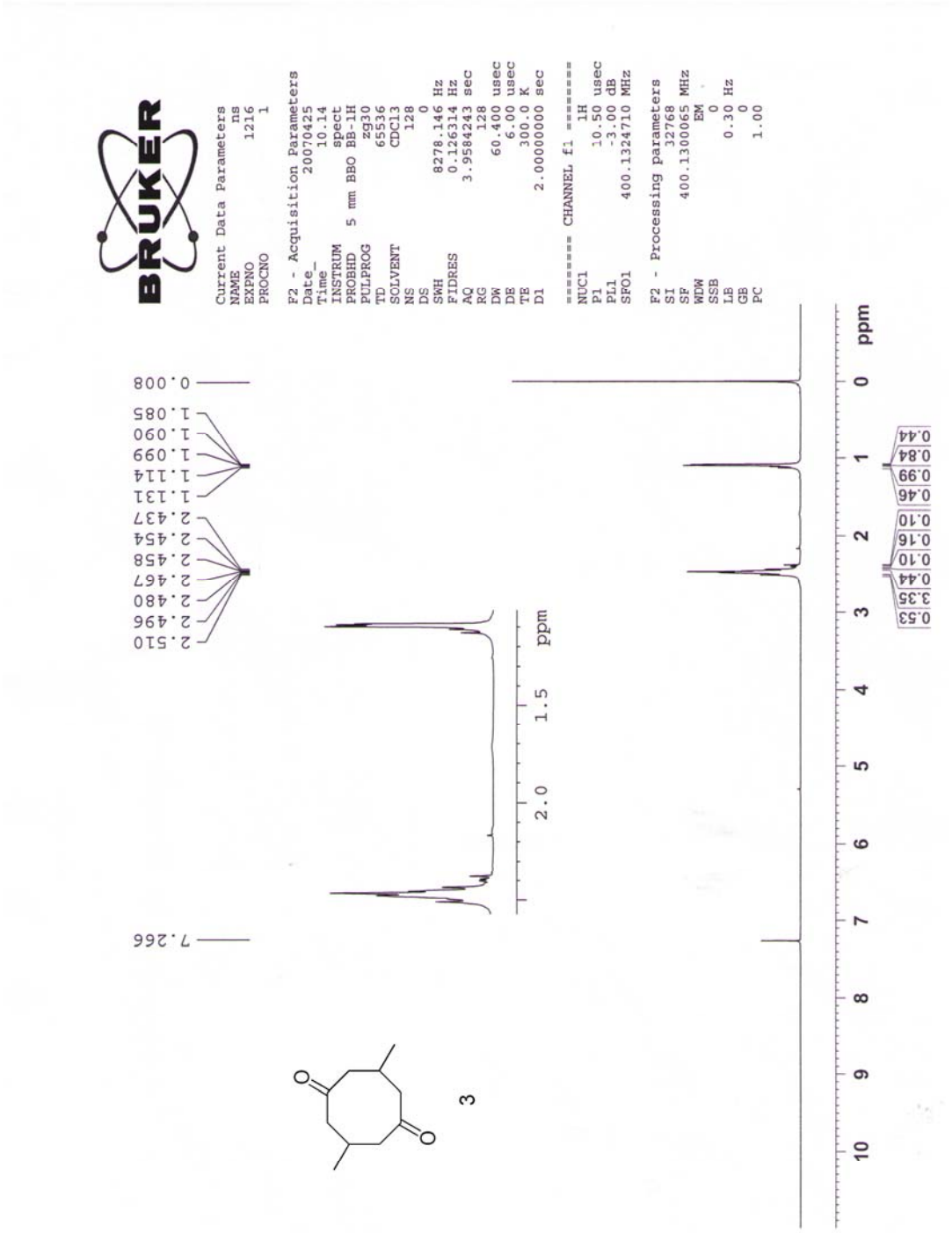

Figure 15. ^{1}H NMR spectrum of 3,7-dimethylcyclooctane-1,5-dione (**3**).

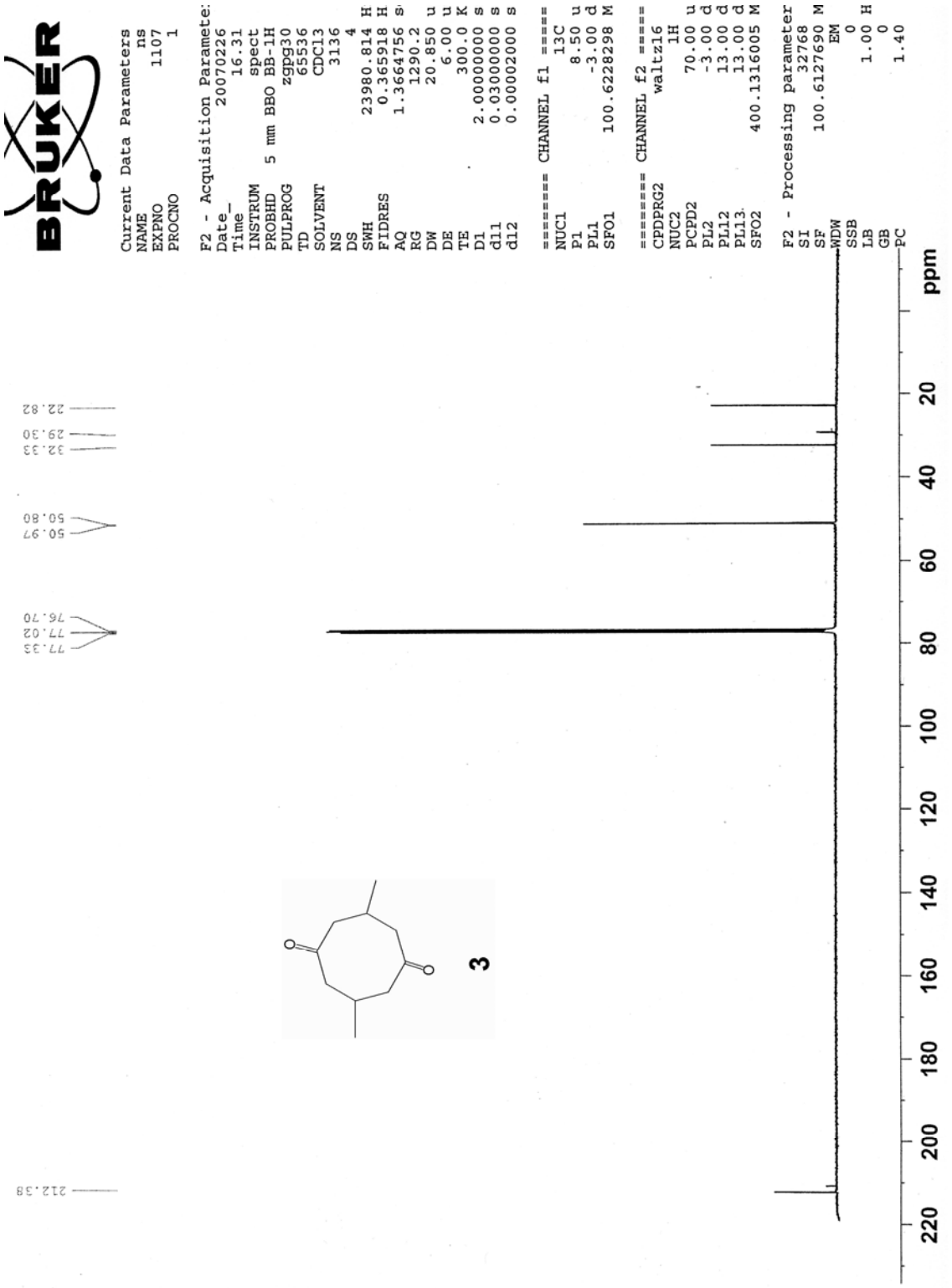

Figure 16. ^{13}C NMR spectrum of 3,7-dimethylcyclooctane-1,5-dione (**3**).

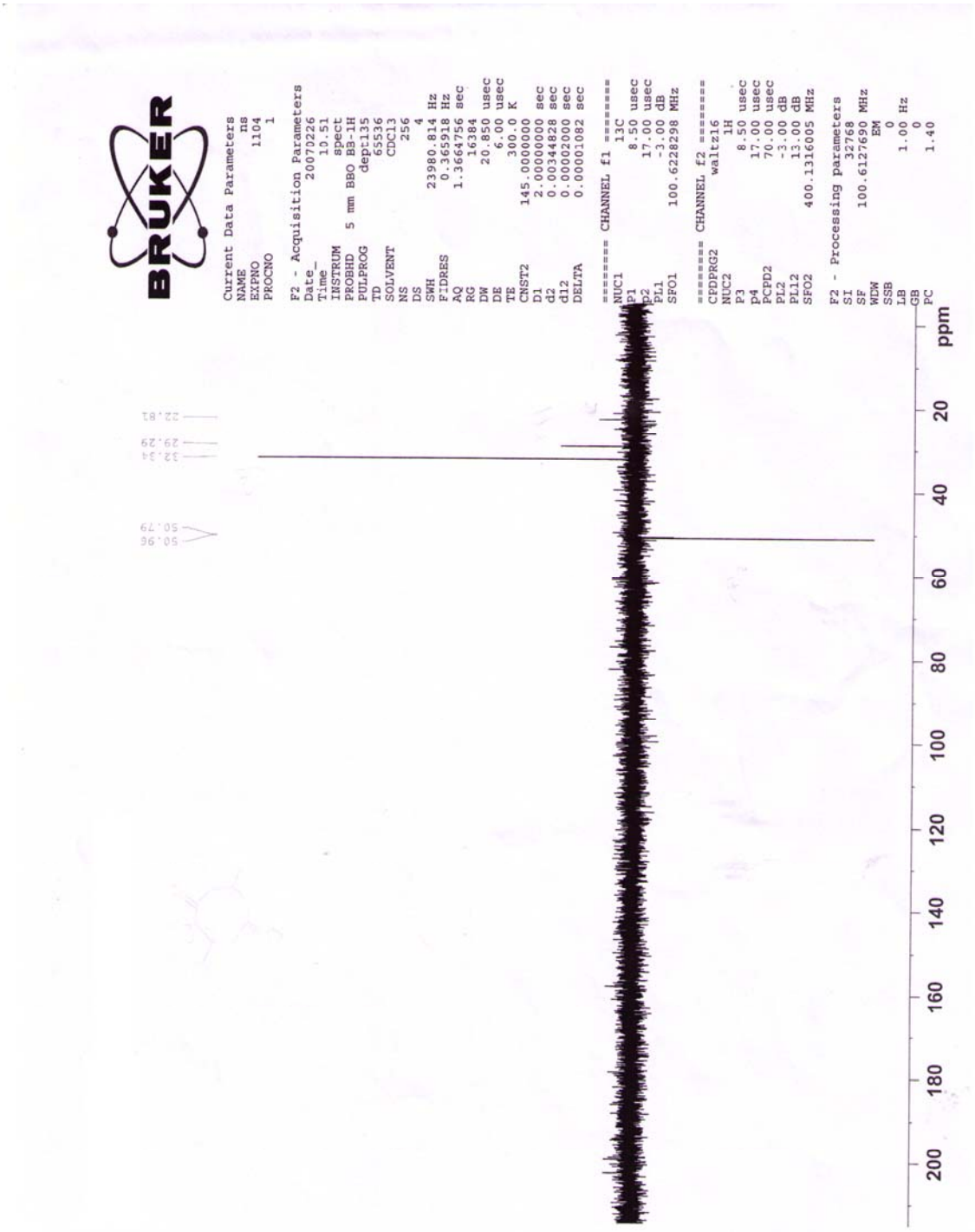

Figure 17. DEPT 135 NMR spectrum of 3,7-dimethylcyclooctane-1,5-dione (**3**).

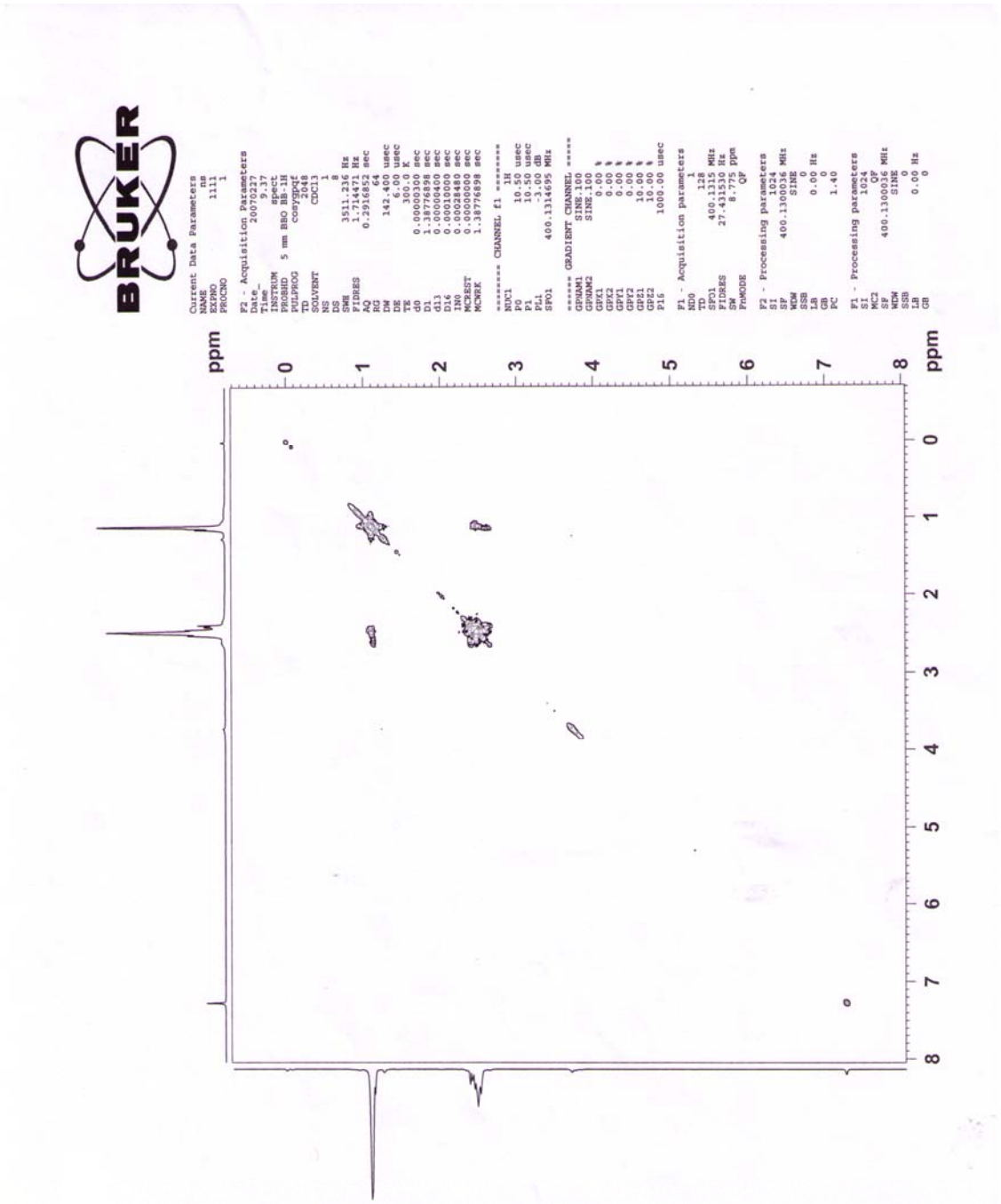

Figure 18. cosy NMR spectrum of 3,7-dimethylcyclooctane-1,5-dione (**3**).

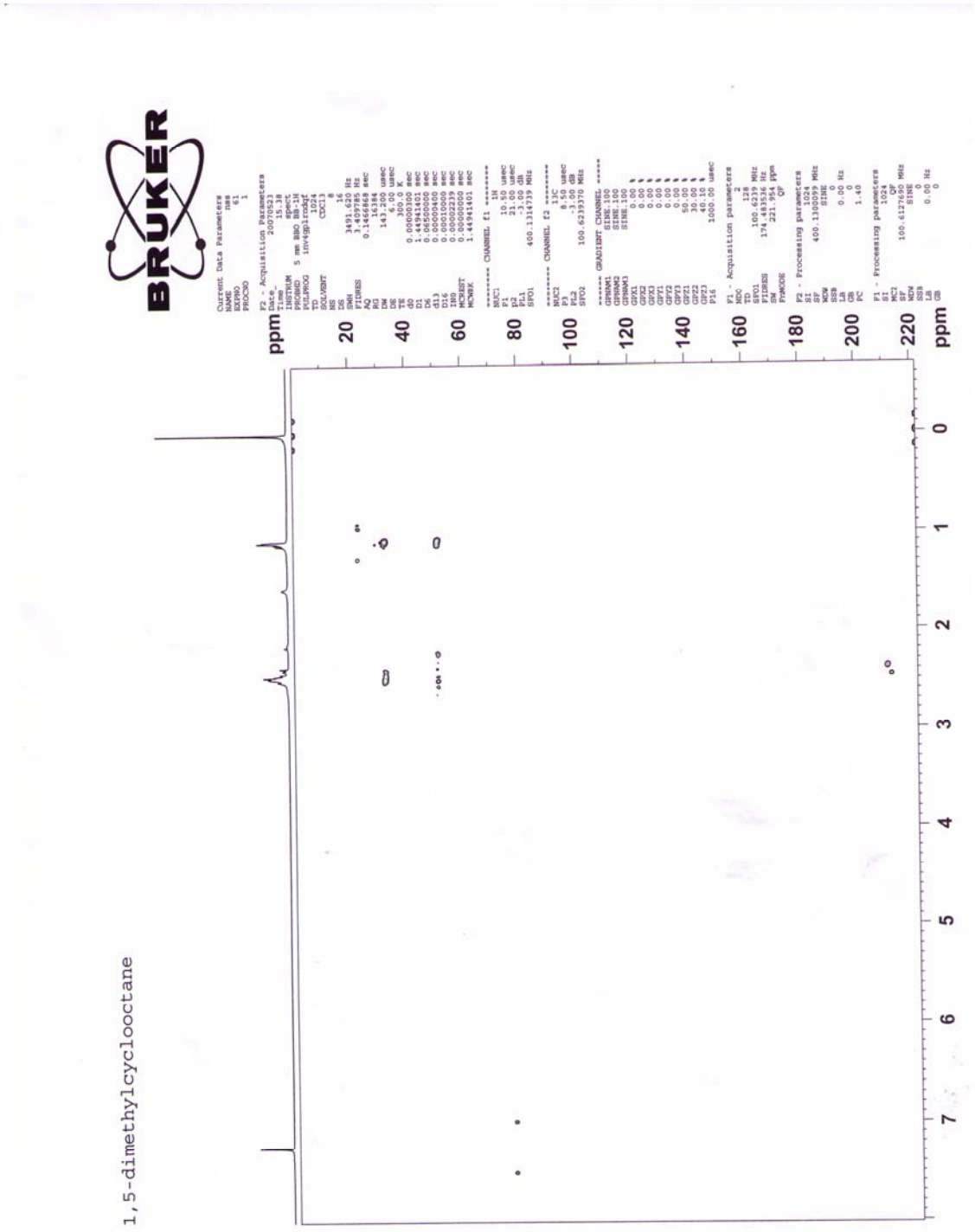

Figure 19. HMBC spectrum of 3,7-dimethylcyclooctane-1,5-dione (**3**).

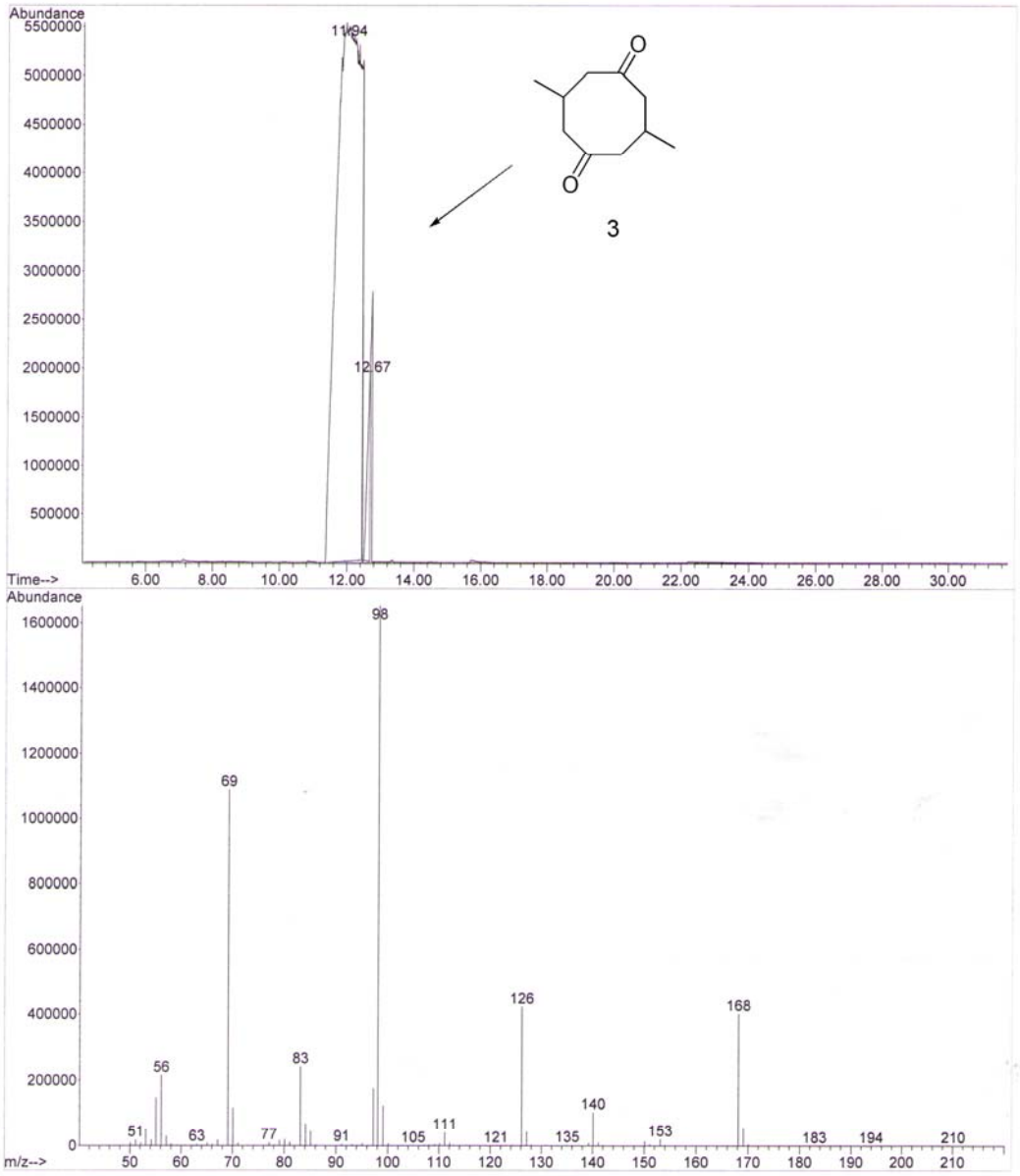

Figure 20. GC/MS spectrum of 3,7-dimethylcyclooctane-1,5-dione (**3**).

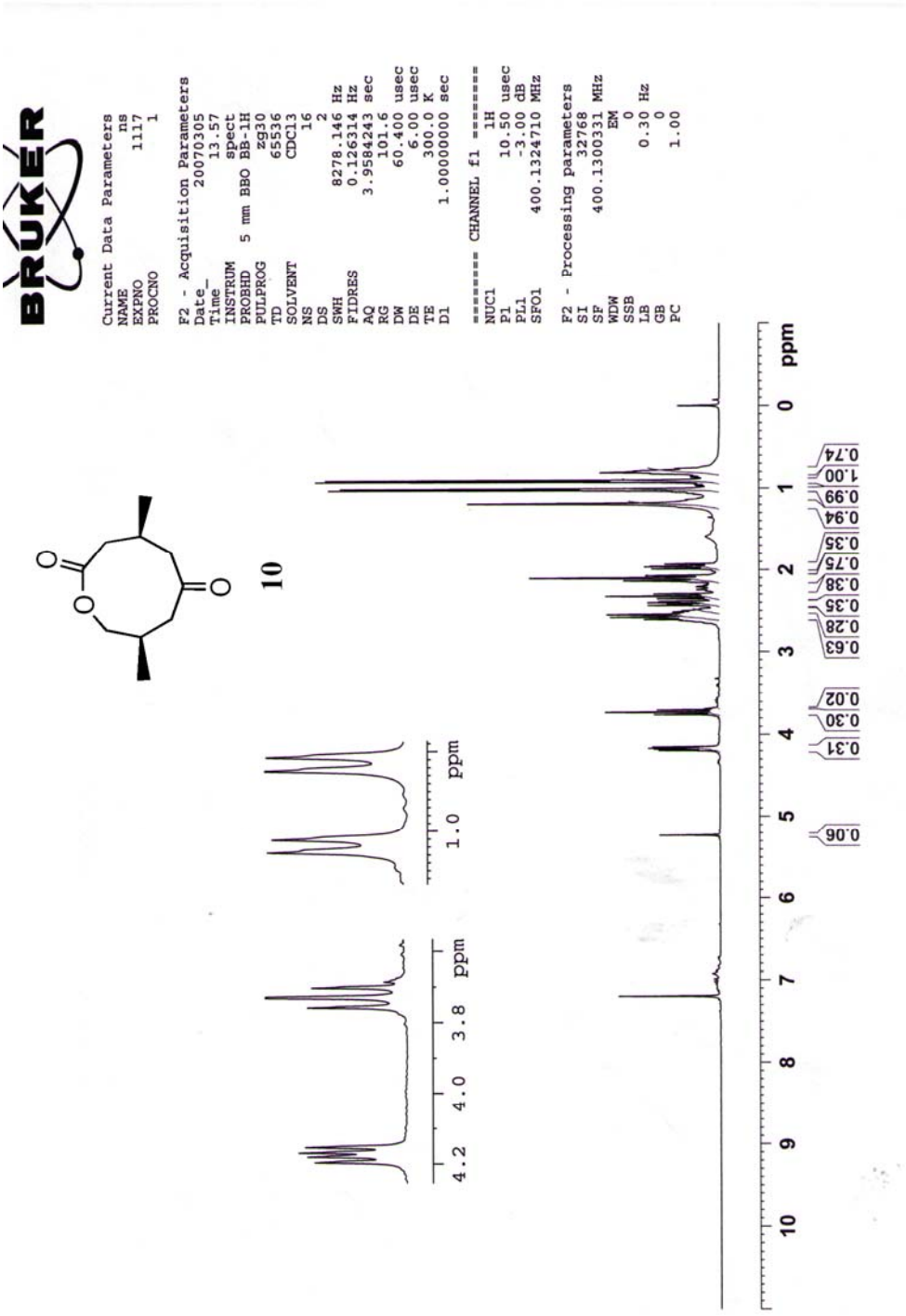

Figure 21. ^{1}H NMR spectrum of 4,8-dimethyloxonane-2,6-dione (**10**).

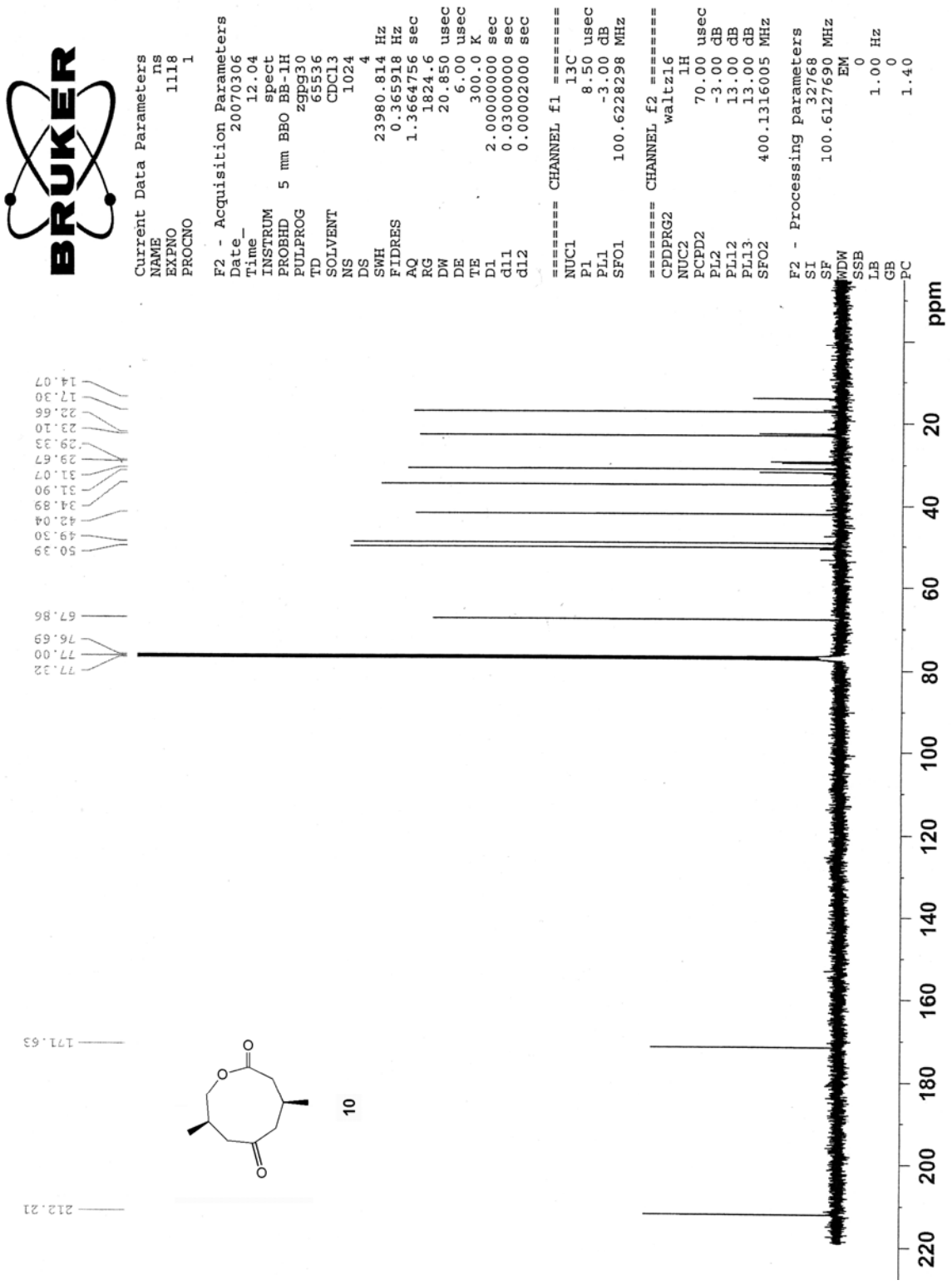

Figure 22. ^{13}C NMR spectrum of 4,8-dimethyloxonane-2,6-dione (**10**).

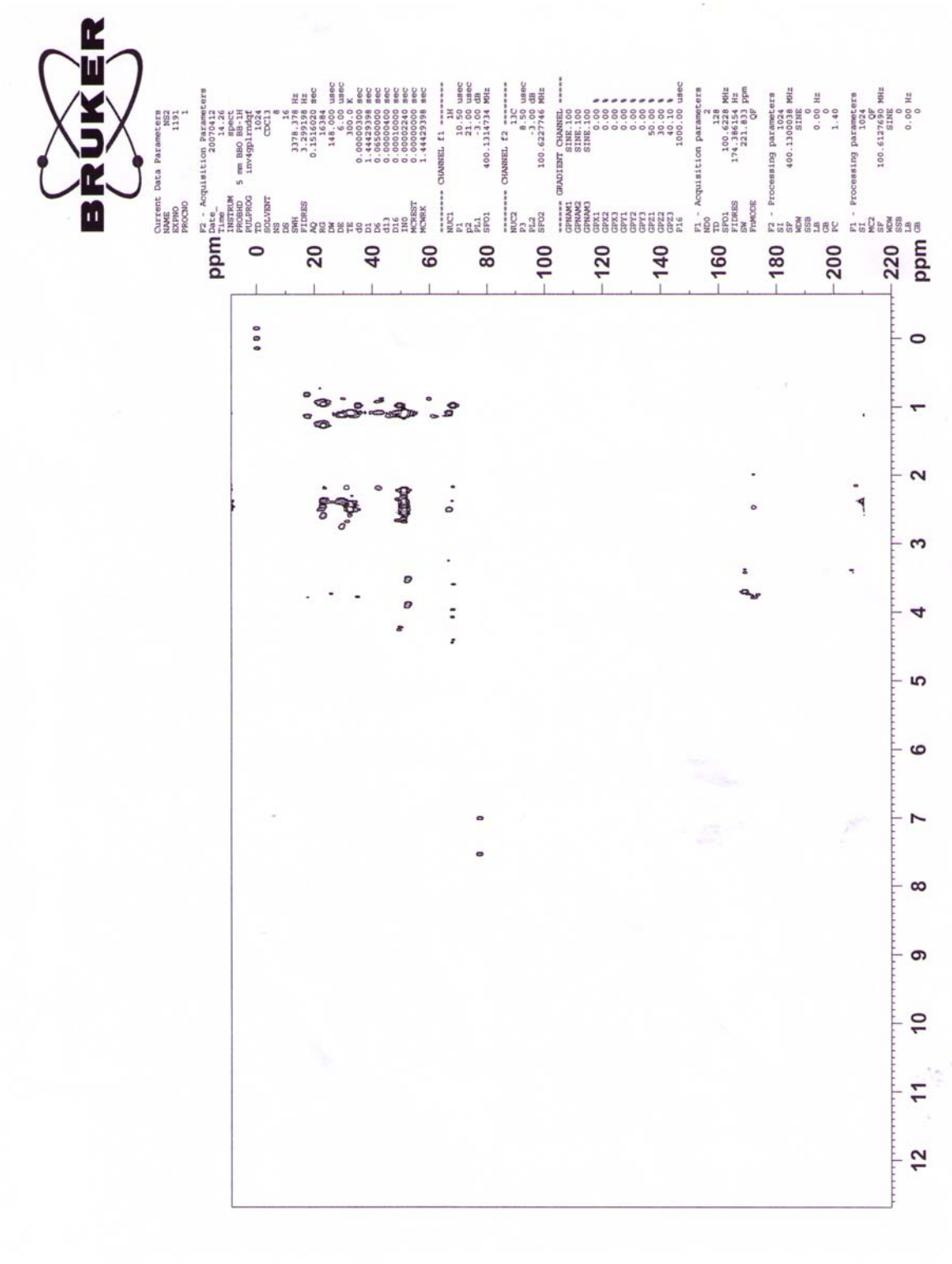

Figure 23. HMBC spectrum of 4,8-dimethyloxonane-2,6-dione (**10**).

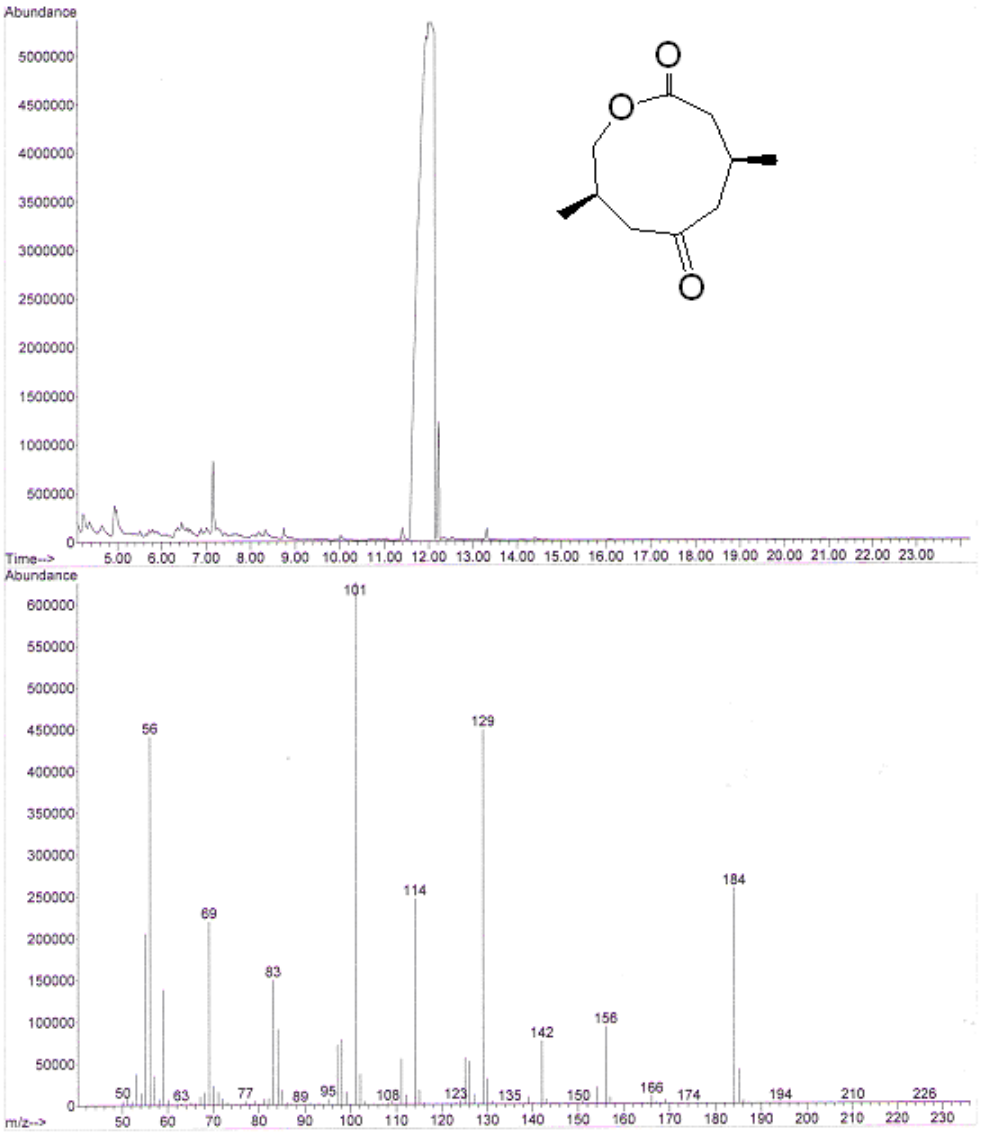

Figure 24. GC/MS spectrum of 4,8-dimethyloxonane-2,6-dione (**10**).

3.4 References

1. Sawwan, N.; Greer, A. *J. Org. Chem*. **2006**, *71*, 5796.
2. (a) Cassidei, L.; Fiorentino, M.; Mello, R.; Sciacovelli, O.; Curci, R. *J. Org. Chem.* **1987**, *52*, 699. (b) Murray, R. W.; Singh, M.; Jeyaraman, R. *J. Am. Chem. Soc.* **1992**, *114*, 1346. (c) Tomioka, H.; Mizutani, K.; Matsumoto, K.; Hirai, K. *J. Org. Chem.* **1993**, *58*, 7128. (d) Kirschfeld, A.; Muthusamy, S.; Sander, W. *Angew. Chem., Int. Ed. Engl.* **1994**, *33*, 2212. (e) Sander, W.; Schroeder, K.; Muthusamy, S.; Kirschfeld, A.; Kappert, W.; Boese, R.; Kraka, E.; Sosa, C.; Cremer, D. *J. Am. Chem. Soc*. **1997**, *119*, 7265. (f) Block, K.; Kappert, W.; Kirschfeld, A.; Muthusamy, S.; Schroeder, K.; Sander, W.; Kraka, E.; Sosa, C.; Cremer, D. *Peroxide Chem.* **2000**, 139. (g) Schroeder, K.; Sander, W. *Eur. J. Org. Chem.* **2005**, *3*, 496.
3. Umehara, M.; Hishida, S.; Okuda, M.; Ohba, S.; Ito, M.; Saito, Y.; Zen, S. *Bull. Chem. Soc. Jpn.* **1990**, *63*, 2002.
4. Strenge, A.; Rademacher, P. *Eur. J. Org. Chem.* **1999**, 1601.
5. Alvik, T.; Borgen, G.; Dale, J. *Acta Chem. Scand.* **1972**, *26*, 1805.
6. Schreiber, S. L.;. Smith, D. B *J. Org. Chem*. **1989**, *54*, 5994.
7. Miller, R. W.; McPhail, A. T. *J. Chem. Soc*., *Perkin Trans*. 2 **1979**, 1527.
8. Still, W. C.; Galynker, I. *Tetrahedron* **1981,** *37*, 23, 3981.
9. Gurst, J. E.; Schubert, E. M.; Boiadjiev, S. E.; Lightner, D. A. *Tetrahedron* **1993**, *49*, 9191.
10. Doerner, T.; Gleiter, R.; Robbins, T. A.; Chayangkoon, P.; Lightner, D. A. *J. Am. Chem Soc*. **1992**, *114*, 3235.
11. Spanka, G.; Boese, R.; Rademacher, P. *J. Org. Chem*. **1987**, *52*, 3362.
12. Spanka, G.; Rademacher, P. *J. Org. Chem*. **1986**, *51*, 592.

13. Rademacher, P. *Germany Chemical Society Reviews* **1995**, *24*, 143.

14. Anet, F. A. L.; Basus, V. J. *J. Am. Chem. Soc*. **1973**, *95*, 4424.

15. Dorofeeva, O. V.; Mastryukov, V. S.; Allinge, N. L.; Almenningen, A. *J. Phys. Chem*. **1985**, *89*, 252.

16. Srinivasan, R.; Srikrishnan, T. *Tetrahedron*, **1971**, *17*, 1009.

17. Dunitz, D. J. *Pure Appl. Chem*. **1971**, *25*, 495.

18. Anet, F. A. L. *Top Curr. Chem*. **1974**, *45*, 169.

19. Dale, J. *Pure Appl. Chem*. **1971**, *25*, 169.

20. Burkert, U.; Allinger, N. L. *Molecular Mechanics*, Am. Chem. Soc., Washington, D. C., 1982.

21. Hendrickson, J. B. *J. Am. Chem Soc*. **1964**, *86*, 4854.

22. Engler, E. M.; Andose, J. D.; Schleyer, P. V. R. *J. Am. Chem Soc*. **1973**, *95*, 8005.

23. Ferguson, D. M.; Raber, D. J. *J. Am. Chem. Soc*. **1989**, *111*, 4371.

24. Elied, E. L.; Wilen, S. H.; Mander, L. N. *Stereochemistry of Organic Compounds*; Wiley & Sons, New York, 1994.

25. Cinquini, M.; Cozzi, F.; Sannicolo, F.; Sironi, A. *J. Am. Chem. Soc*. **1988**, *110*, 4363.

26. Blouin, M.; Beland, M. C.; Brassard, P. *J. Org. Chem*. **1990**, *55*, 1466.

27. Gelin, S.; Gelin, R. *Bull. Soc. Chim. Fr*. **1968**, 288.

28. Gelin, S.; Gelin R. *Bullet Soc. Chim. Fr*. **1969**, 4090.

29. Paquette, L. A.; Ley, S. V.; Traynor, S. G.; Martin, J. T.; Geckle, J. M. *J. Am. Chem. Soc*. **1976**, *98*, 8162.

30. Wiberg, K. B. *J. Org. Chem*. **2003**, *68*, 9322.

Chapter 4. Rather Exotic Types of Cyclic Peroxides: Heteroatom Dioxiranes

4.1 Introduction

This chapter discusses the heteroatom-containing dioxiranes in organic chemistry. Heteroatom-containing dioxiranes are 3-membered ring peroxides with the form XO_2, where X is R_3P, RN, R_2Si, R_2S, R_2Se, R_2Ge, R_2Sn, R_2Pb, R_2Te, S, or Se. The R group represents hydrogen, halogen, alkyl, or aryl substituents. In light of the remarkable success that R_2CO_2 dioxiranes have had in oxygen-transfer reactions in organic chemistry, a review of XO_2 dioxiranes is expected to encourage and uncover new possible oxidation reactions. The synthetic utility for chemical oxidations with XO_2 dioxiranes is presently untapped.

4.2 Background

XO_2 dioxiranes are intermediates in photochemical and thermal reactions. In some cases, XO_2 dioxiranes have been detected with low-temperature techniques (e.g., matrix isolation, NMR, X-ray crystallography). In other cases, evidence for the existence of XO_2 dioxiranes comes from indirect studies, such as chemical trapping data or unimolecular rearrangements of the dioxirane congeners to more stable products.

An approach to the generation of XO_2 dioxiranes is often based on the reaction of an oxidant with mono-, di-, or trivalent (neutral) centers, such as, nitrenes, silylenes, phosphines, phosphites, phosphoranide anions, phosphonium ion betaines, phosphine selenides, sulfides, selenides, and tellurides. Oxidants that have been used in the generation of these high-energy XO_2 dioxiranes include lowest excited singlet state oxygen ($^1O_2$), ground state triplet oxygen ($^3O_2$), ozone (O_3), superoxide ion ($O_2^{\bullet -}$), and hydrogen peroxide (H_2O_2).

Two general types of reactions give rise to XO_2 dioxiranes (Scheme 1). In the first case, XO_2 dioxiranes can arise from a "side-on" addition of the O_2 on the heteroatom center (e.g., reaction of Ph_3P with $^1O_2$). In the second case, XO_2 dioxiranes originate from cyclization of the acyclic XOO form, which arose from an initial "end-on" addition of O_2 (e.g., reaction of F_2Si with $^3O_2$). Methods that can generate XO_2 dioxiranes often do so in the presence of other reactive species, such as acyclic XOO or $^1O_2$.

The experimental requirements for producing XO_2 dioxiranes are not well defined, which leads to the question of how to develop this area. This chapter of XO_2 dioxirane data in the solid-, solution-, and gas-phases will attempt to include substituent effects on the stability of XO_2 dioxiranes. The issues and challenges encountered in the synthesis of heteroatom-containing dioxiranes will be explored. Upon formation of XO_2 dioxiranes, subsequent intra- and intermolecular reactions take place. The analysis of structure and kinetics presented here can help guide thinking for the factors that underlie XO_2 dioxirane reactivity.

One aim of the chapter will be to consider the benefits of interplay between computational and experimental lines of evidence to help establish reactions that can generate XO_2 dioxiranes. Existing computational evidence will be summarized for XO_2 structures and their reactivities that are not yet characterized experimentally, such as in the case where X is R_2Ge, R_2Sn, R_2Te, S, or Se.

It should be noted that no comprehensive and critical coverage exists for cyclic XO_2 peroxide chemistry. Three previous reviews concerned with some aspects of XO_2 dioxiranes were published in 1995,[1] 1996,[2] 2000,[3] and 2005.[4] The metallodioxiranes,

MO_2 (M = metal, e.g., Mo, etc.) will not be covered in this chapter. No comprehensive review exists for metallodioxiranes, MO_2.[5]

4.3 Scope

This chapter will treat sequentially heteroatom-substituted dioxiranes possessing a tetrahedral and trigonal bipyramidal geometry. In Section 4.4.1, tetrahedral "pyramidal" dioxiranes are discussed based upon the order of heteroatoms in the periodic table with the exception of cyclic SO_2 and cyclic SeO_2. In Section 4.4.2, a similar approach will be used for the trigonal bipyramidal (TBP) dioxiranes. Each subsection will describe the structure, generation, and reactions involving the XO_2 dioxiranes, where data are available. The description of a particular XO_2 dioxirane will vary in length based upon whether investigations involved direct spectroscopic, indirect trapping, and/or computational techniques.

In Section 4.4.3, the energetics of the intercoversion between cyclic and ring-open XO_2 peroxides are discussed. A unimolecular reaction pathway is discussed in which XO_2 dioxiranes undergo an O-O bond homolysis to give the acyclic O-X-O isomer. In some cases XO_2 dioxiranes are thought to arise from the acyclic XOO form. Factors involved with intermolecular oxygen-transfer reactions of the XO_2 dioxiranes will be discussed in Section 4.4.4. Lastly, the synthetic implications of XO_2 dioxiranes will be the topic of Section 4.4.5.

We intend to compare R_2CO_2 dioxiranes with XO_2 dioxiranes. Some examples of R_2CO_2 dioxiranes will be mentioned, but not explicitly covered. There is a substantial literature on R_2CO_2 dioxiranes. We emphasize that R_2CO_2 dioxiranes are a topic of their own, which has been previously reviewed,[6] and is beyond the scope of this review. The

restriction also applies to the carbonyl oxide/dioxirane pair. Carbon-based dioxiranes have proven to be highly useful in synthetic chemistry.

4.4 Heteroatom-Containing Dioxiranes

Heteroatom-containing dioxiranes, XO_2, possess either tetrahedral or trigonal bipyramidal geometry (Scheme 2). A trigonal bipyramidal structure where both oxygens are equatorial has only been suggested in one case as opposed to one apical and one equatorial. Evidence for the existence of these 3-membered-ring XO_2 peroxides, their possible rearrangements, and their oxygen-transfer reactions are outlined. Different levels of confidence exist in the assignment of XO_2 structures.

4.4.1 Tetrahedral Dioxiranes

Experimental evidence exists for tetrahedral XO_2 dioxiranes that take the form RNO_2 and R_2SiO_2, but is not available for R_2GeO_2, R_2SnO_2, R_2PbO_2, SO_2, and SeO_2. The matrix isolation technique has played a key role in identifying RNO_2 and R_2SiO_2 dioxiranes. All of the tetrahedral XO_2 dioxiranes have been explored computationally except SeO_2.

4.4.1.1 Dioxaziridine, RNO_2

4.4.1.1.1 Background Information

Dioxaziridine (azadioxirane, **1**, Scheme 3) has not been isolated as a pure compound, but has been proposed as an unstable intermediate in glassy solutions (e.g., 2-methyltetrahydrofuran at 77 K) [7] and in inert solvents (e.g., acetonitrile at 298 K).[8] Dioxaziridines are not stable at room temperature. To date ten studies have proposed the formation of dioxaziridine via nitrene—O_2 chemistry from aryl azide and *O*-substituted diazeniumdiolate photooxidations (Scheme 4).[7-16] Tars also form in photooxidations of aryl azides.[17-22] A non-nitrene route to dioxaziridine has not been suggested. The idea of dioxaziridine as an intermediate in azide—ozone chemistry has not been put forward.[23]

Dioxaziridine may arise from the spin-allowed reaction of triplet nitrene with $^3O_2$, generated by cyclization of the initially formed nitroso oxide (Scheme 3). The reaction is analogous to the reaction of triplet carbenes with $^3O_2$. Owing to its ability to hydroxylate toluene,[8] nitroso oxide has been described as possessing diradical character ($RN^{\bullet}OO^{\bullet}$) rather than the zwitterionic character ($RN^{+}OO^{-}$); the latter is related to nucleophilic oxidants carbonyl oxides ($R_2C^{+}OO^{-}$) and persulfoxides ($R_2S^{+}OO^{-}$). However, there are differences of opinion as to the fate of the nitroso oxide. These differences may be reconciled based on nitroso oxide concentrations. High concentrations of nitroso oxide lead to dimerization to a 6-membered-ring diperoxide, [1,2,4,5]-tetraoxa-3,6-diazinane, rather than intramolecular cyclization to the dioxaziridine. A compilation of the methods and reaction conditions proposed to generate dioxaziridine or tetraoxadiazinane is given in Table 1.

Matrix-isolation has only been employed in one study to characterize structurally dioxaziridines.[7] Dioxaziridines have been directly detected by UV-visible spectroscopy.[7] Structural identification methods that use IR, EPR, luminescence, or NMR spectroscopy have not produced clear evidence for their detection. Dioxaziridines have so far not been trapped and are not capable of oxygen transfer to hydrocarbon molecules. This may be due to the powerful oxidation chemistry displayed by the precursor of the dioxaziridine, nitroso oxide.

4.4.1.1.2 Low Temperature

UV-Visible Spectroscopy. We have only located one study that provided UV-visible spectroscopic evidence for the formation of dioxaziridines in the reaction of nitrenes with O_2 (Table 2). In 1999, the formation of 4-(dioxaziridin-yl)stilbene (**1a**), 4-(dioxaziridin-yl)-4'-nitrostilbene (**1b**), 4'-(dioxaziridin-yl)-4-(dimethylamino)stilbene (**1c**), 4'-(dioxaziridin-yl)-4-aminobiphenyl (**1d**), and 4-(dioxaziridin-yl)-4'-(nitrene-substituted)stilbene (**1f**) was reported in rigid "glassy" 2-methyltetrahydrofuran (MTHF) at 77 K.[7,24] UV or visible irradiation of various aryl azides in air-saturated MTHF solution produced the corresponding triplet nitrene precursors,[25] which can be detected by EPR and UV-visible spectroscopy.[24,26,27] The reaction between the triplet nitrenes and O_2 is a thermal process and gives the corresponding nitroso oxides **2a**-**2e**, respectively, where **2f** arises from subsequent loss of N_2. Upon irradiation at 95 K, nitroso oxides **2a**-**2f** rearrange unimolecularly to dioxaziridines **1a**-**1f**. This process has a large barrier (computed value 45 kcal/mol).[7] MTHF is a rigid medium at 77 K and thus bimolecular reactions leading to [1,2,4,5]-tetraoxa-3,6-diazinanes appear to be unlikely. The dioxaziridines **1a**-**1e** subsequently isomerizes to give the corresponding nitro compounds

(**3a**-**3e**).

EPR Spectroscopy. In 1971, the intermediacy of dioxaziridine **4** or tetraoxadiazinane **5** was proposed in a photooxidation reaction with *p*-diazidobenzene (Scheme 5).[9,28] The UV photolysis (λ = 365 nm) of *p*-diazidobenzene in O_2-saturated hydrocarbon solvents (3-methylpentane, methylcyclohexane, or ethanol) at 77 K produced the triplet mono-nitrene (**7**) in an early step.[9,29] EPR, luminescence, and visible spectroscopy followed the course of the reaction. Interestingly, the thermal reaction between triplet nitrene and O_2 gave higher nitroso oxide concentrations in 3-methylpentane compared to methylcyclohexane glasses, likely due to enhanced O_2 solubility or diffusion in the 3-methylpentane matrix at 77 K. Compound **8** was suggested to possess triplet character (based on an observed triplet species with D* = 0.110 cm^{-1} in the EPR spectrum, a signal only present in O_2-containing samples), whereas **9** possessed singlet dipolar character (based on the observed diamagnetic yellow intermediate). On irradiation, the nitroso oxide(s) converted to the *p*-nitrophenyl azide product (**10**) via dioxaziridine or [1,2,4,5]-tetraoxa-3,6-diazinane intermediates. Only tentative evidence for dioxaziridine **4** was found, based on the possible interconversion of the nitroso oxide(s) to *p*-nitrophenyl azide **10**.

4.4.1.1.3 Room Temperature

Time-Resolved Infrared Study: Oxynitrene—O_2 Reaction. In 2001, a solution-phase *O*-substituted diazeniumdiolate (**11**) photooxidation reaction was conducted at room temperature.[10] Laser light (λ = 266 nm) was used to irradiate **11** in O_2-saturated acetonitrile-d_3, which led to an O-substituted nitrene (**12**) and $Et_2NN{=}O$ (Scheme 6).[10,30-32] Time-resolved infrared (TRIR) spectroscopy provided kinetic insight

that dioxaziridine (**14**) and tetraoxadiazinane (**15**) are both present as transient intermediates in the reaction. A first-order pathway for the nitroso oxide **13** lead to dioxaziridine **14**, whereas a second-order pathway for **13** afforded tetraoxadiazinane **15**. The relative contributions of the uni- and bimolecular pathways depended on the initial concentration of nitroso oxide **13**. A higher concentration of **13** was achieved from the use of high laser power, which then favored the bimolecular reaction to give **15**. Low laser power resulted in low steady-state concentrations of **13**. This consequently favored the unimolecular conversion of nitroso oxide to dioxaziridine **14** or diradical **16**. Formation of benzyl nitrate (**17**) is proposed to take place via dioxaziridine and tetraoxadiazinane. Benzaldehyde and nitrous acid (HONO) are additional products, thought to arise from **13** to **16** or produced by fragmentation of **15** into $\bullet NO_2$ and benzyloxy radical **18** and subsequent coupling. Interestingly, oxynitrenes are known to react faster with $^3O_2$ compared to arylnitrenes due to a possible electron-transfer to form an ion pair, coupling to generate the nitrene oxide, which cyclizes to the dioxaziridine (Scheme 7).[39b]

Laser Flash Photolysis: Aryl Nitrene—O_2 Reaction. In 1987, the photooxidation of *p*-nitrophenyl azide was reported in benzene and acetonitrile solution.[17] The reaction of *p*-nitrophenyl nitrene reacted with O_2 afforded the corresponding nitroso oxide. Dimerization of the nitroso oxide was suggested to give [1,2,4,5]-tetraoxa-3,6-diazinane (Scheme 8).[10,18.34-36] Cleavage of [1,2,4,5]-tetraoxa-3,6-diazinane yields ArN=O and O_2 (in a spin-forbidden process giving $^3O_2$ or in a spin-allowed process giving $^1O_2$) or it can fragment to give two equivalents of $ArNO_2$. $ArNO_2$ may also come directly from nitroso oxide ArNOO. ArN=O reacts with triplet nitrene to give

dinitroazobenzene [ArN(O)=NAr], or nitrene dimerizes when their concentrations are raised, as in the case of the high-power irradiation (Scheme 9). The observation that variation of the laser irradiation power leads to different product distributions constitutes an important discovery. One may anticipate that low-power irradiation conditions facilitate the unimolecular reaction of nitroso oxide **13** to dioxaziridine **14** (Scheme 6) by analogy with the *p*-nitrophenyl nitrene photooxidation reaction in dilute homogeneous solution (Scheme 8).[10]

^{18}O Isotope Labeling. ^{18}O labeling experiments carried out from 1987-1996 suggested that *p*-methoxyphenyl dioxaziridine (**19**), phenyl dioxaziridine (**20**), and *p*-nitrophenyl dioxaziridine (**21**) arise in the photooxidation of *p*-methylphenyl azide, phenyl azide, and *p*-nitrophenyl azide, respectively (Scheme 10).[8,11,12] The ^{18}O-tracer experiments were conducted in acetonitrile solvent at 20 °C ($\lambda > 350$ nm) by using a mixture of $^{18}O_2$ and $^{16}O_2$ gas. GC/MS determined the content of ^{18}O and ^{16}O within the products. Indirect evidence pointed to a dioxaziridine intermediate since retention of two ^{18}O atoms in the nitro product originated from one $^{18}O_2$ molecule. A unimolecular cyclization of nitroso oxide to dioxaziridine accounts for retention of the two oxygen atom labels in the nitro product (Table 3). Scrambling would have indicated that the oxygen atoms come from different O_2 molecules. Table 3 also shows that the unimolecular rearrangement of nitroso oxide to dioxaziridine is competitive with oxygen-transfer (trapping) from the nitroso oxide to PhN=O, Ph_2S, Ph_2SO, and benzene. The work identified the electrophilic character in the phenyl nitroso oxide ($PhN^{\bullet}OO^{\bullet}$).

$PhN^{\bullet}OO^{\bullet}$ is capable of hydroxylating toluene-4-*d* and anisole-4-*d* via an NIH shift to give the products 4-methylphenol-*d* (**23**; R = Me), 4-methoxyphenol-*d* (**23**; R =

OMe), 4-methylphenyl-2-*d*-ol (**24**; R = Me), and 4-methoxyphen-2-*d*-ol (**24**; R = OMe) (Scheme 11).

According to computations, a large energy barrier separates the nitroso oxide and dioxaziridine (~45 kcal/mol) (Section 4.1.1.5). Thus, it is likely that a photochemical interconversion is necessary to overcome the high barrier,[7] although some authors argue that a greater diradical character (versus zwitterion resonance form) will enable cyclization of the RNOO intermediate (Scheme 12).[8,11,12]

Sensitized Reaction. In 1983, a photooxidation reaction of aryl azides was conducted in acetonitrile, acetone, and benzene solvents at 30 °C (Scheme 13).[37] While dioxaziridine and tetraoxadiazinane were not suggested as intermediates in the reaction, this study is worth mentioning. This appears to be the only example of triplet sensitization in connection with the addition of oxygen during the photolysis of organic azides. A medium-pressure mercury lamp was used as the light source. When the triplet sensitizers acetone or acetophenone were added, an increased yield of nitrobenzene product resulted. Addition of a triplet quencher (piperylene) led to negligible yields of nitrobenzene product; however, addition of singlet oxygen sensitizers, Rose Bengal or methylene blue, had no effect on the product yields, which suggested that $^1O_2$ is not playing a role in the photooxidation. The presence of amine additives influenced the product distribution, in that 1° or 2° amines increase production of tar while 3° amines lower it.[38] Such effects with added amines have also been observed by others.[18,38-40]

4.4.1.1.4 Miscellaneous

In 2002, it was suggested that formation of dioxaziridine takes place in 4,4'-diazobiphenyl-containing rubber polymer samples which had been applied to a glass

surface and dried before photolysis.[13] The photooxidation reaction has been proposed to proceed via a nitrene and then subsequently to dioxaziridine $N_3C_6H_4$-$C_6H_4NO_2$, where the dioxaziridine was suggested to luminesce at λ_{max} = 456, 457, 461, 462, and 470 nm. Unfortunately, these rubber polymer experiments provide only tentative evidence for the presence of dioxaziridine since the intermediate(s) responsible for the luminescence have not been detected. Other experiments have proposed the formation of dioxaziridines from photooxidations of phenylazide and 4,4'-diazodiphenyl in acetonitrile or ethanol solutions at room temperature.[14-16] It should be mentioned that reactions of molecular oxygen with imidogen (NH) have been studied in combustion processes. The addition of NH ($^3\Sigma^-$) and O_2 ($^3\Sigma_g^-$) is predicted to give imine peroxide, HNOO. Imidogen is generated in the laboratory, for example, by photolysis of hydrazoic acid where NH ($^1\Delta$) is generated.[40,41] As yet, there are no experimental data that suggest the formation of unsubstituted dioxaziridine HNO_2 in the imidogen—O_2 reactions, although other HNO_x species have been observed.

4.4.1.1.5 Calculations

Structure. Computational results for the dioxaziridine are addressed in this section. HNO_2 and $PhNO_2$ dioxiranes are minima at the G2(MP2), B3LYP/6-31G(d), MP2/6-31G(d), and multiconfigurational MC-SCF/6-31G(d) levels and have been used to explain the experimental data on the nitrene—O_2 reactions.[7,42-50]

Calculated bond distances and a bond angle are shown in Table 4. Dioxaziridine HNO_2 and $PhNO_2$ bond distances for O-O range from a high of 1.487 Å to a low of 1.404 Å. The sensitivity of the dioxaziridine geometry to the identity of the substituent R has not been examined in detail. Dioxaziridine HNO_2 and $PhNO_2$ bear a resemblance to each

other independent of the computational method used. For example, at the B3LYP/6-31G* level, the O-O bond distance is 0.002 Å shorter and the N-O bond 0.002 Å shorter in the HNO_2 dioxirane than the $PhNO_2$ dioxirane. However, the reported literature value for O-O is 1.404 Å at the MP2/6-31G(d) level and 1.487 Å at the MP2/6-31G(d,p) level. This represents a large difference in the predicted O-O bond distance, which has not been explained. The bond distances for the computed N-O range from a high of 1.451 Å to a low of 1.373 Å. The O-N-O bond angle ranges from a high of 61.8° to a low of 59.2°, with the exception of the MCSCF/6-31G(d) value of 68.3°. A sample computed structure for the unsubstituted dioxaziridine is given in Figure 1.

Dioxaziridines HNO_2 and $PhNO_2$ have C_s symmetry and negatively charged oxygen atoms. The atomic charges, as predicted by Mulliken, indicate negative charge density at the oxygen atoms (-0.202) and positive ones on the hydrogen (+0.341) and nitrogen atoms (+0.063) (Table 5). Other properties that have been calculated for dioxaziridine HNO_2 include dipole moment (Table 6), energies of the HOMO and LUMO (Table 7), and vibrational frequencies (Table 8).

Energetics. Saddle points connecting the nitroso oxide and dioxaziridine have been located in four studies (Table 9). The cyclization barrier for MeO-NOO to $MeONO_2$ dioxirane is 21.6 kcal/mol at the B3LYP/6-311+G(d,p)//B3LYP/6-31G(d) level,[39b] for PhNOO to $PhNO_2$ dioxirane is 40.9 kcal/mol at the B3LYP/6-31G(d) level, and for HNOO to HNO_2 dioxirane is 43.8 kcal/mol at the MCSCF level.[43] The barrier is lower at the MP4/6-31G(d,p)//HF/6-31G(d) level, 12 kcal/mol.[49]

Dioxaziridine is apparently isoenergetic with the nitroso oxide in the gas phase. The interconversion of *trans* nitroso oxide HNOO to dioxaziridine HNO_2 has been

calculated to be endothermic by 4.2 kcal/mol (MCSCF) and 4 kcal/mol [MP4/6-31G(d,p)//HF/6-31G(d)], and exothermic by -3.1 kcal/mol [MP2/6-31G(d,p)]. It should be worthwhile to compute the energetics and barrier for conversion of nitroso oxide to the 6-membered diperoxide, [1,2,4,5]-tetraoxa-3,6-diazinane. Calculated structures on model systems provide evidence for the formation of dioxaziridine, but they have not been scrutinized against the dimerization pathway thus far.

The activation energies for the interconversion of dioxaziridine to the corresponding nitro compound are 33.2 kcal/mol [$MeONO_2$, B3LYP/6-311+G(d,p)//B3LYP/6-31G(d)], 14.2 kcal/mol [HNO_2, B3LYP/6-31G(d)], and 18.8 kcal/mol [$PhNO_2$, B3LYP/6-31G(d)] (Table 9). However, a discrepancy exists since there is a reported value of 2 kcal/mol for HNO_2 [MP2/6-31G(d)]. Exothermicity of the reaction is -70.2 kcal/mol [$MeONO_2$, B3LYP/6-311+G(d,p)//B3LYP/6-31G(d)], -74.0 kcal/mol [HNO_2, B3LYP/6-31G(d)], -80.7 kcal/mol [$PhNO_2$, B3LYP/6-31G(d)], -66 kcal/mol ($PhNO_2$), -64 kcal/mol ($PhNO_2$, MCSCF), -77.7 kcal/mol [HNO_2, MP2/6-31G(d,p)], -76 kcal/mol [HNO_2, MP4/6-31G(d,p)//HF/6-31G(d)]. For calculated energetics, isomerization and fragmentation are provided in Table 9. This includes conversion of dioxaziridine HNO_2 to acyclic HOON. The reaction of NH ($^3\Sigma^-$) and O_2 ($^3\Sigma_g^-$) to give acyclic HNOO has been investigated by SCF and MRD-CI calculations with the 6-31G(d,p) basis set.[43,49,50] The reaction between NH ($^1\Delta$) + O_2 ($^1\Delta_g$) has been suggested to give dioxaziridine HNO_2 in a concerted addition process, where acyclic HNOO does not intercede. The reaction of HNO_2 dioxirane to ^{1}HNO + O(^{3}P) is predicted to be endothermic by 7.0 kcal/mol from MCSCF calculations.[43] The activation energies for nitroso oxide or dioxaziridine to release an oxygen atom intramolecularly

have not been computed to date. Formation of the dioxaziridine by the isomerization of peroxynitrite has not been proposed (Scheme 14), presumably due to the high instability expected; however, the isomerization of peroxynitrite to nitrate is known.[23e]

In conclusion, dioxaziridines do not arise as a primary species from a side-on attack of $^3O_2$ with electron-deficient triplet nitrene. Instead, these nitrene reactions with O_2 produce nitroso oxide, which subsequently may cyclize to dioxaziridine. Persistent isolable dioxaziridines have so far not been prepared. The generation of dioxaziridine as a transient intermediate has been achieved; however, other reactive species are also present, such as azide excited states, nitrenes, nitroso oxides, and tetraoxadiazinanes. To avoid the formation of such reactive intermediates in nitrene chemistry presents a challenge for the clean production of dioxaziridines.

4.4.1.2 Dioxasilirane, R_2SiO_2

4.4.1.2.1. Background Information

Dioxasilirane (also known as, siladioxirane or dioxasilacyclopropane, **27**) has not yet been isolated as a pure compound due to its instability. Dioxasilirane can be formed in a reaction of singlet or triplet silylene (silanediyl, R_2Si) with $^3O_2$. Silylenes generated from azo-, fluoro-, chloro-, methyl-, and methoxy-containing silanes in argon matrices have served as precursors to dioxasiliranes (Scheme 15).[51-58] Studies also suggest the intermediacy of dioxasilirane from solution-phase, SiO_2-surface, and combustion experiments.[59-74] A compilation of reaction conditions thought to give rise to dioxasiliranes is given in Table 10.

To date, three studies provide direct spectroscopic evidence for the formation of dioxasilirane intermediates. Surprisingly little indirect evidence has been collected to

support the existence of dioxasiliranes. On reaction of silylene with O_2, silanone *O*-oxide (**28**) is thought to form initially and then rapidly interconvert to the dioxasilirane **27**, given the low barrier separating **27** and **28**. Silanone *O*-oxide is the congener of carbonyl oxide, but its oxygen transfer or other chemical reactivity is unknown, so that clarification about the importance of diradical character ($R_2Si^{\bullet}OO^{\bullet}$) and zwitterionic character ($R_2Si^{+}OO^{-}$) is not available. Bimolecular reactions of **27** or **28** are unknown in matrix and solution phases. 3,3,6,6-Tetrasubstituted-[1,2,4,5]-tetraoxa-3,6-disilinane and silanone [RSi(O)R] are not proposed as products formed in silyene—O_2 reactions; however, dioxasilirane can rearrange unimolecularly to a silaester [RSi(O)OR]. A large body of literature is available for silylenes, but only a fraction of it focuses on silylene—O_2 chemistry. The literature on silylenes under oxygen-free conditions will not be covered here.

4.4.1.2.2 Low Temperature

Infrared Spectroscopy. Three studies that provide IR spectroscopic evidence for dioxasilirane have been located.[51-58] In 2000, the synthesis of methylphenyldioxasilirane ($MePhSiO_2$, **31**) in an oxygen-doped argon matrix at 10 K was reported (Scheme 16).[51] UV irradiation ($\lambda > 305$ nm) of phenylsilyldiazomethane (**29**) in the argon matrix produces methylphenylsilylene via a 2-silapropene intermediate (**30**). Thermal annealing of the argon matrix to 30-45 K led to the reaction of silylene with O_2 giving dioxasilirane **31**. IR spectroscopy detected both silylene and dioxasilirane intermediates. Dioxasilirane **31** displays a strong Si-O stretching mode at 1002 cm^{-1} (1005 cm^{-1} predicted) and a weak O-O stretching mode at 577 cm^{-1} (608 cm^{-1} predicted) (Table 11). The predictions were made on the basis of B3LYP/6-311++G(2d,p) calculations. $^{18}O_2$

labeling confirms the assignment of methylphenyldioxasilirane, in which the Si-O stretching vibration is red-shifted by 25.3 cm^{-1} (28 cm^{-1} predicted) and the O-O stretching vibration by 23.5 cm^{-1} (21 cm^{-1} predicted). The DFT calculations reveal a barrier of about 1 kcal/mol for the cyclization of the silanone *O*-oxide **32** to dioxasilirane **31**. The silanone *O*-oxide **32** is not observed experimentally probably because of a rapid interconversion to the dioxasilirane. Since silanone *O*-oxide **32** exists in a very shallow minimum, and may not be chemically relevant, the generation of dioxasilirane **31** via MePhSi and O_2 is conceivable as a direct addition. Dioxasilirane **31** is photolabile and with 420-nm light interconverts to the silaester, MeSi(O)OPh, via a [1,2]-phenyl migration or to PhSi(O)OMe via a [1,2]-methyl migration.

In 1990, the pyrolysis of hexafluorodisilane and hexachlorodisilane was reported (Scheme 17).[52,55,56] The loss of SiF_4 and $SiCl_4$ takes place in an argon or argon—oxygen matrix, in which difluorosilylene and dichlorosilylene were subsequently trapped at 10 K. UV-visible photolysis of matrix-isolated difluorosilylene and dichlorosilylene in an O_2-containing matrix at 45 K yielded difluorodioxasilirane (**33**, R = F) and dichlorodioxasilirane (**33**, R = Cl). Isotopic labeling with $^{16}O_2/^{16}O^{18}O/^{18}O_2$ mixtures and HF/6-31G(d) calculations aided in the analysis of the IR spectra and in assigning the dioxasilirane structures (Table 12). ^{18}O-Isotopic labeling reveals the equivalence of the oxygen atoms in C_{2v}-symmetric dioxasilirane **33**. When one ^{16}O atom in **33** (R = F) is replaced with ^{18}O, the strong band at 1153 cm^{-1} (4 peaks) shifts to a lower frequency (by 9.6 cm^{-1}). Replacement of both oxygens by ^{18}O results in a shift to lower frequency by 19.3 cm^{-1}. A photolysis reaction was required to generate the dioxasiliranes **33** (R = F, Cl). Thermal reactions (up to 45 K) between O_2 and difluorosilylene and dichlorosilylene

did not yield the corresponding dioxasiliranes. The dioxasilirane stability depends on substituent effects. Dioxasiliranes **33** (R = F, Cl) are stable to UV irradiation unlike methylphenyldioxasilirane **31** and dimethyldioxasilirane **37**. The stronger Si-F and Si-Cl versus Si-C bonds play a role so that the [1, 2]-fluoro or chloro (rearranged) products, namely fluorine fluorosilanoate [FSi(O)OF] and chlorine chlorosilanoate [ClSi(O)OCl], are not easily formed.

In 1989, a matrix-isolation study[53,54] demonstrated that dimethyldioxasilirane **37** forms in the 254-nm photolysis of diazidodimethylsilane [$Me_2Si(N_3)_2$, **34**] in O_2-doped argon at 10 K or by pyrolysis (700 °C) of 1,2-dimethoxytetramethyldisilane (**35**), followed by O_2 trapping in an argon matrix (Scheme 18).[55,56] A photochemical equilibrium exists between 2-silapropene (**36**) and dimethylsilylene (Me_2Si),[75-80] in which dimethylsilylene is subsequently trapped by O_2.[81] IR spectroscopy revealed the splitting of an 1021 cm^{-1} absorption with ^{18}O labeling, which when coupled with the propensity of the intermediate to rearrange to methoxymethylsilanone [MeSi(O)OMe] led to the assignment of the intermediate as dimethyldioxasilirane **37**. The strong Si-O stretching mode at 1013 cm^{-1} and the weak O-O stretching mode at 554 cm^{-1} for dimethyldioxasilirane **37** are consistent with similar assignments made for methylphenyldioxasilirane **31** of 1002 cm^{-1} and 577 cm^{-1}.[51] Dioxasilirane **37** is photochemically unstable and with 436 nm light rearranges to the corresponding silaester. MP2/6-31G(d) and HF/6-31G(d) calculations aided in the interpretation of the experimental IR data (Table 13). There is no evidence for the dimethylsilanone *O*-oxide intermediate.

In one study, the formation of a silanone *O*-oxide was suggested instead of dioxasilirane. In 1988, the reaction of di-2,4,6-trimethylphenylsilylene (dimesitylsilylene, **39**) was conducted in a cryogenic solid-oxygen matrix at 16 K (Scheme 19).[82] An analysis of the products by IR spectroscopy concluded that a triplet-state silanone *O*-oxide **40** was present and not the dioxasilirane **41** based on data from isotopic mixtures of oxygen gas ($^{18}O_2$ and $^{16}O_2$) and HF/6-31G(d) computations. Dimerization of dimesitylsilylene **39** to form stable tetramesityldisilene **42** can take place in the absence of O_2.[83] This example for the intermediacy of silanone *O*-oxide stands in contrast to other reports of O_2 with silylenes (MePhSi, F_2Si, Cl_2Si, and Me_2Si), which point to a facile interconversion to the dioxasilirane.[51-54,61,62]

4.4.1.2.3 Room Temperature

Silylene—O_2 Reaction. While some work has been performed on the silylene—O_2 reaction in low-temperature argon matricies, little is known about the involvement of dioxasilirane in solution or at room temperature.[59-62] In 1987, laser photolysis (λ = 266 nm) of $(Me_3Si)_2SiMePh$ was conducted in air-saturated cyclohexane solutions at 298 K. This reaction yielded methylphenylsilylene, which subsequently reacted with O_2.[59,61,62] Only a tentative suggestion was made for formation of the silanone *O*-oxide **32** or dioxasilirane **31** intermediates;[3,61,62,84] thus, there is some uncertainty as to whether the dioxasilirane had been generated in cyclohexane solution.

4.4 .1.2.4 Miscellaneous

In work that has spanned the period from 1988-2004,[63-73] a surface-bound dioxasilirane [$(Si\text{-}O)_2SiO_2$, **45**] was suggested in the reaction of O_2 with silylene **43**, generated by vacuum pyrolysis of methoxylated silica (Scheme 20). Experiments were conducted on

heterogeneous samples (aerosil SiO_2), in which defects in the aerosil were thought to give rise to silylene **43** in SiO_2. Previous EPR work came to a different conclusion about the identity of the silicon intermediate in SiO_2 pyrolysis reactions and suggested formation of diradical **44** rather than silylene **43**.[85-88] UV-visible and IR spectroscopy cannot easily identify reactive species (e.g., silylene **43**, $R_2Si^{\bullet}OOSi^{\bullet}R_2$ diradical **44**, and dioxasilirane **45**) on silicon surfaces, and there are difficulties in establishing the structure of intermediate(s) formed in the reaction. The surface-bound dioxasilirane **45** was suggested to react with ethylene to give **46** and not oxirane. A series of radical reactions were also proposed, such as the formation of **47** and **48**, in addition to reactions of dioxasilirane **45** with H_2, D_2, carbon monoxide, and ethane. In 2006, evidence was obtained that suggested that dehydroxylation of either silica or hydroxlyated silicon form defects that lead to silylene and dioxasilirane at temperatures ranging from 100-400 °C.[58]

In 1996, a laser photolysis of silane (SiH_4)—oxygen (O_2) mixtures was reported.[74] The combustion reaction conditions generated silyl radical $H_3Si^{\bullet}$, which reacted with O_2 to give an excited acyclic H_3SiOO species. It was proposed that acyclic H_3SiOO cyclized to the unsubstituted dioxasilirane H_2SiO_2 radical (**50**), which then rearranged to silaformic acid [$H_2Si(=O)OH$] (Scheme 21). MP2(full)/6-31G(d) and G2(MP2) calculations predicted dioxasilirane **50** to be a minimum on the potential energy surface, in which TS structure **49** involved the loss of a hydrogen atom. Silanoic acid is not the only product in the reaction, since silicon oxide (SiO) is also a final product that arises by high computed barriers (e.g., 67.6 kcal/mol), made possible by the combustion conditions.

A recent report suggested the formation of unsubstituted dioxasilirane H_2SiO_2 in a dihydrogensilylene—O_2 reaction. In 2006, the gas phase reaction of silylene, SiH_2 (generated from the photolysis of phenylsilane) with O_2 was carried out at 297-600 K.[57] G3 calculations pointed to the formation of H_2SiOO, followed by cyclization to the dioxasilirane H_2SiO_2.

4.1.2.5 Calculations

Structure. Dioxasilirane structures optimize to minima at various levels of theory.[51,57,89-92] Calculated bond distances and bond angles are shown in Table 14. Dioxasilirane $((HO)_3CO)_2SiO_2$, $MePhSiO_2$, and H_2SiO_2 bear a resemblance to each other regardless of the computational method used. Dioxasilirane bond distances for O-O range from a high of 1.81 Å to a low of 1.571 Å. Bond distances for Si-O range from a high of 1.678 Å to a low of 1.632 Å. A sample computed structure for methylphenyldioxasilirane is given in Figure 2. Computed data for the Si-O-O and O-Si-O bond angles are also given in Table 14. The strain energy has been calculated for dioxasilirane H_2SiO_2 (Table 15). Bach estimated strain energies by using the CBS-Q method, along with cyclopropane and a 6-membered ring Si-, O-, and C-containing heterocycle reference compound.[89] Calculated atomic charges are in Table 16, and the vibrational frequencies and infrared intensities are in Table 17. Dioxasilirane H_2SiO_2 possesses negative charge density on the oxygen atoms.

Energetics. Saddle points which connect silanone *O*-oxide and dioxasilirane have been located in four studies in the gas phase (Table 18).[51,57,90-92] The cyclization barrier for silanone *O*-oxide MePhSiOO to dioxasilirane $MePhSiO_2$ is 0.8 kcal/mol at the B3LYP/6-311++G(d,p) level.[51] The barrier for converting acyclic Me_2SiOO to

dioxasilirane Me_2SiO_2 is 6.5 kcal/mol at the HF/6-31G(d) level[53,54] and for acyclic H_2SiOO to dioxasilirane H_2SiO_2 is 6.5 kcal/mol and 2.2 at the HF/6-31G(d) and GVB/6-31G(d) levels.[92] Silanone *O*-oxide is predicted to be higher in energy than dioxasilirane. The conversion of singlet acyclic MePhSiOO to dioxasilirane $MePhSiO_2$ is calculated to be exothermic by –49.6 kcal/mol at the B3LYP/6-311++G(d,p) level.[51] Subsequent conversion of dioxasilirane $MePhSiO_2$ to silaester [PhSi(O)OMe] is calculated to be exothermic by –59.3 kcal/mol. The conversion of singlet acyclic Me_2SiOO to dioxasilirane Me_2SiO_2 is calculated to be exothermic by –63.8 kcal/mol at the HF/6-31G(d) level, and the subsequent conversion from dioxasilirane Me_2SiO_2 to MeSi(O)OMe exothermic by –63.8 kcal/mol.[53,54]

The computational work predicts a facile conversion of singlet silanone *O*-oxide to dioaxsilirane in an exothermic low-barrier process. In all cases the dioxasilirane is calculated to be more stable than silanone *O*-oxide. A suggestion has also been made that this highly exothermic isomerization process could lead to vibrationally "hot" dioxasiliranes with excess energy.[92] The silanone *O*-oxide to dioxasilirane barrier height is much lower compared to the carbon analog $H_2C^+OO^-$ to dioxirane H_2CO_2 (23 kcal/mol barrier at various levels of theory).[3,53-58] Relative energies for other bimolecular and isomerization reactions are listed in Table 18.[51,53,54,57,74,82,89,90,92-95]

In conclusion, Section 4.1.2 provides evidence that is compelling for the direct detection of dioxasiliranes from matrix-isolation experiments of the reaction of silylene with O_2. The generation of dioxasilirane has been achieved in the absence of other reactive species such as silylenes and silanone *O*-oxides; however, formation of a stable isolable dioxasilirane has not yet been achieved.

4.4.1.3 Dioxagermirane, Dioxastannirane, and Dioxastilbirane

A photooxidation reaction of germanium has been conducted with deposited germanium chalcogenides with sulfur, selenium, and tellurium onto thin films, but peroxides were not suggested as intermediates.[96] Spectroscopic detection has been achieved for the heavy carbenes,[97-101] germylenes and stannylenes (e.g., H_2Ge, Me_2Ge, and Me_2Sn), but there are no experimental reports of the corresponding dioxiranes. Dioxagermirane (**51**), dioxastannirane (**52**), and dioxastilbirane (**53**) have been examined with computational methods, but have not been investigated experimentally (Scheme 22).[90,10]

Structure. In 1999, a computational study examined H_2GeO_2 **51**, H_2SnO_2 **52**, and H_2SbO_2 **53** at the B3LYP and CCSD(T) levels with various basis sets and an effective core potential (ECP) treatment.[90,102] These heteroatom-substituted dioxiranes optimize to minima on the potential energy surface (PES). Calculated bond distances are shown in Table 19. The B3LYP/TZ2P-ECP computed dioxirane structures show decreasing O-O bond distances in the order Ge > Sn > Pb with bond lengths of 1.566 Å (H_2GeO_2), 1.561 Å (H_2SnO_2), and 1.555 Å (H_2PbO_2). The O-O bond distances show a similar trend at the B3LYP/DZP-ECP level. The O-O bond distance decreases by increments of 0.005 Å and 0.006 Å in the series of H_2GeO_2, H_2SnO_2, and H_2SbO_2 dioxiranes. Other bond distances include Ge-O (1.778 Å), Sn-O (1.931 Å), and Pb-O (1.992 Å) at the B3LYP/TZ2P-ECP level. The natural atomic charges indicate a negative density at the oxygen and hydrogen atoms and a positive charge density on Ge, Sn, and Pb (Table 20). Natural bond order data are also presented in Table 20.

Energetics. Calculated energetics are provided in Table 21, in which data compare the higher homologue dioxiranes (cyclic H_2YO_2) with dihydroxycarbenes (HOYOH) and formic acid congeners [HY(=O)OH] (Y = Ge, Sn, and Pb). According to B3LYP/TZ2P-ECP calculations, the conversion of H_2GeO_2 dioxirane to HGe(=O)OH is exothermic by -76.9 kcal/mol. Similar exothermicities are calculated for dioxastannirane (-70.6 kcal/mol) and dioxastilbirane (-71.8 kcal/mol) in their conversion to the corresponding formic acid congeners. H_2YO_2 dioxiranes vary in their Y-O bond strengths, namely Y=Ge (77.4 kcal/mol), Y=Sn (63.6 kcal/mol), and Y=Pb (34.0 kcal/mol). The heteroatom-substituted dioxiranes are less stable for the heavier members of group 14. For example, the H_2PbO_2 dioxirane is 149.4 kcal/mol less stable than the corresponding dihydroxy species (plumbous hydroxide) according to B3LYP/TZ2P-ECP calculations. This instability correlates with a decrease in Y-O bond dissociation energies.

4.4.1.4 Cyclic Sulfur Dioxide, SO_2

The literature of the sulfur dioxide structure is enormous. Studies that have considered SO_2 structural isomers span a period of 50 years.[103-110] A variety of experimental methods have been used, but none have provided evidence for cyclic SO_2. Experimental methods have included, for example, flash photolysis of SO_2, gaseous CS_2—oxygen mixtures in explosions, and flash-initiated explosions of H_2S, CS_2, and COS. In 1996, an infrared absorption study of SO_2 in an argon matrix was conducted using 193-nm light from an ArF eximer laser.[111] From ^{18}O-labeling experiments, along with the analysis of IR intensities and B3LYP/cc-pVTZ calculations, it was concluded that the acyclic SOO was present, but not cyclic SO_2.[111] In 2006, cyclic SO_2 was

suggested to form in a two-photon irradiation (248 nm) of acyclic SO_2 in a MTHF or ethanol matrix at 11 K, based on the temperature dependent shift of the SO_2 λ_{max}.[112] There is uncertainty in the spectral assignment of the cyclic SO_2 structure due to the strong absorption of acyclic SO_2.

Structure. Given the absence of experimental data on cyclic SO_2, computational approaches have been used. Cyclic SO_2 optimizes to a minimum at many levels of theory, such as B3LYP/cc-pVTZ, BP86/cc-pVTZ, CCSD(T)/TZ2P(*f*), SCF/DZP, MRCI/cc-pVTZ, and GVB.[111,113-118] Calculated bond distances and a bond angle are shown in Table 22. The O_1-O_2 bond distances range from a high of 1.504 Å to a low of 1.479 Å,[111,113,114] the S-O bond distances range from 1.705 Å to 1.686 Å, and the O-S-O bond angle range from 52.7° to 51.9°. Calculated vibrational frequencies, IR intensities, and excitation energies for cyclic SO_2 are shown in Table 23.

Energetics. According to gas-phase CCSD(T)/TZ2P(*f*), B3LYP/cc-pVTZ, and BP86/cc-pVTZ calculations, cyclic SO_2 is 1-18 kcal/mol more stable than acyclic SOO. Cyclic SO_2 is highly unstable, the exothermicity on the ring opening to acyclic OSO is about 99-111 kcal/mol according to the above computed methods (Table 24).[111,114] The barrier to breaking the O-O bond of cyclic SO_2 is predicted to be 15.6 kcal/mol, based on MCSCF calculations.[117] The computed energetics and barrier for conversion of SO_2 to the 6-membered ring diperoxide has not been conducted, although DFT studies have focused on other combinations of dimers, trimers, and oligomers of sulfur oxides.[119-121] A series of calculations have been performed on the ground-state PES of SO_2.[122-129] The activation energies for SOO or cyclic SO_2 to release O-atom intermolacularly have not been computed to date. Additional work in this area is needed, such as the success found

in the computed and still theoretical complexes $[S_3W(NO)_3]^{3+}$, $[O_3M(NO)_3]^{3+}$ (M = Cr, Mo, W, Fe, Ru, Os), and $[S_3W(NO)_2(CO)]^{2+}$ containing cyclic O_3 and S_3.[123,130]

4.4.1.5 Cyclic Selenium Dioxide, SeO_2

A number of studies have been carried out on selenium oxide [SeO_x (x = 1, 2, 3)], but no experimental evidence exists for the cyclic SeO_2 intermediate. However, in 1996, a study of the reaction of selenium and O_2 provided evidence for various acyclic Se_xO_y molecules, such as SeO, OSeO, SeOO, SeOOO, and OSeOO.[131,132] Complex infrared absorptions in solid argon identified the selenium oxide species. The observed frequencies were corroborated with B3LYP/LANL1DZ calculations, from which frequency, intensity, and isotopic-shift data for the absorptions of Se_xO_2 molecules were obtained. It was proposed that the formation of OSeO in the reactions of Se with O_2 and photolysis of SeOO may go through a cyclic intermediate (cyclic SeO_2) (Scheme 23). The open isomer OSeO product is considerably lower in energy than the acyclic SeOO or cyclic SeO_2 intermediates.

4.4.2 Trigonal Bipyramidal Dioxiranes

Trigonal bipyramidal (TBP) XO_2 dioxiranes are hypervalent peroxides of the form R_3PO_2, R_2SO_2, R_2SeO_2, and R_2TeO_2. Peroxide structures bearing two or more oxygen bonds to hypervalent phosphorus, sulfur, selenium, or tellurium centers are uncommon, although, molecules such as phosphine and phosphite ozonides R_3PO_3 are known.[133-135] Spectroscopic evidence exists for the R_3PO_2 dioxirane, but not for R_2SO_2, R_2SeO_2, and R_2TeO_2. Computational studies have focused on the R_3PO_2 and R_2SO_2 dioxiranes, but not on R_2SeO_2 and R_2TeO_2.

4.4.2.1 Dioxaphosphirane, R_3PO_2

4.4.2.1.1. Background Information

A phosphoranide ion,[136] a sterically hindered aryl phosphine,[137] a 1,1'-binaphthyl phosphine,[138] and a PH_3—ozone complex[139] served as precursors to dioxaphosphiranes (**54-56**), for which direct spectroscopic evidence was obtained (Chart 1 and Table 25). Dioxaphosphirane **55** is a hexacoordinated species. A number of other studies have provided indirect experimental evidence for the formation of dioxaphosphiranes. Various oxidants have been used in the generation of dioxaphosphiranes, such as, $^1O_2$, $^3O_2$, O_3, and hydrogen peroxide.[136-144] A previous review has summarized recent work on phosphine—$^1O_2$ reactions.[4] Early work on phosphine autoxidation reactions dates from 1962-1984,[145-147] although dioxaphosphiranes were not proposed as intermediates.

There is no evidence yet for the formation of peroxyphosphine oxide **57**, although it was proposed in a ring-closure phosphoranide—O_2 reaction.[136] Dioxaphosphirane **54** readily reacts with the substrate (PR_3) to form two equivalents of phosphine oxide **58**, but **54** also rearranges to the phosphonate **59** or is converted to hydroperoxyphosphine **60** and hydroxyphosphorane **61** in methanol. There is no experimental evidence that dioxaphosphirane dimerizes to a 6-membered-ring diperoxide tetradiphosphinane (**62**).

4.4.2.1.2. Low Temperature

NMR Spectroscopy. In 2003, the synthesis of tris(*o*-methoxyphenyl)dioxaphosphirane was reported in CH_2Cl_2 and CH_2Cl_2/toluene solutions at 193 K and was followed by ^{31}P and ^{17}O NMR spectroscopy (Scheme 24 and Table 26).[137a] The reaction of singlet oxygen from irradiated air-saturated solutions containing tetraphenylporphyrin sensitizer in the presence of tris(*o*-methoxyphenyl)phosphine produced the dioxaphosphirane. Chemical quenching of $^1O_2$ by the phosphine was very

efficient and led to phosphine oxide (o-$MeOC_6H_4)_3P{=}O$. The ability of phosphine to convert $^1O_2$ to $^3O_2$ (physical quenching) has not been observed in these reactions. The *ortho*, *meta*, and *para* isomers of $(MeOC_6H_4)_3P$ also show no physical quenching of $^1O_2$ regardless of the solvent.[137,143] With enriched $^{17}O_2$ gas used in the photooxidation, ^{17}O-NMR data showed a broad peak at 740 ppm, which along with the ^{31}P-NMR peak at –48.3 ppm was assigned to the 3-membered ring system (o-$MeOC_6H_4)_3PO_2$. The *ortho*-methoxyphenyl groups exerted steric interactions that slowed the bimolecular reaction of the dioxaphosphirane with the substrate (o-$MeOC_6H_4)_3P$. For phosphines that possess small cone angles, as described for metal complexes,[148,149] the dioxaphosphirane has a longer lifetime by slowing bimolecular reactions. Alkene-trapping experiments showed that (o-$MeOC_6H_4)_3PO_2$ dioxaphosphirane transfers an oxygen atom to alkenes to yield epoxides, analogous to R_2CO_2 dioxiranes such as dimethyldioxirane (Table 27). As yet no information is available whether the apical or the equatorial dioxaphosphirane oxygen is donated, although the equatorial oxygen should be the more electrophilic.[150-152] There is a reduced computed charge on O_{eq} compared to the O_{ax} atom. In the absence of an external trap, the intramolecular rearrangement of dioxaphosphirane afforded the phosphonate **59**. In the presence of methanol as solvent, its addition leads to hydroperoxyphosphine and subsequently to hydroxyphosphorane and tris(o-methoxyphenyl)phosphine oxide, after reaction with the substrate.

In 2006, a dioxaphosphirane intermediate **63** was observed in the reaction of 1,1'-binaphthyl-di-*tert*-butyl-2-phosphine with $^1O_2$ in toluene at temperatures ranging from -40 to -80 °C (Scheme 25 and Table 26).[138] Evidence for the existence of the dioxaphosphirane came from an assignment of the ^{31}P-NMR signal at -18.6 ppm, and the

subsequent decomposition of this intermediate upon warming to give the corresponding phosphine oxide. Warming of the mixture in the presence of cyclohexene afforded its epoxide. The intramolecular oxidation of dioxaphosphirane **63** gave naphthalene epoxide, and subsequently a hydroxylated naphthalene product was found via a NIH-shift mechanism. A similar rearrangement was observed in the reaction of *R*-(+)-2-(diphenylphosphino)-2'-methoxy-1,1'-binaphthyl (**63'**) with $^1O_2$ according to ^{31}P-NMR spectroscopy.[138]

X-ray Crystallography. In 1999, the synthesis of a hexacoordinate 12-P-6 dioxaphosphirane **68** was accomplished in a reaction of $^3O_2$ with 3,3,3',3'-tetrakis-(trifluoromethyl)-1,1'-spirobi[3H,2,1λ^5-benzoxaphosphoranide ion] (**65**), generated from a P-H phosphorane **64** at 273 K (Scheme 26).[136] Exposure of the 10-P-4 phosphoranide to O_2 in a thermal process involved electron transfer (phosphoranyl radical/superoxide radical pair, **66**) to give the corresponding dioxaphosphirane **68**. A cyclization of peroxyphosphine oxide **67** was proposed with pseudo rotation to place the oxygen atom equatorial and the aryl carbons axial. On the basis of ^{31}P and ^{19}F NMR spectroscopy the dioxaphosphirane structure was assigned (Table 26). The dioxaphosphirane crystallized with potassium 18-crown-6 as the salt and was found to be stable in the solid state at room temperature. With Ph_3P it rapidly deoxygenated in solution to give oxidophosphorane **69** and Ph_3P=O. Except for Ph_3P, oxygen-transfer reactions to alkenes or other trapping agents were not explored. The synthesis of diasteromeric analogs was conducted, in which one of the CF_3 groups was replaced by CH_3. A slow interconversion of the *endo* and *exo* forms of the R side groups implies rigid 3-membered peroxide rings in **68a'** and **68a''**, and thus inefficient pseudorotation.

IR Spectroscopy. In 1987, the generation of a dioxaphosphirane [$HP(=O)O_2$] in the visible-light photolysis of a phosphine(PH_3)—ozone complex in solid argon (12-18 K) was reported (Scheme 27 and Table 26).[139] The infrared study in an argon matrix of the reaction of $^{16,18}O_3$ with PH_xD_{3-x} (x = 0, 1, 2, 3) and subsequent decomposition of the phosphine—O_3 complex showed the presence of a number of compounds, which included phosphine oxide $H_3P=O$, phosphinic acid H_2POH, phosphonic acid $(HO)_2HP=O$, and metaphosphoric acid $HOPO_2$. The reaction is thought to produce the HP=O intermediate, which adds O_2 to give acyclic HOOP=O and the $HP(=O)O_2$ dioxaphosphirane upon further irradiation. The results do not support the interconversion between the acyclic HOOP=O and the dioxaphosphirane $HP(=O)O_2$. On the basis of the observed fundamental vibrational frequencies, $HP(=O)O_2$ and $DP(=O)O_2$ structures were assigned, which are given in Table 26. Rotationally, vibrationally, and electronically excited intermediates were suggested.

4.4.2.1.3 Room Temperature

Trapping, intramolecular rearrangement, and ^{18}O-tracer experiments provided indirect evidence for the dioxaphosphirane intermediates in reactions of $^1O_2$ with phosphites and phosphines. Phosphites are less reactive and may be used as trapping agents in the $^1O_2$ reactions.[153] For example, trimethylphosphite traps the anethole—singlet oxygen intermediate(s) because it reacts slowly with $^1O_2$.[150]

In 1993, the photooxidation of tributylphosphite and triphenylphosphine was conducted with sulfoxides [$(p\text{-}YC_6H_4)_2SO$; Y = MeO, Me, H, and Cl] and sulfides [$(p\text{-}YC_6H_4)_2S$; Y = Me and H] as trapping agents (Scheme 28 and Table 28).[143]

Singlet oxygen was generated by irradiation (λ > 400 nm) in air-saturated acetonitrile solutions with methylene blue as sensitizer. The reactivity of the intermediate in the reaction with these trapping agents correlated well with electrophilic dioxaphosphirane. A negative ρ value (-0.63) for trapping by diaryl sulfide was obtained. Oxygen transfer to Ph_2S and to Ph_2SO were inefficient compared to the more oxophilic $(BuO)_3P$ molecule. The relative reactivity was 300:4:1 for $(BuO)_3P$:Ph_2S:Ph_2SO. An ^{18}O-tracer experiment indicated retention of the two ^{18}O atoms, which suggests a unimolecular rearrangment of dioxaphosphirane ($Ph_3P^{18}O_2$) to phenyl diphenylphosphinate $Ph^{18}OP(^{18}O)Ph_2$. Retention indicates that the two oxygen atoms in the phosphinate product are derived from one O_2 molecule. Scrambling implies that the oxygen atoms come from different O_2 molecules. The labeling data do not rule out unimolecular rearrangment of an acyclic peroxyphosphine oxide (Scheme 29).

The reaction of $^1O_2$ with *para*-substituted arylphosphines was investigated in detail (Scheme 30).[137b] Formation of the corresponding phosphine oxides took place efficiently (no physical quenching of $^1O_2$), which showed a correlation with the Hammett σ parameter (ρ = -1.53 in $CDCl_3$) and with the Tolman electronic parameter.[148,149] The phosphine oxide products were proposed to arise from the reaction of phosphine with dioxaphosphirane intermediates.

In 1993 and 1994, indirect evidence for the existence of a dioxaphosphirane came from the reaction of $^1O_2$ with a bicyclic phosphite (1-methyl-4-phospha-3,5,8-trioxabicyclo[2.2.2]octane) in the presence of norbornene (Scheme 31).[154,155] The data point to a dioxaphosphirane intermediate in view of the epoxidation of norbornene. The bicyclic dioxaphosphirane would have no possibility for pseudorotation. The reaction

was followed by GLC analysis and the corresponding phosphate was formed as the product. Addition of the radical trap triphenylmethane did not influence the epoxidation reaction, which is similar to work on (o-$MeOC_6H_4)_3P$ in 2003.[137a] Less nucleophilic olefins such as stilbene and styrene are oxidized less efficiently. Analysis with the thianthrene 5-oxide probe also confirmed electrophilic oxidation behavior.[154,155,168-170]

In 1974, the formation of trialkyl phosphates was reported in the dye-sensitized photooxidation reactions of phosphites [$(MeO)_3P$, $(EtO)_3P$, (i-$PrO)_3P$, (n-$BuO)_3P$, (cyclic-$C_6H_{11}O)_3P$, and $(CH_2{=}CHCH_2O)_3P$].[156] Singlet oxygen was generated in benzene-methanol mixtures (4:1) with methylene blue or in acetone with Rose Bengal as sensitizers at 298 K. The transient formation of a phosphite—O_2 intermediate was implicated, but its structure was not suggested at that time.

4.4.2.1.4 Miscellaneous

Diethyl azodicarboxylate—H_2O_2 Reaction. In one paper the use of hydrogen peroxide was suggested to generate triphenyldioxphosphirane.[108] In 1983, a betaine(**70**)—H_2O_2 reaction was reported (Scheme 32).[144] Migration of the phenyl group to give **73** was taken as evidence for the presence of the dioxaphosphirane or tetradiphosphinane intermediate (Scheme 33). Further experiments to probe the nature of the intermediate(s) in the reaction have not been reported.

Arylphosphines Used as Jet-Fuel Stabilizers. Over the past decade, arylphosphines have been examined as possible stabilizers of jet fuels.[158-163] Thermal oxidative and pyrolytic stability of the jet fuel was enhanced with additions of triphenylphosphine or dicyclohexylphenylphosphine over a temperature range of 190-250 °C. Oxophilic stabilizers such as phosphines are selectively oxidized rather than the jet

fuel. Autoxidation of the phosphines has been suggested to take place by an electron-transfer and/or a charge-transfer process (Scheme 34). High temperatures were necessary to initiate a reaction between Ar_3P and $^3O_2$ in view of the large activation energy ($E_a < 30$ kcal/mol). Thus, decomposition of a possible dioxaphosphirane intermediate is expected to take place rapidly under the high temperature conditions.

Thermolysis of a Bisdiphenylphosphinic Peroxide. In 1965, a reaction was reported, that involved the thermal decomposition of a bisdiphenylphosphinic peroxide **74** (Scheme 35).[157] Decomposition of bisdiphenylphosphinic peroxide with phenyl migration occurred in chloroform, tetrachloroethane, DMF, and acetic acid, but not in alcohol solvents, in which an anhydride is formed. The result was interpreted tentatively in terms of a heterolytic cleavage reaction and production of transient peroxidic intermediates, such as, the acyclic $Ph_2(RO)POO$ (**76**) and dioxaphosphirane $Ph_2(RO)PO_2$ (**77**), prior to formation of the anhydride product. It is uncertain whether a dioxaphosphirane is formed in the reaction. Further experiments and computations are needed to validate the mechanistic suggestion.

4.4.2.1.5 Calculations

Structure. Dioxaphosphiranes H_3PO_2, Me_3PO_2, and $(HO)_3PO_2$ optimize to minima at various levels of theory and basis set extension, including HF/STO-3G(d), HF/3-21G(d), HF/6-31G(d), MP2/6-31G(d), and CASSCF/6-31G(d).[143,164] Calculated bond distances and bond angles are shown in Table 29. The parent dioxaphosphirane HPO_2 has also been studied and optimizes to a minimum at the SCF and SCF/CEPA-1 levels.[165] Calculations predict that peroxyphosphine oxide does not form in phosphine—$^1O_2$ reactions.[164] The acyclic peroxyphosphine oxides $(HO)_3POO$, H_3POO, and Me_3POO

are not found as minima at any level of theory.[143,164,165] Dioxaphosphiranes H_3PO_2, $(HO)_3PO_2$, and Me_3PO_2 bond distances for the O_1-O_2 bond range from 1.599 Å to 1.560 Å. The dioxaphosphirane structure is calculated with one of the peroxide oxygens in an equatorial position and the other in an apical position. The apical P-O_1 bond is 0.059 to 0.202 Å longer than the equatorial P-O_2 bond as would be expected for a TBP structure (Table 29). A sample computed structure for the unsubstituted dioxaphosphirane is given in Figure 3. The sensitivity of the dioxaphosphirane geometry to the R substituent has not been examined in detail.

Wilke and Weinhold have recently calculated resonance bonding patterns in H_3PO_3 dioxaphosphirane (Scheme 36).[141] The use of Natural Resonance Theory (NRT) and Natural Bond Orbitals (NBOs)[166] predicted that the nonhypervalent ionic resonance forms II and III are more important than the valence-shell expanded[167] (octet-violating hypervalent structures) I, ionic IV, and π-complex V forms. The hypervalent form I, with participation of d orbitals in the hydridized structure, is a minor contributor in the structures I-V according to the NRT/NBO analysis.

Energetics. A computational investigation of the phosphine—singlet oxygen reaction appeared in 1993 (Table 30).[164] The barrier connecting PH_3 and $^1O_2$ with dioxaphosphirane H_3PO_2 is 24.8 kcal/mol at the MP2/6-31G(d) level. The conversion of PH_3 and $^1O_2$ to dioxaphosphirane H_3PO_2 is calculated to be -32.0 kcal/mol exothermic at the MP2/6-31G(d) level. The formation of dioxaphosphirane Me_3PO_2 from PMe_3 and $^1O_2$ is calculated to be exothermic by -52.5 kcal/mol at the MP2/6-31G(d)//HF/6-31G(d) level, whereas the cyclization of the acyclic $HP(=O)_2$ to dioxaphosphirane HPO_2 is endothermic by 85.0 kcal/mol at the SCF level.

In conclusion, the spectroscopic evidence for dioxaphosphiranes **54-56** is now in hand. Dioxaphosphirane **54** arises from the reaction of phosphine or phosphite with $^1O_2$, but not from the primary formation of peroxyphosphine oxide. Singlet oxygen attaches in a side-on manner to the trivalent phosphorus center. Dioxaphosphiranes derived from sterically bulky phosphine ligands have synthetic versatility that should be further investigated.

4.4.2.2 Dioxathiirane, R_2SO_2

4.4.2.2.1. Background Information

Dioxathiirane (thiadioxirane, **79**) has been suggested as an intermediate in sulfur oxidation reactions. Since seven previous reviews have focused on organic sulfide or metal thiolate-ligand photooxidations, and the possible formation of R_2SO_2 dioxathiiranes,[2,4,171-176] we shall focus our discussion the new findings.

No direct spectroscopic data exist yet for the dioxathiirane R_2SO_2 intermediate. Routes that have been suggested to give dioxathiirane include reagents such as $^1O_2$, $^3O_2$, and superoxide.[2,4,171-176] Dioxathiirane **79** may arise from the reaction of the sulfide radical cation with superoxide ion. There is no evidence that dioxathiirane is present in sulfide—$^1O_2$ reactions.

Experimental and computational data suggest that various species arise in sulfide oxidation chemistry, which include dioxathiirane **79**, persulfoxide **80**, sulfide radical ion superoxide pair **81**, *S*-hydroperoxysulfonium ylide **82**, sulfoxide **83**, and sulfone **84** (Chart 2). Sulfide photooxidations can lead to hydroperoxysulfurane **85** or a hydrogen bonded persulfoxide **86** in alcohol solvents.[4,171-187] The acidity of the medium and dependence on the trapping efficiency suggest the presence of **86**,[171] ^{17}O-labeled

substrates implied the participation of **85**. Alcohol adducts and nucleophilic oxygen-transfer chemistry suggest a dipolar form of the persulfoxide ($R_2S^+OO^-$) rather than a diradical form ($R_2S^{\bullet}OO^{\bullet}$) in solution.[188] There is no evidence that $R_2S^+OO^-$ persulfoxide or R_2SO_2 dioxathiirane dimerize to a 6-membered-ring diperoxide **87**. Quantum calculations have been used to predict the structures and energetics of intermediates generated in the oxidation of sulfur compounds.[164,176,184,188]

4.4.2.2.2 Room Temperature

Electron-Transfer Photooxidation. Dioxathiiranes may arise from electron-transfer photooxidations with the use of electron-deficient sensitizers.[184,185,189,190] In 2005 and 2006, experiments conducted in O_2-saturated acetonitrile implied that the sulfide radical ion **90** (R = H or Me), dioxathiirane **91** (R = H or Me), and sulfoxide **92** (R = H or Me) are generated in the photooxidation of dibenzothiophene **89** (R = H) and 4,6-dimethyldibenzothiophene **89** (R = Me), sensitized by *N*-methylquinolinium tetrafluoborate ($NMQ^+BF_4^-$), 10-methylacridine hexafluorophosphate ($AcrH^+PF_6^-$), or 2-(4-methoxyphenyl)-4,6-diphenylpyrylium ($MOPDPP^+BF_4^-$) in Scheme 37.[189,190] Laser photolysis, ESR, and fluorescence-quenching data were collected and the formation of dioxathiirane **91** was proposed. It was speculated that the superoxide ion[189] added to the sulfide radical ion in one step (Scheme 37A). It was also suggested that ground state $^3O_2$[190] reacted with the sulfide radical ion in a stepwise manner (via **93** followed by back electron transfer to $MOPDPP^{\bullet}$ or $AcrH^{\bullet}$, as shown in Scheme 37B).

EPR data indicated that the superoxide ion is formed by electron transfer from the sensitizer radical (e.g., $NMQ^{\bullet}$). Sulfoxide production is reduced in the presence of the electron trap 1,4-benzoquinone, which reacts with $NMQ^{\bullet}$ and superoxide to give NMQ^+

and O_2. Compound **89** does not form the *S*-hydroperoxysulfonium ylide **82** due to the absence of α protons.

In 2003, the photooxidation of dibutylsulfide (**94**) and thioanisole (**95**) in O_2-saturated acetonitrile, sensitized by NMQ^+ and 9,10-dicyanoanthracene (DCA) was conducted at 298 K (Scheme 37).[184] Time-resolved laser flash photolysis of NMQ^+ revealed the formation of sulfide radical cations [dimeric $(Bu_2S)_2^{+\bullet}$, $PhSMe^{+\bullet}$, and dimeric $(PhSMe)_2^{+\bullet}$]. DCA photolysis also led to the production of radical ions for PhSMe, but not Bu_2S. The persulfoxide exists as a primary intermediate in sulfide—$^1O_2$ reactions,[188] but in the NMQ^+ and DCA systems, dioxathiirane was suggested to arise from a direct reaction between sulfide radical ion and the superoxide ion. The evidence for dioxathiirane derives from the electrophilic character of the intermediate in bimolecular trapping experiments, as confirmed by data from computations. The computations predict an energetically facile conversion of $R_2S^{+\bullet}$ (from **94** and **95**) with the superoxide ion to give the corresponding dioxathiiranes.[184]

Other work has also focused on generation of sulfide radical ions, some via electron transfer photosensitizers [DCA (free or covalently bound to silica), triphenylpyrylium tetrafluoroborate, 2,3,5,6-tetrachloro-1,4-benzoquinone, Ru(2,2'-bipyrazine)$_3^{2+}$, TiO_2, CdS, and acetone], although the intermediacy of dioxathiiranes as not suggested in these cases.[191-203]

Singlet Oxygen Reactions.[171-264] Early sulfide photooxidation work of Schenck (from 1962 to about 1970) suggested a sensitizer-oxygen complex (moloxide) rather than a diffusible $^1O_2$ species.[204,205] In the 1980s and 1990s, efforts were increased to understand the intermediates generated in the sulfide—$^1O_2$ chemistry. In these studies,

the production of dioxathiiranes was searched for by using flash photolysis and competitive kinetic techniques. The reaction mechanism in Scheme 39 proposes the persulfoxide **80** as the first intermediate. The high energy barrier computed for the formation of the dioxathiirane from the persulfoxide suggests that the *S*-hydroxysulfonium ylide is a key reaction intermediate. The *S*-hydroxysulfonium ylide is most likely an additional intermediate in the photosensitized oxidations of sulfides in aprotic solvents. The formation of a *S*-hydroperoxysulfonium ylide explains the experimental results in many cases.[207-216] For example, in 2002, the reaction of $^1O_2$ with ethyl γ-phenylthiocrotonate (**96**) was conducted in C_6D_6 at 298 K (Scheme 40).[215] From the observation of the sulfoxide **101** and sulfone products **100** and **102** by ^{1}H-NMR spectroscopy, the intermediacy of the *S*-hydroperoxysulfonium ylides **98** and **99** was implied. In this study, the source of $^1O_2$ was 1,4-dimethylnaphthalene endoperoxide.

Despite all the work conducted on the reactions of $^1O_2$ with nickel-, platinum-, and cobalt-thiolate complexes, little is known about the formation of the corresponding dioxathiiranes in these systems (Scheme 41 and 42).[255-263] The nickel- and platinum-thiolate ligand photooxidations were conducted in aprotic solvents (*N*,*N*-dimethylformamide, acetonitrile, and DMSO), which paralleled the organic sulfide—$^1O_2$ reactions observed in aprotic solvents.[175] Kinetic data and trapping experiments suggest a mechanism analogous to the photooxidation of organic sulfides. The singlet oxygen oxidizes the thiolato group of the complex $[Co(III)(en)_2(S\text{-}cys)]^+(BF_4)^-$ (**103**) in water to give the corresponding sulfenato complex (Scheme 41A). The Pt(bpy)(bdt) [bpy=2,2'-bipyridine (**104**); bdt=1,2-benzenedithiolate (**105**)] is oxidized by the $^1O_2$ to form the sulfinate [Pt(bpy)($bdtO_2$)]] and disulfinate [Pt(bpy)($bdtO_4$)] products (Scheme 41B,C).

Nickel dithiolate complexes react with $^3O_2$ or $^1O_2$ to generate the corresponding sulfenate and sulfonate products through the persulfoxide **107** and dioxathiirane **108** intermediates (Scheme 42).

4.4.2.2.3 Calculations

Structure. A number of computational papers have focused on the reaction of $^1O_2$ with sulfides. Theory suggests that the dioxathiirane is a minimum on the potential energy surface. The calculated O-O and S-O bond distances are shown in Table 31. The dioxathiirane structures resemble each other in many of the basic geometric trends. Dioxathiirane O-O bond distances range from 1.562 Å to 1.527 Å, which depends on the structure and the level of theory; the dioxathiirane ring is unsymmetric, with two nonequivalent S-O bonds. The oxygen atoms occupy apical and equatorial positions, with the apical bonds longer than the equatorial ones by ca. 0.08 to 0.48 Å. A sample computed structure for dimethyldioxathiirane is given in Figure 4.

Dioxathiiranes have negative charges on the oxygen atoms. The atomic charges as predicted by the NBO method for a series of dioxathiiranes $MeS(O_2)X$ (where X=Me, NMe_2, F, OMe, SMe, NH_2, NHMe, OH, and SH), indicate a greater negative charge at the apical oxygens (O_1) compared to the equatorial ones (O_2), see Table 32. MP2/6-31G(d) computed vibrational frequencies, IR intensities, and isotropic shifts of dioxathiirane Me_2SO_2 are shown in Tables 33 and 34.

Energetics. The transition state that connects the persulfoxide and the dioxathiirane is high in energy with a barrier of ~20 kcal/mol; thus, the dioxathiirane is not expected to form as a reaction intermediate along this route. Once formed, the persulfoxide converts to the *S*-hydroperoxysulfonium ylide by a lower barrier process

(~10 kcal/mol). The strongest experimental evidence for the formation of dioxathiiranes comes from the use of electron-poor sensitizers in the photooxidation of sulfides. In contrast, the *S*-hydroperoxysulfonium ylide is in most cases the second intermediate formed in sulfide—$^1O_2$ reactions (Table 35).

5. 4.2.3. Dioxaselenirane and Dioxatellurirane

In 1994, the reaction of singlet oxygen with diaryl selenides and benzyl-substituted selenides was reported.[265] Surprisingly, the identities of the R groups of the starting selenides **111** were not explicitly stated in the publication.[265] The diaryl selenides yielded the corresponding selenoxides $Ar_2Se{=}O$, while the benzyl-substituted selenides afforded benzaldehyde and diselenide ArSeSeAr. Initial formation of a peroxyselenoxide **112** was proposed; however, the mechanism is not well understood. No mention was made of R_2SeO_2 dioxaselenirane **113** as a possible reaction intermediate (Scheme 43).

In 1976, a selenide photooxidation reaction was conducted in anhydrous methanol at room temperature.[266] Unfiltered light from an iodine lamp was employed, and Rose Bengal served as the sensitizer; the selenoxide yields are given in Table 36. No trapping reactions were conducted, although aryl selenides and selenoxides have been used as trapping agents[267] in other photooxidation processes.[268-270]

Little data exist on the dioxatellurirane, R_2TeO_2. Near-IR-absorbing tellurapyrylium dyes **114-118** have been suggested to form either $R_2Te^+OO^-$ pertelluroxide or R_2TeO_2 dioxatellurirane intermediates upon photooxidation with singlet oxygen,[271,272] but no distinction between the two intermediates was made (Scheme 44). The irradiation of the tellurapyrylium dyes was conducted in air-saturated aqueous

solutions with unfiltered light from a tungsten bulb in the absence of trapping agents. A reaction between pertelluroxide or telluradioxirane and substrate R_2Te may take place, to account for the formation of the $R_2Te{=}O$ product, which is readily hydrated to the diol $R_2Te(OH)_2$. The tellurium-containing dyes **114-116** reacted with singlet oxygen 20-80 times faster than the corresponding selenium and oxygen derivatives **117** and **118**. The tellurium-containing dye **114** reacted two times faster with singlet oxygen than **116**. The impetus to study the photooxidation of the tellurapyrylium dyes was their potential use in photodynamic therapy (PDT). Theoretical studies on the photooxygenation of selenides and tellurides should be informative. The possible formation of R_2SeO_2 and R_2TeO_2 heterodioxiranes, their cleavage products, and *Se*-hydroperoxyselenium and *Te*-hydroperoxytellurium ylides should be of interest.

4.4.3 Cyclic and Ring-Open Species

To assess the difference in stability between the various XO_2 heterodioxiranes, the computed energies between ring-closed and ring-open structures shall be compared. With the exception of Sawaki's review,[3] no comparison of this sort exists for the XO_2 dioxiranes. The relative energetics of the XO_2 dioxiranes compared to O-X-O acyclic compounds are summarized in Table 37. Cleavage of the O-O bond in XO_2 dioxiranes may lead, for example, to a nitro compound in the case of dioxaziridine (cf. entries 1-5, Table 37). In contrast, a Baeyer-Villiger reaction for some of the XO_2 dioxiranes may afford heteroatom-substituted esters or acids (cf. entries 6-11, Table 37). The above reactions are highly exothermic favoring the acyclic structures rather than the corresponding XO_2 dioxiranes. It was found that the energy difference is the greatest in the SO_2 system. Schaefer et al. have noted a decrease in this energy change for the

heavier XO_2 dioxiranes (H_2C > H_2Si > H_2Ge > H_2Sn ~ H_2Pb).[90] More systematic computational data is needed to recognize the factors that determine dioxirane stability. The data on the transition states for unimolecular O-O bond breaking process in XO_2 dioxiranes are scarce.

The calculated cyclization barriers for X-O-O into XO_2 dioxirane (X = RN, R_2Si, R_2S, and S) can be compared with the ~19 kcal/mol barrier for carbonyl oxides to dioxiranes (Table 38).[273] Computational data is not available for the acyclic X-O-O to cyclic XO_2 conversion (where X = R_3P, R_2Se, R_2Ge, R_2Sn, R_2Pb, R_2Te, and Se). Not for all XO_2 dioxiranes has an acyclic XOO counterpart been computationally found. For example, R_3P appears to be such a case, for which many theoretical methods conclude that the acyclic R_3POO species does not intervene in reactions of R_3P with $^1O_2$. Sawaki has conducted B3LYP/6-31G(d) calculations of the reaction enthalpies and activation energies for the cyclization of X-O-O to cyclic XO_2 (where X = O, HN, H_2C, S, HP, H_2Si, Se, HAs, and H_2Ge).[3] A lower activation energy was predicted for the cyclization of X-O-O in higher-row elements, for example H_2Si < H_2Ge < HP < H_2C ~ H_2S < HN < O. The second-row elements have more prominent 1,3-dipoles and enhanced double bond character in the X-O bond, whereas the higher-row elements have less double bond character.[3] It has also been suggested that a larger difference in the electronegativity between the X and O atoms results in a lower rotation barrier of X-O-O, which facilitates cyclization to the dioxirane.[143b]

4.4.4 Intermolecular Reactions

Carbon-based dioxiranes may donate an oxygen atom to acceptor molecules, such as alkenes, phosphines, sulfides, and in some cases even saturated hydrocarbons.[4,6,274-276]

Since R_2CO_2 dioxiranes have low strain energies (~11 kcal/mol for R=Me; ~16 kcal/mol for R=H); their enhanced oxidative reactivity[277] does not derive from the strain release in the oxygen-transfer process.[89,278-280] Instead, it is a result of the weak peroxide bond.[89,278-280] Some heteroatom-substituted XO_2 dioxiranes are able to transfer an oxygen atom to acceptor molecules (Table 39), but the literature is limited in comparison to R_2CO_2 dioxiranes.[4,6] An oxygen-transfer reaction of dioxaziridine RNO_2 or dioxasiliranes R_2SiO_2 has not yet been established. Oxygen-transfer studies of other XO_2 dioxiranes (X = R_2Se, R_2Ge, R_2Sn, R_2Pb, R_2Te, S, and Se) have also not been done.

Alkenes. Dioxaphosphirane (*o*-$MeOC_6H_4)_3PO_2$ has been used to convert alkenes to epoxides.[99] This alkene epoxidation appears to be a non-radical process. The mechanism of deoxygenation of (*o*-$MeOC_6H_4)_3PO_2$ does not involve a unimolecular fragmentation of an oxygen atom.[137] A dioxaphosphirane derived from 1-methyl-4-phospha-3,5,8-trioxabicyclo[2.2.2]octane reacts supposedly with norbornene to give norbornene oxide.[154,155a] There are no data available that demonstrates an intermolecular oxygen-transfer from an intermediary dioxaziridine to an alkene. A problem is that the alkene, e.g., 2,3-dimethyl-2-butene, reacts with the ground-state triplet nitrene to form an aziridine instead of a reaction with dioxaziridine to give the epoxide. An oxygen-substituted nitrene reaction exemplifies this, in which the triplet nitrene CH_3ON (**119**) reacts with 2,3-dimethyl-2-butene to produce aziridine **120** (Scheme 45).[10,23f] Acyclic nitroso oxides have been proposed to convert alkenes to epoxides **121**.[3] Nitroso oxide (e.g., PhNOO) and dioxaziridine (e.g., $PhNO_2$) will also rapidly oxidize additional triplet nitrene, since the reaction of nitrene with $^3O_2$ is slower.[39b] The highly reactive $PhN^{\bullet}OO^{\bullet}$ transfers an oxygen atom to toluene and anisole. At present, there are not

sufficient data available for comparing possible oxygen-transfer reactions of dioxaziridines and nitroso oxides.

Phosphorus- and Sulfur-Containing Reactants. Dioxaphosphiranes are capable of delivering an oxygen atom to phosphines, sulfides, and sulfoxides.[136-140,142,143,154,155] Also dioxathiiranes, e.g., $PhMeSO_2$ and Bu_2SO_2 (generated from sulfide radical cation—superoxide reactions) react presumably with phenyl sulfide to give phenyl sulfoxide.[184,185]

4.5 Synthetic Prospectives

Disappointingly, heteroatom-containing dioxiranes have not yet been found useful as oxidant alternatives for the popularly used carbon-based dioxiranes. Except for dioxaphosphirane, the XO_2 dioxiranes have only been of mechanistic interest, but their synthetic versatility remains still to be established, whereas the mechanistic aspects of XO_2 dioxiranes (X = R_3P, RN, R_2Si, and R_2S) are becoming better understood, little or no experimental evidence confirms the existence of the remaining XO_2 dioxiranes (X = R_2Se, R_2Ge, R_2Sn, R_2Pb, R_2Te, S, and Se).

Early research on R_2CO_2 dioxiranes showed that they were formed in carbene—O_2 reactions under conditions (e.g., low temperature matrix, combustion, etc.) that proved of little use in synthetic applications. The versatility of R_2CO_2 dioxiranes in synthetic organic chemistry emerged after the discovery of their generation from aqueous oxone—ketone reactions.[4,6] The use of oxone to generate dioxiranes from ketones was an important discovery. R_2CO_2 dioxiranes are generated from ketones in other ways, including the reaction with arenesulfonic peracids [generated from (arenesulfonyl)imidazole/H_2O_2/NaOH],[272] peroxyimidic acid MeC(=NH)OOH (thought

to be generated from MeCN/H_2O_2),[274] and possibly peroxynitrite.[275,276] Overcoming obstacles in generating experimentally useful concentrations of R_2CO_2 dioxiranes and in developing catalytic processes for their production were essential for synthetic applications to be realized.

No XO_2 dioxiranes have yet been generated from their corresponding X=O precursors, analogous to the preparation of R_2CO_2 dioxiranes from ketones. Attempts in this regard have been sparsely reported. For example, generating dioxaphosphirane Ph_3PO_2 by the oxidation of Ph_3P=O with MCPBA or H_2O_2-trifluoroacetic acid-trifluoroacetic anhydride was unsuccessful.[2] A reaction of ^{18}O-labeled dimethylsulfoxide with oxone failed to generate the Me_2SO_2 dioxathiirane.[1] In view of their considerable instability and tendency to form polymers, the reaction of oxone with R_2Si=O silanones has not been explored, in an attempt to generate dioxasilirane.

4.5 Summary

Progress has been made in regard to the direct experimental evidence for the generation of R_3PO_2, RNO_2, and R_2SiO_2 dioxiranes. The R_2SO_2 and R_2TeO_2 dioxiranes are tentatively assigned based on indirect experimental methods; however, experimental evidence is lacking for the homologue dioxiranes R_2SeO_2, R_2GeO_2, R_2SnO_2, R_2PbO_2, SO_2, and SeO_2. Theoretical calculations predict that the XO_2 dioxiranes should persist under a variety of reaction conditions, but no computations have as yet been reported on the cyclic SeO_2.

The chemistry of XO_2 dioxiranes is still not well understood and far less developed compared to R_2CO_2 dioxiranes,[4,6] a serious shortcoming for the effective use of XO_2 dioxiranes in synthetic chemistry. In this regard, the dioxaphosphiranes are the

only XO_2 dioxiranes that display synthetic utility in intermolecular (oxygen-transfer) reactions.

Challenging problems that await exploration include: (i) the discovery of methods to generate XO_2 dioxiranes from their corresponding X=O (monoxide) precursors, (ii) the development of asymmetric XO_2 oxygen-transfer reactions (precursors or catalysts bearing chiral substituents on X), (iii) the discovery of a possible synthetic advantage of XO_2 over R_2CO_2 in cases where X itself is a chiral center, (iv) the design of heterogeneous reactions to tether XO_2 dioxiranes onto solid surfaces to minimize unwanted bimolecular reactions, (v) the creation of "persistent" or at least sufficiently long-lived XO_2 dioxiranes to enable their isolation under the more common laboratory conditions by stabilizing the dioxiranes kinetically (e.g., utilizing sterically bulky substituents to shield the peroxide center or by caging dioxiranes in host molecules such as carcerands or dendrimers) or thermodynamically (e.g., electronic substituent effects to reduce the energy difference between reactants and intermediate), and (vi) assessment of the nucleophilic or ambiphilic oxidation character of the XO_2 dioxirane oxygen atoms.

Scheme 1. Formation of XO_2 Dioxiranes

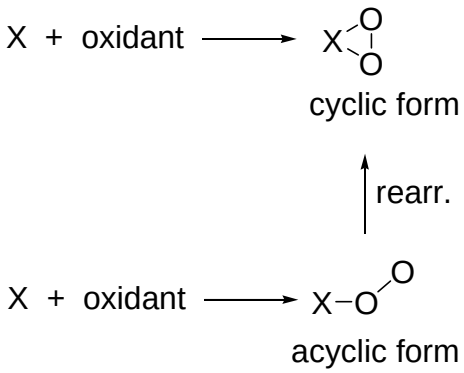

Scheme 2. Types of XO_2 Dioxiranes

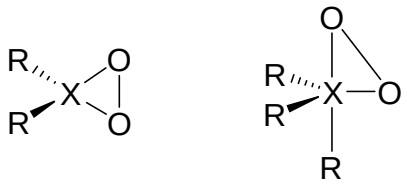

tetrahedral trigonal bipyramidal

An R group can be a lone pair of electrons

Scheme 3. Reaction of Nitrene with O_2

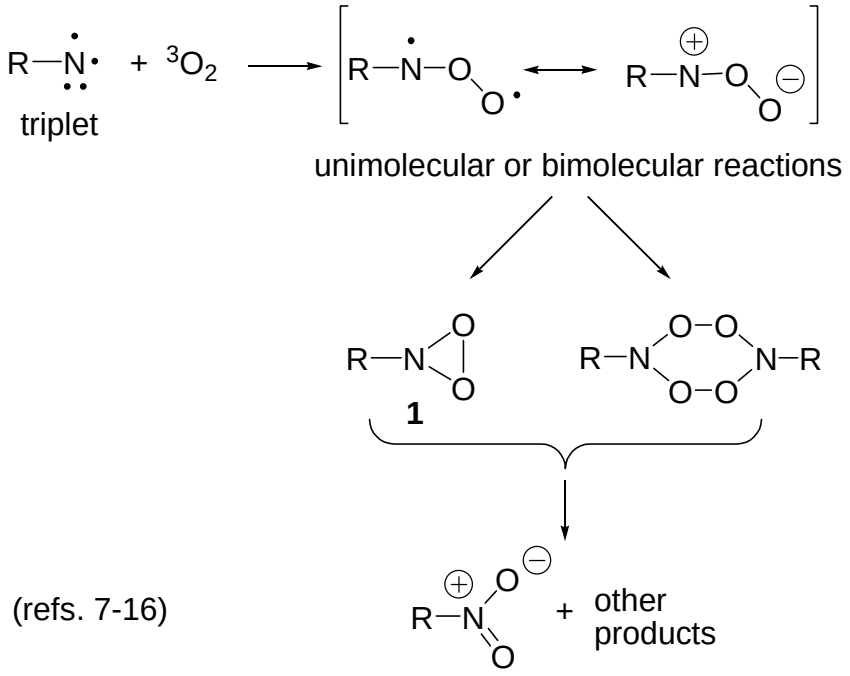

(refs. 7-16)

Scheme 4. Dioxaziridine Precursors

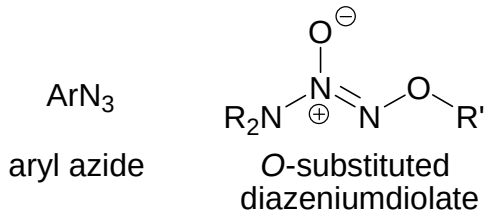

Scheme 5. Photooxidation of *p*-Diazidobenzene

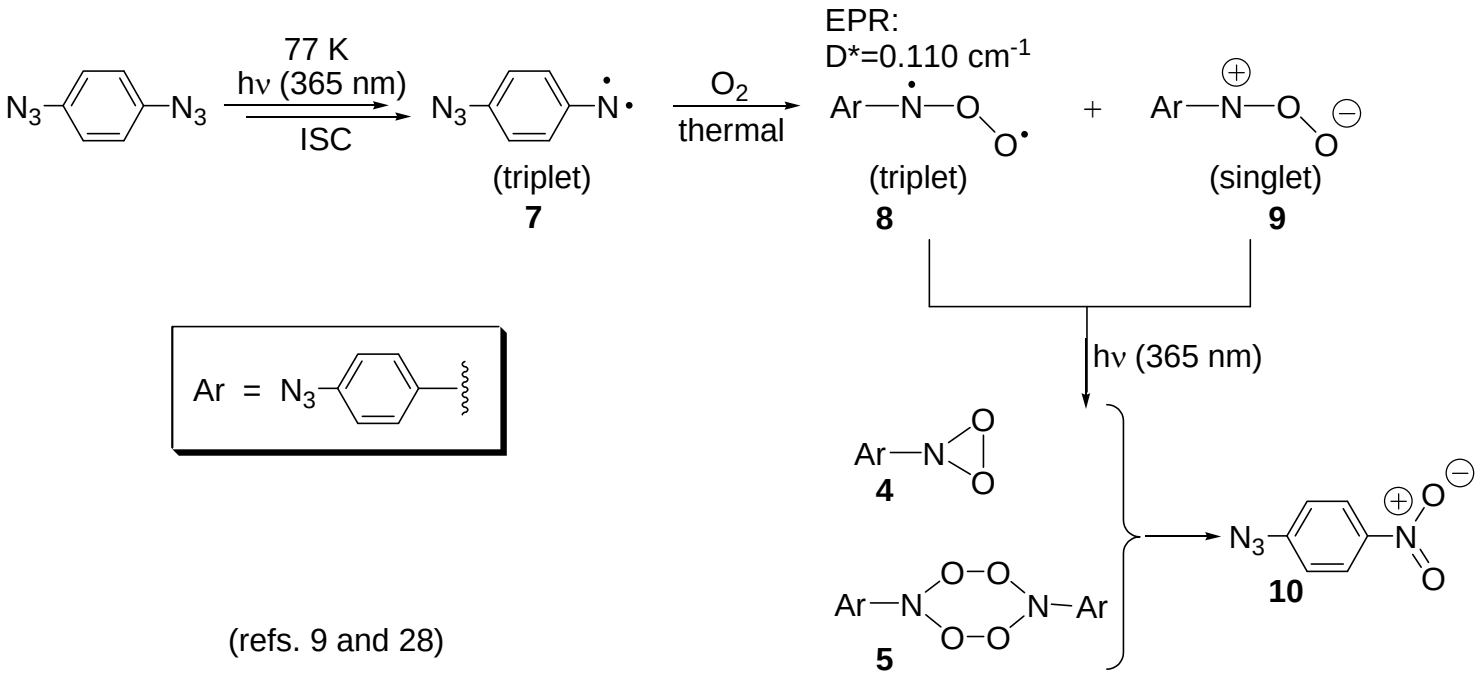

(refs. 9 and 28)

Scheme 6. Photooxidation of *O*-substituted Diazeniumdiolate

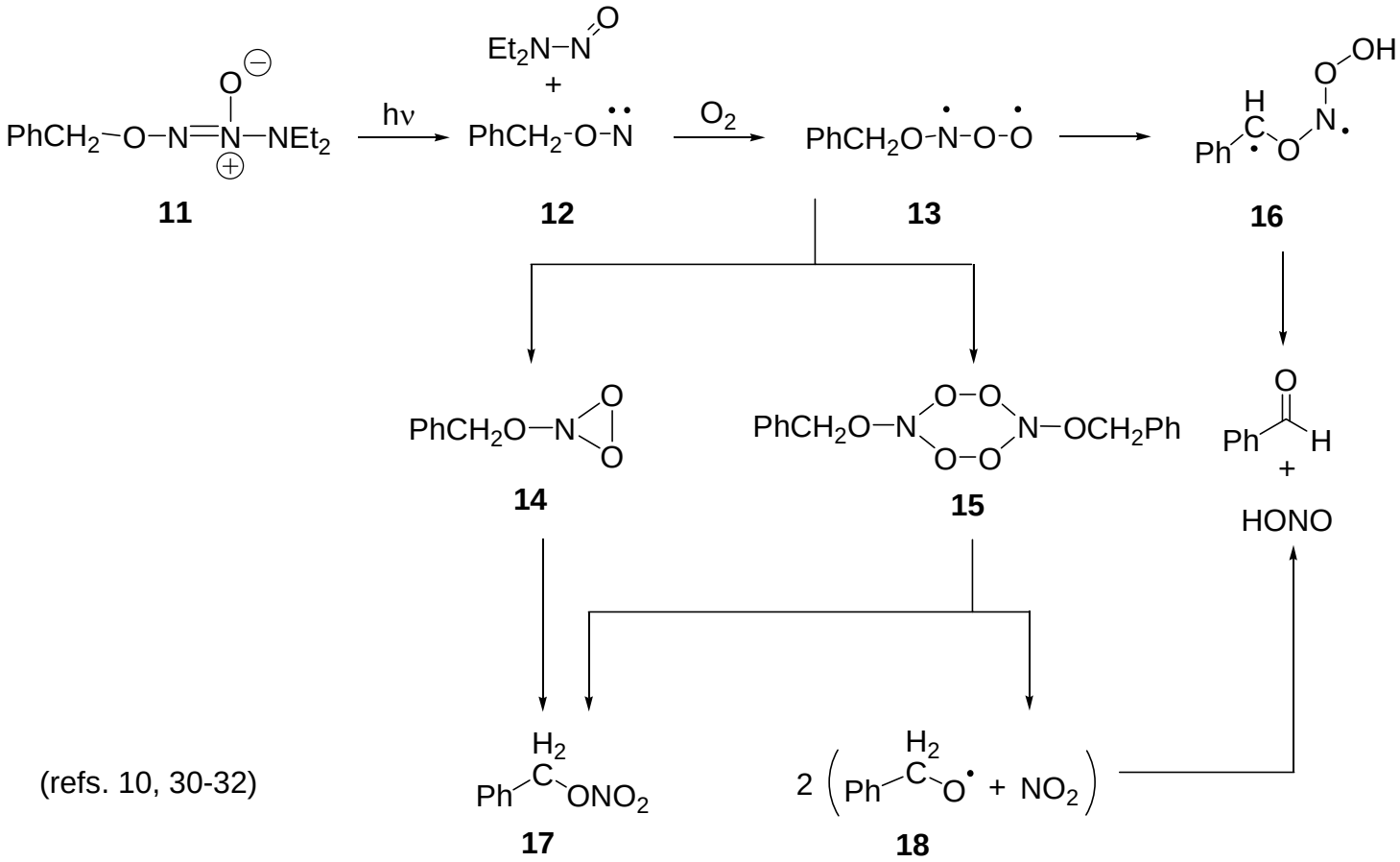

(refs. 10, 30-32)

Scheme 7. Formation of an Ion Pair Transition State

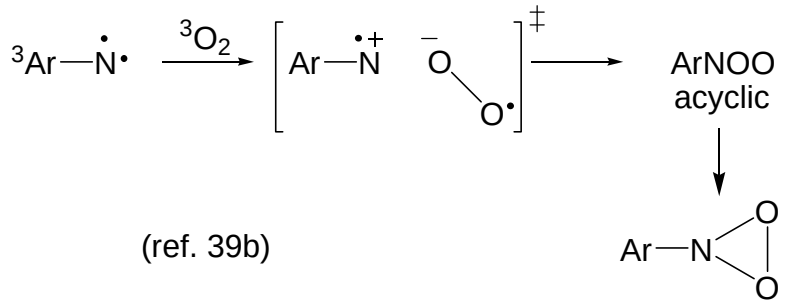

(ref. 39b)

Scheme 8. Reactions of Nitroso Oxides

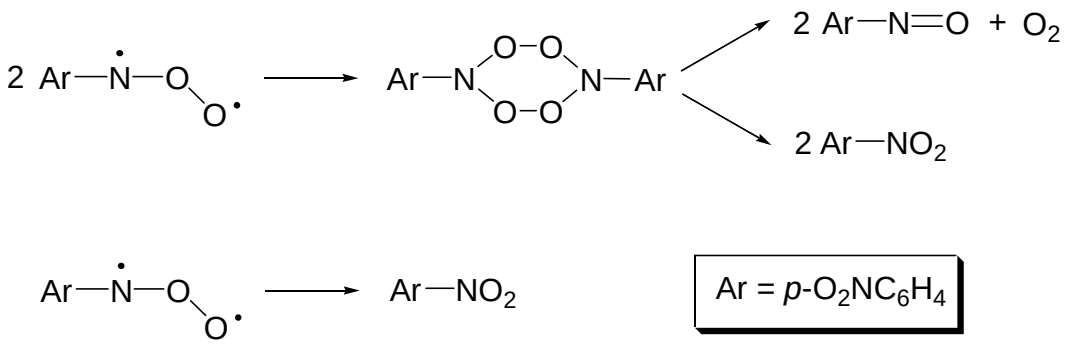

(refs. 10, 18, 34-36)

Scheme 9. Nitrene Dimerization

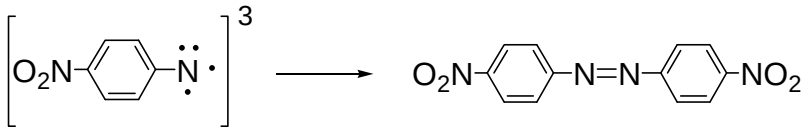

high
concentration

(refs. 10 and 18)

Scheme 10. ^{18}O-Labeling Study in Aryl Azide Photooxidations

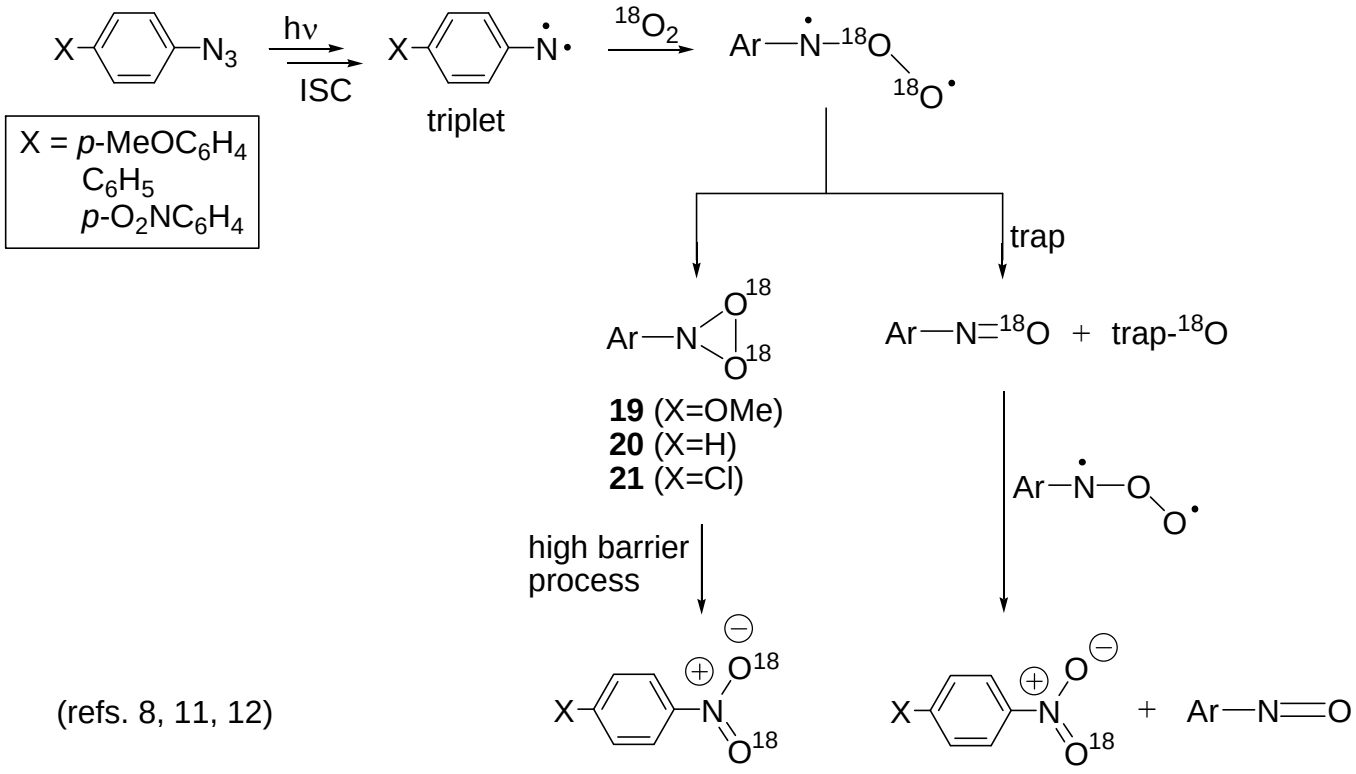

(refs. 8, 11, 12)

Scheme 11. Oxygen Transfer from Phenyl Nitroso Oxide to Toluene-4-*d* and Methoxybenzene-4-*d*

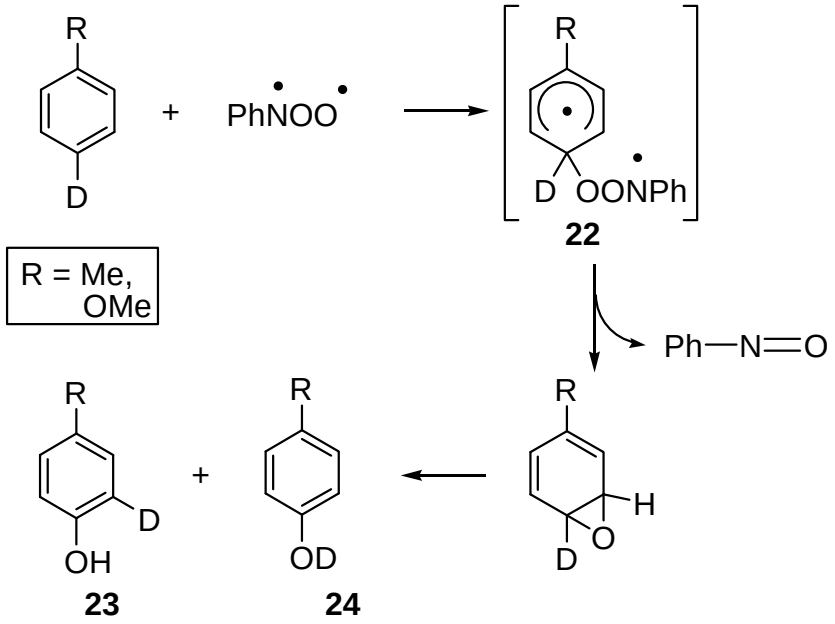

(ref. 11)

Scheme 12. Resonance Forms of Nitroso Oxide

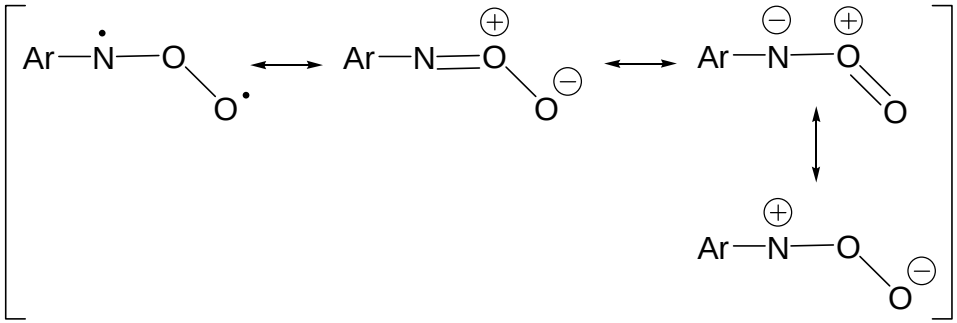

(ref. 8)

Scheme 13. Photooxidations of Aryl Azides

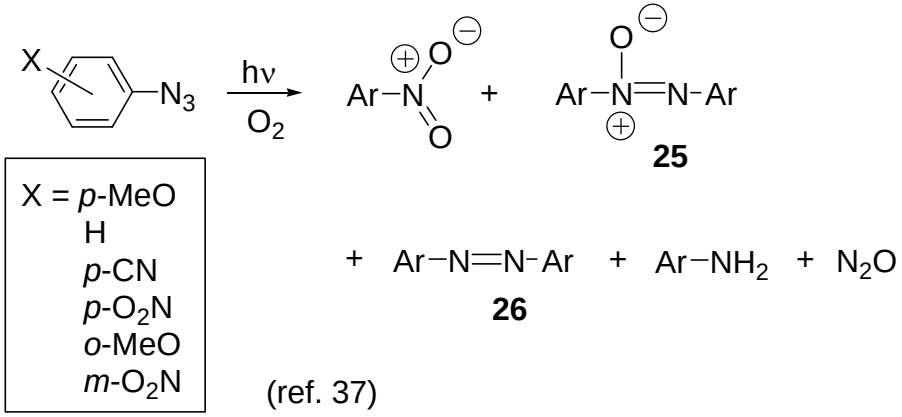

X = *p*-MeO
H
p-CN
p-O_2N
o-MeO
m-O_2N

(ref. 37)

Scheme 14. Cyclization of Peroxynitrite

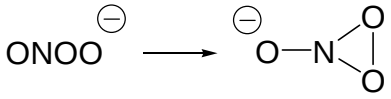

Scheme 15. Reaction of Silylene with O_2

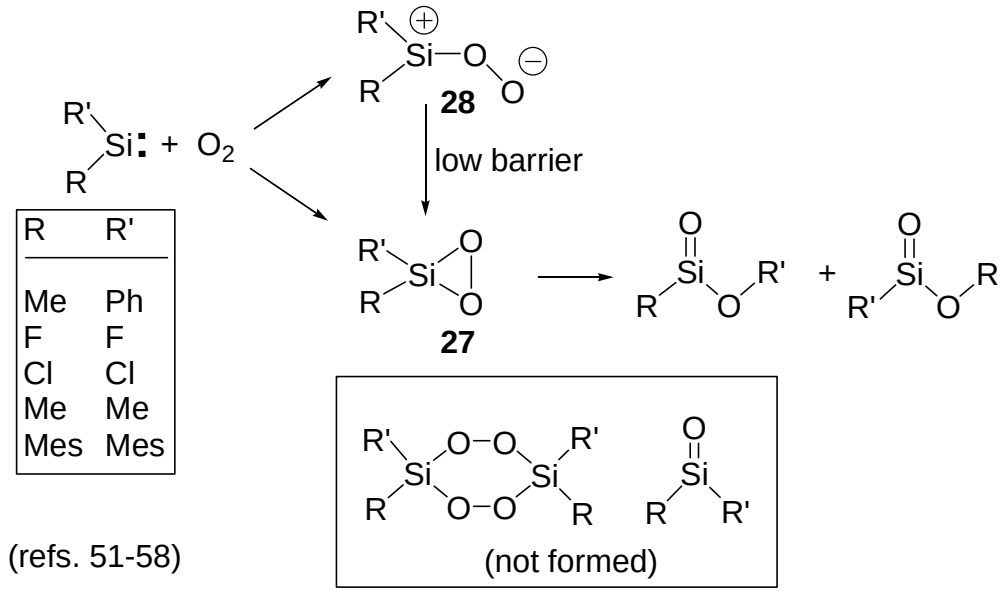

Scheme 16. Reaction of Silylene with O_2

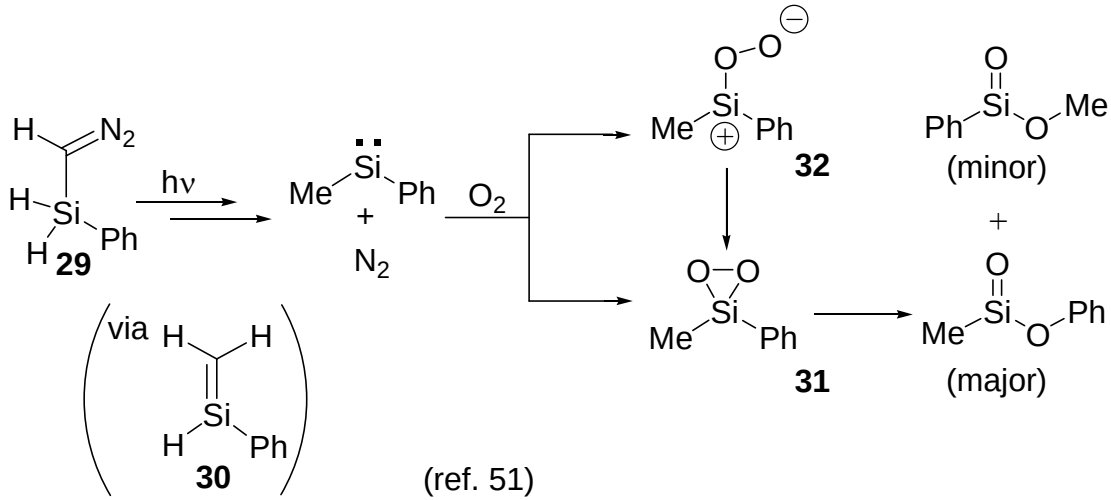

(ref. 51)

Scheme 17. Pyrolysis of Hexahalodisilane

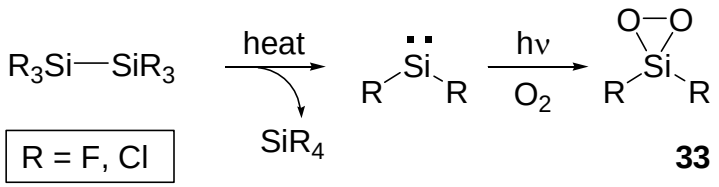

(refs. 52, 55, 56)

Scheme 18. Generation of Silylene and a Subsequent Reaction with O_2

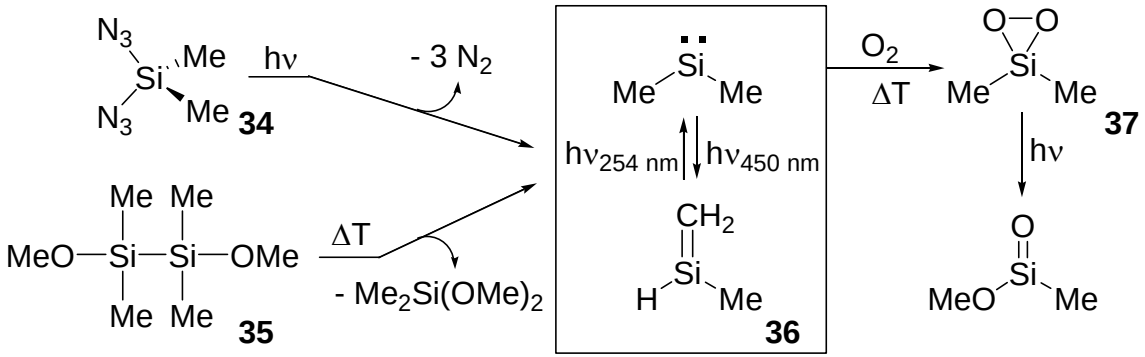

(refs. 53, 54)

Scheme 19. Irradiation of 2,2-bis(2,4,6-Trimethylphenyl)hexamethyltrisilane

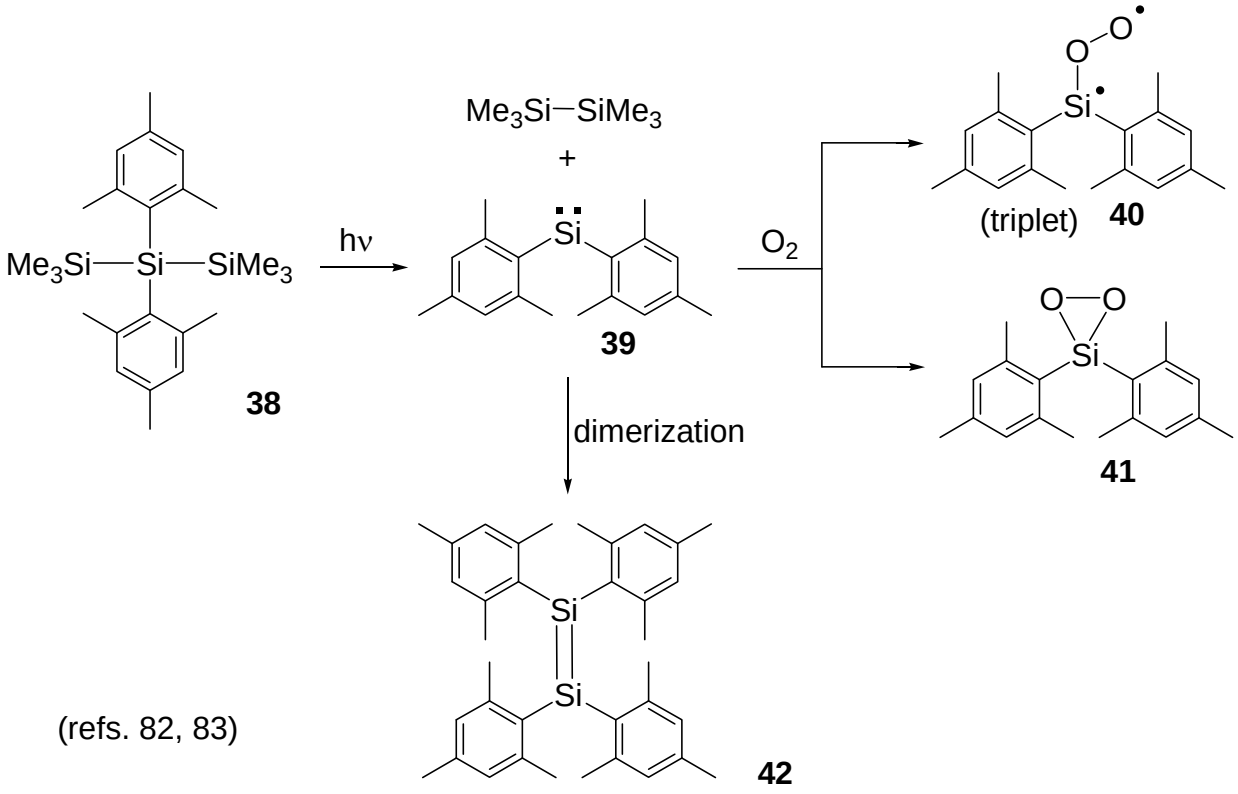

(refs. 82, 83)

Scheme 20. A Possible Surface-Bound Dioxasilirane

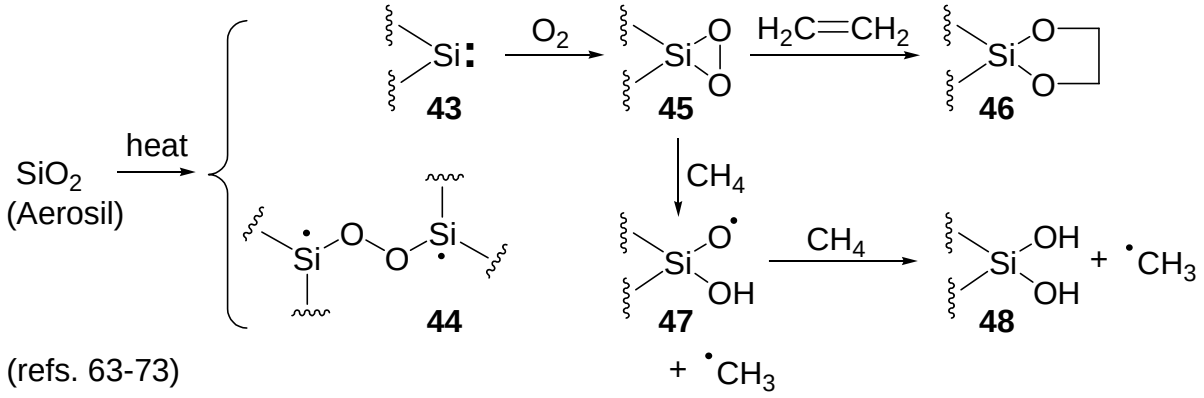

(refs. 63-73)

Scheme 21. Possible Reaction of the SiH_3 Radical with O_2

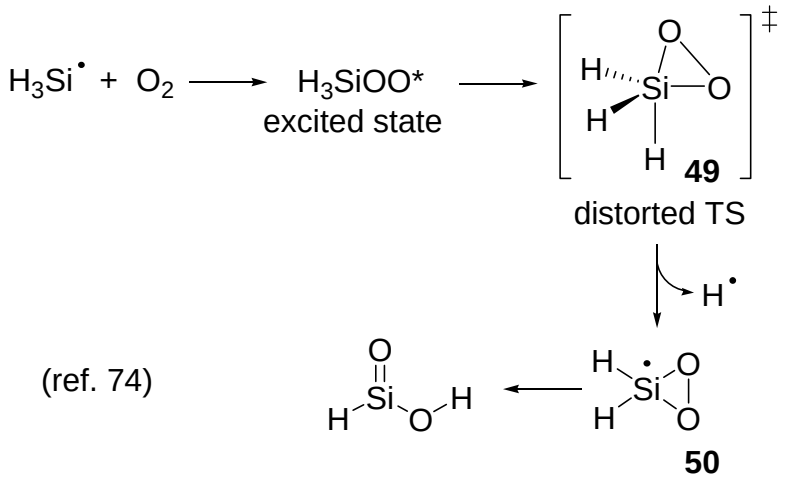

Scheme 22. Dioxagermirane, Dioxastannirane, and Dioxastilbirane

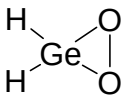

51

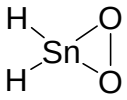

52

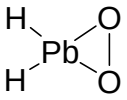

53

(ref. 90)

Scheme 23. Reaction of Selenium with O_2

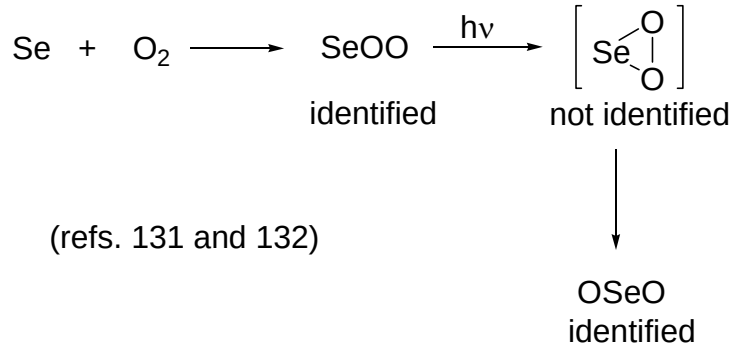

(refs. 131 and 132)

Scheme 24. Reaction of tris(*o*-Methoxyphenyl)phosphine with Singlet Oxygen

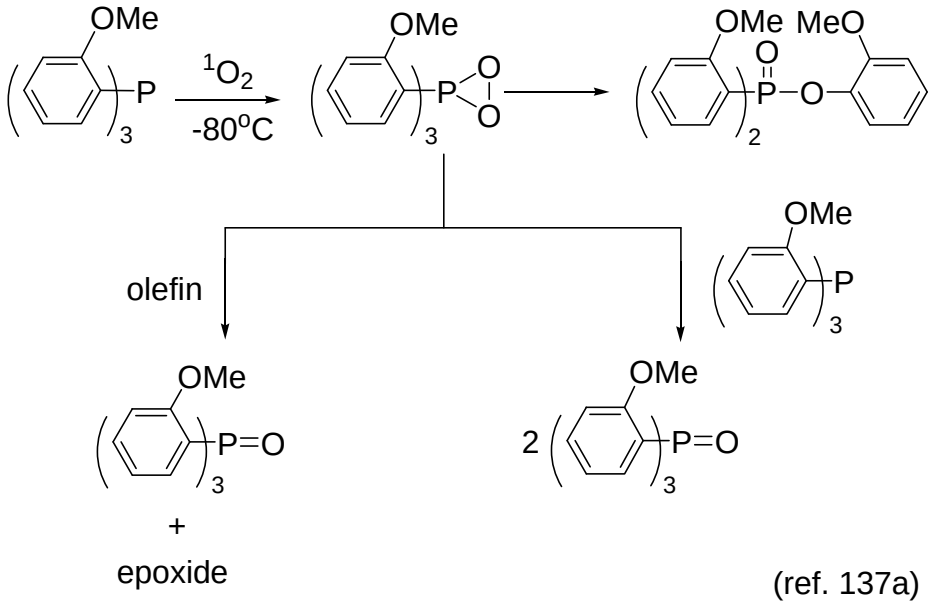

(ref. 137a)

Scheme 25. Reaction of Binaphthyl-Containing Phosphines with Singlet Oxygen

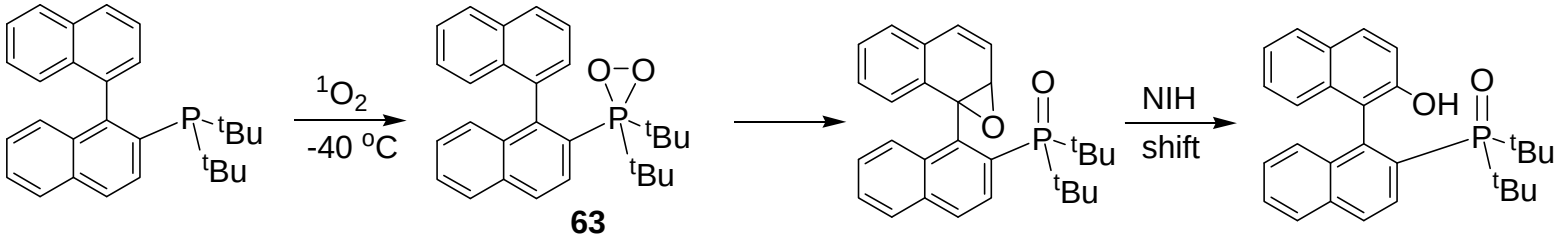

63

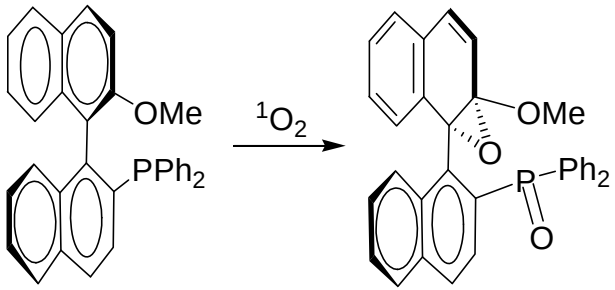

63'

(ref. 138)

Scheme 26. Reaction of a Phosphoranide Ion with O_2

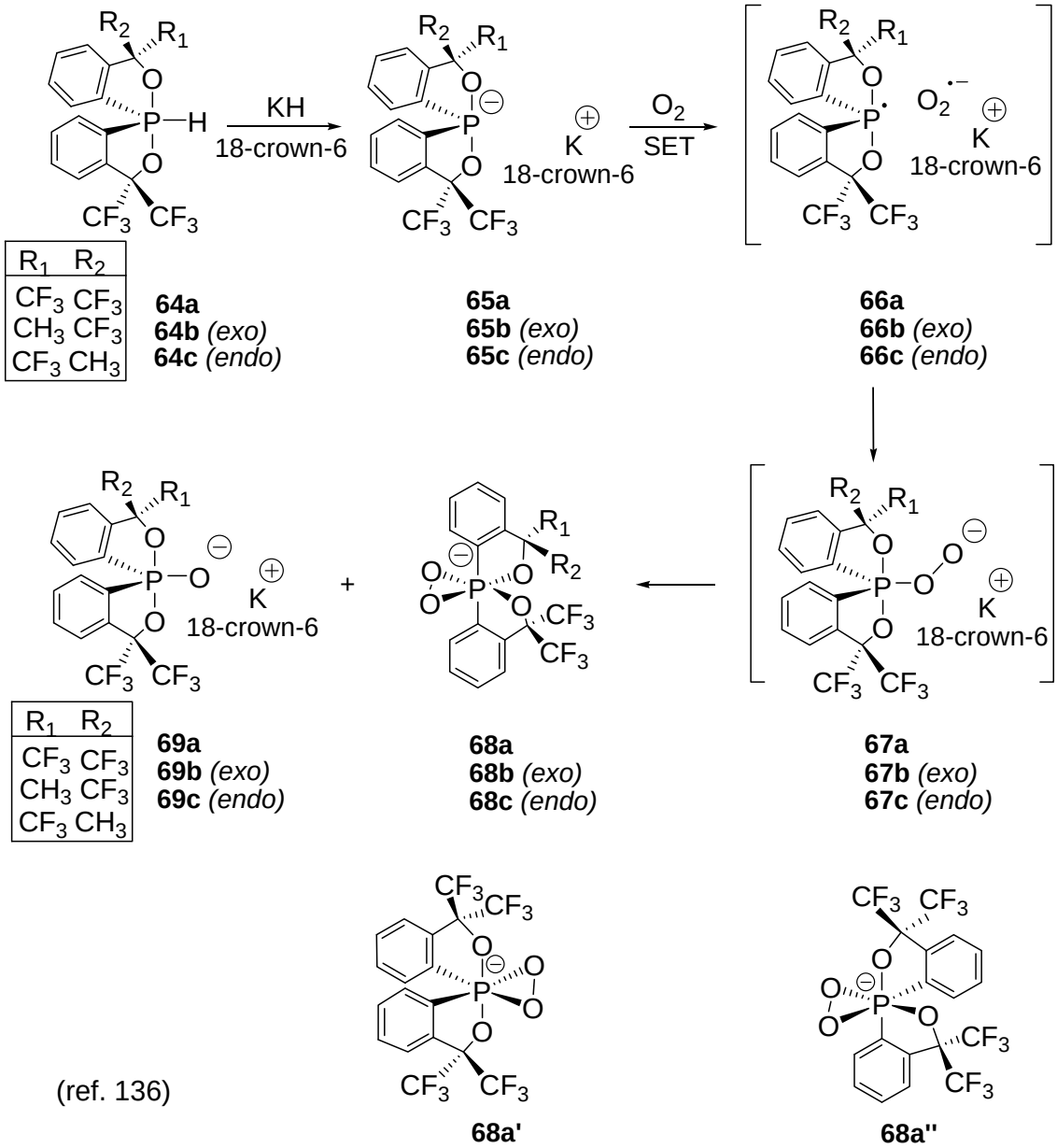

R_1	R_2
CF_3	CF_3
CH_3	CF_3
CF_3	CH_3

64a
64b *(exo)*
64c *(endo)*

65a
65b *(exo)*
65c *(endo)*

66a
66b *(exo)*
66c *(endo)*

67a
67b *(exo)*
67c *(endo)*

68a
68b *(exo)*
68c *(endo)*

R_1	R_2
CF_3	CF_3
CH_3	CF_3
CF_3	CH_3

69a
69b *(exo)*
69c *(endo)*

(ref. 136)

68a'

68a''

Scheme 27. Photolysis of a Phosphine--Ozone Complex[a]

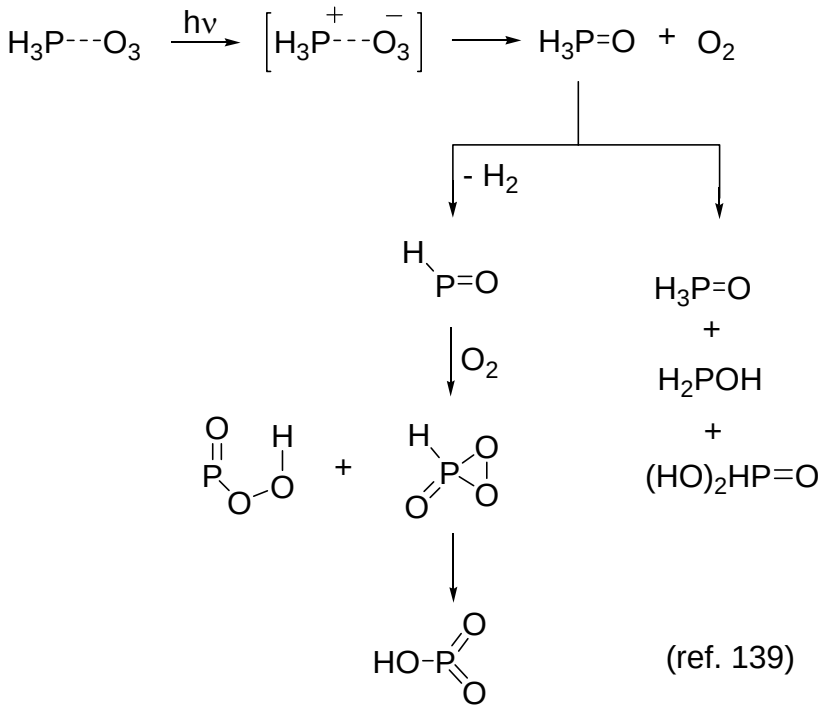

[a]Participation of intermediates that are rotationally excited, vibrationally excited or electronically excited are not noted here.

Scheme 28. ^{18}O-Labeling Study of a Dioxaphosphirane Rearrangement

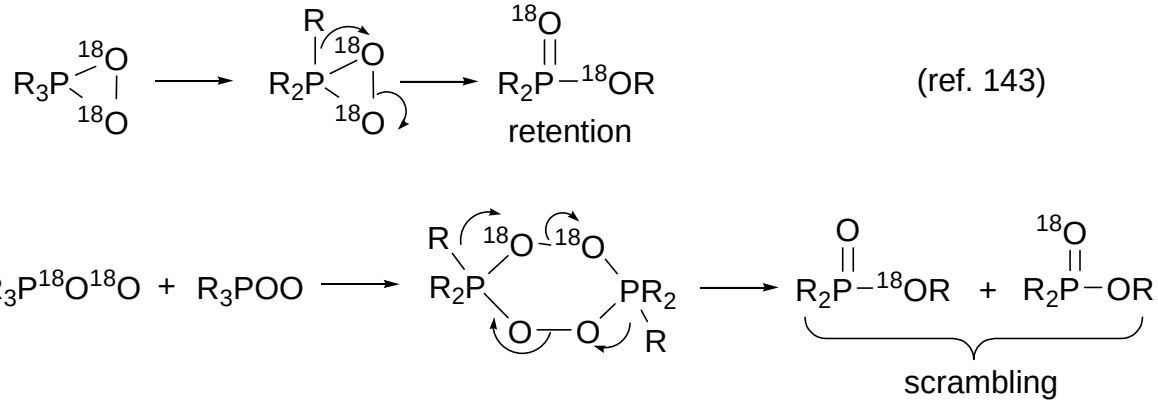

Scheme 29. Peroxyphosphine Oxide Rearrangement

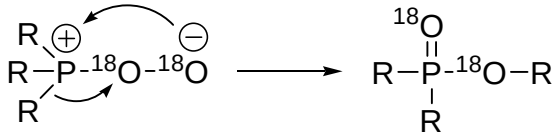

(ref. 143)

Scheme 30. Reaction of Aryl Phosphines with Singlet Oxygen

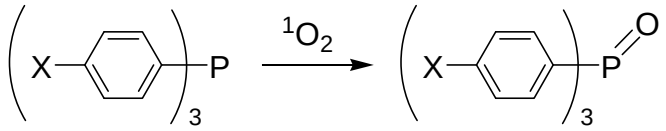

X = MeO, H, F, Cl, CF_3

(ref. 137b)

Scheme 31. Reaction of a Bicyclic Phosphite with Singlet Oxygen

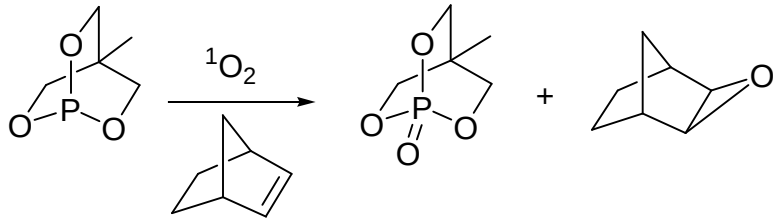

(refs. 154 and 155)

Scheme 32. Reaction of a Betaine with Hydrogen Peroxide

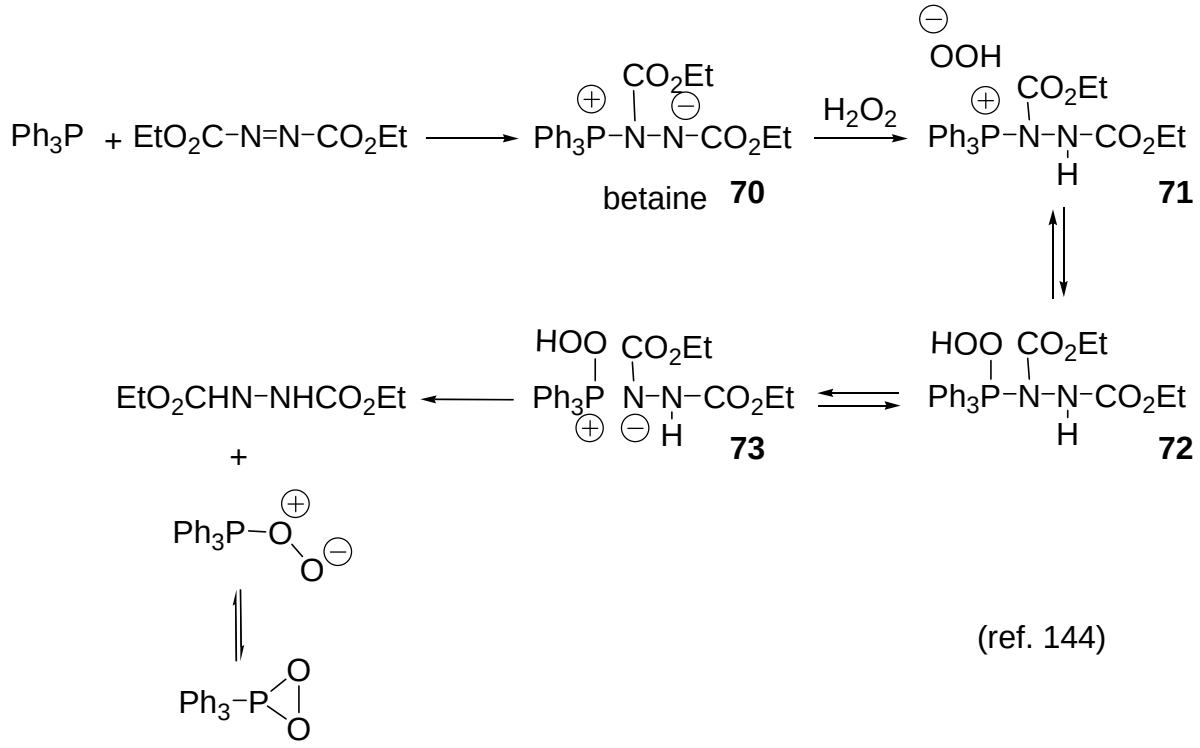

(ref. 144)

Scheme 33. Phenyl Migration in Triphenyldioxaphosphirane

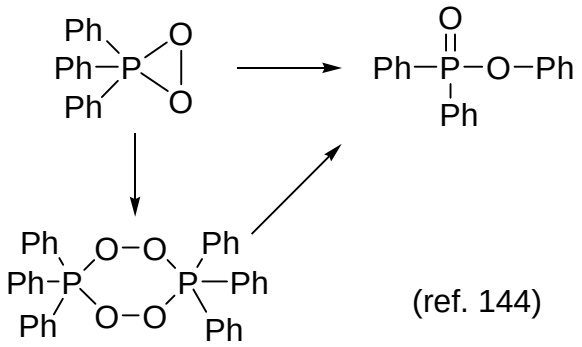

(ref. 144)

Scheme 34. Reaction of Triarylphosphine with O_2

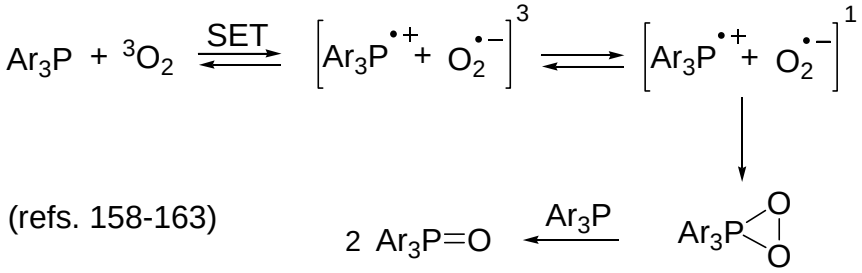

(refs. 158-163)

Scheme 35. Thermal Reaction of Bisdiphenylphosphinic Peroxide

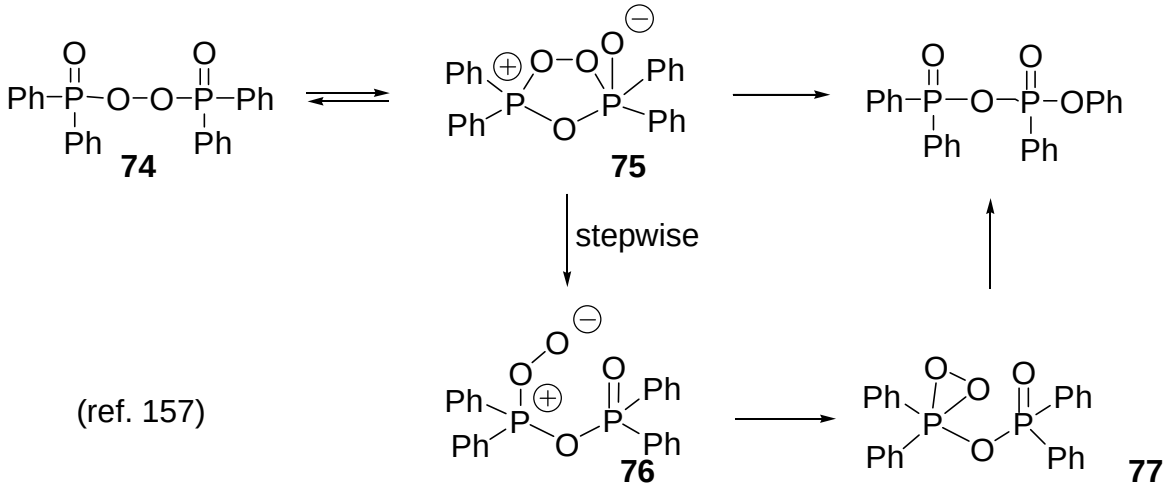

Scheme 36. Resonance Forms of Dioxaphosphirane

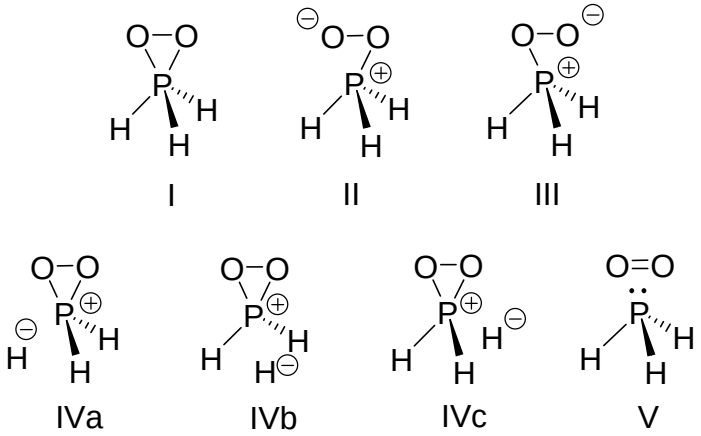

(ref. 141)

Scheme 37. Electron-Transfer Photooxidation of Dibenzothiophenes

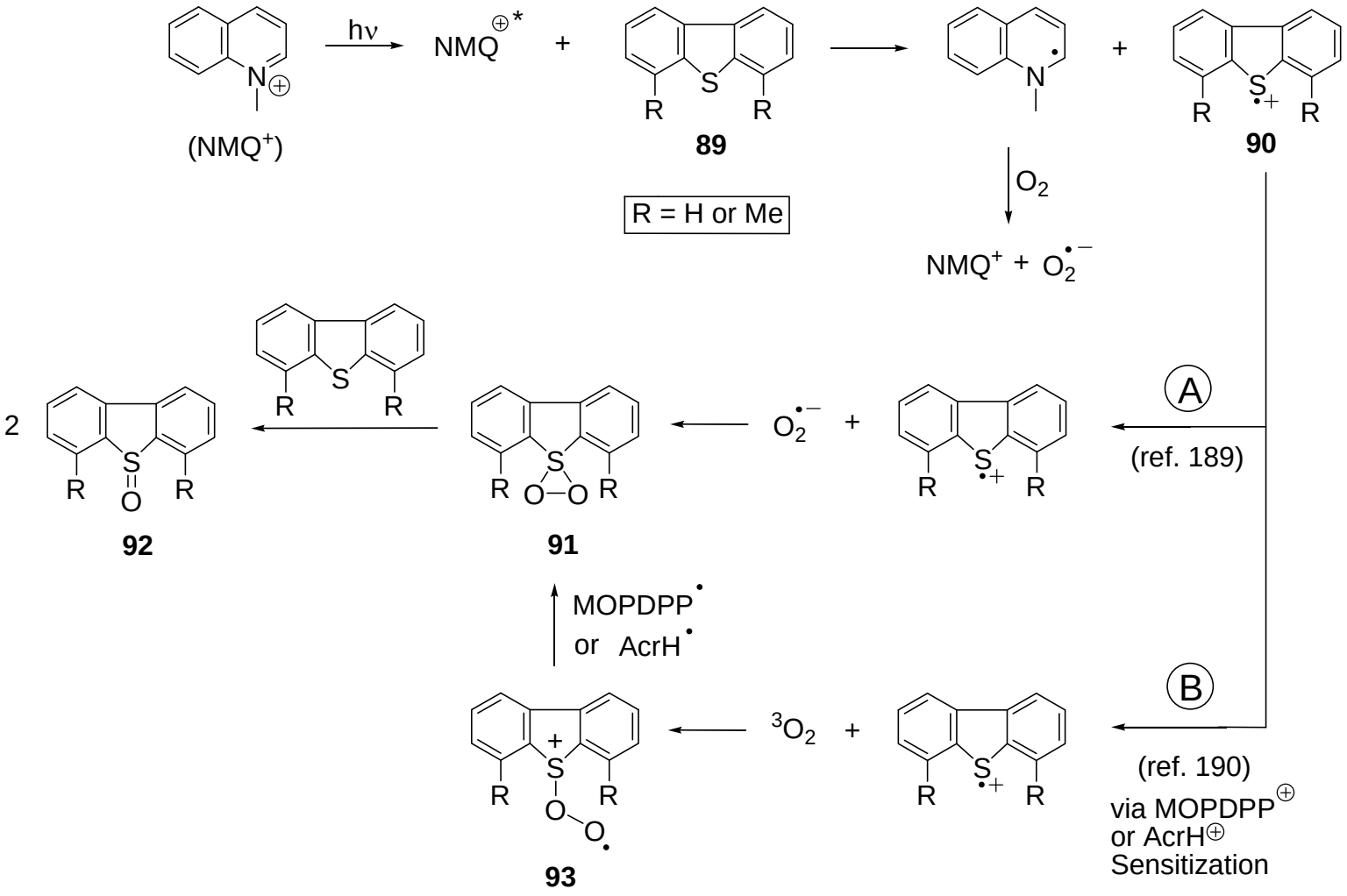

Scheme 38. Electron-Transfer Photooxidation of Dibutylsulfide and Thioanisole

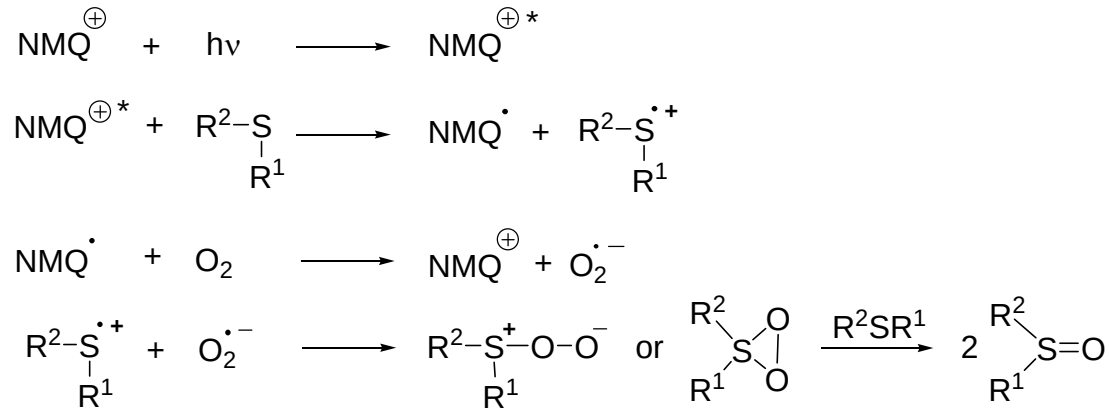

$R^1 = R^2 = Bu$ (**94**)

$R^1 = Me$; $R^2 = Ph$ (**95**)

(ref. 184)

Scheme 39. Reaction of Sulfides with Singlet Oxygen

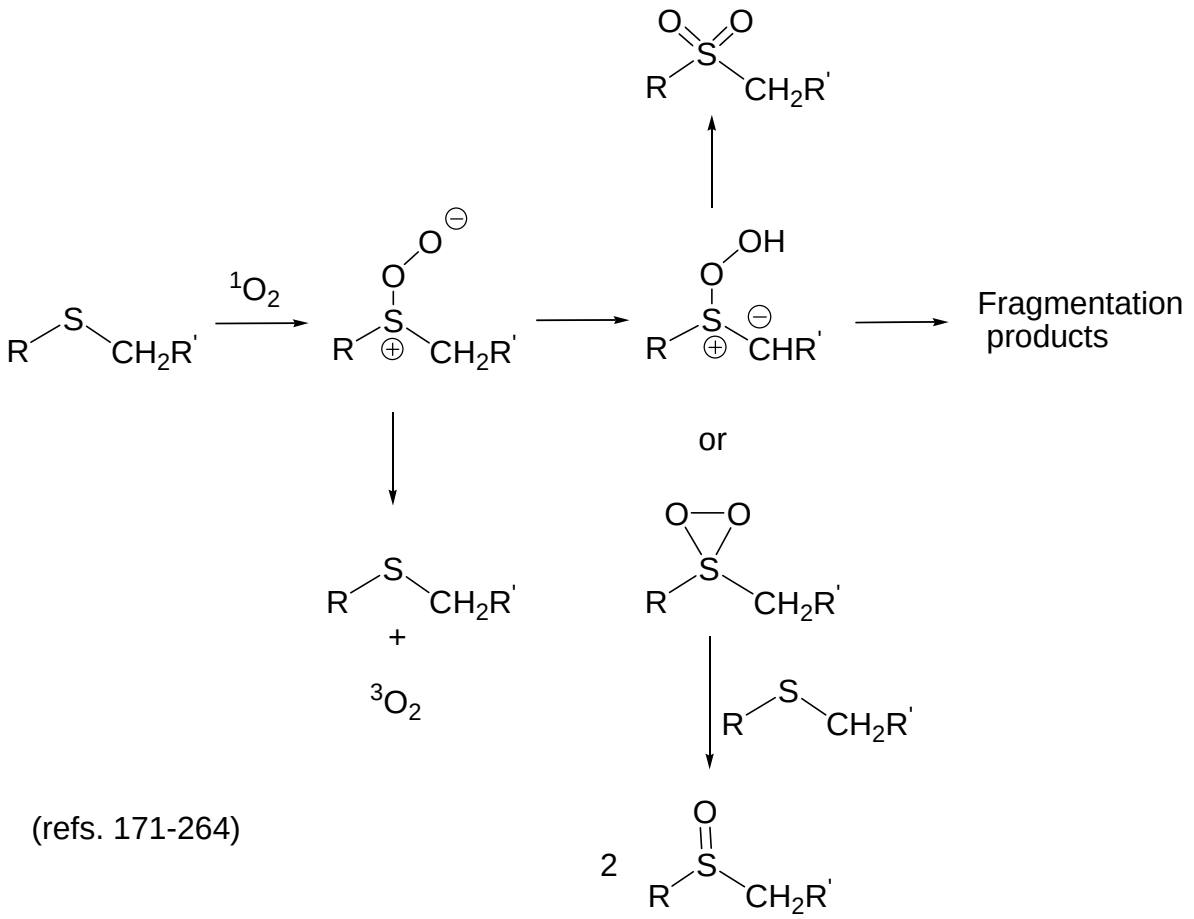

(refs. 171-264)

Scheme 40. Reaction of γ-Phenylthiocrotonate with Singlet Oxygen

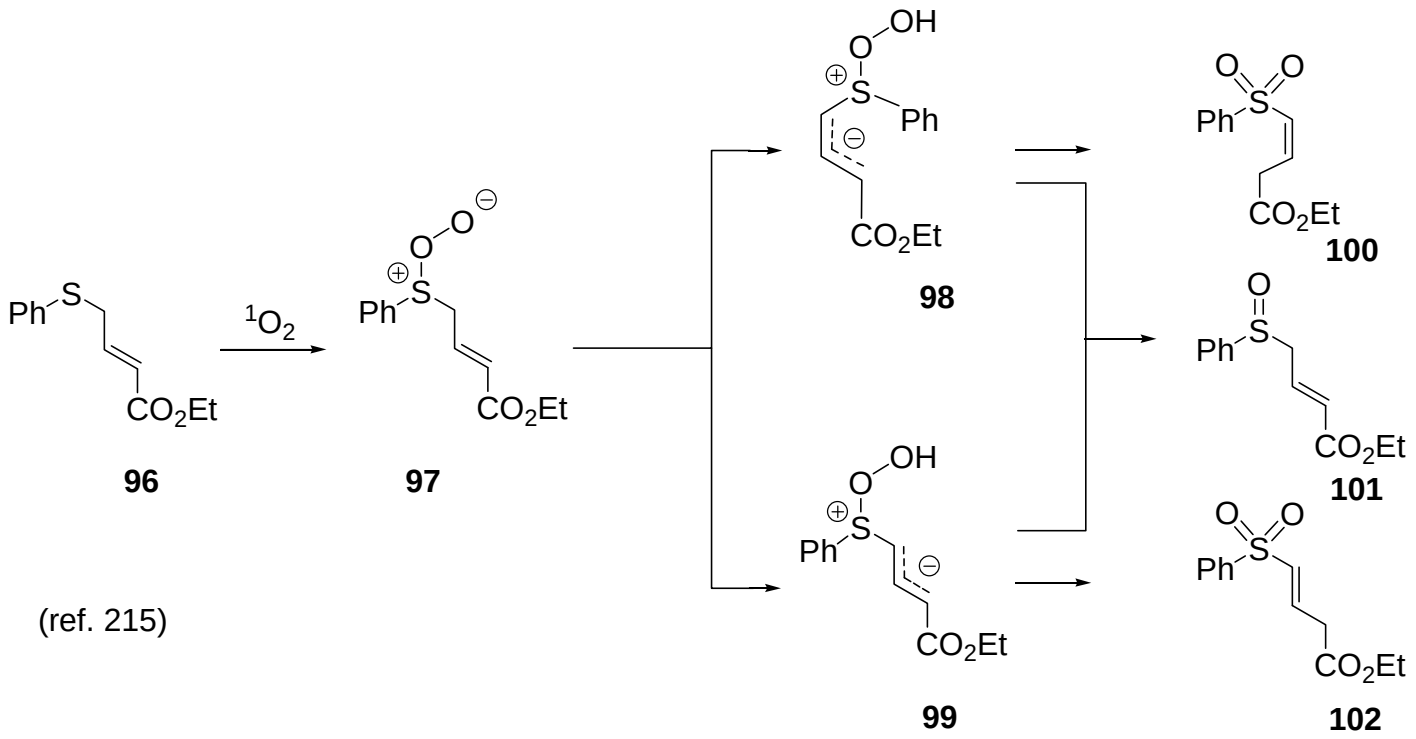

(ref. 215)

Scheme 41. Photooxidation of Cobalt- and Platinum-Thiolate Complexes

A

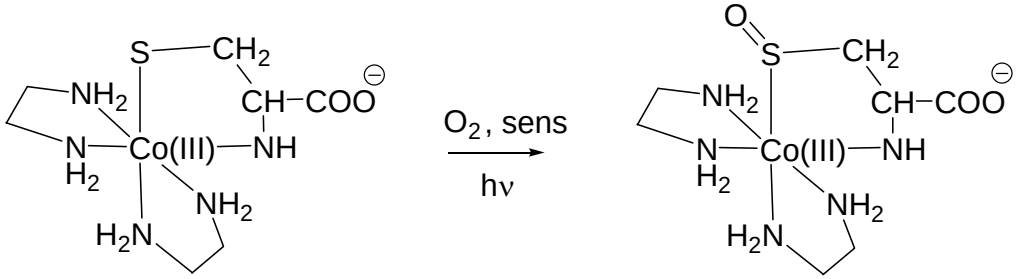

102 **103**

(refs. 255-263)

B

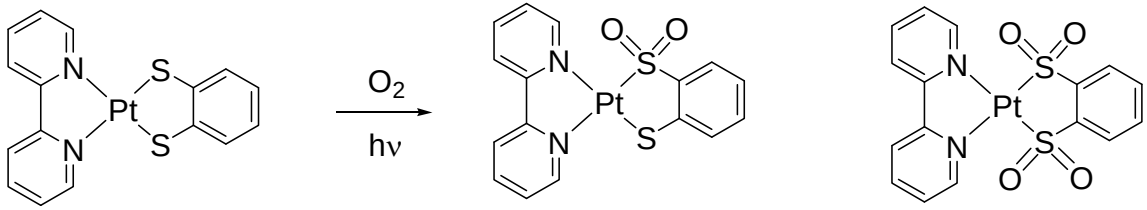

Pt(bpy)(bdt)

104

C

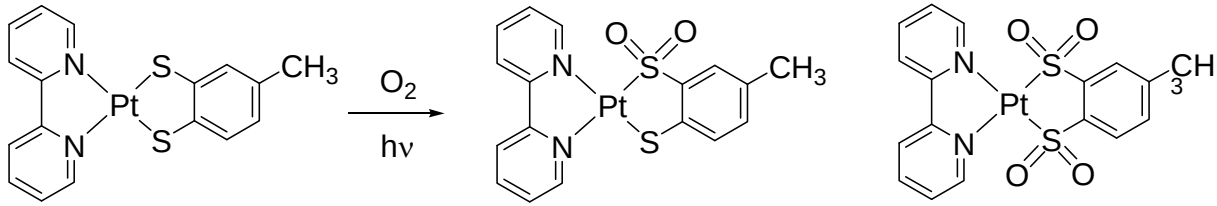

Pt(bpy)(tdt)

105

Scheme 42. Photooxidation of a Nickel-Thiolate Complex

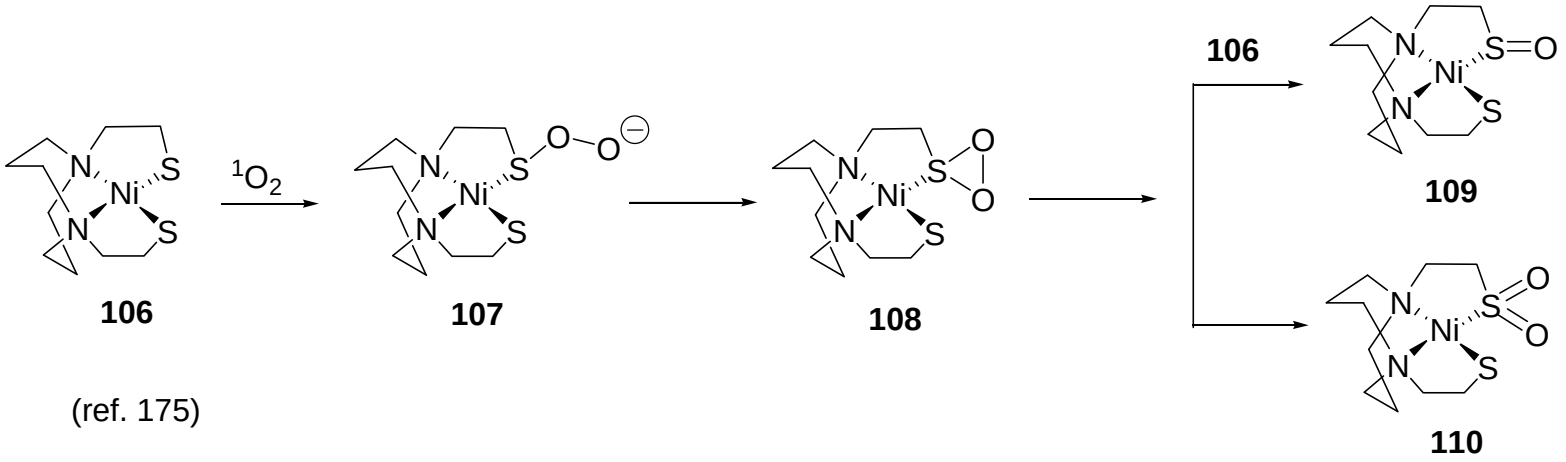

(ref. 175)

Scheme 43. Selenide, Peroxyselenoxide, and Dioxaselenirane

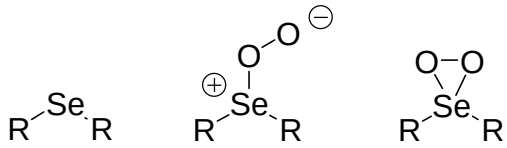

111 **112** **113**

(ref. 265)

Scheme 44. Photooxidation of Tellurium-, Selenium-, and Oxygen-Containing Dyes

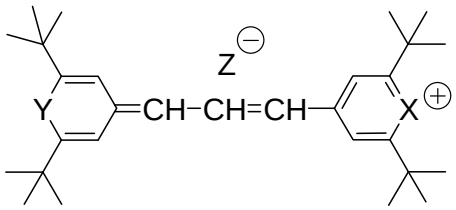

(ref. 271)

Structure	X	Y	Z
114	Te	Te	BF_4^-
115	Te	Se	ClO_4^-
116	Te	O	ClO_4^-
117	Se	O	ClO_4^-
118	O	O	ClO_4^-

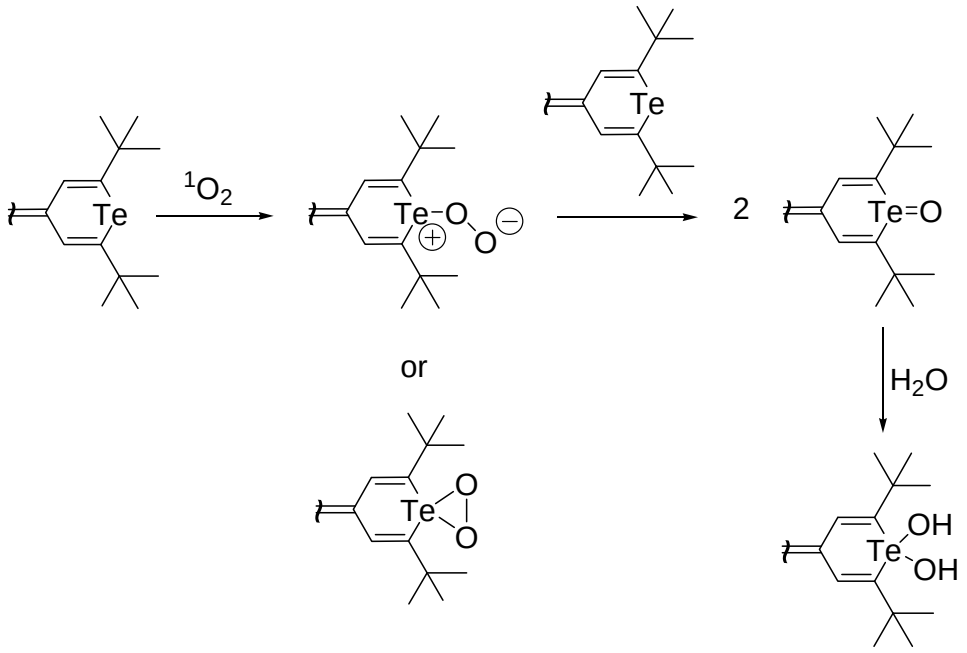

Scheme 45. Reaction of a Nitrene or Nitroso Oxide with an Alkene

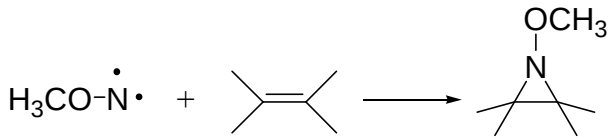

119 **120**

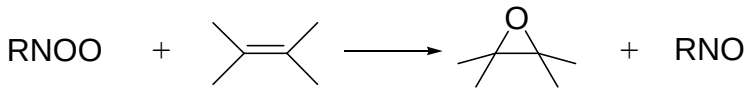

121

(refs. 8 and 10)

Chart 1. Phosphorus- and Oxygen-Containing Compounds

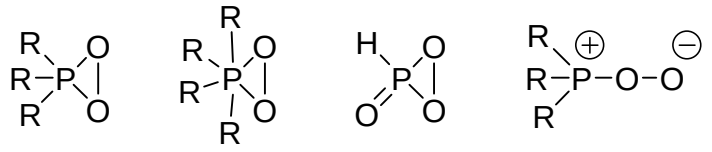

54 **55** **56** **57**

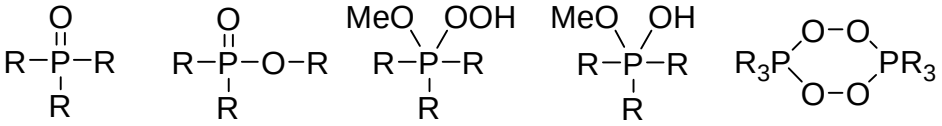

58 **59** **60** **61** **62**

(refs. 136-144)

Chart 2. Sulfur- and Oxygen-Containing Compounds

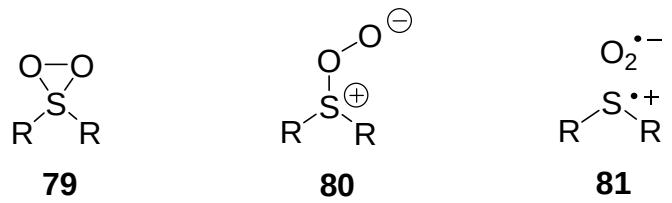

79 **80** **81**

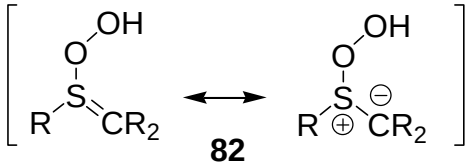

82

83 **84**

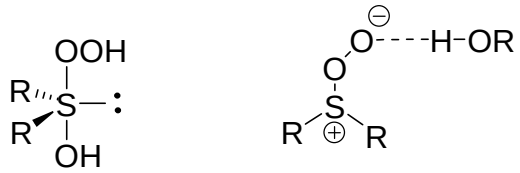

85 **86**

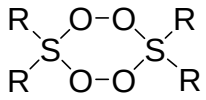

87

(refs. 2, 4, 171-264)

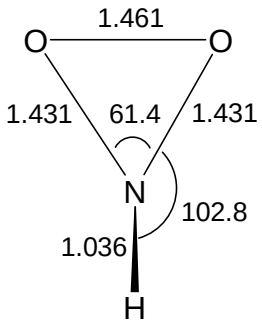

Figure 1. B3LYP/6-31G(d) computed structure of the unsubstituted dioxaziridine from Ref. 7. Bond lengths in Å; bond angles in degrees.

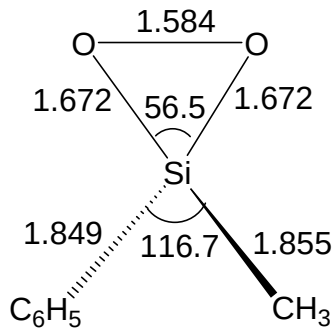

Figure 2. B3LYP/6-311++G(d,p) computed structure of the methylphenyldioxasilirane from Ref. 51. Bond lengths in Å; bond angles in degrees.

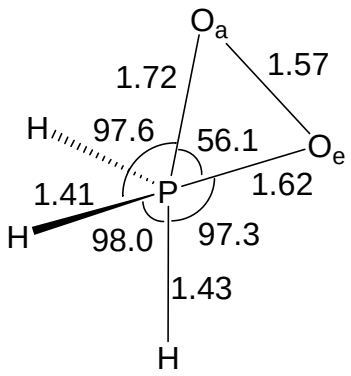

Figure 3. B3LYP/6-31+G(d) computed structure of the unsubstituted dioxaphosphirane from Ref. 141. Bond lengths in Å; bond angles in degrees.

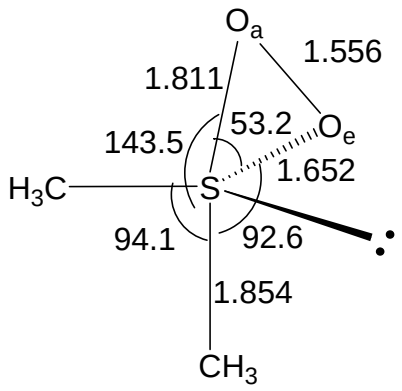

Figure 4. MP2/6-31G(d) computed structure of the dimethyldioxathiirane from Ref. 213. Bond lengths in Å; bond angles in degrees.

Table 1. Generation of Dioxaziridines (RNO_2 Dioxirane) or Tetraoxadiazinane (Diperoxide)

Year	Structure	Evidence of Formation	T(K)	Method of Preparation[a]	Ref.	Comments
2004	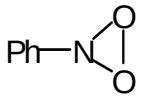	Luminescence data	298	A	14, 15	
2002	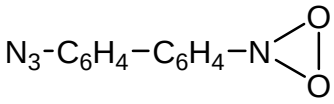	Luminescence data	298	C	13	Dioxaziridine contained within a rubber polymer was proposed
2001	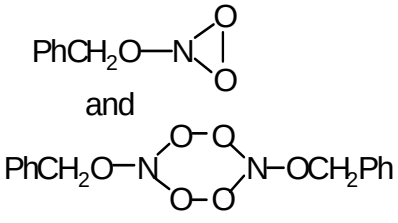	Kinetic and product study	298	D	10	Light source power suggested to influence dioxaziridine-to-tetraoxadiazinane contribution

Table 1 (cont.)

2001	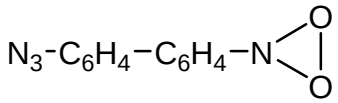	Luminescence data	293	A	16	
1999	**1a - 1f**	UV-Visible detection	77	A	7	Presumably formed by nitroso oxide isomerization
1996	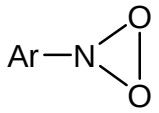 Ar = *p*-$MeOC_6H_4$ Ph, *p*-$NO_2C_6H_4$	$^{18}O_2$ labeling	298	B	8	Dioxiaziridine suggested to have a very short lifetime and convert rapidly to $ArNO_2$ nitrobenzene
1991	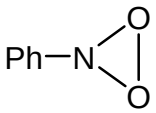	$^{18}O_2$ labeling	298	B	11	Suggestion of whether dioxaziridine was an intermediate or TS was not made

Table 1 (cont.)

1987	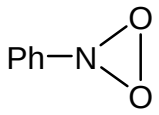	$^{18}O_2$ labeling	298	B	12	Unimolecular isomerization of PhNOO to nitrobenzene suggested to go via phenyldioxaziridine
1987	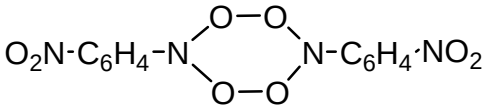	Product study	298	B	17	Product distribution varies based upon high- vs low power light source. Intractable tarry polymer product also formed
1971	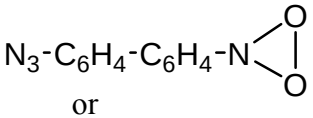 or 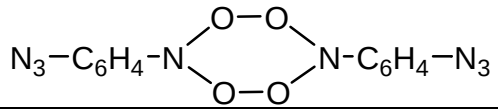	Product study	77	A	9	Suggested assignment of dioxaziridine or tetraoxadiazinane is only tentative

[a]A, Matrix isolation of ArN_3 photooxidation; B, Room-temperature solution-phase ArN_3 photooxidation; C, Substrates adsorbed to natural rubber; D, Room temperature solution-phase diazeniumdiolate photooxidation.

Table 2. UV-visible Spectral Data Obtained From Aryl Azide Photooxidations[a]

R	**2** λ_{max} (nm)	**1** λ_{max} (nm)	**3** λ_{max} (nm)
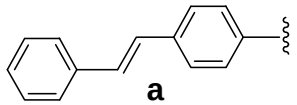 **a**	514	333, 348	373
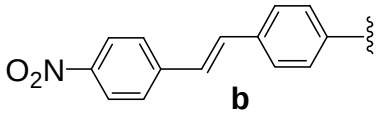 **b**	486	367	357, 374, 394
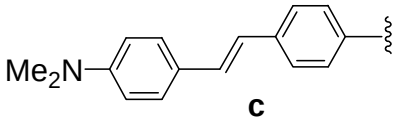 **c**	703	414	477
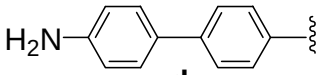 **d**	612	362	432
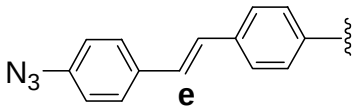 **e**	541	-	389
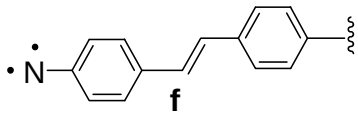 **f**	554	355, 371	379, 396, 425, 454

[a]Matrix detection of nitroso oxides, dioxaziridines, and nitro compounds at 77 K. Ref 7.

Table 3. ^{18}O-Tracer Study in the Photooxidation of Aryl Azides[a]

ArN_3	additive	conv. (%)	yield (%) of $ArNO_2$	mass data of $ArNO_2$ M/(M+2)/(M+4)	retention: scrambling[b]
	-			100/0.6/8.4	100:0 (calculated)
	-			100/16.8/0.7	0:100 (calculated)
p-$MeOC_6H_4$	Ph_2S	85	14	100/10.8/3.3	35:65
p-$MeOC_6H_4$	Ph_2SO	94	25	>100/55.7/7.5	16:84
C_6H_5	-	41	28	100/10.7/4.0	41:59
p-$O_2NC_6H_4$	Ph_2SO	90	30	100/14.0/2.1	19:81

[a]Irradiation of ArN_3 ($\lambda = 350$ nm) in acetonitrile under oxygen ($^{32}O_2$:$^{34}O_2$:$^{36}O_2$ = 100:0.6:8.4). Ref 8.
[b]Retention means the formation of $PhNO_2$ from one molecule of oxygen. Scrambling means that the two oxygen atoms in $ArNO_2$ are derived from two different oxygen molecules.

Table 4. Calculated Energies and Geometries of the Dioxaziridines

Year	Structure	State	Energy[a]	Method and Basis Set	O-O[b]	N-O[b]	O-N-O[c]	Ref.	Comments
1999		S_o	-205.5670	B3LYP/6-31G(d)	1.461	1.431	61.4	7	Both N-O bond distances are equal in length
1999	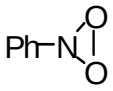	S_o	-436.6261	B3LYP/6-31G(d)	1.463	1.443	60.9	7	
1998		S_o	-205.32839	G2(MP2)	_	1.449	61.8	46	
1997		S_o	-205.07655	MP2/6-31G(d,p)	1.487	1.451	59.2	45	
1997		S_o	_	MP2/6-311G (2df,2p)	1.464	1.435	61.4	45	
1992		S_o	–	MCSCF/6-31G(d,p) 6-electron-6-orbital	–	1.374	68.3	43	Geometries also optimized for singlet and triplet acyclic HNOO

Table 4 (cont.)

1989		S_o	_	MP2/6-31G(d)	1.404	1.373	61.5	44	Basis set dependence on HNOO dihedral angle also reported
1987		S_o	_	HF/4-31G(d)	1.405	1.374	61.5	47	Structure for dithiaziridine (HNS_2) also reported

[a]Energies in au. [b]Bond distances in Å. [c]Bond angles in degrees.

Table 5. Calculated Change Densities of the Unsubstituted Dioxaziridine

Year	Structure	Mulliken Charge				Method and Basis Set	Ref.	Comment
		H	N	O	O			
1997		0.341	0.063	-0.202	-0.202	MP2/6-31G(d,p)	45	
1987		-	0.094	0.090	0.090	HF/6-31G(d,p)	47	A Mullliken gross population was calculated, where q = d_{xx}+ d_{yy} + d_{zz} + d_{xy} + d_{yz} + d_{xz}

Table 6. Calculated Dipole Moment of the Unsubstituted Dioxaziridine[a]

Year	Structure	μ (Debyes)	Method and Basis Set
1989		2.22	MP2/6-31G(d)

[a]Ref 44.

Table 7. Calculated HOMO and LUMO Energies of the Unsubstituted Dioxaziridine[a]

Year	Structure	HOMO(au)	LUMO(au)	Method and Basis Set	Ref.	Comments
1999		-0.49245	0.20580	HF/6-31G(d)	7	An orbital diagram for the conversion of the following is also given: 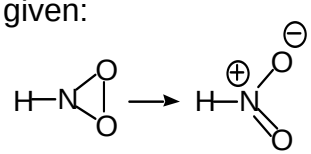
1989		-0.49111	0.21799	MP2/6-31G(d)	44	HOMO and LUMO values also reported for TS for NH inversion process

[a]Both N-O bond distances are equal in length.

Table 8. Calculated Vibrational Frequencies of the Unsubstituted Dioxaziridine

Year	Structure	Symmetry	a'	a''	a'[a]	a''[b]	a'	a'[b]	Method and Basis Set	Ref.
		Scaled Harmonic Vibrational Frequencies (cm^{-1})								
1997		Scaled Freq.	748	761	1035	1140	1344	3177	MP2/6-31G(d,p)	45
		Unscaled Freq.	801	814	1107	1219	1437	3398		
		IR intensity	0.3	2.9	0.5	39.3	34.8	2.6		

[a]Cyclic breathing vibration. [b]Exo N-H stretching vibration.

Table 9. Calculated Relative Energies of Species on the Dioxaziridine Reaction Surface[a, b]

Year	A	B	$\Delta E_{A \rightarrow B}$	Method and Basis Set	Ref.	Comments
2006	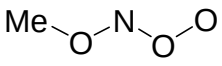	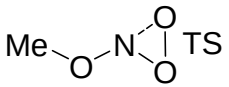 (Ring closing)	21.6[b]	B3LYP/6311+G(d,p)// B3LYP/6-31G(d)	39b	Energies are given as ΔG(298K). Calculations were also performed at the CBS-QB3 level.
	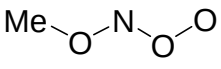	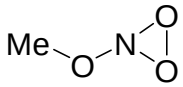	8.6			
	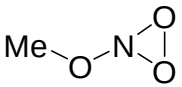	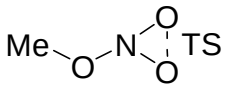 (Ring opening)	33.2[b]			
	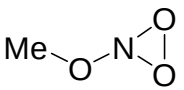	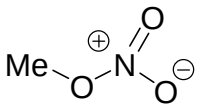	-70.2			

Table 9 (cont.)

	^{3}PhN + PhNOO	2 PhN=O	-79.5			
	^{3}PhN + 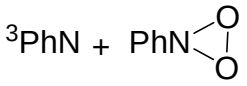	2 PhN=O	-93.5			
2002	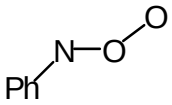	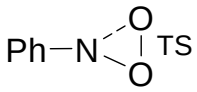 (Ring closure)	40.9[b]	B3LYP/6-31G(d)	13	Singlet-triplet gap for acyclic PhNOO is 19.0 kcal/mol with the CASSCF/6-31G(d) method
1999	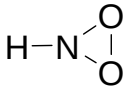	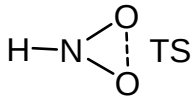 (Ring opening)	14.2[b]	B3LYP/6-31G(d)	7	Zero-point energy (ZPE) correction included
	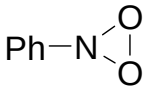	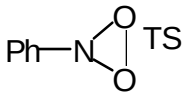 (Ring opening)	18.8[b]			

Table 9 (cont.)

	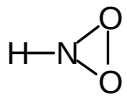	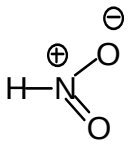	-74.0			
	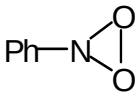	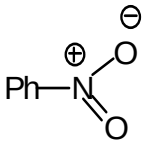	-80.7			
	$PhNO_2$	$PhNO_2$ perpendicular Ph group	3.5			Energy represents the barrier to forcing the phenyl ring to be perpendicular to the dioxaziridine ring
1998	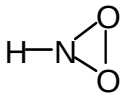 + 2 NH_2OH + HOOH	2NH2OOH + HON(H)OH	-28.0	G2 (MP2)	46	Atomization energies were also reported

Table 9 (cont.)

	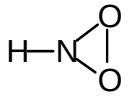 + $2NH_3$ + $2HO_2$	2 NH_2OH + HOOH	11.8			
1997	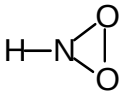	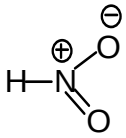	-74.7	MP4 SDTQ//MP2/ 6-31G(d,p)	45	ZPE corrected values also available
	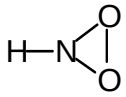	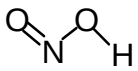 (trans)	-82.0			
	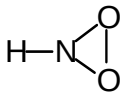	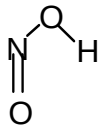 (cis)	-83.2			

Table 9 (cont.)

1996	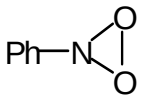	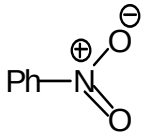	-66		8	Computational method used was not mentioned
1992	H-NOO	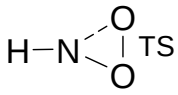 (Ring closure)	43.8[b]	6-electron/6-orbital MCSCF	43	A multiconfigurational SCF procedure was used and the transition state calculated with CI (full)
	H-NOO	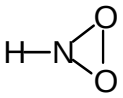	4.2			
1992	H-NOO	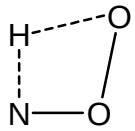 TS	17.2[b]	6-electron/6-orbital MCSCF	43	Favors route from HNOO to NOOH and then cleavage to NO+OH rather than less stable route of HNOO to cyclic HNO_2

Table 9 (cont.)

H-NOO	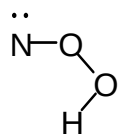	-35.7
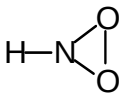	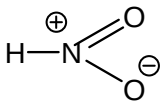	-64.0
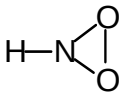	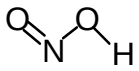	-81.6
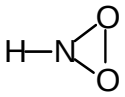	HNO + O(^{3}P)	7.0

Table 9 (cont.)

1989	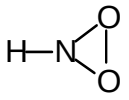	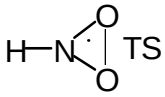 (Ring opening)	60.7	MP2/6-31G(d)	44	Values from the SCF method, the MP3 method and 6-31G, 6-31G+R. F., and 6-31G+(d) basis set were alsoreported. Inversion barrier of dioxaziridine is greater than 1H-azirine (46.3), oxaziridine(41.5), 1H-diazirine (34.7), and aziridene (19.9) at the MP2/6-31G(d) level. MP2/6-31G(d) inversion barrier reported on rotation about the HNOO dihedral angle.
	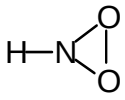	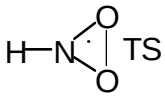 (Ring opening)	56.8	MP2/6-31+G(d)		

Table 9 (cont.)

1987	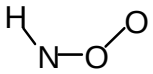 (cis)	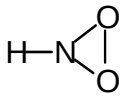	-1.3	MP2/6-31G(d,p)	47	Values also reported at the levels RHF/4-31G, RHF/4-31G(d), RHF/6-31G(d), and MP2/6-31G(d,p)
	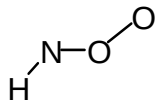 (trans)	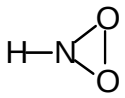	-3.1			
	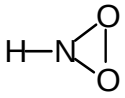	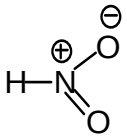	-77.7			
	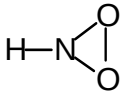	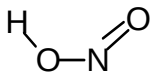 (cis)	-83.8			

Table 9 (cont.)

	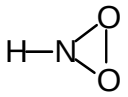	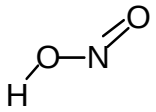 (trans)	-82.4			
	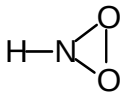	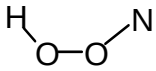 (cis)	-9.8			
	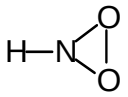	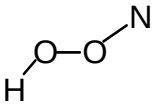 (trans)	-18.0			
1984	HNOO	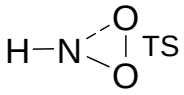 (Ring closure)	12[b]	MP4/6-31G(d,p)// HF/6-31G(d)	49	ZPE correction included. Bond additivity-type conections also included giving sufficient electron correlation contribution. Energy values are taken from a Figure in the original manuscript and are subject to errors of ± 3 kcal/mol.

Table 9 (cont.)

HNOO	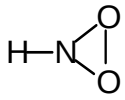	4	
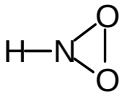	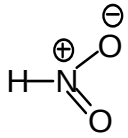 TS	2^{b}	
	(Ring opening)		
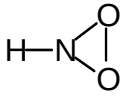	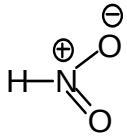	-76	
$^{1}NH + {}^{1}O_{2}$	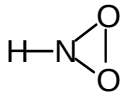	-20	Path does not proceed through the HNOO species

Table 9 (cont.)

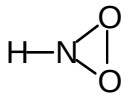	HONO	-81	Path proceeds through the species 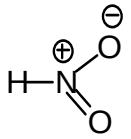

[a]Energies in kcal/mol. [b]Transition state energies in kcal/mol.

Table 10. Generation of Dioxasiliranes ($R^1R^2SiO_2$) or Silanone O-oxides (R^1R^2SiOO)

Year	R^1	R^2	Evidence of Formation	T (K)	Method of Generation[a]	Ref.	Comments
2000	Me	Ph	IR spectroscopy	30-40	A	51	Direct evidence for dioxasilirane obtained
1996	H	H	Product Analysis		B	74	Dioxasilirane proposed among other reactive intermediates
1990	F	F	IR spectroscopy	10	C	52	Direct evidence for dioxasilirane obtained
1990	Cl	Cl	IR spectroscopy	10	C	52	Direct evidence for dioxasilirane obtained
1989	Me	Me	IR spectroscopy	35-42	D	53, 54	Direct evidence for dioxasilirane obtained

Table 10 (cont.)

1988	Mes	Mes	IR spectroscopy	16	E	82	Silanone O-oxide suggested as the intermediate rather than dioxasilirane
1988-2004	—	—	UV-Vis and IR spectroscopy	700	F	63-73	Conclusion for surface-bound silylene contradicts that of previous researchers
1987	Me	Ph	Product Analysis	298	G	59	Tentative indirect evidence for the existence of dimesityldioxasilirane

[a] A, Matrix isolation from phenylsilyldiazomethane photooxidation; B, laser photolysis of a $SiH_4/O_2/CCl_4$ mixture; C, matrix isolation from X_3SiSiX_3 (X=F, Cl) pyrolysis and subsequent photooxidation; D, matrix isolation from diazidodimethylsilane photolysis and pyrolysis of 1,2-dimethoxytetramethyldisilane; E, matrix isolation from reaction of dimesitylsilylene with O_2; F, silica-gel reaction; G, solution-phase reaction of methylphenylsilylene with O_2.

Table 11. IR Data for Matrix-Isolated Methylphenyldioxasilirane, $MePhSiO_2$

Argon, 10 K			B3LYP/6-311++G(d,p)				
$\tilde{\nu}$, cm^{-1}	I[a]	$\tilde{\nu}_i/\ \tilde{\nu}$ [b]	$\tilde{\nu}$, cm^{-1}	I[a]	$\tilde{\nu}_i/\ \tilde{\nu}$[b]	sym	Assignment
3086.3	2	1.000	3191	11	1.000	A'	C-H str
3075.2	1		3183	13	1.000	A'	C-H str
3071.6	3	1.000	3175	5	1.000	A'	C-H str
3058.7	2	1.000	3156	3	1.000	A'	C-H str
3024.7	1		3122	1	1.000	A'	CH_3 str
3015.1	3	1.000	3099	2	1.000	A"	CH_3 str
1596.8	17	1.000	1629	10	1.000	A'	ring str
1435.0	30	1.000	1461	13	1.000	A'	skel. ring, in pl. C-H
1432.5	2	1.000	1456	3	1.000	A'	HCH bend
1429.5	7	1.000	1455	6	1.000	A"	HCH bend
1336.9	3	1.000	1357	4	1.000	A'	skel. ring, in pl. C-H

Table 11 (cont.)

1307.5	5	1.000	1311	10	1.000	A'	HCH bend, ring str
1260.3	10	0.998	1301	20	1.000	A'	HCH bend
1218.0	4		1211	2	1.000	A'	in pl. C-H bend
1135.6	92	0.999	1139	97	0.999	A'	skel. ring, in pl. C-H
1033.7	4	0.999	1049	1	0.999	A'	skel. ring, in pl. C-H
1013.1	1		1013	3	1.000	A'	ring breathing
1002.1	81	0.975	1005	100	0.972	A'	SiO str
998.2	28						
792.7	100	0.999	820	72	0.998	A'	CH_3 rock
783.4	4	0.994	800	15	0.998	A"	CH_3 twist
777.0	4						
737.5	29	0.999	750	40	1.000	A"	C-H wag
729.9	17	1.004	747	38	0.996	A'	SiC str, CH_3 def
717.6	3	0.952	731	3	0.956	A"	SiC def, CH_3 def

Table 11 (cont.)

694.5	39	1.000	710	31	1.000	A"	C-H wag
678.8	8	0.991	695	8	0.986	A'	
576.7	28	0.959	608	25	0.965	A'	O_2 str, CH_3 def
456.3	11	0.999	466	9	1.000	A"	C-H wag

[a]Relative intensity based on the strongest peak. [b]Ratio of the frequencies of the ^{18}O versus ^{16}O isotopomers. [c]The assignment of experimental and calculated IR absorption is based on peak positions and peak intensities and is only tentative for the weak absorptions. Ref 51.

Table 12. IR-Spectroscopic Data of F_2SiO_2 and Cl_2SiO_2 Dioxiranes, Matrix-Isolated in O_2 at 10 K and *Ab initio*Data of F_2SiO_2 Dioxirane Calculated at the HF/6-31G(d) Level[a]

Matrix				6-31G(d)				
$\tilde{\nu}$ [b]	I[c]	$\Delta\tilde{\nu}_1$ [d]	$\Delta\tilde{\nu}_2$ [e]	$\tilde{\nu}$ [b]	I[c]	$\Delta\tilde{\nu}_1$ [d]	$\Delta\tilde{\nu}_2$ [e]	Assignment[f]
1155.2								
1153.5 1152.0	1.00	-9.6	-19.3	1120.0	1.00	-12.7	-25.9	δ (Si-F)
1150.8								
1013.7	0.86	-0.5	-3.7	967.0	0.87	-0.1	-0.1	δ (Si-F)
862.7	0.02	[g]	-32.4	800.0	0.12	-9.0	-26.2	δ (Si-O)
				615.0	0.08	-13.7	-28.1	δ (O-O)
1054.4	1.00	-14.5	-30.9					δ (Si-O)
649.9	0.71	0.0	0.0					δ (Si-O)

Table 12 (cont.)

647	0.63	0.0	0.0	δ (Si-Cl)
576.1	0.30	-11.1	21.1	δ (O-O)

[a]Refs 52, 55, and 56. [b]Wavelength in cm^{-1}. [c]Relative intensity. [d]Isotopic shift if one ^{16}O atom is replaced by ^{18}O. [e]Isotopic shift if two ^{16}O atom are replaced by ^{18}O. [f]Approximate description on the basis of observed isotopic shifts and the calculated mode vectors. [g]This weak peak of the O-O isotopomer could not be observed.

Table 13. IR-Spectroscopic Data of Dimethyldioxasilirane (**37**), matrix-isolated in Ar at 10 K ($\tilde{\nu}$ [cm^{-1}], $\Delta\tilde{\nu}$ isotopic shift).

Frequencies ($\tilde{\nu}$)		$\Delta\tilde{\nu}$	[$^{18}O_2$]-**37**	$\Delta\tilde{\nu}$	assignment[c]
[$^{16}O_2$]-**37**	[$^{16}O^{18}O$]-**37**[b]				
1431.4(w)	1430.9 (w)	-0.5	1430.4 (w)	-1.0	δ_{as} (CH_3)
1260.3 (m)	1260.0 (m)	0.0	1258.8 (m)	-1.5	δ_s (CH_3)
1021.1 (s)	1009.6 (s)	-11.5	997.0 (s)	-24.1	$\tilde{\nu}_{as}$(Si-O)
1012.9 (w)	1005.2 (m)	-7.7	988.8 (w)	-24.1	[d]
1005.7 (w)	993.2 (w)	-12.5	981.1 (w)	-24.6	$\tilde{\nu}_{as}$(Si-O)[d]
820.1 (m)	814.8 (m)	-5.3	810.4 (m)	-9.7	
820.1 (m)	814.8 (m)	-5.3	809.5 (m)	-10.6	δ (CH_3)[e]
809.5 (m)			800.8 (w)	-8.7	δ (CH_3)[e]
554.4 (w)			530.8 (w)	-23.6	$\tilde{\nu}$ (O-O)

[a]Refs 53 and 54. [b]Due to the presence of three isotopomers in the spectra, not all bands could be assigned. [c]Approximate description on the basis of observed isotopic shifts and by comparison with *ab initio* calculations. [d]The assignment of the weak bands at 1012.9 and 1005.7 is not definite. [e]Rocking mode.

Table 14. Calculated Geometries of Dioxasiliranes

Year	Structure	State	Method and Basis Set	O-O[a]	Si-O[a]	Si-O-O[b]	O-Si-O[b]	Ref.	Comments
2006	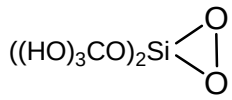	S_o	B3LYP/6-31G(d)	1.614	1.650, 1.666	–	–	58	
2005	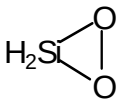	S_o	MP2(Full)/ 6-31G(d)	1.628	1.672	–	58.3	58	Computed data also reported at the MCSCF (FORS) level with the 6-31G(d) basis set
2000	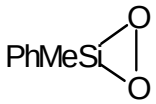	S_o	B3LYP/ 6-311++G(d,p)	1.584	1.672	61.7	56.5	51	Both Si-O bond distances are equal in length

Table 14 (cont.)

1999	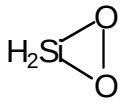	S_o	B3LYP/TZ2P	1.571	1.678	_	_	90	Computed data also reported at the B3LYP level with DZP and DZP-ECP basis sets
1996	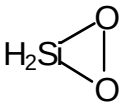	S_o	SCF/6-31G(d,p)	_	1.632	_	55.6	91	
1993	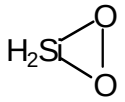	S_o	MP2/6-31G(d)	1.628	1.672	_	_	93	
1989	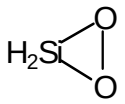	S_o	MP2/6-31G(d)	1.628	1.672	60.9	_	92	
1989	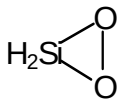	S_o	GVB/6-31G(d)	1.81	1.66	57.0	_	92	CASSCF calculation also carried out with 6 electrons distributed in 6 active orbitals

[a] Bond distances in Å. [b]Bond angles in degrees.

Table 15. Calculated Properties of the Dioxasilirane Ring

Year	Structure	Estimated Strain Energy	Method and Basis Set	Ref.	Comments
2006	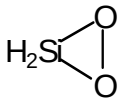	36.0	CBS-Q	89	Calculated from a 6-membered ring reference compound and a combination reaction of cyclopropane and dioxasilirane. In the same study, the strain energy for H_2CO_2 dioxarane was calculated to be 16-17 kcal/mol.
1996	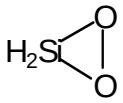	34.1	MP2/6-31G(d,p)	91	Calculated from 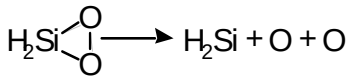
		44.9	SCF/6-31G(d,p)		
		27.7	MP2/6-31G(d,p)		Calculated from 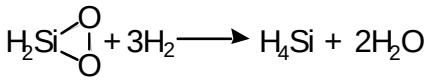
		26.6	SCF/6-31G(d,p)		

[a]Energies in kcal/mol.

Table 16. Calculated Properties of the Dioxasilirane Ringa

Year	Structure	Natural Atomic Charge			Natural Bond Order			Method	Comments
		Si	O	H	Si-O	O-O	Si-H		
1999	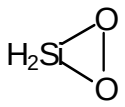	1.82	-0.56	-0.34	0.42	1.00	0.66	B3LYP/DZP	
		1.60	-0.57	-0.23	0.41	1.00	0.76	B3LYP/DZP-ECP	ECP = effective core potential

[a]Ref 90.

Table 17. Harmonic Vibrational Frequencies ($\tilde{\nu}$) and Infrared Intensities of the Dioxasilirane H_2SiO_2[a]

MP2/6-31G(d)		GVB/6-31G(d)		Assignment	
$\tilde{\nu}$, cm^{-1}	I[b]	$\tilde{\nu}$, cm^{-1}	I[b]		
490	0	526	0	a_2	SiH_2 twist
613	21	284	10	a_1	OSiO bend
734	97	755	126	b_1	SiH_2 rock
792	11	822	1	b_2	OSiO a-str[c]
871	141	923	192	b_2	SiH_2 bend
976	2	956	40	a_1	OSiO a-str[c]
1083	174	1123	206	a_1	SiH_2 bend
2377	79	2464	106	a_1	SiH_2 a-str
2393	168	2464	228	b_1	SiH_2 a-str

[a]Ref 92. [b]Infrared intensities. [c]Strongly coupled with the bending of SiH_2.

Table 18. Calculated Relative Energies for Intramolecular and Intermolecular Reactions of Dioxasilirane[a, b]

Year	A	B	$\Delta E_{A \rightarrow B}$	Method and Basis Set	Ref.	Comments
2006	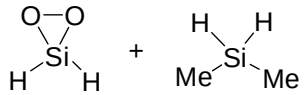	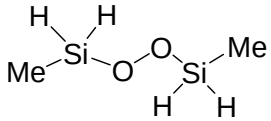	-35.5	CBS-Q	89	These represent homodesmotic reactions
	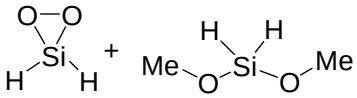	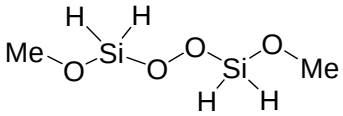	-36.0			
	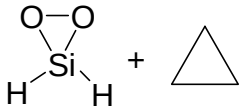	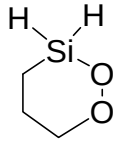	-31.2			
2005	H_2SiOO	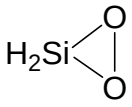	-64.5	G3	57	

Table 18 (cont.)

H_2SiOO	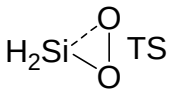 (ring closure)	4.5[b]	G3	
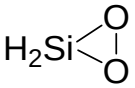	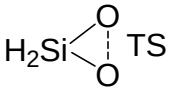 (ring opening)	14.4[b]	MRMP2/ 6-31G(d)	Computed values vary widely depending on the theoretical method. Values also reported at the MCSCF level. Use of the Cc-pVTZ basis set also reported
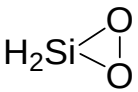	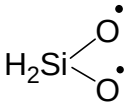	8.8	MRMP2/ 6-31G(d)	
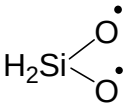	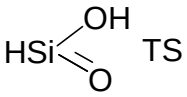 (H-rearrange)	1.4[b]	MRMP2/ 6-31G(d)	

Table 18 (cont.)

	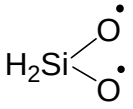	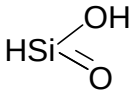	-85.9	MRMP2/ 6-31G(d)	
2000	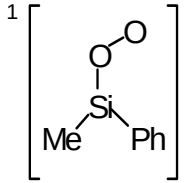	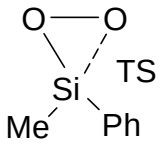 (ring closure)	0.8[b]	B3LYP/ 6-311++G(d,p)	51
	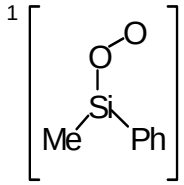	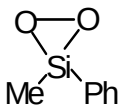	-49.6	B3LYP/ 6-311++G(d,p)	
	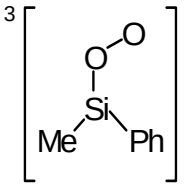	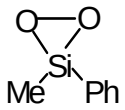	-57.8	B3LYP/ 6-311++G(d,p)	

Table 18 (cont.)

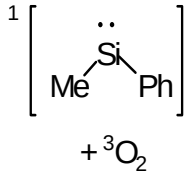	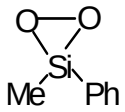	-77.4	B3LYP/ 6-311++G(d,p)
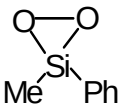	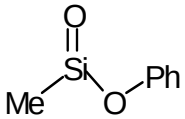	-61.7	B3LYP/ 6-311++G(d,p)
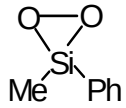	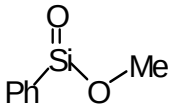	-59.3	B3LYP/ 6-311++G(d,p)
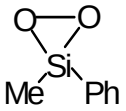	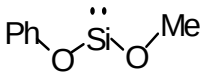	-49.1	B3LYP/ 6-311++G(d,p)

Table 18 (cont.)

1999	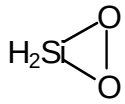	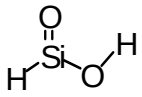	-81.1	B3LYP/DZP	90	Calculations also performed at other levels of theory levels such as B3LYP/DZP-ECP, BLYP/ DZP, B3LYP/TZ2P, B3LYP/TZ2P-ECP, BLYP/DZ2P, BLYP/ TZ2P-ECP CCSD/TZ2P//BLYP/TZ2P, BLYP/DZ2P, BLYP/ TZ2P-ECP CCSD/TZ2P//BLYP/TZ2P, CCSD/TZ2P-ECP//BLYP/TZ2P-ECP, CCSD(T)/TZ2P-ECP//BLYP/TZ2P-ECP
	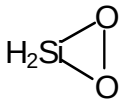	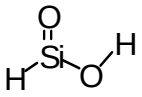	-80.1	CCSD(T)/TZ2P-ECP//BLYP/TZ2P-ECP		

Table 18 (cont.)

	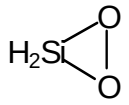	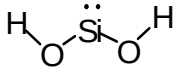	-88.6	B3LYP/DZP		
	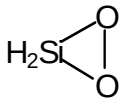	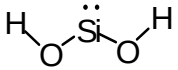	-88.0	CCSD(T)/TZ2P-ECP//BLYP/TZ2P-ECP		
	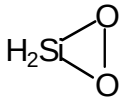	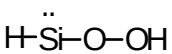	20.9	B3LYP/DZP		
	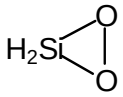	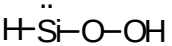	24.6	CCSD(T)/TZ2P-ECP//BLYP/TZ2P-ECP		
1996	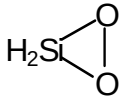	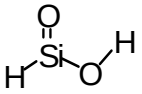 TS (rearrangement)	6.4[b]	CASSCF(6/6)/ 6-31G(d)	74	6 electrons in 6 orbitals

Table 18 (cont.)

	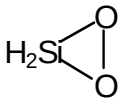	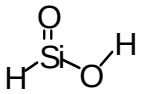	-8.3	CASSCF(6/6)/ 6-31G(d)		Predictions of the $SiH_3 + O_2$ reaction to give SiH_3OO and then cyclization to H_2SiO_2 atom
	—	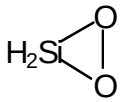	-28.1	G2	93, 94	Calculated heat of formation at 298 K
1989	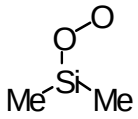	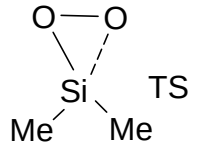 TS (ring closure)	6.5[b]	HF/6-31G(d)	53, 54	
	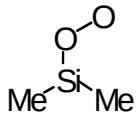	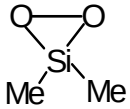	-63.8	HF/6-31G(d)		

Table 18 (cont.)

H_2SiOO	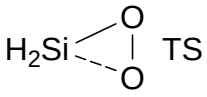 (ring closure)	6.5[b]	MP2/6-31G(d)	92	Single point values also calculated at various levels: MP3, MP4, CI with the 6-31G(2d,p) basis set
H_2SiOO	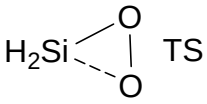 (ring closure)	2.2[b]	GVB/6-31G(d)		Single point energies also calculated with GVB/6-31G(2d,p) and CASSCF/6-31G(d)
H_2SiOO	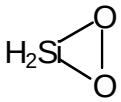	-63.8	MP2/6-31G(d)		
H_2SiOO	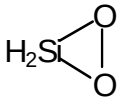	-62.1	GVB/6-31G(d)		

Table 18 (cont.)

1988	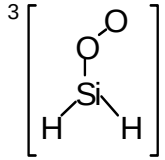	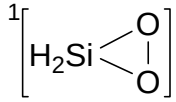	-61.5	MP4SDTQ/ 6-31G(d)// HF/6-31G(d)	82
	$^1H_2Si + {}^3O_2$	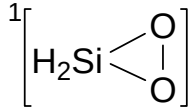	-84.2	MP4SDTQ/ 6-31G(d)// HF/6-31G(d)	

[a]Energies in kcal/mol. [b]Transition-state energies.

Table 19. Calculated Geometries of Dioxagermirane, Dioxastannirane, and Dioxastilbirane[a]

Year	Structure	State	Method of Basis Set	O-O[b]	Y-O[b]
1999	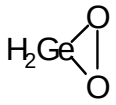	S_o	B3LYP/TZ2P-ECP	1.566	1.778 (Y=Ge)
	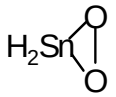	S_o		1.561	1.931 (Y=Sn)
	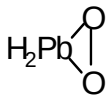	S_o		1.555	1.992 (Y=Pb)
	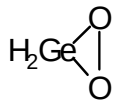	S_o	B3LYP/DZP-ECP	1.555	1.785 (Y=Ge)
	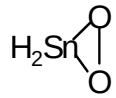	S_o		1.550	1.936 (Y=Sn)
	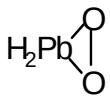	S_o		1.544	2.001 (Y=Pb)

[a]Ref 90. [b]Bond distances in Å.

Table 20. Calculated Structural Properties of Dioxagermirane, Dioxastannirane, and Dioxastilbiranea

Year	Structure	Natural Atomic Charge			Natural Bond Order			Method and Basis Set
		Y	O	H	Y-O	O-O	Y-H	
1999	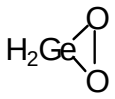 (Y=Ge)	1.42	-0.5	-0.16	0.45	1.00	0.82	B3LYP/DZP
		1.57	-0.6	-0.22	0.42	1.00	0.77	B3LYP/DZP-ECP
	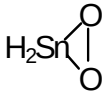 (Y=Sn)	1.88	-0.6	-0.32	0.37	1.00	0.67	B3LYP/DZP-ECP
	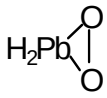 (Y=Pb)	1.54	-0.6	-0.21	0.42	1.00	0.76	B3LYP/DZP-ECP

[a]Ref 90.

Table 21. Calculated Energies for Rearrangements of Dioxagerminane, Dioxastannirane, and Dioxastilbirane[a]

Year	A	B	$\Delta E_{A \rightarrow B}$	Method and Basis Set	Ref.	Comments
1999	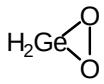	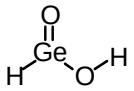	-72.3	B3LYP/DZP-ECP	90	Calculations also performed at different levels of theory including single point calculations at the CCSD(T)/TZP-ECP level
			-76.9	B3LYP/TZ2P-ECP		
	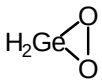	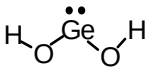	-106.9	B3LYP/DZP-ECP		
			-109.7	B3LYP/TZ2P-ECP		
	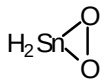	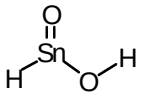	-67.2	B3LYP/DZP-ECP		
			-70.6	B3LYP/TZ2P-ECP		

Table 21 (cont.)

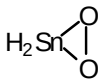	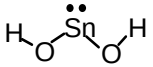	-122.2	B3LYP/DZP-ECP
		-125.9	B3LYP/TZ2P-ECP
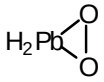	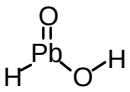	-68.0	B3LYP/DZP-ECP
		-71.8	B3LYP/TZ2P-ECP
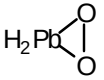	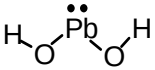	-144.8	B3LYP/DZP-ECP
		-149.4	B3LYP/TZ2P-ECP

[a]Energies in kcal/mol

Table 22. Calculated Geometries of Cyclic SO_2

Year	Structure	State	Method and Basis Set	O-O[a]	S-O[a]	O-S-O[b]	Ref.
1997		S_o	CCSD(T)/TZ2P(*f*)	1.500	1.690	52.7	113, 114
1996		S_o	B3LYP/cc-pVTZ	1.479	1.686	51.9	111
		S_o	BP86/cc-pVTZ	1.504	1.705	51.9	111

[a]Bond distances in Å. [b]Bond angles in degrees.

Table 23a. Calculated Vibrational Frequencies and IR Intensities of Cyclic SO_2

Year	$\tilde{\nu}_1$ (A_1)[a]	$\tilde{\nu}_2$ (A_1)[a]	$\tilde{\nu}_3$ (B_2)[a]	Method and Basis Set	Ref.
1996	1009 (13.3)[b]	682 (3.9)[b]	739 (9.8)[b]	B3LYP/cc-pVTZ	111
	970 (11.0)[b]	662 (4.0)[b]	721 (8.8)[b]	BP86/cc-pVTZ	

[a] Symmetries of vibrational modes listed in parentheses. [b]IR intensities are listed in parentheses.

Table 23b. Calculated Excitation Energies of Cyclic SO_2

	State	Energy (eV) MRCI	Oscillator Strength	Energy (eV) MRCI+Q	Ref.
2005[a]	1^1A_1	4.511		4.465	118
	1^3A_2	6.081	0	5.985	
	1^1A_2	6.752	0	6.660	
	1^3B_1	7.715	0	7.647	
	1^1B_1	8.078	0.00124	8.033	
	2^3B_1	8.887	0	8.738	
	2^3A_2	9.170	0	8.85	
	1^3B_2	9.930	0	9.824	

[a]Cyclic SO_2 was computed for C_{2v} symmetry.

Table 24. Calculated Energies for the Rearrangements of Acyclic and Cyclic SO_2[a]

Year	**A**	**B**	$\Delta E_{A \rightarrow B}$	Method and Basis Set	Ref.
1996	OSO		99.8	B3LYP/ cc-pVTZ	111
	OSO		98.2	BP86/ cc-pVTZ	
	OSO	SOO	107.3	B3LYP/ cc-pVTZ	
	OSO	SOO	99.7	BP86/ cc-pVTZ	
1995	OSO		104.3	CCSD(T)/ TZ2P(*f*)	114
	OSO	SOO	110.8	CCSD(T)/ TZ2P(*f*)	

[a]Energies in kcal/mol.

Table 25. Generation of Dioxaphosphiranes (R_3PO_2 Dioxiranes)[a]

Year	Structure	Evidence of Formation	T (K)	Method of Preparation	Ref.	Comments
2006	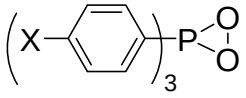 (X=MeO, H, F, Cl, CF_3)	Trapping and rate constant study	298	A	137b	Phosphine oxide products formed
	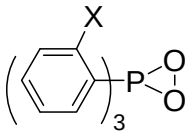 (X=MeO, Me, H)	Trapping and rate constant study	298	A	137b	Phosphinate and phosphine oxide formed
	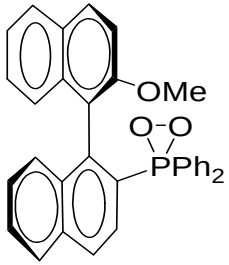	Intramolecular trapping	298	A	138	

Table 25 (cont.)

	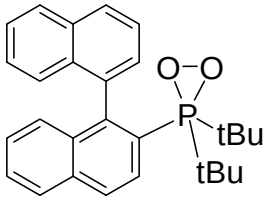	NMR spectroscopy and trapping	218-258	A	138	^{31}P NMR spectroscopy was conducted in addition to trapping with cyclohexene
2003	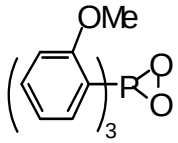	NMR spectroscopy	193	A	137a	^{31}P and ^{17}O NMR spectroscopy was conducted along with olefin trapping studies
2001	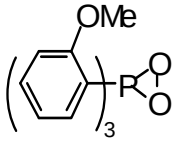	Kinetic analysis	298	A	140	meta- and para-methoxyphenylphosphine reaction with singlet oxygen also conducted

Table 25 (cont.)

1999	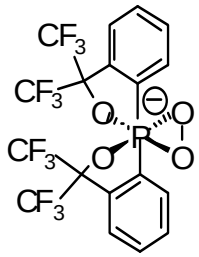	NMR and X-ray crystallography	273	B	136	Potassium 18-crown-6 was the counter ion
1993	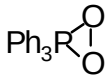 and 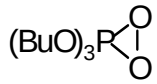	Trapping and ^{18}O labelling	298	A	143a	Peroxyphosphine oxide and [1,2,4,5,3,6]tetradiphosphinirane are not formed
1993	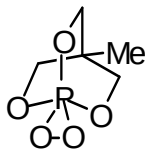	Trapping and product study	293	A	154	Oxidation of olefins and thianthrene-5-oxide provide tentative evidence for the dioxaphosphirane

Table 25 (cont.)

1987	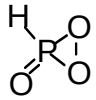	IR spectroscopy	12-18	C	139	Other species formed such as HPO, HOOPO, and $HOPO_2$
1983	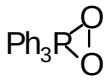	Product study	237	D	144	

[a]A, Solution-phase phosphine or phosphite photooxidation; B, reaction between triplet oxygen and the phosphoramide ion; C, Ar-matrix irradiation of a PH_3--O_3 complex; D, reaction between Ph_3P, H_2O_2, and diethyl azocarboxylate.

Table 26. Spectral Properties of Dioxaphosphiranes[a]

Year	Structure	^{31}P NMR (ppm)	^{17}O NMR (ppm)	Coupling Constants	X-ray structure	IR data (cm^{-1})			Ref.	Comments
						mode	observed	calculated		
2006	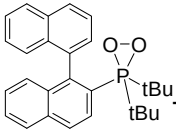	-18.6							138	
2003	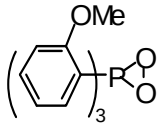	-48.3	740						137a	Also detected as the hydroperoxyphosphine and hydroxyphosphorane in MeOH solvent

Table 26 (cont.)

1999	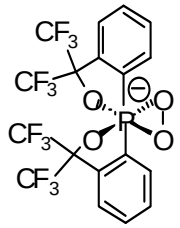	-121.0	δ=-74.73 (q, J_{PF}=8.8Hz), -75.36 (q, J_{PF}=8.8 Hz)	a=10.446 (5)Å b=12.265 (6)Å c=15.206 (6)Å α=70.088 (3)^{o} ß=80.669 (4)^{o} γ=69.164 (3)^{o} (R=0.047)				136	^{1}H and ^{13}C NMR data are also available
1987					$\tilde{\nu}$ (P-H)	2490.1 2489.4	2489.8 2489.7	139	
						1370.3	1370.1		
						1362.4, 1372.0	1366.8		

Table 26 (cont.)

	$\tilde{\nu}$ (P=O)	1331.6	1330.4
		1368.1	1368.4
		1329.3	1328.1
		1326.9	1326.0
	$\tilde{\nu}_s$(-PO_2)	974.1	977.3
		939.4	943.5
		965.9	963.1
		959.0	961.5
		950.8	948.0
		931.8	932.4

Table 26 (cont.)

	δ(HPO)		935.3
			927.6
	$\tilde{\nu}_{as}$(-PO_2)		853.6
		833.2	833.3
		833.2	833.1
			813.8
	$\tilde{\nu}_{s}$(-PO_2)	587.3	586.8
		560.0	559.4
	ϖ(OPO_2)	436.7	436.5
			423.2

[a]Temperatures of the experiments range from 12-298 K.

Table 27. Oxidation of Alkenes by In-situ Generated tris (o-Methoxyphenyl)dioxaphosphirane[a]

Alkene	Epoxide	Yield (%)
	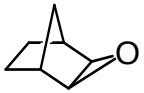	60
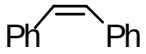	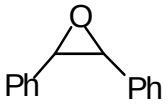	65
	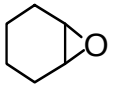	80
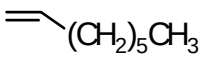	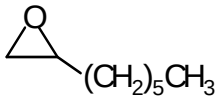	75

[a]Ref 137b.

Table 28. ^{18}O-Tracer Study of the Formation of Phenyl Diphenylphosphinate [$Ph_2P(=O)OPh$] from Ph_3P and $^1O_2$[a]

Entry	Conditions[b]	Product	Masses[b] M	M+2	M+4	
		Observed				
1	20mM $Ph_3P/^{18}O_2$[c]	$Ph_2P(=O)OPh$	100	11.8	5.9	
2	20mM $Ph_3P/^{18}O_2$[d]	$Ph_2P(=O)OPh$	100	10.5	0.3	
			100	1.3	5.6	(Difference between entries 1 and 2[e])
		Calculated				
3			100	0.5	6.2	(Retention)
4			100	3.6	0.0	(Scramble)

[a]Ref 143a. [b]Mass spectral data for $Ph_2P(=O)OPh$, M = 294. The observed values are the mean of two determinations. [c]Oxygen gas: $^{32}O_2/^{34}O_2/^{36}O_2$ = 100:0.5:6.2. [d]Control experiment with natural oxygen gas under the same conditions. [e]Net values for ^{18}O contents.

Table 29. Calculated Energies and Geometries of Dioxaphosphiranes

Year	Structure	Energy[a]	Method of Basis Set	O^1-$O^{2\,b}$	P-O^1_b	P-$O^{2\,b}$	P-O^1-$O^{2\,c}$	Ref.	Comments
2006	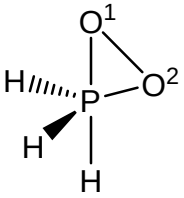		B3LYP/6-31+G(d)	1.570	1.720	1.620	58.6	141	Calculations were also performed with other methods [HF, MP2, QC1SD(T)] and basis sets (3-21G, ang-cc-pVOZ, ang-cc-pVTZ)
1993	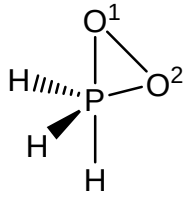	-492.531	MP2/6-31G(d)	1.599	1.697	1.630	63.4	164	

Table 29 (cont.)

	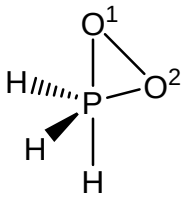	-492.128	CASSCF/6-31G(d)	1.630	1.681	1.622	62.3		Calculation on a 12-orbital system with 10 filled and 2 virtual orbitals
	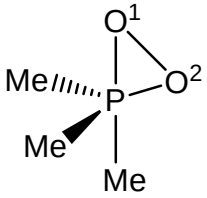	-610.053	MP2(FC)/6-31G(d)	1.560	1.782	1.580	69.2		
1993	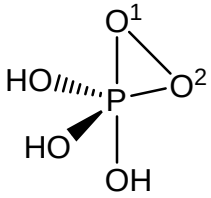	-713.105	HF/3-21G(d)	1.572	1.654	1.568	--	143a	HF/STO-3G(d) calculations have also been reported

[a]Calculated for the S_o state. [b]Bond destances in Å. [c]Bond angles in degrees.

Table 30. Calculated Energies[a] for the Intramolecular and Intermolecular Reactions of Dioxaphosphiranes

Year	**A**	**B**	$\Delta E_{A \rightarrow B}$	Method and Basis Set	Ref.	Comments
1993	$PH_3 + {}^1O_2$	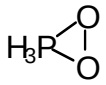	-32.0	MP2/6-31G(d)	164	An energy minimum was not found for acyclic H_3POO nor Me_3POO at any theoretical level
	$PH_3 + {}^1O_2$	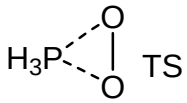 TS	24.8			
	$2\,PH_3 + {}^1O_2$	$2\,H_3PO$	-111.2			
	$Me_3P + {}^1O_2$	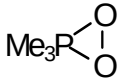	-52.5	MP2/6-31G(d)// HF/ 6-31G(d)		
	$Me_3P + {}^1O_2$	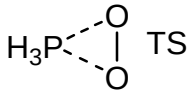 TS	20.7	HF/3-21G(d)		

Table 30 (cont.)

	$2\,Me_3P + {}^1O_2$	$2\,Me_3PO$	-163.0	MP2/6-31G(d)// HF/ 6-31G(d)		
1992	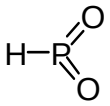	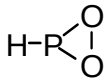	85.0	SCF	165	
			79.6	SCF/CEPA-1	165	Electron correlation was conducted with the CEPA-1 method by using SCF geometries

[a]Energies in kcal/mol.

Table 31. Calculated Geometries of Dioxathiiranes

Year	Structure	Method of Basis Set	O^1-O^{2a}	S-O^{1a}	S-O^{2a}	S-O^1-O^{2b}	Ref.
1998	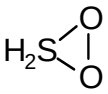	B3LYP/6-31+G(d)	1.535	2.077	1.597		212
1998, 1996	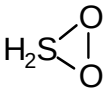	MP2/6-31G(d)	1.556	1.811	1.651		243, 244
		MP2/6-311+G(2df)	1.531	1.817	1.609		
1998	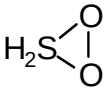	MP2/6-311+G(3df,2p)	1.542	1.755	1.607	67.7	176

Table 31 (cont.)

		QCISD/6-31+G(d)	1.562	1.982	1.597	77.7	
	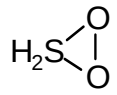	MP2/6-311+G(3df,2p)	1.527	1.809	1.601	70.6	
	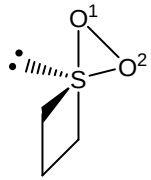	MP2/6-311+G(3df,2p)	1.53	1.798	1.603	70	
1997	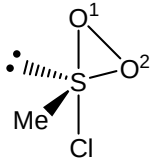	MP2/6-31G(d)	1.556	1.811	1.652		213

Table 31 (cont.)

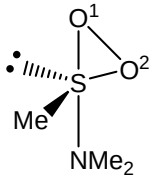	1.547	1.797	1.666
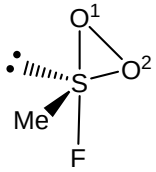	1.555	1.747	1.634
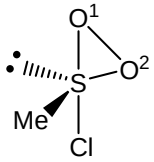	1.555	1.753	1.639
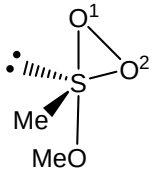	1.549	1.771	1.650

Table 31 (cont.)

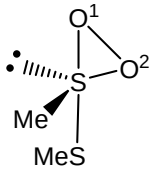	1.551	1.786	1.649
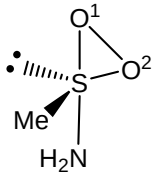	1.546	1.803	1.649
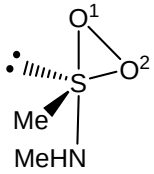	1.546	1.800	1.659
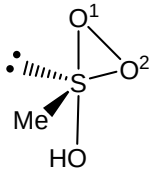	1.549	1.773	1.642

Table 31 (cont.)

	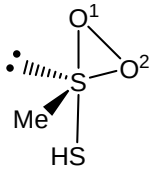		1.552	1.780	1.643	
1996	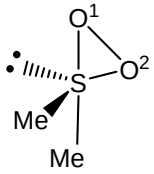	RHF-PM3	1.580	1.790	1.710	242
1996	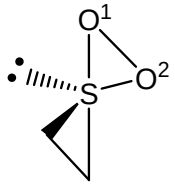		1.564	1.793	1.648	243
	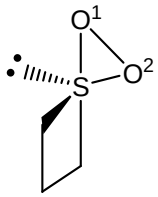		1.555	1.812	1.646	

Table 31 (cont.)

	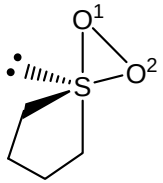		1.553	1.825	1.647	
1992	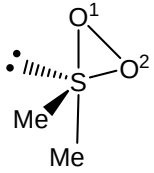	MP2/6-31G(d)	1.555	1.809	1.648	231

[a]Bond distances in Å. [b]Bond angles in degrees.

Table 32. Calculated Charges of the Sulfur and Oxygen Atoms in Dioxathiiranes[a]

Year	Structure	Natural Bond Order Charges			Method
		S	O^1	O^2	
1997	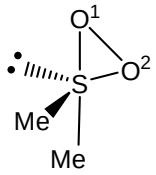	1.32	-0.55	-0.46	MP2/6-31G(d)
	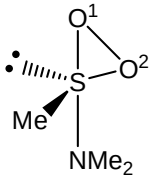	1.45	-0.55	-0.46	
	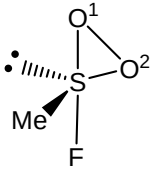	1.59	-0.51	-0.41	

Table 32 (cont.)

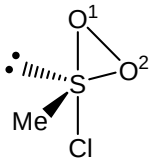	1.34	-0.47	-0.39
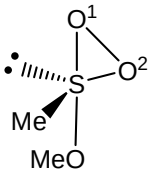	1.52	-0.52	-0.44
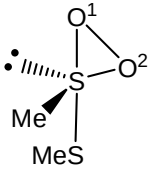	1.20	-0.52	-0.42

Table 32 (cont.)

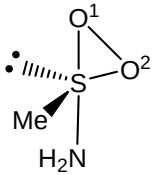	1.45	-0.55	-0.46
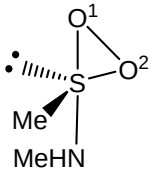	1.45	-0.55	-0.46
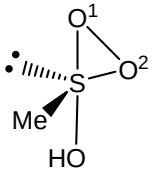	1.52	-0.52	-0.43
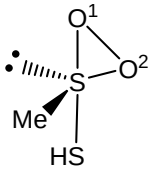	1.22	-0.51	-0.41

[a]Ref 213.

Table 33. Calculated Vibrational Frequencies ($\tilde{\nu}$) and IR Intensities of Dimethyldioxathiirane[a, b]

$\tilde{\nu}$, cm^{-1}	I[c]
156	3.4
235	0.1
270	0.9
326	5.5
359	6.8
366	6.5
450	66.4
649	54.8
740	30.5
807	56.9
945	8.2

Table 33 (cont.)	
963	9.2
966	34.2
1045	25.5
1083	39.0
1389	9.3
1422	8.1
1509	7.8
1517	2.0
1526	2.4
1536	19.5
3107	2.4
3123	3.7
3217	4.4

Table 33 (cont.)		
	3226	3.0
	3229	3.1
	3258	0.8

[a]Ref 231. [b]Calculated at the MP2/6-31G(d) level. [c]IR intensities.

Table 34. Calculated Isotopic Shifts (cm^{-1}) of Selected Vibrations of Dimethyldioxathiirane[a, b]

$\Delta\tilde{\nu}$	$\Delta\tilde{\nu}$	$\Delta\tilde{\nu}$	$\Delta\tilde{\nu}$	$\Delta\tilde{\nu}$
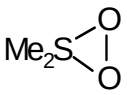	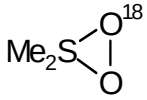	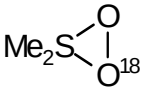	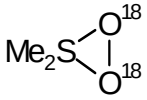	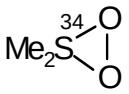
156	-4	-2	-6	0
326	-3	-2	-5	-1
359	-3	-3	-6	-3
366	-1	-3	-4	-1
450	-7	-15	-21	-1
649	-2	0	-2	-5
740	-6	-2	-8	-7
807	-15	-4	-18	-8

Table 34. (cont.)				
945	-4	-8	-28	-1
963	-14	-17	-18	-4
966	-3	-4	-4	-1
1045	-2	-1	-3	-4

[a]Ref 231. [b]Calculated at the MP2/6-31G(d) level.

Table 35. Calculated Energies for Intramolecular and Intermolecular Reactions of Dioxathiiranes[a, b]

Year	A	B	$\Delta E_{A \rightarrow B}$	Method and Basis Set	Ref.	Comments
2003	$Me_2S^{\bullet+} + O_2^{\bullet-}$	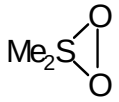	-158.6	MP2/6-31+G(2d,p)	184	
			-151.2	QCISD/6-31+G(2d,p)		
		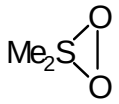	-1.7	MP2/6-31+G(2d,p)		
			2.3	QCISD/6-31+G(2d,p)		
	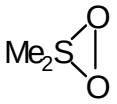	$Me_2S + {}^1O_2$	-11.1	MP2/6-31+G(2d,p)		
			-15.1	QCISD/6-31+G(2d,p)		

Table 35 (cont.)

	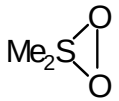	$Me_2S + {}^1O_2$	TS	9.9[b]	MP2/6-31+G(2d,p)		
				6.2	QCISD/6-31+G(2d,p)		
1998	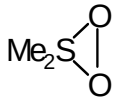	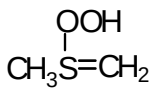		-12.2	B3LYP/6-31+G(d)	212	
				-7.4	QCISD(T)/6-31+G(d)		
				-5.9	QCISD(T)/6-311+G(3df,2p)		
	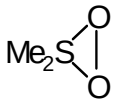	$Me_2S + {}^1O_2$		-22.2	B3LYP/6-31+G(d)		22 kcal/mol experimental value added to $^3O_2$
				-13.9	QCISD(T)/6-31+G(d)		
				-3.5	QCISD(T)/6-311+G(3df,2p)		

Table 35 (cont.)

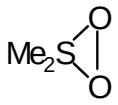	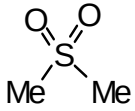	-87.6	B3LYP/6-31+G(d)	
		-85.9	QCISD(T)/6-31+G(d)	
		-101.8	QCISD(T)/6-311+G(3df,2p)	
	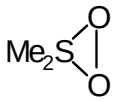	3.0	B3LYP/6-31+G(d)	
		0.9	QCISD(T)/6-311+G(3df,2p)	
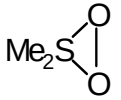	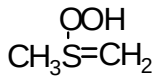	-6.7	MP2/6-31G(d)	176
		-7.2	CCSD(T)/6-311+G(2df)[b]	

Table 35 (cont.)

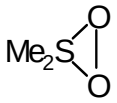	$Me_2S + {}^1O_2$	-19.4	MP2/6-31G(d)
		-3.2	CCSD(T)/6-311+G(2df)[b]
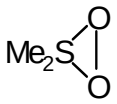	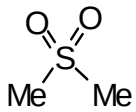	-94.5	MP2/6-31G(d)
	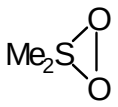	-3.0	MP2/6-31G(d)
		1.4	CCSD(T)/6-311+G(2df)[b]
$Me_2S + {}^1O_2$	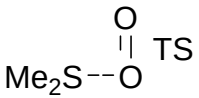	32.8[b]	MP2/6-31G(d)
		11.2	CCSD(T)/6-311+G(2df)[b]

Table 35 (cont.)

	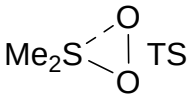	19.0[b]	MP2/6-31G(d)	
	(Ring closure)			
		20.6	CCSD(T)/6-311+G(2df)[b]	
	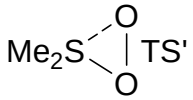	13.2[b]	MP2/6-31G(d)	TS' represents a second pathway found to the dioxathiirane
	(Ring closure)			
		11.1	CCSD(T)/6-311+G(2df)[b]	

Table 35 (cont.)

1998	$H_2S\overset{\oplus}{O}\overset{\ominus}{O}$	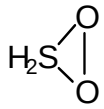	-6.3	MP2/6-31+G(d)	176
			-0.1	CCSD(T)/631+G(d) //MP2/6-31+G(d)	
			1.5	QCISD/6-31+G(d)	
			-7.9	MP2/6-31++G(2d,p)	
			-10.7	MP2/6-31+G(2df,p)	

Table 35 (cont.)

			-10.6	MP2/6-31+G(2df,p)	
1997, 1998	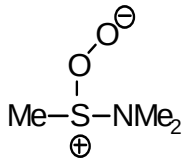	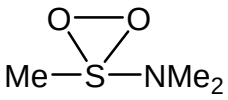	-9.3	MP2/6-31G(d)	213, 214
	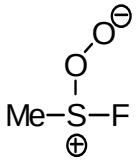	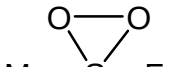	-31.1	MP2/6-31G(d)	
			-24.3	CCSD(T)/6-31G(d)	
			-30.1	MP2/6-311G(2d)	

Table 35 (cont.)

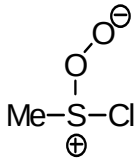	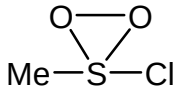	-13.6	MP2/6-31G(d)
		-15.9	CCSD(T)/6-31G(d)
		-14.4	MP2/6-311G(2d)
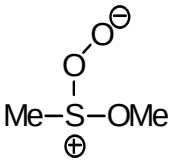	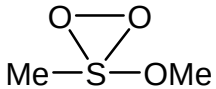	-19.7	MP2/6-31G(d)

Table 35 (cont.)

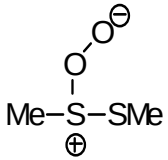	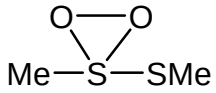	-25.6	MP2/6-31G(d)
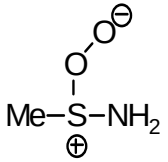	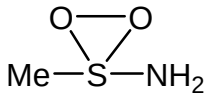	-12.2	MP2/6-31G(d)
		-7.2	CCSD(T)/6-31G(d)
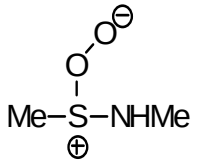	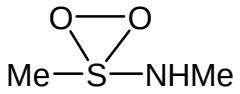	-10.8	MP2/6-311G(2d)

Table 35 (cont.)

		-11.8	MP2/6-31G(d)
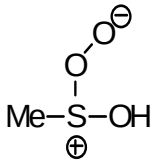	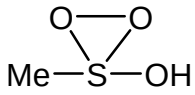	-22.9	MP2/6-31G(d)
		-16.7	CCSD(T)/6-31G(d)
		-21.6	MP2/6-311G(2d)
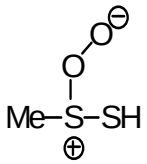	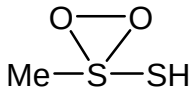	-18.0	MP2/6-31G(d)

Table 35 (cont.)

			-10.9	CCSD(T)/6-31G(d)	
			-16.5	MP2/6-311G(2d)	
1996	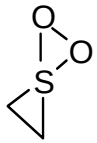	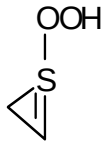	11.5	MP2/6-31G(d)	243
	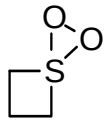	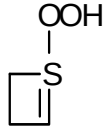	1.7		
	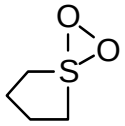	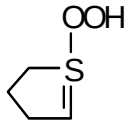	-7.8		

Table 35 (cont.)

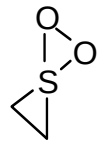	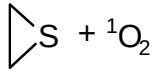	-24.1
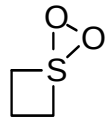	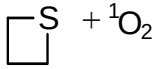	-11.9
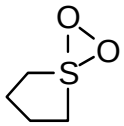	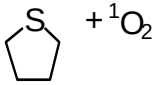	-19.0
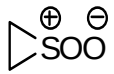	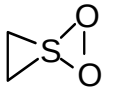	-4.4

Table 35 (cont.)

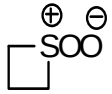	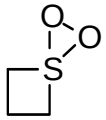		-8.0		
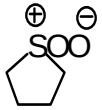	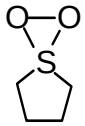		-2.3		
	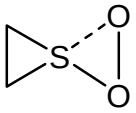	TS	16.4[b]		
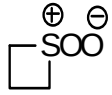	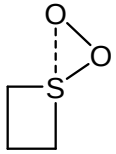		21.6[b]		
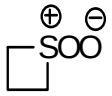	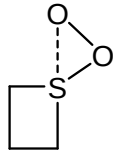	TS’	13.2[b]	176	TS’ represents a second pathway found to the dioxathiirane

Table 35 (cont.)

1996		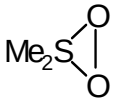	-2.6	PM3	242
		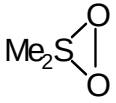	17.6		

[a]Energies in kcal/mol. [b]Transition state energies in kcal/mol.

Table 36. Selenoxide Yields in the Reaction of Singlet Oxygen with Selenides (R^1SeR^2)[a]

R^1	R^2	Yield (%)
Ph	Me	95
Ph	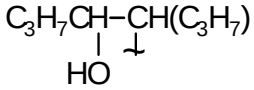	70
Me	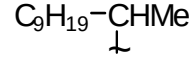	85
Me	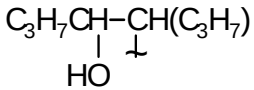	70

[a]Ref 266.

Table 37. Relative Energetics of the Heteroatom Dioxiranes Compared to Their Corresponding O-X-O Acyclic Counterparts[a]

Entry	XO_2 Cyclic Structure	O-X-O Acyclic Structure	Method and Basis Set	$\Delta E_{A \rightarrow B}$	Ref.
1	$PhNO_2$ dioxaziridine	$PhNO_2$ nitrobenzene	B3LYP/6-31G(d)	-80.7	7
2	HNO_2 dioxaziridine	HNO_2 nitro compound	B3LYP/6-31G(d)	-74.0	7
3	SO_2 cyclic	O=S=O	B3LYP/cc-pVTZ	-99.8	111
4	HPO_2 dioxaphosphirane	$HP(=O)_2$	SCF-CEPA-1	-79.6	165
5	Me_2SO_2 dioxathiirane	$Me_2S(=O)_2$ sulfone	B3LYP/6-31+G(d)	-87.6	212

Table 37 (cont.)

6	$MeSi(O)_2Ph$ dioxasilirane	MeSi(=O)OPh ester	B3LYP/6-311++G(d,p)	-61.7	51
7	H_2SiO_2 dioxasilirane	HSi(=O)OH acid	B3LYP/TZ2P-ECP	-81.0	90
8	H_2GeO_2 dioxagermirane	HGe(=O)OH acid	B3LYP/TZ2P-ECP	-74.9	90
9	H_2SnO_2 dioxastannirane	HSn(=O)OH acid	B3LYP/TZ2P-ECP	-70.6	90
10	H_2PbO_2 dioxastilbirane	HPb(=O)OH acid	B3LYP/TZ2P-ECP	-71.8	90
11	H_2CO_2 dioxirane	HC(=O)OH acid	B3LYP/TZ2P	-94.6	90

[a]Energies in kcal/mol.

Table 38. Calculated Cyclization Barriers for the Reaction of Acyclic X-O-O to the Corresponding XO_2 Dioxiranes[a]

X-O-O Acyclic Structure	XO_2 Cyclic Structure	Method and Basis Set	$\Delta E_{A \rightarrow B}$	TS Barrier	Ref.
trans HNOO nitroso oxide	HNO_2 dioxaziridine	SFC/6-31G+p	4.2	43.8	44
MeSi(OO)Ph silanone O-oxide	$MeSi(O_2)H$ dioxasilirane	B3LYP/6-311++G(d,p)	-49.6	0.8	51
SOO acyclic	SO_2 cyclic	B3LYP/cc-pVTZ	-7.5		111
Me_2SOO peroxysulfoxide	Me_2SO_2 dioxathiirane	MP2/6-31G(d)	-3.0	19.0	176
H_2COO carbonyl oxide	H_2CO_2 dioxirane	MP2/6-31G(d)	-28.6	19.1	273a

[a]Energies in kcal/mol.

Table 39. Bimolecular Reaction of XO_2 Dioxiranes

Year	Structure	Trap	Product	Ref.	Comments
2006, 2003	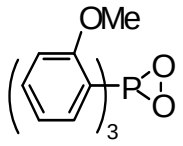	alkenes	epoxides[a]	137	
2004	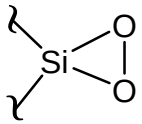	$CH_2=CH_2$	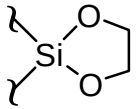	63-73	Tentative assignment of a silica gel-attached dioxasilirane
2003	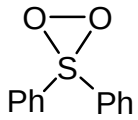	Ph_2S	Ph_2SO	184	
2001	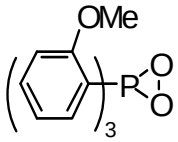	Ar_3P	Ar_3PO	140	

Table 39 (cont.)

1999	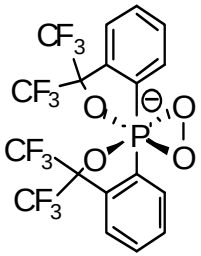	Ph_3P	Ph_3PO	136
1993	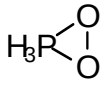	Ph_2SO	Ph_2SO_2 (sulfone)	143a
1993	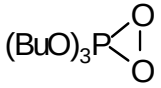	Ar_2S	Ar_2SO	143a
	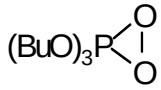	Ar_2SO	Ar_2SO_2 (sulfone)	143a

Table 39 (cont.)

1993	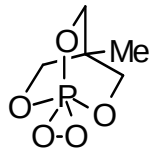	norbornene	norbornene oxide	154
	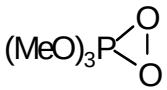	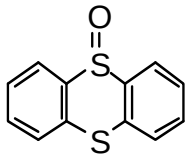	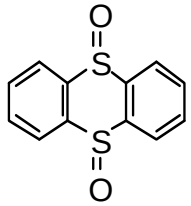 (major product)	154
	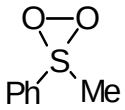	Ph_2S	Ph_2SO	
	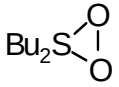	Ph_2S	Ph_2SO	

[a]Corresponding epoxides from norbornene, cis-stilbene, cyclohexene and 1-octene.

4. 6. References

1. Clennan, E. L. *Trends in Org. Chem.* **1995**, *5*, 231.

2. Clennan, E. L. *Sulfur Reports* **1996**, *19*, 171.

3. Ishiguro, K.; Sawaki, Y. *Bull. Chem. Soc. Jpn.* **2000**, *73*, 535.

4. Clennan, E. L.; Pace, A. *Tetrahedron* **2005**, *61*, 6665.

5. A sample of references on metallodioxiranes, MO_2, includes:

   (a) Ho, R. Y. N.; Liebman, J. F.; Valentine, J. S. Biological Reactions of Dioxygen: An Introduction; In *Active Oxygen in Biochemistry*, Valentine, J. S.; Foote, C. S.; Greenberg, A.; Liebman, J. F., Eds.; Blackie Academic & Professional: New York, NY; 1995, pp 1.

   (b) Vaska, L. *Acc. Chem. Res.* **1976**, *9*, 175.

   (c) $MoO(O_2)_2(OPR_3)$ Mimoun-type complexes and $ReO(O_2)_2Me$ Herrmann-type complexes: Deubel, D. V.; Frenking, G.; Gisdakis, P.; Herrmann, W. A.; Rosch, N.; Sundermeyer, J. *Acc. Chem. Res.* **2004**, *37*, 645. Abu-Omar, M. M.; Hansen, P. J.; Espenson, J. H. *J. Am. Chem. Soc.* **1996**, *118*, 4966.

   (d) Copper dioxygen complexes: Mirica, L. M.; Ottenwaelder, X.; Stack, T. D. P. *Chem. Rev.* **2004**, *104*, 1013. Zhang, C. X.; Liang, H.-C.; Humphreys, K. J.; Karlin, K. D. *Catal. Metal Complexes* **2003**, *26* (Advances in Catalytic Activation of Dioxygen by Metal Complexes), 79. Fox, S.; Karlin, K. D. Dioxygen Reactivity in Copper Proteins and Complexes; In *Active Oxygen in Biochemistry*, Valentine, J. S.; Foote, C. S.; Greenberg, A.; Liebman, J. F., Eds.; Blackie Academic & Professional: New York, NY; 1995, pp 188. Mattar, S. M.; Ozin, G. A. *J. Phys. Chem.* **1988**, *92*, 3511.

(e) Cobalt dioxygen complexes: Basolo, F.; Hoffman, B. M.; Ibers, J. A. *Acc. Chem. Res.* **1975**, *8*, 384. McLendon, G.; Martell, A. E. *Coord. Chem. Rev.* **1976**, *19*, 1. Tovrog, B. S.; Kitko, D. J.; Drago, R. S. *J. Am. Chem. Soc.* **1976**, *98*, 5144. Dedieu, A.; Rohmer, M. M.; Veillard, A. *J. Am. Chem. Soc.* **1976**, *98*, 5789.

(f) Dioxygen complexes of manganese porphyrins: Hanson, L. K.; Hoffman, B. M. *J. Am. Chem. Soc.* **1980**, *102*, 4602.

(g) Dioxygen complex of a titanium porphyrin: Guilard, R.; Fontesse, M.; Fournari, P. *J. Am. Chem. Soc. Chem. Commun.* **1976**, 161.

(h) Heme and non-heme dioxygen complexes: Momenteau, M.; Reed, C. A. *Chem. Rev.* **1994**, *94*, 659. Feig, A. L.; Lippard, S. J. *Chem. Rev.* **1994**, *94*, 759. Roelfes, G.; Vrajmasu, V.; Chen, K.; Ho, Raymond Y. N.; Rohde, J.-U.; Zondervan, C.; la Crois, R. M.; Schudde, E. P.; Lutz, M.; Spek, A. L.; Hage, R.; Feringa, B. L.; Muenck, E.; Que, L., Jr. *Inorg. Chem.* **2003**, *42*, 2639.

(i) Vanadium dioxygen complexes: Sam, M.; Hwang, J. H.; Chanfreau, G.; Abu-Omar, M. M. *Inorg. Chem.* **2004**, *43*, 8447.

(j) $Ir(CO)Cl(PPh_3)_2O_2$ complex: Selke, M.; Foote, C. S. *J. Am. Chem. Soc.* **1993**, *115*, 1166.

(k) $Rh(CO)Cl(PPh_3)_2O_2$ complex: Selke, M.; Foote, C. S.; Karney, W. L. *Inorg. Chem.* **1993**, *32*, 5425.

(l) Other examples exist for symmetrical dioxygen complexes with Nb, Cr, W, U, and Pt.

(m) For a comparison between metal-peroxo species and dioxiranes, see: Adam, W.; Mitchell, C. M.; Saha-Moller, C. R.; Weichold, O. *Structure and Bonding* **2000**, *97*, 237. Adam, W.; Mitchell, C. M.; Saha-Moeller, C. R. *J. Org. Chem.* **1999**, *64*, 3699.

6. (a) Bach, R. D. *Chemistry of Peroxides*, Rappoport, Z., Ed.; Wiley & Sons Ltd.: Chichester, U.K., 2006; Vol. 2, Part 1, pp 1.

(b) Adam, W.; Zhao, C.-G. *Chemistry of Peroxides*, Rappoport, Z., Ed.; Wiley & Sons Ltd.: Chichester, U.K., 2006; Vol. 2, Part 1, pp 1129.

(c) Curci, R.; D'Accolti, L.; Fusco, C. *Acc. Chem. Res.* **2006**, *39*, 1.

(d) Yang, D. *Acc. Chem. Res.* **2004**, *37*, 497.

(e) Levai, A. *ARKIVOC* **2003**, *14*, 14.

(f) Adam, W.; Saha-Moeller, C. R.; Zhao, C.-G. *Org. Reactions* **2002**, *61*, 219.

(g) Shi, Y. *Yuki Gosei Kagaku Kyokaishi* **2002**, *60*, 342.

(h) Adam, W.; Saha-Moller, C. R.; Ganeshpure, P. A. *Chem. Rev.* **2001**, *101*, 3499.

(i) Adam, W.; Degen, H.-G.; Pastor, A.; Saha-Moller, C. R.; Schambony, S. B.; Zhao, C.-G. *Peroxide Chemistry* **2000**, 78.

(j) Frohn, M.; Shi, Y. *Synthesis* **2000**, *14*, 1979.

(k) Bach, R. D. *Peroxide Chemistry* **2000**, 569.

(l) Kazakov, V. P.; Voloshin, A. I.; Kazakov, D. V. *Russ. Chem. Rev.* **1999**, *68*, 253.

(m) Denmark, S. E.; Wu, Z. *Synlett* **1999**, 847.

(n) Dryuk, V. G.; Kartsev, V. G. *Russ. Chem. Rev.* **1999**, *68*, 183.

(o) Kabal'nova, N. N.; Khursan, S. L.; Shereshovets, V. V.; Tolstikov, G. A. *Kinetics and Catalysis* (Translation of Kinetika i Kataliz) **1999**, *40*, 207.

(p) Murphree, S. S.; Padwa, A. *Prog. Heterocyclic Chem.* **1998**, *10*, 49.

(q) Adam, W.; Smerz, A. K. *Bull. Soc. Chim. Belg.* **1996**, *105*, 581.

(r) Curci, R.; Dinoi, A.; Rubino, M. F. *Pure Appl. Chem.* **1995**, *67*, 811.

(s) Sauter, M.; Adam, W. *Acc. Chem. Res.* **1995**, *28*, 289.

(t) Adam, W.; Hadjiarapoglou, L. *Topics Current Chem.* **1993**, *164*, 45.

(u) Padwa, A. *Prog. Heterocyclic Chem.* **1993**, *5*, 54.

(v) Adam, W.; Hadjiarapoglou, L. P.; Curci, R.; Mello, R. *Org. Peroxides* **1992**, 195.

(w) Bunnelle, W. H. *Chem. Rev.* **1991**, *91*, 335.

(x) Curci, R. *Adv. Oxygenated Proc.* **1990**, *2*, 1.

(y) Murray, R. W. *Chem. Rev.* **1989**, *89*, 1187.

(z) Adam, W.; Curci, R.; Edwards, J. O. *Acc. Chem. Res.* **1989**, *22*, 205.

(aa) Murray, R. W. *Molecular Struct. Energetics* **1988**, *6*, 311.

(bb) Kafafi, S. A.; Martinez, R. I.; Herron, J. T. *Molecular Struct. Energetics* **1988**, *6*, 283.

(cc) Adam, W.; Curci, R. *Chimica e l'Industria* **1981**, *63*, 20.

7. Harder, T.; Wessig, P.; Bendig, J.; Stösser, R. *J. Am. Chem. Soc.* **1999**, *121*, 6580.

8. Ishikawa, S.; Nojima T.; Sawaki, Y. *J. Chem. Soc., Perkin Trans. 2*, **1996**, *1*, 127.

9. Brinen, J. S.; Singh, B. *J. Am. Chem. Soc.* **1971**, *93*, 6623.

10. Srinivasan, A.; Kebede, N.; Saavedra, J. E.; Nikolaitchik, A. V.; Brady, D. A.; Yourd, E.; Davies, K. M.; Keefer, L. K.; Toscano, J. P. *J. Am. Chem. Soc.* **2001**, *123*, 5465.

11. Ishikawa, S.; Tsuji, S.; Sawaki, Y. *J. Am. Chem. Soc.* **1991**, *113*, 4282.

12. Sawaki, Y.; Ishikawa, S. *J. Am. Chem. Soc.* **1987**, *109*, 584.

13. Zelentsov, S. V.; Zelentsova, N. V.; Shchepalov, A. A. *High Energy Chem.* (Translation of Khimiya Vysokikh Energii) **2002**, *36*, 326.

14. Zelentsov, S. V.; Zelentsova, N. V. *Peroxides at the Beginning of the Third Millennium,* Antonovsky, V. L.; Kasaikina, O. T.; Zaikov, G. E., Eds.; Nova Sciences Publishers, Inc.: New York, 2004, pp 239.

15. Safiullin, R. L.; Khursan, S. L.; Chainikova, E. M.; Danilov, V. T. *Russian Kinetics Catal.* (Translation of Kinetika i Kataliz) **2004**, *45*, 640.

16. Makareeva, E. N.; Lozovskaya, E. L.; Zelentsov, S. V. *High Energy Chem.* (Translation of Khimiya Vysokikh Energii) **2001**, *35*, 177.

17. Liang, T. Y.; Schuster, G. B. *J. Am. Chem. Soc.* **1987**, *109*, 7803.

18. Schuster, G. B.; Platz, M. S. *Adv. Photochem.* **1992**, *17*, 69.

19. Zelentsov, S. V.; Zelentsova, N. V.; Zhezlov, A. B.; Oleinik, A. V. *High Energy Chem.* (Translation of Khimiya Vysokikh Energii) **2000**, *34*, 164.

20. Zhezlov, A. B.; Zelentsov, S. V.; Oleinik, A. V. *High Energy Chem.* (Translation of Khimiya Vysokikh Energii) **1999**, *33*, 87.

21. Zelentsov, S. V.; Bykova, E. A.; Ezhevskii, A. A.; Oleinik, A. V. *High Energy Chem.* (Translation of Khimiya Vysokikh Energii) **1997**, *31*, 397.

22. Treushnikov, V. M.; Pomerantseva, L. L.; Frolova, N. V.; Zelentsov, S. V.; Oleinik, A. V. *Zhurnal Prikladnoi Spektroskopii* **1978**, *28*, 484.

23. (a) Betterton, E. A.; Craig, D. *J. Air Waste Management Assoc.* **1999**, *49*, 1347.

(b) Uppu, R. M.; Squadrito, G. L.; Cueto, R.; Pryor, W. A. *Methods Enzymol.* **1996**, *269B*, 311.

(c) Janowicz, K.; Kurzawa, J. *Chem. Analityczna* **1996**, *41*, 77.

(d) Neumann, D. K.; Coombe, R. D.; Ongstad, A. P.; Stech, D. J. *Proc SPIE International Soc. Opt. Eng.* **1988**, *875*, 142.

(e) Manuszak, M.; Koppenol, W. H. *Thermochim. Acta* **1996**, *273*, 11.

(f) Carey, F. A.; Hayes, L. J. *J. Org. Chem.* **1973**, *38*, 3107.

24. Harder, J.; Bendig, J.; Scholz, G.; Stösser, R. *J. Inf. Recording*. **1996**, *23*, 147.
25. (a) Harder, T.; Bendig, J.; Scholz, G.; Stösser, R. *J. Am. Chem. Soc.* **1996**, *118*, 2497.

(b) Harder, T.; Stösser, R.; Wessig, P.; Bendig, J. *J. Photochem. Photobiol. A* **1997**, *103*, 105.

26. Wasserman, E. *Prog. Phys. Org. Chem.* **1971**, *8*, 319.
27. (a) Platz, M. S. In *Azides and Nitrenes: Reactivity and Utility*, Scriven, E. F. V., Ed.; Academic Press: New York, 1984, pp 359-393.

(b) For a recent example that uses femtosecond UV/Vis spectroscopy, see: Burdzinski, G.; Hackett, J. C.; Wang, J.; Gustafson, T. L.; Hadad, C. M.; Platz, M. S. *J. Am. Chem. Soc.* **2006**, *128*, 13402.

28. Singh, B.; Brinen, J. S. *J. Am. Chem. Soc.* **1971**, *93*, 540.
29. Trozzolo, A. M.; Murray, R. W.; Smolinsky, G.; Yager, W. A.; Wasserman, E. *J. Am. Chem. Soc.* **1963**, *85*, 2526.
30. D'Sa, R. A.; Wang, Y.; Ruane, P. H.; Showalter, B. M.; Saavedra, J. E.; Davies, K. M.; Citro, M. L.; Booth, M. N.; Keefer, L. K.; Toscano, J. P. *J. Org. Chem.* **2003**, *68,* 656.
31. (a) Bushan, K. M.; Xu, H.; Ruane, P. H.; D'Sa, R. A.; Pavlos, C. M.; Smith, J. A.; Celius, T. C.; Toscano, J. P. *J. Am. Chem. Soc.* **2002**, *124*, 12640.

(b) Wasylenko, W. A.; Kebede, N.; Showalter, B. M.; Matsunaga, N.; Miceli, A. P.; Liu, Y.; Ryzhkov, L. R.; Hadad, C. M.; Toscano, J. P. *J. Am. Chem. Soc.* **2006**, *128*, 13142.

(c) Celius, T. C.; Toscano, J. P. *CRC Handbook of Organic Photochemistry and Photobiology (2nd Edition)* 2004, 92/1-92/10.

(d) Ruane, P. H.; Bushan, K. M.; Pavlos, C. M.; D'Sa, R. A.; Toscano, J. P. *J. Am. Chem. Soc.* **2002**, *124*, 9806.

(e) Pavlos, C. M.; Xu, H.; Toscano, J. P. *Free Rad. Biol. Med.* **2004**, *37*, 745.

32. Pavlos, C. M.; Cohen, A. D.; D'Sa, R. A.; Sunoj, R. B.; Wasylenko, W. A.; Kapur, P.; Relyea, H. A.; Kumar, N. A.; Hadad, C. M.; Toscano, J. P. *J. Am. Chem. Soc.* **2003**, *125*, 14934.

33. (a) Go, C. L.; Waddell, W. H. *J. Org. Chem*. **1983**, *48*, 2897.

(b) Waddell, W. H.; Go, C. L. *J. Am. Chem. Soc.* **1982**, *104*, 5804.

34. Leyva, E.; Platz, M. S.; Persy, G.; Wirz, J. *J. Am. Chem. Soc.* **1986**, *108*, 3783.

35. Liang, T. Y.; Schuster, G. B. *J. Am. Chem. Soc.* **1986**, *108*, 546.

36. Liang, T. Y.; Schuster, G. B. *Tetrahedron Lett.* **1986**, *27*, 3328.

37. Abramovitch, R. A.; Challand, S. R. *J. Chem. Soc., Chem. Commun.* **1972**, 964.

38. Nay, B.; Scriven, E. F. V.; Suschitzky, H.; Thomas, D. R.; Carroll, S. E. *Tetrahedron Lett.* **1977**, *21*, 1811.

39. (a) Platz, M. S. *Reactive Intermediate Chemistry*, Moss, R. A.; Platz, M. S.; Jones, M. Jr., Eds.; Wiley: New York, 2004, pp 501-559.

(b) Liu, J.; Hadad, C. M.; Platz, M. S. *Org. Lett.* **2005**, *7*, 549.

(c) Borden, W. T.; Gritsan, N. P.; Hadad, C. M.; Karney, W. L.; Kemnitz, C. R.;

Platz, M. S. *Acc. Chem. Res.* **2000**, *33*, 765.

40. Abramovitch, R. A.; Davis, B. A. *Chem. Rev.* **1964**, *64*, 149.

41. Atkinson, R. S. In *Azides and Nitrenes: Reactivity and Utility,* Scriven, E. F. V., Ed.; Academic Press: New York, 1984, pp 290.

42. Shchepalov, A. A.; Zelentsov, S. V.; Razuvaev, A. G. *Russian Chemical Bulletin* (Translation of Izvestiya Akademii Nauk, Seriya Khimicheskaya) **2001**, *50*, 2346.

43. Fueno, K.; Yokoyama, K.; Takane, S-Y. *Theor. Chim. Acta*. **1992**, *82*, 299.

44. Alcami, M.; de Paz, J. L. G.; Yanez, M. *J. Comput. Chem*. **1989**, *10*, 468.

45. Li, Y.; Iwata, S. *Bull. Chem. Soc. Jpn*. **1997**, *70*, 79.

46. Alcami , M.; Mo, O.; Yanez, M. *J. Comput. Chem*. **1998**, *19*, 1072.

47. Nakamura, S.; Takahashi, M.; Okazaki, R.; Morokuma, K. *J. Am. Chem. Soc.* **1987**, *109*, 4142.

48. (a) Yamaguchi, K.; Yabushita, S.; Fueno, T. *J. Chem. Phys*. **1979**, *71*, 2321.
(b) Jones, W. H. *J. Phys. Chem*. **1992**, *96*, 594.

49. Melius, C. F.; Binkley, J. S. ACS Symposium Series; The Chemistry of Combustion Processes, T. M. Sloane, Ed. 1984, 249, pp 103.

50. Takane, S-Y.; Fueno, K. *Theor. Chim. Acta*. **1994**, *87*, 431.

51. Bornemann, H.; Sander, W. *J. Am. Chem. Soc*. **2000**, *122*, 6727.

52. Patyk, A.; Sander, W.; Gauss, J.; Cremer, D. *Chem. Ber.* **1990**, *123*, 89.

53. Patyk, A.; Sander, W.; Gauss, J.; Cremer, D. *Angew. Chem*. **1989**, *101*, 920.

54. Patyk, A.; Sander, W.; Gauss, J.; Cremer, D. *Angew. Chem. Int. Ed. Engl*. **1989**, *28*, 898.

55. Sander, W.; Kirschfeld, A. *Matrix-Isolation of Strained Three-Membered Ring Systems*, Halton, B., Ed.; JAI Press: London, U.K., 1995; Vol. 4, Chapter 2, pp 1-80.

56. Sander, W.; Trommer, M.; Patyk, A. *Organosilicon Chemistry III*: From Molecules to Materials; Auner, N; Weis, J., Eds.; Wiley-VCH, Weinheim, Germany, 1996, 86.

57. Becerra, R.; Bowes, S.-J.; Ogden, J. S.; Cannady, J. P.; Adamovic, I.; Gordon, M. S.; Almond, M. J.; Walsh, R. *Phys. Chem. Chem. Phys.* **2005**, *7*, 2900.

58. Uchino, T.; Kurumoto, N.; Sagawa, N. *Phys. Rev. B* **2006**, *73*, 2031.

59. (a) Gaspar, P. P.; Boo, B.-H.; Chari, S.; Ghosh, A. K.; Holten, D.; Kirmaier, C.; Konieczny, S. *Chem. Phys. Lett*. **1984**, *105*, 153.

(b) Gasper, P. P.; Holten, D.; Konieczny, S.; Corey, J. Y. *Acc. Chem. Res*. **1987**, *20*, 329.

60. Sabdhu, V.; Jodhan, A.; Safarik, I.; Strausz, O. P. *Chem. Phys. Lett.* **1987**, *135*, 260.

61. Hartman, J. R.; Famil-Ghiriha, J.; O'Neal, H. E. *Combust. Flame* **1987**, *68*, 43.

62. Inoue, G.; Suzuki, M. *Chem. Phys. Lett.* **1985**, *122*, 361.

63. Permenov, D. G.; Radzig, V. A. *Kinetics Catal.* **2004**, *45*, 273.

64. Radtzig, V. A. *Kinetics Catal.* (Translation of Kinetika i Kataliz) **1996**, *37*, 302.

65. Radtzig, V. A.; Baskir, E. G.; Korolev, V. A. *Kinetics Catal.* (Translation of Kinetika i Kataliz), **1995**, *36*, 568.

66. Radtzig, V. A. *Khimicheskaya Fizika* **1995**, *14*, 125.

67. Radtzig, V. A. *Sov. J. Chem. Phys*. **1993**, *10*, 1958.

68. Bobyshev, A. A.; Radtzig, V. A. *Sov. J. Chem. Phys*. **1991**, *7*, 1641.

69. Radtzig, V. A. *Khim. Fiz*. **1991**, *10*, 1262.

70. Bobyshev, A. A.; Radtzig, V. A. *Kinetika i Kataliz* **1990**, *31*, 925.

71. Radtzig, V. A.; Senchenya, I. N.; Bobyshev, A. A.; Kazanskii, V. B. *Kinetika i Kataliz* **1989**, *30*, 1334.

72. Bobyshev, A. A.; Radtzig, V. A. *Khim. Fiz.* **1988**, *7*, 950.

73. Bobyshev, A. A.; Radtzig, V. A. *Kinetika i Kataliz* **1988**, *29*, 638.

74. Murakami, Y.; Koshi, M.; Matsui, H.; Kamiya, K.; Umeyama, H. *J. Phys. Chem.* **1996**, *100*, 17501.

75. Conlin, R. T.; Gaspar, P. P. *J. Am. Chem. Soc.* **1976,** *98*, 868.

76. Drahnak, T. J.; Michl, J.; West, R. *J. Am. Chem. Soc.* **1981,** *103*, 1845.

77. Arrington, C. A.; West, R.; Michl, J. *J. Am. Chem. Soc.* **1983,** *105*, 6176.

78. Maier, G.; Mihm, G.; Reisenauer, H. P.; Littmann, D. *Chem. Ber*. **1984**, *117*, 2369.

79. Arrington, C. A.; Klingensmith, K. A.; West, R.; Michl, J. *J. Am. Chem. Soc.* **1984,** *106*, 525.

80. (a) Raabe, G.; Michl, J. *Chem. Rev*. **1985**, *85*, 419.
(b) Raabe, G.; Vancik, H.; West, R.; Michl, J. *J. Am. Chem. Soc*. **1986**, *108*, 671.

81. Trommer, M.; Sander, W.; Patyk, A. *J. Am. Chem. Soc.* **1993**, *115*, 11775.

82. (a) Akasaka, T.; Nagase, S.; Yabe, A.; Ando, W. *J. Am. Chem. Soc*. **1988**, *110*, 6270.
(b) Akasaka, T.; Yabe, A.; Nagase, S.; Ando, W. *Nippon Kagaku Kaishi* **1989**, *8*, 1440.

83. West, R.; Fink, M. J.; Michl, J. *Science* **1981**, *214*, 1343.

84. Gaspar, P. P. *Reactive Intermediates*; John Wiley: New York, 1978; Vol. 1, pp 229; 1981, Vol. 2, 335; 1985, Vol. 3, 333.

85. Morterra, C.; Low. M. J. D. *Ann. N. Y. Acad. Sci*. **1973**, *220*, 133.

86. Morterra, C.; Low. M. J. D. *J. Phys Chem.* **1969**, *73*, 327.

87. Morterra, C.; Low. M. J. D. *J. Phys. Chem*. **1969**, *73*, 321.

88. Morterra, C.; Low. M. J. D. *J. Am. Chem. Soc. Chem. Commun*. **1968**, 203.

89. Bach, R. D.; Dmitrenko, O. *J. Am. Chem. Soc.* **2006**, *128*, 4598.

90. Richardson, N. A.; Rienstra-Kiracofe, J. C.; Schaefer, H. F. *Inorg. Chem*. **1999**, *38*, 6271.

91. Liebman, J. F.; Skancke, P. N. *Int. J. Quant. Chem*. **1996**, *58*, 707.

92. Nagase, S.; Kudo, T.; Akasaka, T.; Ando, W. *Chem. Phys. Lett*. **1989**, *163*, 23.

93. Darling, C. L.; Schlegel, H. B. *J. Phys. Chem.* **1993**, *97*, 8207.

94. Darling, C. L.; Schlegel, H. B. *J. Phys. Chem.* **1994**, *98*, 8910.

95. Zachariah, M. R.; Tsang, W. **1995**, *99*, 5308.

96. Harshavardhan, K.; Solomon, A.; Hegde, M. S. *Solid State Comm.* **1989**, *69*, 117.

97. Neumann, W. P. *Chem. Rev.* **1991**, *91*, 311.

98. Becerra, R.; Walsh, R. *Spectrum* **2004**, *17*, 16.

99. J asinski, J. M.; Becerra, R.; Walsh, R. *Chem. Rev.* **1995**, *95*, 1203.

100. Becerra, R.; Walsh, R. Kinetics & mechanisms of silylene reactions: A prototype for gas-phase acid/base chemistry. In *Research in Chemical Kinetics*; Compton, R. G.; Hancock, G., Eds.; Elsevier: Amsterdam, 1995; Vol. 3, pp 263.

101. Driess, M.; Grützmacher, H. *Angew. Chem., Int. Ed. Engl.* **1996**, *35*, 828.

102. Richardson, N. A.; Rienstra-Kiracofe, J. C.; Schaefer, H. F. *J. Am. Chem. Soc*. **1999**, *121*, 10813.

103. Myerson, A. L.; Taylor, F. R.; Hanst, P. L. *J. Chem. Phys.* **1957**, *26*, 1309.

104. Norrish, R. G. W.; Zeelenberg, A. P. *Proc. R. Soc. London, Ser. A* **1957**, *240*.

105. Norrish, R. G. W.; Oldershaw, G. A. *Proc. R. Soc. London, Ser. A* **1957**, *249*, 498.

106. Meyer, B.; Philips, L. F.; Smith, J. J. *Proc. Natl. Acad. Sci*. **1968**, *61*, 7.

107. Deveze, D.; Rumpf, P. *C. R. Acad. Sci., Ser. C* **1968**, *266*, 1001.

108. Brown, J.; Burns, G. *Can. J. Chem*. **1969**, *47*, 4291.

109. Plach, H. J.; Troe, *J. Int. J. Chem. Kinetics* **1984**, *16*, 1531.

110. Zen, C. C.; Chen, I. C.; Lee, Y. P. *J. Phys. Chem. A* **2000**, *104*, 771.

111. Chen, L.-S.; Lee, C.-I.; Lee, Y.-P. *J. Chem. Phys.* **1996**, *105*, 9454.

112. Kaupp, G. *J. Mol. Struct.* **2006**, *786*, 140.

113. Kellogg, C. B.; Schaefer, H. F. *Theor. Chem. Acc.* **1997**, *96*, 7.

114. Kellogg, C. B.; Schaefer, H. F. *J. Chem. Phys.* **1995**, *102*, 4177.

115. Dunning, T. H. Jr.; Raffenetti, R. C. *J. Phys. Chem.* **1981**, *85*, 1350.

116. Hayes, E. F.; Pfeiffer, G. V. *J. Am. Chem. Soc.* **1968**, *90*, 4773.

117. Ivanic, J.; Atchity, G. J.; Ruedenberg, K. *J. Chem. Phys*. **1997**, *107*, 4307.

118. Elliott, R.; Compton, R.; Levis, R.; Matsika, S. *J. Chem. Phys*. *A* **2005**, *109*, 11304.

119. Martinez, R. I.; Herron, J. T. *Chem. Phys. Lett.* **1980**, *72*, 77.

120. Groves, C.; Lewars, E. *THEOCHEM* **2000**, *530*, 265.

121. Studies have also been conducted on oligomers of NO_2: Liebman, J. F. *J. Chem. Phys.* **1974**, *60*, 2944.

122. Hoffmann, R. *Am. Sci.* **2004**, *92*, 23.

123. Sung, S.; Hoffmann, R. *J. Molecular Sci.* **1983**, *1*, 1.

124. Plass, R.; Egan, K.; Collazo-Davila, C.; Grozea, D.; Landree, E.; Marks, L. D.; Gajdardziska-Josifovska, M. *Phys. Rev. Lett.* **1998**, *81*, 4891

125. Xie, D. Q.; Guo, H.; Bludsky, O.; Nachtigall, P. *Chem. Phys. Lett*. **2000**,

329, 503.

126. Zuniga, J.; Bastida, A.; Requena, A. *J. Chem. Phys*. **2001**, *115*, 139.

127. Rodrigues, S. P. J.; Sabin, J. A.; Varandas, A. J. C. *J. Phys. Chem. A* **2002**, *106*, 556.

128. Ma, G. B.; Chen, R. Q.; Guo, H. *J. Chem. Phys*. **1999**, *110*, 8408.

129. Kamiya, K.; Matsui, H. *Bull. Chem. Soc. Jpn*. **1991**, *64*, 2792.

130. Flemmig, B.; Wolczanski, P. T.; Hoffmann, R. *J. Am. Chem. Soc.* **2005**, *127*, 278.

131. Brabson, G; Andrews, L. *J. Phys. Chem.* **1996**, *100*, 16487.

132. Brabson, G; Citra, A.; Andrews, L.; Davy, R. D.; Neurock, M. *J. Am. Chem. Soc.* **1996**, *118*, 5469.

133. Bartlett, P. D.; Mendenhall, G. D. *J. Am. Chem. Soc*. **1970**, *92*, 210.

134. Schaap, A. P.; Bartlett, P. D. *J. Am. Chem. Soc.* **1970**, *92*, 6055.

135. Stephenson, L. M.; McClure, D. E. *J. Am. Chem. Soc*. **1973**, *95*, 3074.

136. Nakamoto, M.; Akiba, K.-Y. *J. Am. Chem. Soc.* **1999**, *121*, 6958.

137. (a) Ho, D. G.; Gao, R.; Celaje, J.; Chung, H.-Y.; Selke, M. *Science*, **2003**, *302*, 259. (b) Zhang, D.; Ye, B.; Ho, D. G.; Gao, R.; Selke, M. *Tetrahedron* **2006**, *62*, 10729.

138. Zhang, D.; Gao, R.; Afzal, S.; Vargas, M.; Sharma, S.; McCurdy, A.; Yousufuddin, M.; Stewart, T.; Bau, R.; Selke, M. *Org. Lett.* **2006**, *8*, 5125.

139. Withnall, R.; Andrews, L. *J. Phys. Chem.* **1987**, *91*, 784.

140. (a) Gao, R.; Ho, D. G.; Dong, T.; Khuu, D.; Franco, N.; Sezer, O.; Selke, M. *Org. Lett*. **2001**, *3*, 3719.

141. Wilke, J. J.; Weinhold, F. *J. Am. Chem. Soc.* **2006**, *128*, 11850.

142. Armstrong, A.; Knight, J. D. Ann. Rep. Prog. Chem.: *Org. Chem.* **2004**, 100, 51.

143. (a) Tsuji, S.; Kondo, M.; Ishiguro, K.; Sawaki, Y. *J. Org. Chem*. **1993**, *58*, 5055.

(b) Bennett, G. D.; Paquette, L. A. *Chemtracts—Org. Chem.* **1994**, *7*, 21.

144. Itzstein, M. V.; Jenkins, I. D. *J. Chem. Soc., Chem. Commun*. **1983**, 165.

145. Buckler, S. A. *J. Am. Chem. Soc.* **1962**, *84*, 3093.

146. Burkett, H. D.; Hill, W. E.; Worley, S. D. *Phosphorus Sulfur* **1984**, *20*, 169.

147. (a) Howard, J. A.; Tait, J. C. *Can. J. Chem.* **1978**, *56*, 2163.

(b) Phosphines have been suggested to reduce hydroperoxides by nonradical paths: Hiatt, R.; McColeman, C. *Can. J. Chem.* **1971**, *49*, 1709.

(c) A radiolysis study was published: Alfassi, Z. B.; Neta, P.; Beaver, B. *J. Phys. Chem. A* **1997**, *101*, 2153.

148. Tolman, C. A. *Chem. Rev*. **1977**, *77*, 313.

149. Crabtree, R. H. *The Organometallic Chemistry of the Transition Metals*; John Wiley & Sons: New York, 1988; pp 72.

150. Greer, A.; Vassilikogiannakis, G.; Lee, K.-C.; Koffas, T. S.; Nahm, K.; Foote, C. S. *J. Org. Chem.* **2000**, *65*, 6876.

151. Hayes, R. A.; Martin, J. C. *Organic Sulfur Chemistry. Theoretical and Experimental Advances*; Elsevier: Amsterdam, 1985; Vol. 19, pp 408.

152. Kucsman, A.; Kapovits, I. *Organic Sulfur Chemistry. Theoretical and Experimental Advances*; Elsevier: Amsterdam, 1985; Vol. 19., pp 191.

153. Nahm, K.; Foote, C. S. *J. Am. Chem. Soc.* **1989**, *111*, 909.

154. Akasaka, T.; Kita, I.; Haranaka, M.; Ando, W. *Quimica Nova* **1993**, *16*, 325.

155. (a) Akasaka, T.; Ando, W. *Phosphorus, Sulfur, Silicon Relat. Elem.* **1994**, *95-69*, 437.

(b) Tamagaki, S.; Akatsuka, R. *Bull. Chem. Soc. Jpn*., **1982**, *55*, 3037.

156. Bolduc, P. R.; Goe, G. L. *J. Org. Chem*. **1974**, *39*, 3178.

157. Dannley, R.; L. Kabre, K. R. *J. Am. Chem. Soc.* **1965**, *87*, 4805.

158. Sobkowiak, M.; Clifford, C. E. B.; Beaver, B. *Preprints-ACS Division of Petroleum Chem.* **2004**, *49*, 450.

159. Beaver, B.; Gao, L.; Fedak, M. *Preprints-ACS Division of Petroleum Chem.* **2004**, *49*, 448.

160. Beaver, B. D.; Burgess Clifford, C.; Fedak, M. G.; Gao, L.; Iyer, P. S.; Sobkowiak, M. *Energy & Fuels* **2006**, *20*, 1639.

161. Beaver, B. D.; Gao, Li; Fedak, Mitchel G.; Coleman, Michael M.; Sobkowiak, M. *Energy & Fuels* **2002**, *16*, 1134.

162. Beaver, B.; DeMunshi, R.; Heneghan, S. P.; Whitacre, S. D.; Neta, P. *Energy & Fuels* **1997**, *11*, 396.

163. Beaver, B.; Rawlings, D.; Neta, P.; Alfassi, Z. B.; Das, T. N. *Heteroatom Chem.* **1998**, *9*, 133.

164. Nahm, K.; Li, Y.; Evanseck, J, D.; Houk, K. N.; Foote, C. S. *J. Am. Chem. Soc.* **1993**, *115*, 4879.

165. Schoeller, W. W.; Busch, T. *Chem. Ber.* **1992**, *125*, 1319.

166. Weinhold, F.; Landis, C. R. *Valency and Bonding: A Natural Bond Orbital Donor—Acceptor Perspective*; Cambridge University Press: Cambridge, U.K., 2005; pp 275.

167. Trippett, S. *Phosphorus Sulfur* **1976**, *73*, 1.

168. Adam, W.; Haas, W.; Sieker, G. *J. Am. Chem. Soc.* **1984**, *106*, 5020.

169. Adam, W.; Golsch, D. *J. Org. Chem.* **1997**, *62*, 115.

170. Adam, W.; Blancafort, L. *J. Org. Chem.* **1997**, *62*, 1623.

171. Clennan, E. L. Sulfide Photooxidation: A Question Of Mechanism, In *Advances in Oxygenated Processes*; JAI Press, Inc., 1995, Vol. 4, pp. 49-80.

172. Clennan, E. L. *ACS Symposium Series* (Petroleum Chemistry) **1992**, 377.

173. Ando, W. *Sulfur Reports* **1981**, *1*, 147.

174. Ando, W.; Takata, T. In *Singlet O_2. Reaction Modes and Products. Part 2*; Frimer, A. A., Ed.; CRC Press: Boca Raton, 1985; Vol. III; pp 1.

175. Grapperhaus, C. A.; Darensbourg, M. Y. *Acc. Chem. Res.* **1998**, *31*, 451.

176. Jensen, F.; Greer, A.; Clennan, E. L. *J. Am. Chem. Soc.* **1998**, *120*, 4339.

177. Liang, J.-J.; Gu, C.-L.; Kacher, M. L.; Foote, C. S. *J. Am. Chem. Soc*. **1983**, *105*, 4717.

178. Bonesi, S. M.; Fagnoni, M.; Albini, A. *J. Org. Chem*. **2004**, 69, 928.

179. Clennan, E. L.; Greer, A. *J. Org. Chem*. **1996**, *61*, 4793.

180. Sysak, P. K.; Foote, C. S.; Ching, T.-Y. *Photochem. Photobiol.* **1977**, *27*, 19.

181. Miskoski, S.; Garcia, N. A. *Photochem. Photobiol.* **1993**, *57*, 447.

182. Bonesi, S. M.; Albini, A. *J. Org. Chem.* **2000**, *65*, 4532.

183. Bonesi, S. M.; Mella, M.; d'Alessandro, N.; Aloisi, G. G.; Vanossi, M.; Albini, A. *J. Org. Chem.* **1998**, *63*, 9946.

184. Baciocchi, E.; Giacco, T. D.; Eliesi, F.; Gerini, M. F.; Guerra, M.; Lapi, A.; Liberali, P. *J. Am. Chem. Soc*. **2003**, *125*, 16444.

185. Baciocchi, E.; Del Giacco, T.; Ferrero, M. I.; Rol, C.; Sebastiani, G. V. *J. Org. Chem.* **1997**, *62*, 4015.

186. Baciocchi, E.; Del Giacco, T.; Gerini, M. F.; Lanzalunga, O. *Org. Lett.* **2006**, *8*, 641.

187. Baciocchi, E.; Del Giacco, T.; Gerini, M. F.; Lanzalunga, O. *Tetrahedron* **2006**, *62*, 6566.

188. Clennan, E. L. *Acc. Chem. Res.* **2001**, *34*, 875.

189. Che, Y.; Ma, W.; Ren, Y.; Chen, C.; Zhang, X.; Zhao, J.; Zang, L. *J. Phys. Chem. B* **2005**, *109*, 8270.

190. Che, Y.; Ma, W.; Ji, H.; Zhao, J.; Ling, Z. *J. Phys. Chem. B* **2006**, *110*, 2942.

191. Latour, V.; Pigot, T.; Simon, M.; Cardy, H.; Lacombe, S. *Photochem. Photobiol. Sci.* **2005**, *4*, 221.

192. Lacombe, S.; Cardy, H.; Simon, M.; Khoukh, A.; Soumillion, J. P.; Ayadim, M. *Photochem. Photobiol. Sci.* **2002**, *1*, 347.

193. Soggiu, N.; Cardy, H.; Habib Jiwan, J. L.; Leray, I.; Soumillion, J. P.; Lacombe, S. *J. Photochem. Photobiol. A* **1999**, *124*, 1.

194. Clennan, E. L.; Zhou, W.; Chan, J. *J. Org. Chem.* **2002**, *67*, 9368.

195. Thanasekaran, P.; Rajagopal, S.; Ramaraj, R.; Srinivasan, C. *Radiat. Phys. Chem.* (Symposium) **1996**, *49*, 103.

196. Gu, K.; Cao, Y.; Zhang, B. *Huaxue Xuebao* **1989**, *47*, 668.

197. Miller, B. L.; Kuczera, K.; Schoeneich, C. *J. Am. Chem. Soc.* **1998**, *120*, 3345.

198. Baciocchi, E.; Del Giacco, T.; Gerini, M. F.; Lanzalunga, O. *Org. Lett.* **2006**, *8*, 641.

199. Rehorek, D. *Zeitschrift Chem.* **1990**, *30*, 447.

200. Fox, M. A.; Miller, P. K.; Reiner, M. D. *J. Org. Chem.* **1979**, *44*, 1103.

201. Inoue, K.; Matsuura, T.; Saito, I. *Tetrahedron* **1985**, *41*, 2177.

202. Ando, W.; Nagashima, T.; Saito, K.; Kohmoto, S. *J. Chem. Soc,. Chem. Comm.* **1979**, 154.

203. Eriksen, J.; Foote, C. S.; Parker, T. L. *J. Am. Chem. Soc.* **1977**, *99*, 6455.

204. Schenck, G. O.; Krauch, C. H. *Angew. Chem.* **1962**, *74*, 510.

205. Schenck, G. O. *Ann. N. Y. Acad. Sci.* **1970**, *171*, 67.

206. Corey, E. J.; Ouannes, C. *Tetrahedron Lett*. **1976**, *47*, 4263.SA33.

207. Ando, W.; Kabe, Y.; Miyazki, H. *Photochem. Photobiol.* **1979**, *31*, 191.

208. Jori, G.; Cauzzo, G. *Photochem. Photobiol.* **1970**, *12*, 231.

209. Casagrande, M.; Gennari, G.; Cauzzo, G. *Gazzetta Chim. Ital.* **1979**, *104*, 1251.

210. Takata, T.; Hoshino, K.; Takeuchi, E.; Tamura, Y.; Ando, W. *Tetrahedron Lett.* **1984**, *25*, 4767.

211. Ando, W.; Sonobe, H.; Akasaka, T. *Tetrahedron Lett.* **1986**, *27*, 4473.

212. McKee, M. L. *J. Am. Chem. Soc.* **1998**, *120*, 3963.

213. Greer, A.; Chen, M.-F.; Jensen, F.; Clennan, E. L. *J. Am. Chem. Soc*. **1997**, *119*, 4380.

214. Clennan, E. L.; Chen, M.-F.; Greer, A.; Jensen, F. *J. Org. Chem*. **1998**, *63*, 3397.

215. Clennan, E. L.; Aebisher, D. *J. Org. Chem*. **2002**, *67*, 1036.

216. Foote, C. S.; Peters, J. W. *J. Am. Chem. Soc.* **1971**, *93*, 3795.

217. Gu, C.-L.; Foote, C. S.; Kacher, M. L. *J. Am. Chem. Soc.* **1981**, *103*, 5949.

218. Sawaki, Y.; Ogata, Y. *J. Am. Chem. Soc*. **1981**, *103*, 5947.

219. Gu, C.-L.; Foote, C. S. *J. Am. Chem. Soc*. **1982**, *104*, 6060.

220. Kacher, M. L.; Foote, C. S. *Photochem. Photobiol.* **1978**, 29, 765.

221. Jensen, F.; Foote, C. S. *J. Am. Chem. Soc*. **1987**, *109*, 1478.

222. Bhardwaj, R. K.; Davidson, S. *Tetrahedron* **1987**, *43*, 4473.

223. Jensen, F.; Foote, C. S. *J. Am. Chem. Soc*. **1988**, *110*, 2368.

224. Ando, W.; Akasaka, T. The Role of Oxygen in Chemistry and Biochemistry, Proceeding of an International Symposium on Activation of Dioxygen and Homogeneous Catalytic Oxidation, In *Studies of Organic Chemistry*, Vol. 33, Tsukoba, Japan, 1988, pp. 99.

225. Nahm, K.; Foote, C. S. *J. Am. Chem. Soc.* **1989**, *111*, 1909.

226. Clennan, E. L.; Chen, X. *J. Am. Chem. Soc.* **1989**, *111*, 5787.

227. Clennan, E. L.; Yang, K. *J. Am. Chem*. *Soc*. **1990**, *112*, 4044.

228. Akasaka, T.; Sakurai, A.; Ando, W. *J. Am. Chem. Soc*. **1991**, *113*, 2696.

229. Akasaka, T.; Haranaka, M.; Ando, W. *J. Am. Chem. Soc.* **1991**, *113*, 9898.

230. Watanabe, Y.; Kuriki, N.; Ishiguro, K.; Sawaki, Y. *J. Am. Chem*. *Soc*. **1991**, *113*, 2677.

231. Jensen, F. *J. Org. Chem*. **1992**, *57*, 6478.

232. Clennan, E. L.; Wang, D. X.; Yang, K.; Hodgson, D. J.; Oki, A. R. *J. Am. Chem. Soc.* **1992**, *114*, 3021.

233. Laakso, D.; Marshall, P. *J. Phys. Chem*. **1992**, *96*, 2471.

234. Clennan, E. L.; Yang, K. *Tetrahedron Lett.* **1993**, *34*, 1697.

235. Clennan, E. L.; Zhang, H. *J. Org. Chem*. **1994**, *59*, 7952.

236. Pasto, D. J.; Cottard, F. *J. Am. Chem. Soc*. **1994**, *116*, 8973.

237. Clennan, E. L.; Wang, D.; Zhang, H.; Clifton, C. H. *Tetrahedron Lett.* **1994**, 4723.

238. Clennan, E. L.; Zhang, H. *J. Am. Chem*. *Soc.* **1994**, *116*, 809.

239. Clennan, E. L.; Chen, M.-F. *J. Org. Chem*. **1995**, *60*, 6444.

240. Clennan, E. L.; Dobrowolski, P.; Greer, A. *J. Am. Chem. Soc*. **1995**, *117*, 9800.

241. Clennan, E. L.; Greer, A. *Tetrahedron Lett.* **1996**, *37*, 6093.

242. Ishiguro, K.; Hayashi, M.; Sawaki, Y. *J. Am. Chem. Soc*. **1996**, *118*, 7265.

243. Greer, A.; Jensen, F.; Clennan, E. L. *J. Org. Chem.* **1996**, *61*, 4107.

244. Shangguan, C.; McAllister, M. A. *Theochem*, **1998**, *422*, 123.

245. Toutchkine, A.; Clennan, E. L. *J. Org. Chem*. **1999**, *64*, 5620.

246. Toutchkine, A.; Clennan, E. L. *J. Am. Chem. Soc.* **2000**, *122*, 1834.

247. Madhavan, D.; Pitchumani, K. *Tetrahedron* **2001**, *57*, 8391.

248. Toutchkine, A.; Aebisher, D.; Clennan, E. L. *J. Am. Chem. Soc.* **2001**, *123,* 4966.

249. Sofikiti, N.; Rabalakos, C.; Stratakis, M. *Tetrahedron Lett.* **2004**, *45*, 1335.

250. Bonesi, S. M.; Fagnoni, M.; Albini, A. *J. Org. Chem.* **2004**, *69*, 928.

251. Clennan, E. L.; Hightower, S. E.; Greer, A. *J. Am. Chem. Soc.* **2005**, *127*, 11819.

252. Shiraishi, Y.; Koizumi, H.; Hirai, T. *J. Phys. Chem. B* **2005**, *109*, 8580.

253. Clennan, E. L.; Hightower, S. E. *J. Org. Chem.* **2006**, *71*, 1247.

254. Akasaka, T.; Yabe, A.; Ando, W. *J. Am. Chem. Soc*. **1987**, *109*, 8085.

255. Grapperhaus, C. A.; Maguire, M. J.; Tuntulani, T.; Darensbourg, M. Y. *Inorg. Chem.* **1997**, *36*, 1860.

256. Farmer, P. J.; Solouki, T.; Mills, D. K.; Soma, T.; Russell, D. H.; Reibenspies, J. H.; Darensbourg, M. Y. *J. Am. Chem. Soc.* **1992**, *114*, 4601.

257. Darensbourg, M. Y.; Tuntulani, T.; Reibenspies, J. H. *Inorg. Chem.* **1995**, *34*, 6287.

258. Farmer, P. J.; Solouki, T.; Soma, T.; Russell, D. H.; Darensbourg, M. Y. *Inorg. Chem.* **1993**, *32*, 4171.

259. Buonomo, R. M.; Font, I.; Maguire, M. J.; Reibenspies, J. H.; Tuntulani, T.; Darensbourg, M. Y. *J. Am. Chem. Soc.* **1995**, *117*, 963.

260. Buonomo, R. M.; Font, I.; Maguire, M. J.; Reibenspies, J. H.; Tuntulani, T.; Darensbourg, M. Y. *J. Am. Chem. Soc.* **1995**, *117*, 5427.

261. Grapperhaus, C. A.; Darensbourg, M. Y.; Sumner, L. W.; Russell, D. H. *J. Am. Chem. Soc.* **1996**, *118*, 1791.

262. Galvez, C.; Ho, D. G.; Azod, A.; Selke, M. *J. Am. Chem. Soc.* **2001**, *123*, 3381.

263. Connick, W. B.; Gray, H. B. *J. Am. Chem. Soc.* **1997**, *119*, 11620.

264. Zhang, Y.; Ley, K. D.; Schanze, K. S. *Inorg. Chem.* **1996**, *35*, 7102.

265. Akasaka, T.; Ando, W. *Phosphorus, Sulfur, Silicon Relat. Elem.* **1994**, *95-69*, 437.

266. Hevesi, L.; Krief, A. *Angew. Chem., Int. Ed. Eng.* **1976**, *15*, 381.

267. Sofikiti, N.; Rabalakos, C.; Stratakis, M. *Tetrahedron Lett.* **2004**, *45*, 1335.

268. Wasserman, H. H.; Lu, T. J. *Recueil Trav. Chim. Pays-Bas* **1986**, *105*, 345.

269. Tamagaki, S.; Akatsuka, R. *Bull. Chem. Soc. Jpn.* **1982**, *55*, 3037.

270. Kojima, N.; Yamada, A.; Takahashi, K.; Okamoto, T.; Konagai, M.; Saito, K. *Jpn. J. Applied Phys. Lett.* **1993**, *32*, L887.

271. Detty, M. D.; Merkel, P. B.; Powers, S. K. *J. Am. Chem. Soc.* **1988**, *110*, 5920.

272. Schultz, M.; Liebsch, S.; Kluge, R.; Adam, W. *J. Org. Chem.* **1997**, *62*, 188.

273. (a) Bach, R. D.; Andres, J. L.; Owensby, A. L.; Schlegel, H. B.; McDouall, J. J. W. *J. Am. Chem. Soc*. **1992**, *114*, 7207.

(b) Warner, P. M. *J. Org. Chem.* **1996**, *61*, 7192.

274. Shu, L.; Shi, Y. *Tetrahedron Lett.* **1999**, *40*, 8721.

275. Yang, D.; Tang, Y.-C.; Chen, J.; Wang, X.-C.; Bartberger, M. D.; Houk, K. N.;

Olson, L. *J. Am. Chem. Soc.* **1999**, *121*, 11976.

276. Merenyi G.; Lind J.; Goldstein S. *J. Am. Chem. Soc.* **2002**, *124*, 40.

277. Liebman, J. F.; Greenberg, A. *Chem. Rev.* **1989**, *89*, 1225.

278. Bach, R. D.; Dmitrenko, O. *J. Am. Chem. Soc.* **2004**, *126*, 4444.

279. Bach, R. D.; Dmitrenko, O. *J. Org. Chem.* **2002**, *67*, 2588.

280. Bach, R. D.; Dmitrenko, O. *J. Org. Chem.* **2002**, *67*, 3884.